Stony Brook University

Investigation of the mouse sperm acrosome reaction with synthetic glycopolymers

A Dissertation Presented

by

Linghui Wu

to

The Graduate School

in Partial Fulfillment of the

Requirements

for the Degree of

Doctor of Philosophy

in

Chemistry

Stony Brook University

August 2013

Stony Brook University

The Graduate School

Linghui Wu

We, the dissertation committee for the above candidate for the

Doctor of Philosophy degree, hereby recommend

acceptance of this dissertation.

Nicole S. Sampson – Dissertation Advisor
Professor and Chair of Chemistry

Isaac Carrico - Chairperson of Defense
Associate Professor of Chemistry

Erwin London – Third Member of Defense
Professor of Chemistry and Professor of Biochemistry and Cell Biology

W. Todd Miller – Outside Member of Defense
Professor of Physiology and Biophysics

This dissertation is accepted by the Graduate School

Charles Taber
Interim Dean of the Graduate School

Abstract of the Dissertation

Investigation of the mouse sperm acrosome reaction with synthetic glycopolymers

by

Linghui Wu

Doctor of Philosophy

in

Chemistry

Stony Brook University

2013

The sperm acrosome reaction (AR), an essential step in mammalian fertilization, is mediated by a highly species-specific interaction of sperm surface molecules with glycan moieties on the egg. Many previous studies indicate that a subset of terminal carbohydrate residues on the mouse egg zona pellucida (ZP) trigger the AR by cross-linking or aggregating receptors on the sperm membrane. However, the exact role of those carbohydrates in AR has not been identified and the mechanism underlying the induction of the AR still needs further investigation. To study this process, a series of synthetic glycopolymers were synthesized. The glycopolymer is composed of a multivalent scaffold (norbornene), a functional ligand (previously identified ZP terminal carbohydrates), and a linker connecting the ligand and the scaffold. The polymers were tested for their ability to initiate AR and through which signaling pathways AR induction occurred. Our data demonstrate that mannose, fucose, and β-N-acetylglucosamine 10-mers and 100-mers initiate AR in a dose-dependent manner, and the 100-mers are more potent on a per monomer basis than the 10-mers. Although nearly equipotent in inducing the AR at the optimal

concentrations, the 100-mers bind to different receptors on the sperm and their AR activation kinetics are not identical. Similar to mouse ZP3, all 100-mer-activated AR are sensitive to guanine-binding regulatory proteins (G-proteins), protein tyrosine kinase, protein kinase A, protein kinase C and Ca^{2+} related antagonists. Thus, the chemotypes of synthetic glycopolymers mimic the physiologic AR-activation agents and provide evidence that occupation of one of at least three different receptor binding sites is sufficient to initiate the AR.

Table of Contents

List of Figures

Chapter 3

Chapter 4

List of Tables

List of Schemes

List of Appendix Contents

List of Abbreviations

AC	adenylate clyclase
Ac	acetyl
Acm	acetamidomethyl
ADAM	a disintegrin and metalloprotease
AMP	adenosine monophosphate
ATRP	atom transfer radical polymerization
Boc	t-butyloxycarbonyl
BSA	bovine serum albumin
cAMP	cyclic adenosine monophosphate
CatSper	sperm-specific Ca^{2+} channel
CB	cyclobutene
Cbz	benzyloxycarbonyl
CRISP1	cystein-rich secretory protein 1
Cys	cysteine
DAG	1,2-diacylglycerol
DBU	1, 8-diazabicyclo[5.4.0]undec-7-ene
ddI H_2O	distilled and deionized water
DIC	differential interference contrast
DIEA	N,N-diisopropylethylamine
DMAP	4-dimethylaminopyridine
DMF	N,N-dimethylformamide

DMSO	dimethyl sulfoxide
ECD	glutamic acid-cystein-aspartic acid
EGF	epidermal growth factor
Et_2O	diethyl ether
EtOAc	ethyl acetate
Fmoc	fluorenylmethoxycarbonyl
Fuc	fucose
Gal	galactose
Gal	galactose
GalNAc	D-N-acetylgalactosamine
GalT	β-1,4-galactosyltransferase
Glc	glucose
GlcNAc	D-N-acetylglucosamine
Glu, E	glutamic acid
Gly, G	glycine
GPC	gel permeation chromatography
h	hour
IP_3	1,4,5-inositol triphosphate
Man	mannose
Mn	number-average molecular weight
Mo	molybdenum
MS	mass spectormetry
Mw	weight-average molecular weight

N_2	nitrogen gas
NB	norbornene
NHC	N-heterocyclic carbene
NHS	N-hydroxysuccinimide
NMR	nuclear magnetic resonance
NSFG	national survey of family growth
PBS	phosphate-buffered saline
Pd/C	palladium on carbon
PDI	polydispersity index
PIP2	phosphatidylinositol 4,5-bisphosphate
PKA	protein kinase A
PLCβ1	phospholipase C β1
PLCγ	phospholipase C γ
PMA	phosphomolybdic acid
ppm	parts per million
RAFT	reversible addition-fragmentation chain transfer
ROMP	ring opening metathesis polymerization
rt	room temperature
Ru	ruthenium
sp56	sperm protein-56
tBu	*tert*-Butyl
THF	tetrahydrofuran
TLC	thin layer chromatography

Trt	trityl
UV	ultraviolet
WT	wild-type
ZP	zona pellucida

Chapter 1

Introduction

1. Gamete membrane interactions in mammalian fertilization
    1.1. Infertility problem
    1.2. Overview of Mammalian Fertilization
        1.2.1. Sperm Structure and capacitation
        1.2.2. Egg structure, cumulus oophorus and zona pellucida
        1.2.3. Sperm-egg binding
        1.2.4. Acrosome reaction
        1.2.5. Previous studies about acrosome reaction activators
        1.2.6. Proposed acrosome reaction mechanism
        1.2.7. Sperm-egg fusion

2. Specific aims
    2.1. Investigation of mouse sperm acrosome reaction with synthetic glycopolymers
    2.2. Investigation of synthetic methods to prepare fertilization probes

1. Gamete membrane interactions in mammalian fertilization

1.1. Infertility problem

Infertility is a disease of the reproductive system, which leads to the inability to conceive a child. While there is no universal definition of infertility, a couple is generally considered clinically infertile when pregnancy has not occurred after at least twelve months of regular sexual activity without the use of contraceptives (Evens 2004). Although it is difficult to collect accurate data for the incidence of global infertility, it is estimated that infertility affects 70 million couples worldwide, the majority of whom are from developing countries (Ombelet, Cooke et al. 2008). In America alone, the statistics from National Survey of Family Growth (NSFG) show about 7.3 million women are infertile. Infertility has become a public health issue and a major physiological and psychological problem to a growing proportion of the population.

Infertility has a wide range of causes stemming from three general sources: physiological dysfunctions, preventable causes, and unexplained issues (Evens 2004). Among those, known male infertility factors account for about 40% of the total major infertility causes (Kashir, Heindryckx et al. 2010). However, a large portion of the infertility causes are still unexplained. Current evidence suggests that 1 in 7 couples are involuntarily childless after a year of timed intercourse, and that 1 out of 5 of these couples will still have no answer to explain why they have difficulty conceiving, even after a panel of expensive and often, invasive, diagnostics tests (Boivin, Bunting et al. 2007). Though significant efforts have been made to study male/female reproductive systems and gamete interaction, there are a lot of unknown areas that need further

investigation (Evens 2004). Especially, there is a huge unmet need for non-invasive diagnostic tests that can help diagnose infertility upfront and guide treatment protocols down a more efficient path.

1.2. Overview of Mammalian Fertilization

Mammalian fertilization is a chain of sophisticated events, which starts with sperm binding to eggs, fusing with egg plasma membrane, and eventually the development of an embryo (**Figure 1-1**) (Chittaboina, Hodges et al. 2006). Before encountering eggs, sperm need to undergo capacitation, which changes sperm metabolism and motility by a series of biochemical modifications. Most importantly, capacitation appears to alter the sperm's membrane to prepare it for the acrosome reaction in the following step. With the hyperactivated motility and a surface hyaluronidase, capacitated sperm are capable of passing through cumulus cells to the extracellular layer of the egg, known as the zona pellucida (ZP). Sperm must undergo a cellular exocytosis named the acrosome reaction to penetrate the zona pellucida, and bind to and fuse with the egg plasma membrane. The egg rapidly undergoes a number of metabolic and physical changes called egg activation, and then cortical granules are released from the oocyte cortex via the perivitelline space, and change the zona pellucida structure to prevent the fusion of additional sperm that have penetrated the ZP. Meanwhile, free-swimming sperm are no longer able to bind to the ZP either. Following fusion of the fertilizing sperm with the oocyte, the sperm head is incorporated into the egg cytoplasm. Chromatin from both the sperm and egg are soon encapsulated in a nuclear membrane to form pronuclei, and subsequently a diploid organism. At

this point, the egg has been fertilized and becomes a zygote. There has been a longstanding interest in the basic biology of this process (Wassarman 1999), and most of these events are best illustrated in the mouse, although there is considerable information in other species including human.

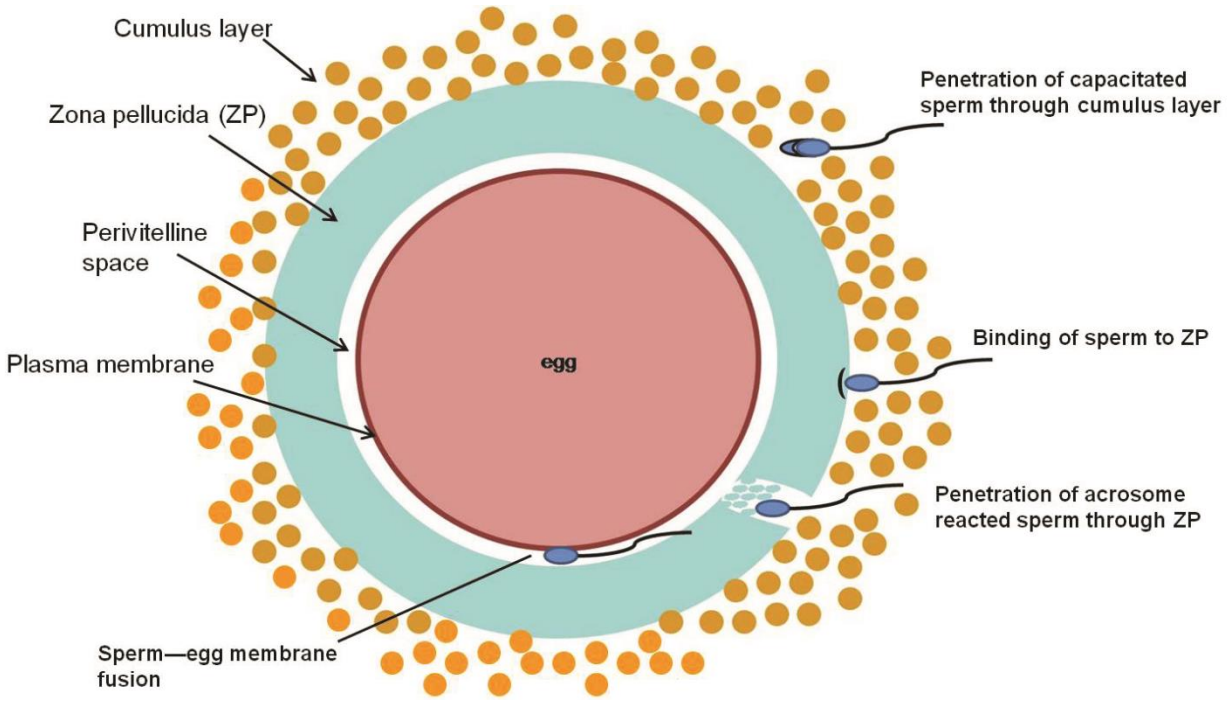

Figure 1-1. Overview of mammalian fertilization.

1.2.1. Sperm structure and capacitation

The role of sperm in fertilization is to activate egg metabolism and provide male pronucleus to the fertilized egg (Cheng, Le et al. 1994). The sperm is made up of two major parts: the flagellum (sperm tail) concerned with energy production and the initiation and maintenance of the motility; and the head containing all important DNAs and proteins for sperm-egg binding and

fusion (Borg, Wolski et al. 2010). Both of the two parts can be further subdivided into several cellular compartments shown in **Figure 1-2**.

Ejaculated mammalian sperm have to stay in the female genital tract for a certain time to gain the ability to fertilize the egg. They undergo several physiological and biochemical modifications collectively called capacitation (Wassarman 1999). These changes include membrane hyperpolarization, changes in membrane lipid composition, intracellular alkalinization, increased level of protein tyrosine phosphorylation, and increases in intracellular pH, calcium and cyclic adenosine monophosphate (cAMP) levels (Hernández-González, Sosnik et al. 2006). There are two major signaling events leading to capacitation: fast and slow (Ickowicz, Finkelstein et al. 2012). The fast event, which happens as soon as the sperm leave the epididymis, includes activation of the vigorous and asymmetric movement of the flagella and protein kinase A (PKA) activation mediated by the Ca^{2+} and HCO_3^- dependent soluble adenylyl cyclase. It has been suggested that Ca^{2+} is transported into the cell by the sperm-specific Ca^{2+} channel (CatSper) (Ren and Xia 2010) and HCO_3^- by the Na/ HCO_3^- co-transporter. The slow event includes changes in the pattern of movement (hyperactivation), which is marked by the removal of cholesterol from the membrane by serum albumin and the increase in its fluidity. Both events take place during the passage of sperm within the female reproductive tract.

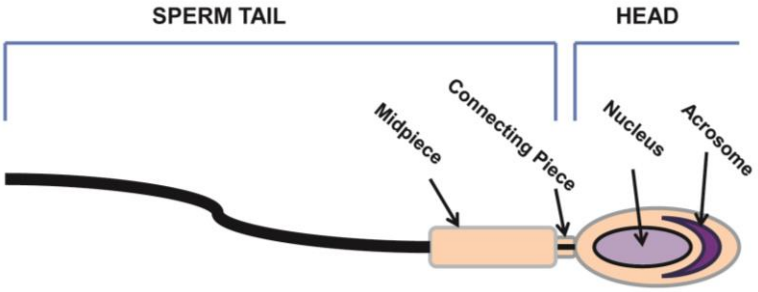

Figure 1-2. Sperm structure.

1.2.2. Egg structure, cumulus oophorus and zona pellucida

As illustrated in **Figure 1-1**, the mammalian egg is surrounded by two egg envelopes: the cumulus oophorus and the zona pellucida. There is also a narrow space called the perivitelline space between the zona pellucida and the egg plasma membrane. The cumulus oophorus is a cluster of cumulus cells and their extracellular matrix surround the egg both in the ovarian follicle and after ovulation. The cumulus matrix contains two functional components associated with fertilization. One is hyaluronic acid, a large polymer of disaccharides composed of D-glucuronic acid and D-N-acetylglucosamine (GlcNAc); the other is progesterone (Hong, Chiu et al. 2009). Both are synthesized by the cumulus cells. The fully developed cumulus oophorus supports egg maturation before ovulation, conducts the egg into the oviduct during ovulation, and participates in a complex mechanism controlling the access of sperm to the egg shortly after ovulation (Tanghe, Van Soom et al. 2002). It has been proposed that cumulus oophorus contributes to fertilization in several aspects: 1) to increase the number of fertilizing sperm around the egg; 2) to create a microenvironment to facilitate sperm capacitation, acrosome reaction and penetration; and 3) prevent unfavorable changes on the egg (Tanghe, Van Soom et al. 2002). However, the exact role of cumulus oophorus in mammalian fertilization still needs further investigation.

Another important extracellular layer surrounding the egg is called zona pellucida, a glycoprotein matrix that mediates the relative species specificity of sperm binding, secondary binding events, blocking polyspermy and protection of growing embryo from fertilization to implantation (Wassarman 1999). In mice, zona pellucida is composed of three glycoproteins

ZP1, ZP2 and ZP3 with molecular weights of 200, 120, and 83 kDa respectively. Each glycoprotein consists of a unique polypeptide that is heterogeneously glycosylated with both complex-type asparagine- (N-) and serine/threonine- (O-) linked oligosaccharides. All three ZPs interact with each other via non-covalent bonds to form a complex matrix where ZP2 and ZP3 assemble into long filaments while ZP1 crosslinks the filaments (**Figure 1-3**) (Wassarman, Jovine et al. 2001). The primary structure of ZP2- and ZP3-related glycoproteins from different species are relatively well conserved (~65% to 98% identity), whereas ZP1-related glycoproteins are less conserved (~40% identity) (Jovine, Darie et al. 2005). Previous experimental results suggest that ZP3 serves as a primary receptor for sperm and ZP2 serves as a secondary receptor (Florman and Wassarman 1985).

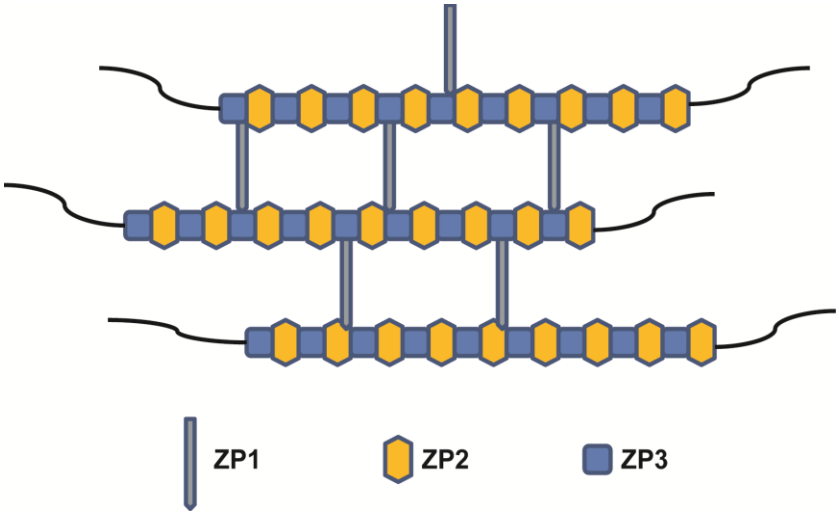

Figure 1-3. The structure of the zona pellucida.

1.2.3. Sperm-egg binding

The species-specific binding of sperm to eggs is the initial event in mammalian fertilization. Mounting evidence indicates that this interaction is mediated by functional ZP carbohydrates,

especially the O-linked carbohydrate moieties located near the carboxyl terminus of the ZP3 glycoprotein, and the lectin-like proteins on the sperm head. (Wassarman 2005, Nixon, Aitken et al. 2007) Several ZP3 terminal monosaccharide residues—*N*-acetylgalactosamine (GalNAc) (Nagdas, Araki et al. 1994), *N*-acetylglucosamine (GlcNAc) (Miller, Gong et al. 1993), mannose (Cornwell and Tulsiani 1991), galactose (Bleil and Wassarman 1988) and fucose (Oh, Ahn et al. 2012) have been proposed to be critical for sperm binding, and the addition of a fucose residue to the GlcNAc and galactose trisaccharides enhances sperm-egg binding affinity (Johnston, Wright et al. 1998). However, it is still difficult to define the exact function of these sugars due to the spatial heterogeneity of zona glycosides. For example, α-galactosyl and *N*-acetylgalactosaminyl residues only exist in the inner portions of the mature ZP, whereas *N*-acetylglucosamine, is dispersed throughout the whole zona (Shur, Rodeheffer et al. 2006). Moreover, recent genetic experiments have challenged the proposed roles of some glycan residues: Mice with genetically modified N- and O-glycans lacking terminal galactose and GlcNAc were still fertile, which suggested these two monosaccharides were unessential for fertilization (Williams, Xia et al. 2007). This result strongly supports the idea that the oligosaccharides on the ZP are far less important for sperm-egg interactions than previously believed. To the best of our knowledge, there are no genetically engineered mouse models to rule out the suggested role of mannose, GalNac, or fucose residue(s) in sperm-egg adhesion. An alternative interpretation could be that the remaining glycans on the ZP like mannose or GalNAc contribute to fertilization.

Like the uncertainty about carbohydrates, details about sperm surface proteins involved in this interaction are still unclear, although a number of mouse egg binding proteins have been proposed (**Table 1-1**). Earlier reports suggested that β-1,4-galactosyltransferase (GalT) on the sperm plasma membrane recognized and bound to N-acetylglucosaminyl residue(s) on the ZP3

(Miller, Macek et al. 1992). However, mice devoid of GalT were still fertile but with reduced fertility (Williams, Xia et al. 2007). Similarly, mice with an sp56 gene deletion exhibited no difference in fertility compared to wild-type mice (Muro, Buffone et al. 2012), although sp56 has been identified as another ZP3 receptor. Again, there could be additional factors mediating the interaction besides GalT-ZP3 and sp56-ZP3 binding pairs, or the ability of an antibody directed against a sperm protein to inhibit binding of sperm to eggs does not necessarily mean that the antigen is an authentic egg binding protein. Some recent studies (Bi, Hickox et al. 2003) also indicate that zonadhesin, together with sp56, could be secondary egg binding molecules and not involved in the primary sperm-egg adhesion. Moreover, capacitated sperm lipid rafts showed affinity for the ZP and a number of ZP binding molecules were indentified to be present in sperm lipid rafts (Khalil, Chakrabandhu et al. 2006). These results corroborate that sperm lipid rafts may be the platforms on the sperm surface for ZP interaction (Tanphaichitr, Carmona et al. 2007). There are four possibilities to account for the confusing state of this area of research (Wassarman 1999): (1) involvement of different sperm proteins as egg binding proteins in different mammalian species; (2) participation of multiple sperm proteins as egg binding proteins, acting either individually or as multiprotein complexes, in a particular mammalian species; (3) participation of multiple sperm proteins as egg binding proteins, each with different affinities particular mammalian species; and (4) some of the *in vitro* assays used to assess egg binding proteins function may not mirror *in vivo* events. Clearly, more research on the mechanism(s) underlying gamete interaction is needed.

Table 1-1. Major proposed mouse egg binding proteins (Wassarman 1999, Tanphaichitr, Carmona et al. 2007)

Candidates	**Comments**
Glycoenzymes	
β-1,4-galactosyltransferase (Lu and Shur 1997)	Binds to GlcNAc residues on mZP3 specifically; located on the plasma membrane overlying the acrosome region
α-D-mannosidase (Cornwall, Tulsiani et al. 1991)	Binds to mannose residues on ZP; located on the plasma membrane overlying the acrosome region
Lectins and glycosaminoglycan binding proteins	
Sperm protein-56 (sp56) (Cheng, Le et al. 1994, Buffone, Zhuang et al. 2008, Wassarman 2009)	Binds to mZP3 oligosaccharides; contains sushi and unique domains; located on acrosome matrix and sperm head plasma membrane
Zonadhesin (Hardy and Garbers 1995)	Binds to the egg zona pellucida; contains multiple types of domains, associated with the luminal aspect of the outer acrosomal membrane and adjacent acrosomal matrix
Others	
SED-1(Ensslin and Shur 2003)	Binds to both ZP2 and ZP3, required for initial adhesion between sperm and egg, an EGF repeat and discoidin domain protein on sperm head plasma membrane

Despite the wide acceptance of the carbohydrate-dependent gamete binding model, a small number of studies have implicated the carboxyl terminal of mouse ZP3 polypeptide backbone as playing a vital role in sperm receptor function (Li, Cao et al. 2007). The authors generated ZP3 polypeptide backbone from E. coli, which is deficient in post translational modification system and an ideal producer of large amount of recombinant protein free of oligosaccharide chains.

And they found polypeptide backbone derived from carboxyl terminal of mouse ZP3 inhibits sperm-ZP binding.

Notably, recent data from genetically modified mice have also drawn attention to the fact that the three-dimensional structure of the zona matrix, rather than a single protein or carbohydrate, is important in mediating sperm binding (Rankin, Coleman et al. 2003). Jurrien Dean and his co-workers developed a ZP2 cleavage model and demonstrated that gamete recognition in mice depends on the cleavage status of ZP2 (Gahlay, Gauthier et al. 2010). The role of carbohydrate recognition in this paradigm is thought to be minimal. This model and the carbohydrate-dependent model were tested by replacing endogenous ZP2 with a mutant ZP2 that cannot be cleaved ($ZP2^{Mut}$) or with ZP3 lacking implicated O-linked glycans ($ZP3^{Mut}$). The results were not consistent with the carbohydrate-dependent model: acrosome reacted sperm instead of acrosome intact ones bond to $ZP2^{Mut}$ eggs, and $ZP3^{Mut}$ mice were fertile. However, the conclusion is controversial and the investigators of the above studies did not address three important points (Visconti and Florman 2010, Tulsiani and Abou-Haila 2012). First, what are the structural similarities or dissimilarities between the endogenous and the mutant ZP2? Second, has the replacement of endogenous ZP2 glycoprotein with mutant ZP2 protein altered the three-dimensional structure of the egg coat? Finally, what are other possible outcomes if all or some of the other carbohydrate residues implicated in sperm-egg recognition are removed from the ZP3?

A domain specific model (Clark 2011) has been proposed to reconcile the contradictory situation. This model suggests that murine gamete binding involves both protein-carbohydrate and protein-protein interactions, and envisions a mouse sperm protein (or complex of proteins) that interacts with the glycans and/or the protein backbone of mZP3 depending on its glycosylation state. It is proposed that, due to stochastic variation in glycosylation, some mouse

ZP3 molecules carry glycans that sterically hinder access to peptide sequences. For those ZP3 molecules, binding is proposed to be solely via lectin-like interactions. In other ZP3 molecules, glycosylation sites will be unoccupied, and the peptide sequences that mediate binding will be accessible. For those mZP3 molecules, protein-protein interactions may predominate. This model is attractive because of the redundancy it offers and the evidence obtained from several laboratories that support it (Clark and Dell 2006). Also, an advantage of this dual adhesion system is that sperm would have enhanced opportunities to bind to the oocyte (Clark 2011). However, continued investigation is required to unveil the molecular basis of the murine sperm-egg binding interaction and eventually lead to a level of understanding that will be useful for practical application in many mammals including humans.

1.2.4. Acrosome reaction

Binding to the ZP3 is relatively easy. Next sperm faces the big challenge of penetrating the zona pellucida to get to the oocyte. Nature's response to this challenge is the acrosome, a very important exocytotic organelle located around the anterior part of the sperm's head. Structurally, the acrosome consists of two compartments: a vesicle filled with soluble components and acrosomal matrix, and the acrosomal membrane surrounding the vesicle. Also, the acrosomal membrane can be further delineated into the outer acrosomal membrane overlying the acrosome, and the inner acrosomal membrane associated with the nuclear membrane (Wassarman 1999). When the acrosome reaction occurs (**Figure 1-4**), the contents of the vesicle—several hydrolases and other proteins—are exposed and the acrosomal constituents are released at different rates,

which provide the sperm with an enzymatic drill to get through the zona pellucida (Kim and Gerton 2003, Wassarman, Jovine et al. 2004). The acrosome reaction plays an essential role in fertilization and only acrosome reacted sperm can participate in the following fertilization steps. During the past 30 years, considerable progress toward delineating the molecular basis of the sperm acrosome reaction has been made. However, four essential questions about this step—where and when does the AR start, what activates the AR and how, still remain to be answered. Unveiling the mechanism of this crucial and complicated stage of fertilization will enable us to better understand this essential process and deal with the problem of infertility and world population control.

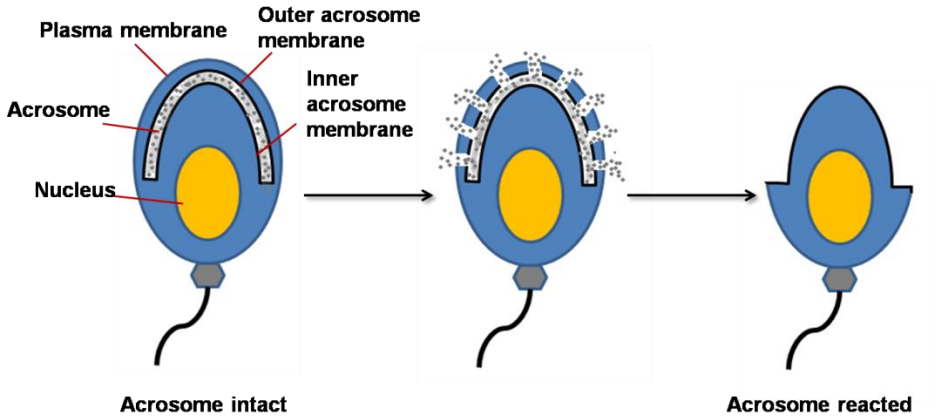

Figure 1-4. Acrosome structure and acrosome reaction.

1.2.5. Previous studies about AR activator

ZP3

Solubilized mouse ZP can stimulate sperm to complete the AR *in vitro* (Florman and Storey 1982), and ZP3 is widely accepted as the active agent in the solubilized ZP and the most important natural AR agonist (Tulsiani 2012). Classical studies done in a mouse model, using native purified protein, established ZP3 as the putative primary sperm receptor (Bleil and Wassarman 1983). These observations were subsequently confirmed by using recombinant mouse ZP3 (Beebe, Leyton et al. 1992). In humans, studies employing purified native ZP3 as well as the recombinant ZP3, expressed either using baculovirus or mammalian expression systems, also exhibited dose-dependent induction of the acrosome reaction (van Duin, Polman et al. 1994, Chakravarty, Suraj et al. 2005, Chakravarty, Kadunganattil et al. 2008).

Chemically deglycosylated mouse ZP3 failed to induce the AR, suggesting that glycosylation of ZP3 is critical for its functional activity (Florman and Wassarman 1985). The saccharides must be presented in a multivalent structure in order to induce AR (Wassarman 2005), but the precise oligosaccharides and the structure of their three-dimensional display are still not definitively identified. Early studies relied on glycosidase treatments of isolated egg ZP3 protein or fragments (Florman and Wassarman 1985, Litscher and Wassarman 1996, Liu, Litscher et al. 1997) followed by testing for sperm binding or inhibition of sperm binding to zona-intact eggs or isolated/recombinant ZP3 protein and identified a large number of oligosaccharide candidates (Tulsiani, Yoshida-Komiya et al. 1997). However, these experiments did not distinguish between ZP adhesion molecules and ZP receptors that mediate the AR.

Recent studies (Loeser and Tulsiani 1999) examined the properties of several neoglycoproteins that are bovine serum albumin (BSA) conjugates with an average of 8 copies of the glycan of interest attached through a 3- or 14- atom spacer. They concluded that mannose-BSA, GlcNAc-BSA, and GalNAc-BSA could mimic ZP3 to initiate AR while glucose-BSA or galactose-BSA had no effect. Moreover, free sugars failed to block neoglycoprotein-induced AR which suggests a multivalent backbone is necessary for AR activation (Chapman, Kessopoulou et al. 1998). Later, Hanna et al (Hanna, Kerr et al. 2004) found that the sperm binding sites Lewis X (Galβ4[Fucα3]GlcNAc) and Lewis A (Galβ3[Fucα4]GlcNAc) when conjugated to BSA could mimic ZP3 to initiate AR, and Lewis X-BSA was more potent than Lewis A-BSA. This finding indicates that fucose may be another glycan ligand involved in AR initiation in addition to the three monosaccharides identified by Loeser et al. However, the GlcNAc-BSA tested in Hanna's work showed no AR activation effect, which disagreed with Loeser's results; and there has been no direct AR activation study on fucosyl bioconjugates so far.

Other proposed AR activators

It is known that a number of other physiological or non-physiological agonists can also activate the AR (Abou-haila and Tulsiani 2009). The physiological agonists are substances that sperm cells will encounter during *in vivo* fertilization. Besides ZP3, progesterone, a hormone produced during ovulation, has been suggested to activate the AR by interacting with the sperm plasma membrane in a receptor-mediated manner (Roldan, Murase et al. 1994, Blackmore 1998). Prostaglandins, sterol sulphate, and glycosamino-glycans present in the follicular fluid and

cumulus cell secretions have also been reported to induce the acrosome reaction (Tulsiani, Abou-Haila et al. 1998, Hong, Chiu et al. 2009). Other physiological agonists include epididymal growth factor, atriopeptin, platelet activating factor and ATP (Abou-haila and Tulsiani 2009). However, no receptors on the surface of capacitated sperm that are recognized by these agonists *in vitro* or *in vivo* have been identified. Thus, their roles in inducing the acrosome reaction remain unclear.

Non-physiological agonists include calcium ionophore, neoglycoproteins, methyl-β-cyclodextrin, BSA, and many more. The calcium ionophore triggers the acrosome reaction by opening the Ca^{2+} channels that allow an influx of calcium ions (Blackmore 1998). Several synthetic neoglycoproteins containing mannose, N-acelylglucosamine or N-acetylgalactosamine covalently conjugated to BSA, described in the last section, have been demonstrated to mimic ZP3 and induce the acrosome reaction in the mouse (Loeser and Tulsiani 1999). Methyl-β-cyclodextrin and BSA both activate sperm AR by mediating cholesterol influx, but methyl-β-cyclodextrin is more effective (Takeo, Hoshii et al. 2008).

1.2.6. Proposed AR mechanisms

Mechanism of ZP3 activated AR

Many researchers believe that ZP3 with multiple sperm-binding carbohydrate residues stimulates AR by cross-linking or aggregating receptors on the sperm plasma membrane (Bleil

and Wassarman 1983, Wassarman, Jovine et al. 2004). At least two different ZP3 receptors have been proposed to be in the sperm plasma membrane (Breitbart and Spungin 1997): a pertussis toxin sensitive G_i protein-coupled receptor, and a putative tyrosine kinase receptor (**Figure 1-5**). Cholera toxin-sensitive Gs proteins have not been found in sperm (Hilderbrandt, Codina et al. 1985). Upon ZP binding, Adenylate cyclase (AC) can be stimulated, resulting in elevation of cAMP and protein kinase A (PKA) activation. G_i protein was found to regulate AC in somatic cells, but how it regulates AC in the sperm hasn't been determined (Leclerc and Kopf 1995). The activated PKA will phosphorylate and trigger downstream proteins, which will further trigger the fusion of sperm plasma membrane and the outer acrosomal membrane. G_i protein coupled phospholipase C β1 ($PLC_{\beta1}$) and tyrosine kinase coupled phospholipase C γ (PLC_{γ}) can hydrolyse phosphatidylinositol 4,5-bisphosphate (PIP_2) in the membrane, leading to the production of 1,4,5-inositol triphosphate (IP_3) and 1,2-diacylglycerol (DAG). DAG mediates PKC translocation to the plasma membrane and its activation, whereas IP_3 mediates calcium entry into the sperm cytosol from intracellular stores. The G_i protein or tyrosine kinase can also activate Ca^{2+} channels and a Na^+/H^+ exchanger, the latter one will lead to alkalinization of the cytosol. The increase in Ca^{2+} concentration and pH will both result in membrane fusion and acrosomal exocytosis. Although considerable progress in the mechanism of ZP activated-AR has been made, the real signaling pathways leading to acrosome reaction are not completely understood (Gupta and Bhandari 2011, Ickowicz, Finkelstein et al. 2012).

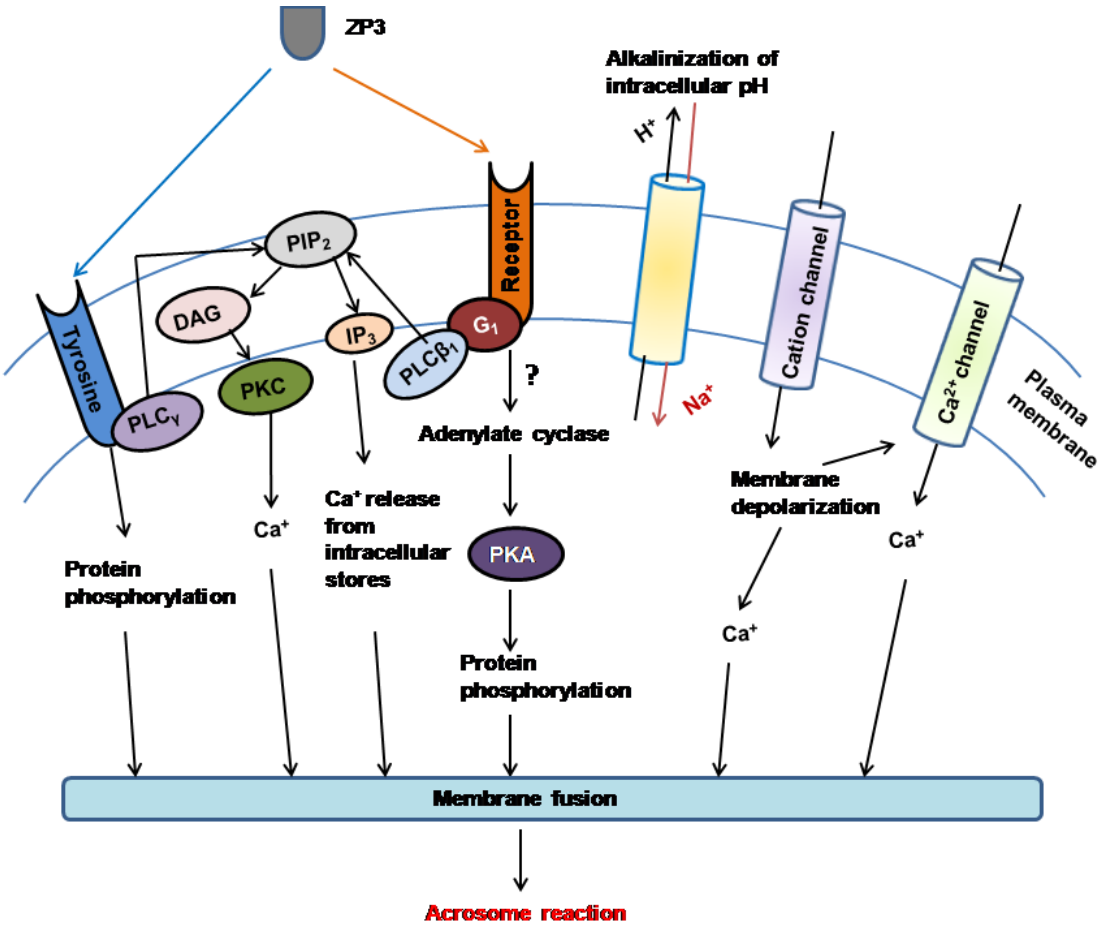

Figure 1-5. Proposed signaling pathways involved in ZP3-activated AR.

Other mechanisms

Recently, some researchers have challenged the concept of ZP as the AR primary activator and the proposed mechanism of AR activation. A model through which sperm induce acrosome exocytosis by mechanosensory signal transduction was reported (Baibakov, Gauthier et al. 2007). The authors illustrated that capacitated, motile and acrosome-intact sperm approach and bind to the zona pellucida. This binding (or the limiting size of the matrix interstices)

immobilizes the sperm plasma membrane, inhibiting further progression of the sperm. However, the continued forward motility of the sperm transduces a mechanosensory signal that leads to increased intracellular Ca^{2+} and induction of the acrosome reaction. The residual acrosomal shroud is left behind bound to the surface of the zona pellucida matrix, and only acrosome-reacted sperm enter into the perivitelline space (**Figure 1-6**). Those researchers argued that ZP3 cannot be considered the sole innate substance that induces the physiological AR (Yanagimachi 2011). These results indicate that redundant mechanisms for sperm binding and the induction of the acrosome reaction could exist. However, it is difficult to imagine how mechanical signals can be transmitted without molecular binding interactions between sperm and egg surface, and some concerns about the experiment methods have also been raised by other researchers (Tulsiani 2012).

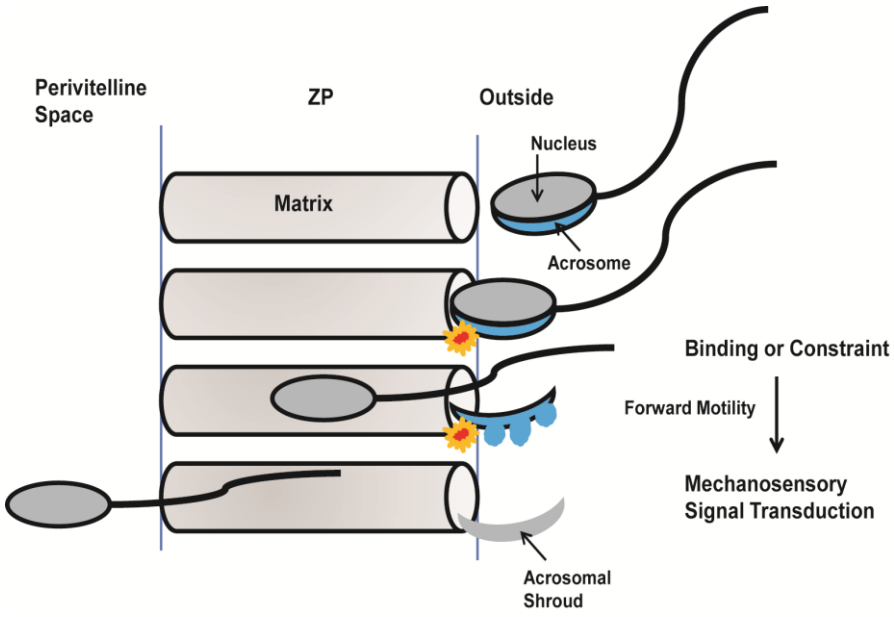

Figure 1-6. Model of mechanosensory induction of sperm acrosome reaction.

It has also been suggested that most fertilizing sperm begin acrosomal exocytosis before binding to ZP through molecular interactions between sperm and female reproductive tract (Jin, Fujiwara et al. 2011). This suggestion draws attention back to the AR inducer debate. However, the precise functional compounds involved and the mechanism under this reaction still have not been worked out. It appears that there are multiple interactions that lead to AR, most likely involving carbohydrates. To what extent signaling is initiated through a single type of receptor-ligand interaction versus multiple types of interactions is poorly understood. A major challenge in the study of AR mechanism is to develop a good AR activation model that fits as much of the data as possible. By now, the mechanism underlying sperm-egg interaction remains an unresolved issue.

1.2.7. Sperm-egg fusion

Acrosome-reacted sperm which traverse the zona pellucida into the perivitelline space will adhere to and fuse with the egg plasma membrane. Several sperm surface proteins fertilin, cyritestin, cystein-rich secretory protein 1 (CRISP1) and Izumo have been identified to be involved in this process (Wolfsberg and White 1996). Fertilin is composed of two integral membrane proteins, fertilinα and fertilinβ. Fertilinα, fertilinβ and cyritestin are members of the ADAM (A disintegrin And Metalloprotease) family and are also called ADAM1 (fertilinα), ADAM2 (fertilinβ) and ADAM3 (cyritestin) respectively (Wolfsberg, Straight et al. 1995). Fertilinβ and cyritestin are located in the equatorial region of the sperm head, and during sperm maturation, their disintegrin domains are exposed on the sperm head. ADAM proteins have a

specific domain structure: a signal sequence, prodomain, metalloprotease domain, disintegrin domain, cysteine-rich domain, an EGF (epidermal growth factor) like repeat, a transmembrane domain and a cytoplasmic tail. The disintegrin domains have a highly conserved peptide sequence, glutamic acid-cysteine-aspartic acid (ECD), which has been reported as the minimal recognition element necessary for the binding to the egg plasma membrane (Yuan, Primakoff et al. 1997).

Adhesion and inhibition studies suggested that fertilin mediates sperm adhesion via $\alpha_6\beta_1$ integrin on the egg plasma membrane, which was also identified as the ECD binding partner on the egg (Chen and Sampson 1999, Zhu, Bansal et al. 2000). Previous Sampson group members have determined that norbornene based polymers displaying multiple ECD peptides showed very high inhibition of sperm-egg plasma membrane binding and fusion, and that the inhibition was mediated through a β_1 integrin receptor on the egg surface (Baessler, Lee et al. 2006, Baessler, Lee et al. 2009). Integrin $\alpha_9\beta_1$ also appears to be a presumable binding partner (Eto, Huet et al. 2002). However, several experiments including knockout experiments implicate that the integrin adhesion step is non-essential (Baessler, Lee et al. 2009, Vjugina, Zhu et al. 2009).

2. Specific aims

2.1. Investigation of mouse sperm acrosome reaction with synthetic glycopolymers

As infertility becomes a rising global issue, it is necessary to develop new strategies for the diagnosis as well as the treatment of infertility in the world. Advances in the understanding of fertilization will provide a valuable model system for the study of sperm-egg interaction and insight into early development. This research focused on the sperm acrosome reaction because sperm dysfunction is a major cause of male infertility and the acrosome reaction plays an essential role in mammalian fertilization. Controversy about the mechanism of AR calls for a modified strategy to elucidate the molecular players in this complicated process. We hypothesized that synthetic glycopolymers would provide further insights into the molecular complexity of sperm AR activation. The length, substitution and ligand density of glycopolymers can be easily controlled. Thus, we applied neoglycopolymers prepared by ring-opening metathesis polymerization (ROMP) to investigate the AR. We further examined the glycopolymer-activated AR in the absence and presence of established pharmacological agents known to prevent the AR by blocking specific signaling pathways.

2.2. Investigation of synthetic methods to prepare fertilization probes

ROMP is widely used to prepare polymers with interesting properties and biological activities. Ruthenium-catalyzed ROMP has been extensively utilized to investigate the mechanism of sperm-egg interaction in the Sampson laboratory. Previously, norbornene-based polymers with a short peptide sequence E(OtBu)C(Trt)D(OtBu) [NB-E(OtBu)C(Trt)D(OtBu) 100-mer] conjugate showed better inhibition properties than the corresponding tripeptide monomer or other shorter norbornene polymers [NB-E(OtBu)C(Trt)D(OtBu) 10-mer]. These studies indicate that NB-E(OtBu)C(Trt)D(OtBu) 100-mer has a specific interaction with the egg plasma membrane receptors. However, due to the three chiral centers in a unit of norbornene, polymers derived from 5- and 6-substituted norbornene monomers have a large number of stereoisomers depending on the length of the polymer. Therefore, it is very important to prepare more homogeneous polymers which have not only reduced number of stereoisomers, but low polydispersities, because those polymers may enable more predictable experimental design and provide clearer experimental information. In this research, 1-substituted cyclobutene was chosen for the synthesis of a stereoregular polymer because it has a structure which is achiral, highly strained and sterically hindered. Thus, CB-ECD polymers in different length were designed to compare the ROMP characteristics of cyclobutyl polymers with norbornyl polymers.

Chapter 2

Multivalent interactions and linear scaffold polymerization

1. Multivalent interactions
    1.1 Multivalency
    1.2. Synthetic multivalent ligands
    1.3. Mechanisms of multivalent interactions

2. Linear scaffold polymerization
    2.1. Ring opening metathesis polymerization (ROMP)
        2.1.1. ROMP catalysts
        2.1.2. Other ROMP conditions
    2.2. Other polymerization methods

3. Norbornene and cyclobutene derived polymers as Fertilinβ mimics

4. Glycopolymer probes for the investigation of the sperm AR mechanism

1. Multivalent interactions

1.1 Multivalency

Multivalency is defined as the interaction between multiple copies of receptors and ligands (**Figure 2-1**), and it is involved in many cell surface protein-protein and protein-carbohydrate interactions (Kiessling, Gestwicki et al. 2000). Multivalency confers several characteristics on a system that are not present in monovalent interactions, for example, more enhanced binding avidity and specificity, larger surface contact between biological surfaces, and more efficient communication (Mammen, Choi et al. 1998). The strength of multivalent ligand-receptor binding is termed 'avidity' whereas a general term for that of monovalent interaction is affinity. The valency of a single multivalent conjugate is defined as the number of binding copies present. In most cases, there is a strong link between valency and binding avidity (Jayaraman 2009).

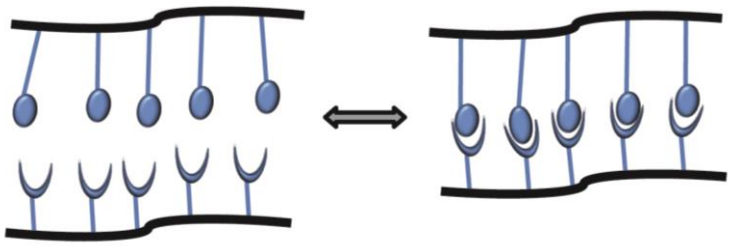

Figure 2-1. Multivalent interaction.

Understanding cell surface ligand-receptor interactions is crucial to grasp a cell's activity in its entirety. Through the elucidation of this interaction, the receptor topology on a cell surface required to initiate or block cellular signaling may be characterized. These types of investigations

can further lead to new strategies for the design of pharmaceutical agents, the practical application of biosensing pathogens and toxins, drug delivery to specific cell types, and tissue engineering (Mammen, Choi et al. 1998, Kiessling, Gestwicki et al. 2000, Bertozzi, Kiessling et al. 2001).

1.2. Synthetic multivalent ligands

Synthetic multivalent ligands have been considered as alternative structures to natural compounds. Their design, which is simple and flexible, requires a multivalent scaffold, a minimal ligand, and a spacer to link the ligand to the scaffold. This concept provides an effective strategy in designing compounds that can modulate the functions of many diverse macromolecular targets, and can often be more easily achieved by chemical methods than the heterogeneous and often too scarce natural examples. Moreover, flexible modification, for instance, variation of linker lengths and ligand valencies, can be made for the preparation of the conjugates, and the addition of functional groups like biolabels are facilitated (Lindhorst 2002). Typical constructs for synthetic multivalent ligands include liposomes, dendrimers, self assembled monolayers (SAM) and linear polymers (**Figure 2-2**).

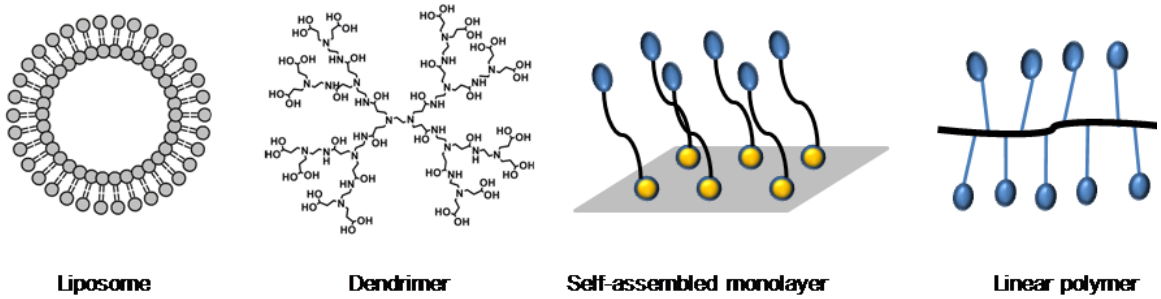

Figure 2-2. Multivalent ligands

Liposomes can accommodate multivalent displays on a spherical surface and represent an ideal mimic of the cell surface membrane. The embedded ligands in the liposome can interact with their targets in a fashion similar to that occurs on an actual cell surface (Crommelin and Storm 2003). Due to their biocompatibility and huge capacities as specific molecule carriers, liposomes are widely used in the biomedical area (Torchilin 2006). However, extra cross-linking method is required to form stable liposomes and it is still challenging to formulate with quality control.

Dendrimers, composed of a core structure that has repetitive branching units, are also attractive scaffolds for multivalent display of natural ligands (Myung, Gajjar et al. 2011). They have several advantages including precise nanometer size, high functionality and easy degradation (Joshi and Grinstaff 2008). Dendrimers are usually prepared by repeating a given set of reactions using either divergent or convergent strategies (Lee, Kim et al. 2006). Many reports showed that dendrimers incorporated with amino acid or carbohydrate ligands mediate multivalent interactions in several biological processes (van Baal, Malda et al. 2005, Lee, Kim et al. 2006).

A self-assembled monolayer is a layer of molecular thickness formed by self-organization of molecules in an ordered manner by chemisorption on a solid surface (Senaratne, Andruzzi et al. 2005). The monolayer is comprised of three significant parts: a surface-active head group that binds strongly to a substrate, an alkyl chain giving stability to the assembly by van der Waals interactions and terminal functional groups. Two of the most widely studied SAMs are gold-alkylthiolate monolayers and alkylsilane monolayers. SAMs offer a unique combination of physical properties that allow fundamental studies of biological recognition such as

carbohydrate-protein interactions, and interactions between DNA bases (Arya, Solanki et al. 2009).

With engineered density and spacing, linear polymers are also of great interest in the study of multivalent interactions. Many groups have reported a wide range of carbohydrate or peptide-substituted polymers that were applied for inhibition of selectin binding (Manning, Strong et al. 1997), biorecognition (David, Kopečková et al. 2001), and modulating bacterial chemotactic response (Gestwicki, Strong et al. 2001). Various synthetic techniques have been developed (Miura 2012) to prepare linear polymers with well-defined chain length. The commonly used techniques include atom-transfer radical polymerization (ATRP), reversible addition–fragmentation chain transfer polymerization (RAFT), nitroxide-mediated polymerization (NMP), and ring opening metathesis polymerization (ROMP). These techniques are relatively more tolerant to different reaction solvents and functional monomers, and are successful in controlling the chain length.

1.3. Mechanisms of multivalent interactions

In contrast to monovalent ligands, multivalent ligands can interact with receptors through many different mechanisms. These mechanisms include the chelate effect, receptor clustering subsite binding, statistical rebinding, and steric stabilization (**Figure 2-3**) (Gestwicki, Cairo et al. 2002). In the chelate effect model (**Figure 2-3a**), the translational entropy cost is paid with the first receptor–ligand contact; subsequent binding interactions proceed without additional translational entropy penalties, although there is a conformational entropy cost. In this case, the

off-rate of the multivalent ligand and multiple receptors is decreased and the avidity can be enhanced. Multivalent ligand binding can also alter the proximity or orientation of the clustered receptors (**Figure 2-3b**), which can affect the signaling functions of the receptors. Some proteins possess secondary binding site in addition to the primary binding site, and these can be occupied by a multivalent ligand (**Figure 2-3c**). In addition, multivalent ligands can display a higher local concentration of binding moieties. Therefore, rebinding of the multivalent ligand is favored and the avidity is improved even if only one receptor is engaged (**Figure 2-3d**). Another effect of multivalent ligand binding that is relevant for inhibition of cell-surface interactions is steric stabilization (**Figure 2-3e**). In this mechanism, the size and hydration shell of the multivalent ligands prevent the binding of the cell surface with an opposing compound or cell. Together, these different modes of interaction contribute to the higher potency of multivalent ligands.

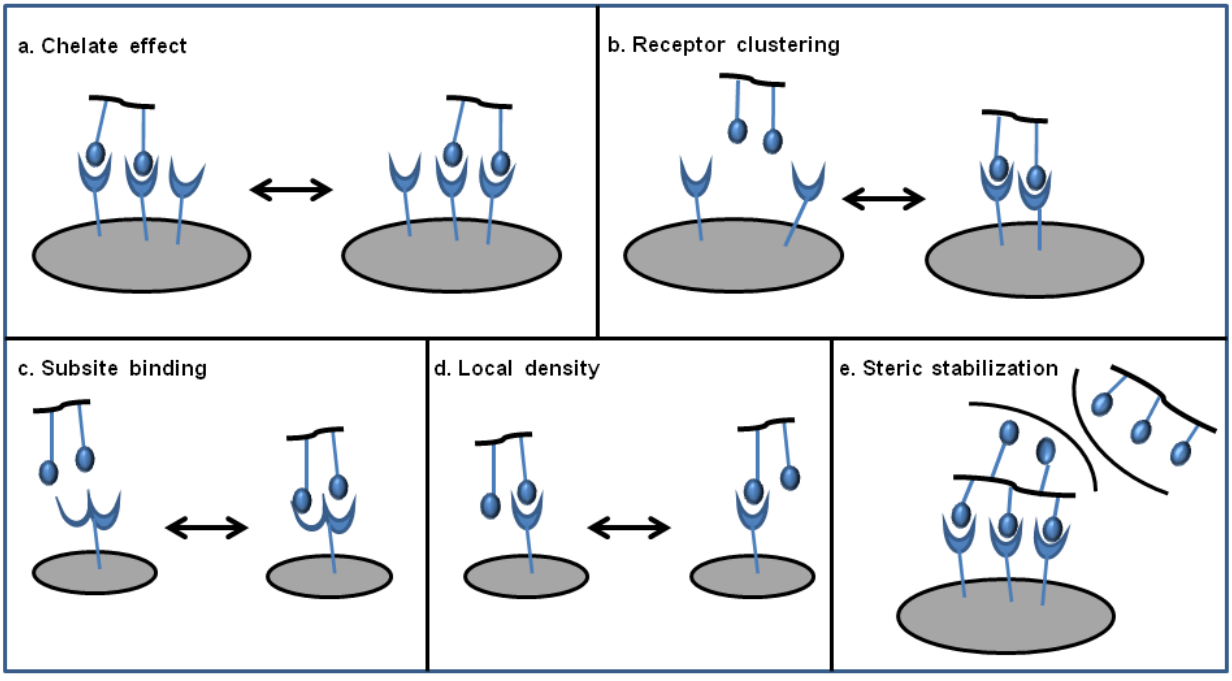

Figure 2-3. Mechanism of multivalent ligand binding

The various binding mechanisms involved in multivalent interaction result from the architecture of multivalent ligands. Though multivalent ligands can potentially access multiple binding mechanisms, one or some of those mechanisms may be preferred by a multivalent ligand. Varying the whole scaffold or altering a single structural feature of a multivalent ligand—such as valency or density of binding epitopes, can change its effect. Thus, a rational decision about all the parameters involved is critical for the successful design of a multivalent ligand.

2. Linear scaffold polymerization

2.1. Ring opening metathesis polymerization (ROMP)

Organic polymers with well-defined lengths and molecular weights can be prepared if the rate of chain initiation is much larger than the rate of chain propagation (Szwarc 1970). In this "living" system, the polymer chains grow at a more constant rate than those in traditional chain polymerization, and the polymer molecular weights are narrowly polydispersed (polydispersity index PDI <1.5) (Darling, Davis et al. 2000). Ring opening metathesis polymerization (ROMP), one of the living polymerization methods, has emerged as a particularly powerful method for synthesizing polymers with tunable sizes, shapes, and functions, as well as an excellent tool for structure-function studies in various biological systems (Bielawski and Grubbs 2007).

ROMP is a chain growth polymerization in which cyclic olefins are elongated to a polymer. The mechanism of ROMP is depicted in **Figure 2-4**. First, the reaction is initiated when the cyclic olefin monomer forms a metal alkylidene complex with a transition metal catalyst. After formation of the metal-carbene complex, subsequent [2+2] cycloaddition generates a highly strained metallacyclobutane intermediate. The ring in the intermediate opens to give a new metal alkylidene. The chain growth process proceeds during the propagation stage until all monomer is consumed. Then the reaction can be terminated by adding a quenching reagent. In ROMP, polymers with exact predetermined length and density can be prepared by varying the monomer/catalyst ratio.

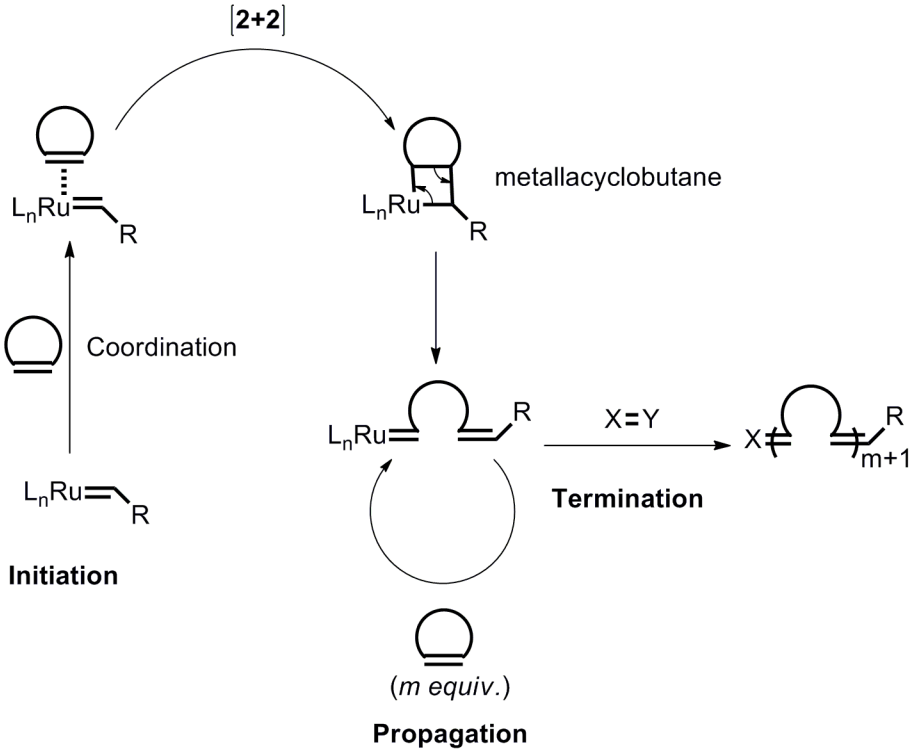

Figure 2-4. Mechanism of ROMP

2.1.1. ROMP catalysts

Early catalytic systems were extremely air and moisture sensitive heterogeneous mixtures. Because the catalyst plays a pivotal role in living polymerizations, an enormous number of studies have been pursued to develop well-defined and functional group tolerant catalysts. Homogenous catalytic systems mediating living ROMP reactions have been reported, such as titanium-based Tebbe reagents (Tebbe, Parshall et al. 1979), tantalum complexes (Schrock and Fellmann 1978), tungsten-based catalysts (Katz and Han 1982, Kress and Osborn 1983), molybdenum-based alkylidenes (Schrock, Murdzek et al. 1990), and ruthenium-based complex (Maughon and Grubbs 1997).

Versatile and robust ruthenium-based catalytic systems have been widely adopted for ROMP because of their exceptional functional group tolerances compared to other transition metal-based catalysts. In addition, the ruthenium-based catalysts are also relatively more stable to air and moisture, and allow the synthesis of polymers with narrowly defined molecular weights. The Grubbs catalysts (**Figure 2-5**) are commonly used ruthenium-based catalysts and in particular, the 3rd Grubbs catalyst is highly reactive with broad functional group tolerance.

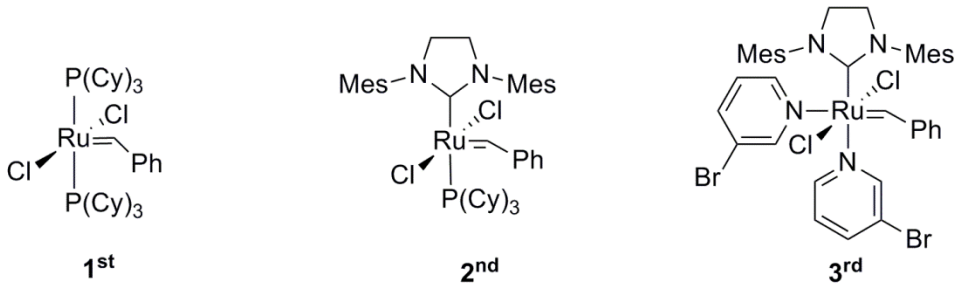

Figure 2-5. Grubbs ruthenium catalysts.

2.1.2. Other ROMP conditions

The driving force behind the ROMP of cyclic olefins is the relief of strain energy, encompassed by the enthalpic term, ΔH, in the equation $\Delta G = \Delta H - T\Delta S$. The minimal strain energy necessary for successful ROMP is about 5 kcal/mol (Hejl, Scherman et al. 2005). The commonly used cyclic olefin monomers for ROMP such as norbornene, cyclobutene, and cyclopentene (**Figure 2-6**) all possess much greater ring strain (Schleyer, Williams et al. 1970). With very low ring strain, cyclic olefins like cyclohexene have very little enthalpic driving force to be polymerized with ROMP.

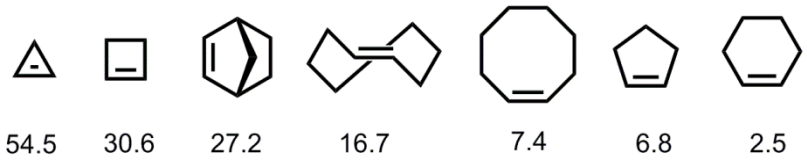

Figure 2-6. Ring strains of common cyclic olefins

Accordingly, the temperature and concentration at which the ROMP is conducted has a strong influence over the outcome of the reaction, because they are intimately associated with the thermodynamics of ROMP (Hejl, Scherman et al. 2005). For every cyclic olefin monomer, there exists a critical monomer concentration below which no polymerization will occur at a given temperature. Performing the ROMP at low temperatures can mitigate the entropic loss inherent to all polymerizations and drive the reaction to high molecular weight polymer. Lower reaction temperatures, however, require catalysts with higher activities. Generally, the most favorable conditions for a successful ROMP reaction are to use the highest monomer concentration at the lowest temperature possible (Bielawski and Grubbs 2007).

Addition of substituents to the monomer can also affect the ROMP and the characteristics of the polymer. Several research groups have demonstrated that introduction of some substituents can increase the rate of reaction (Mutch, Leconte et al. 1998) or precisely control polymer stereo- and regiochemistry (Lee, Parker et al. 2006, Kobayashi, Pitet et al. 2011). Especially in the latter study, cyclobutene carboxylic acid derivatives underwent ruthenium catalyzed ROMP with high regiochemical and geometric preferences (Lee, Parker et al. 2006). The ROMP of 3-substituted *cis*-cyclooctenes also proceeded in a regio- and stereoselective manner to afford polyoctenamers, and the regioselectivity was partially due to the steric interactions between the substituent and the NHC-ligand in the 2rd Grubbs catalyst (Kobayashi, Pitet et al. 2011). Even different rate limiting steps were found for the different substituent sizes (Martinez, Mir ó et al. 2012). However, a proper design of the monomer is necessary as some substituents are deleterious to the catalysts or even decrease the reactivity of the monomers (Mutch, Leconte et al. 1998).

Lastly, the choice of solvent and the addition of some special agents can be used to tune the polymer molecular weights and polydispersity. Solvent plays a vital role in the formation of the ruthenium-carbene complex. Al Samak et al. reported that altering the solvent in metal salt-type catalytic systems can drastically change the microenvironment of the system; these changes affect the tacticity of the polymer, the cis-trans ratio, and can increase the regularity of copolymers (Al Samak, Amir-Ebrahimi et al. 2000). Solvent polarity can also contribute significantly to the chain growth because it affects the solubility of the polymers (Kanai, Mortell et al. 1997). For the special agents, Roberts et al. dramatically improved ROMP of oligopeptides upon addition of LiCl to reduce polymer and oligopeptide aggregation (Roberts and Sampson 2003).

2.2. Other polymerization methods

Besides ROMP, living radical polymerization methods have also been widely utilized to prepare controlled polymers with various architectures and functionality. Atom transfer radical polymerization (ATRP) is one of the most effective living radical polymerization methods. In this reaction (**Figure 2-7**), free radicals are generated in the system via reversible redox reactions catalyzed by transition metal complexes. With the abstraction of a halogen atom from an initiator (R-X), the transition metal complex undergoes a single electron oxidation to generate an active species. The active radical species propagate in a similar manner to standard free radical polymerizations by attacking available monomer. Meanwhile, growing chain ends are free to abstract the halogen atom from the transition metal complex, creating a capped dormant chain. In this manner, an equilibrium is established between dormant and growing chains. When polymerization is finished, the chains remain in a capped dormant state and can be re-initiated to synthesize more complex molecules (Wang and Matyjaszewski 1995).

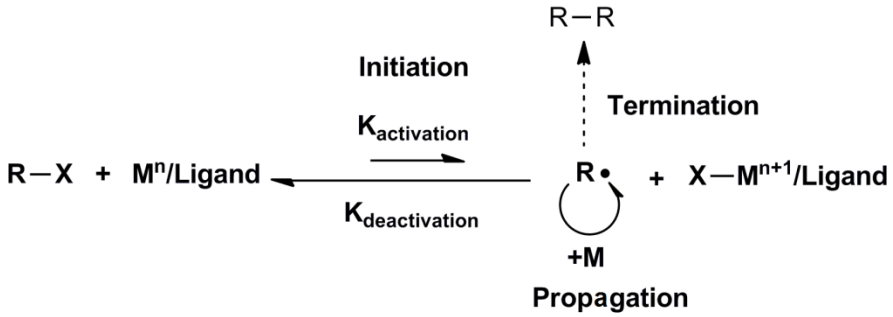

Figure 2-7. Mechanism of ATRP. M: transition metal, R: polymer chain, X: Br or Cl.

ATRP is tolerant of water and oxygen, and can be performed with a broad range of monomers including styrenes, acrylates, methacrylates, acrylonitrile, vinyl pyridine, and dienes (Gao and Matyjaszewski 2009). It is also advantageous due to the readily accessible and inexpensive catalysts (copper complex), pyridine based ligands and initiators (alkyl halides). The polymerization has been widely explored as a method for grafting chains from solid surfaces (Siegwart, Oh et al. 2012). However, while ATRP gives good control over chain growth, reaction rates are typically slow.

Recently, reversible addition–fragmentation chain transfer (RAFT) has emerged as another attractive living radical polymerization method. The same as ATRP, RAFT allows synthetic tailoring of macromolecules with complex architectures and controlled molecular weight, and is applicable to a variety of monomers under a large number of experimental conditions, including the preparation of water-soluble materials (Gregory and Stenzel 2012).

The RAFT process utilizes conventional free radical initiators and monomers but also includes the presence of a suitable chain transfer agent (RAFT agent or CTA) (Chiefari, Chong et al. 1998). These RAFT agents are most commonly dithioesters such as dithiocarbamates and trithiocarbonates (Biasutti, Davis et al. 2005), which mediate the polymerization via a reversible chain-transfer process. RAFT involves two extra equilibrium steps in addition to the three basic steps of a conventional radical polymerization—initiation, propagation, and termination. **Figure 2-8** depicts the mechanism of RAFT polymerization (Barner-Kowollik, Davis et al. 2003). The reaction starts with a free radical (I•) formed from a free-radical source (initiator). It further reacts with a monomer to yield a propagating polymeric radical (P_1•). The radicals at the end of the propagating chain quickly attack the reactive C=S bond of the CTA to produce a carbon centered intermediate radical. This is a reversible step in which the

intermediate RAFT adduct radical is capable of losing either the R group (R•) or the polymeric species (P_n•). The R radical released is free to initiate new chains by attacking monomers or the dithioester capped chains. The following main equilibrium is the most important part in the RAFT process, and it results in a rapid exchange of the dithioester cap. This rapid exchange ensures each chain has the same probability of growth. When polymerization is finished, the chains remain in the capped state and can be re-initiated to form more complex molecules.

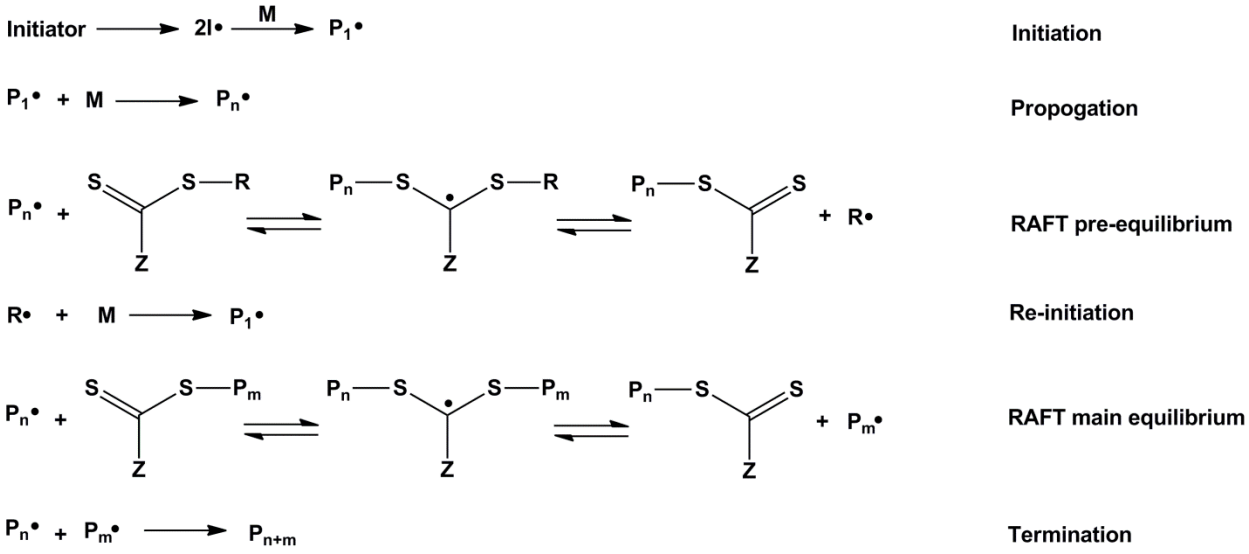

Figure 2-8. Mechanism of RAFT. I: initiator, M: transition metal, R, P: polymer chain, Z: CTA chain.

3. Norbornene and cyclobutene derived polymers as Fertilinβ mimics

Previous Sampson group members have synthesized a series of polymers with the fertilinβ and cyritestin mimic oligopeptides, and their mutated oligopeptides by ROMP for inhibition studies (Baessler, Lee et al. 2006, Baessler, Lee et al. 2009). The ECD sequence from the fertilinβ disintegrin domain and QCD from the cyritestin disintegrin domain, which are the

minimum sequences required for inhibition of sperm-oocyte binding, were chosen as the ligands. Norbornene (NB) served as the backbone because it is highly reactive and prevalently used with ruthenium catalysts in ROMP. However, NB monomers generated stereochemically heterogeneous products due to several uncontrolled stereochemical variables on NB (**Figure 2-9**). To overcome the stereochemistry difficulties, ROMP with 1-substituted cyclobutene (CB) monomers were developed to yield stereoregular, regio- and stereo-selective polymers (Lee, Parker et al. 2006, Song, Lee et al. 2010). The synthesized polymer length ranged from 10-mer to 50-mer with low PDIs (1.3-1.5) and accurate molecular weight control. This provides an entry to synthesize the linear polymers containing tactic bioactive functional groups in the biomedical studies.

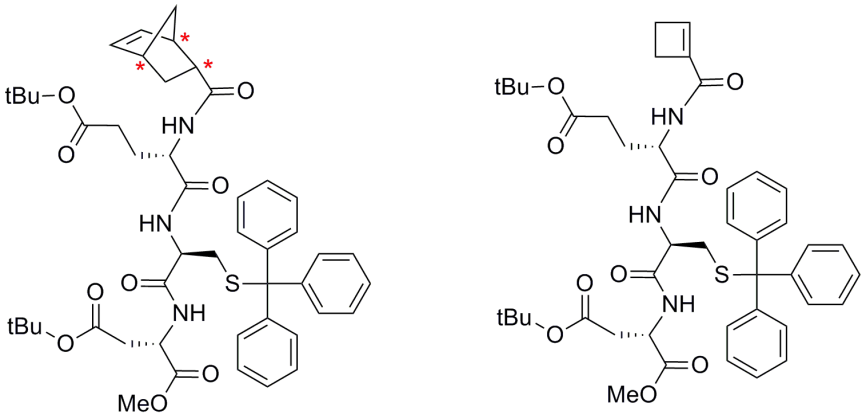

NB-E(OtBu)C(Trt)D(OtBu) **CB-E(OtBu)C(Trt)D(OtBu)**

Figure 2-9. The structures of NB-E(OtBu)C(Trt)D(OtBu) and CB-E(OtBu)C(Trt)D(OtBu). *: the asymmetric centers.

To compare the inhibition properties of ROMP-derived cyclobutyl polymers with norbornyl polymers, cyclobutyl Glu(OtBu)Cys(Trt)Asp(OtBu) and E(OtBu)C(Trt)D(OtBu) polymers of different lengths were designed. However, only CB-E(OtBu)C(Trt)D(OtBu) 4-mer was obtained. Several factors may lead to the failure of CB-E(OtBu)C(Trt)D(OtBu) polymerization. First, the

steric hindrance from the 1-substituted tripeptide side chains may prevent the completion of CB-E(OtBu)C(Trt)D(OtBu) polymerization. To test this hypothesis, amino acids without large side chains (e. g. Gly and Ala) were used to replace the bulky Cys (**Figure 2-10**). Due to the fast cyclization rate of GD(OtBu), E(OtBu)AD(OtBu) was chosen instead of E(OtBu)GD(OtBu). GC(Trt)D(OtBu) and the unhindered GGG were also prepared for testing. Second, the trityl group on Cys is not very stable; it may fall off in during ROMP and the free sulfur exposed can deactivate the catalyst. Thus, Cys with a more stable protecting group—acetyl methyl group (Acm) was designed. Though there may be some other possible reasons for this problem, at the first stage, only the ROMP properties of the above tripeptides were evaluated.

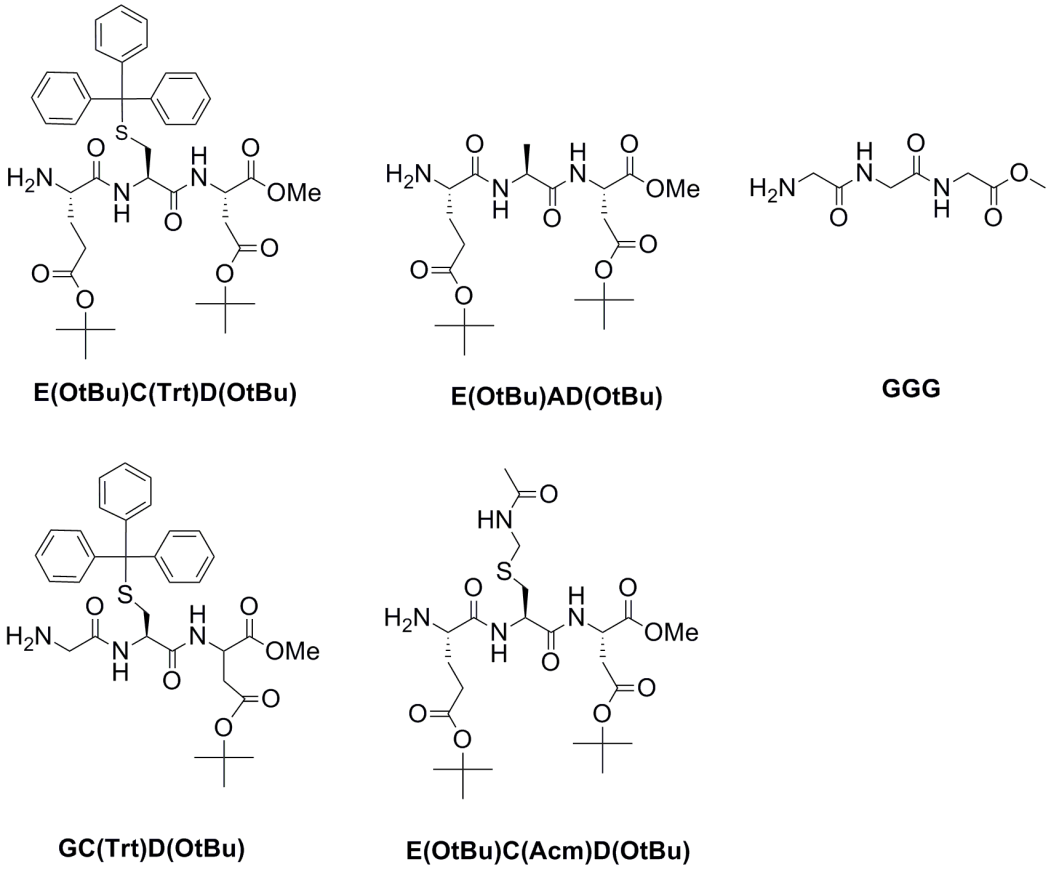

Figure 2-10. Tripeptide structures.

4. Glycopolymer probes for the investigation of sperm AR mechanism

Chemical approaches are powerful allies to genetics and biochemistry in the study of biological systems. Especially, synthetic multivalent mimics of the complex assemblies found on cell surfaces can modulate cellular interactions and are very useful tools for the development of therapeutic agents. In mammalian fertilization, sperm bind to the egg through multivalent carbohydrate-protein interactions. The interactions can result in receptor communication and signal transduction, which further leads to the acrosome reaction (AR). Although mounting

evidence has shown that the multivalent interactions between carbohydrates on the ZP and the corresponding receptors on the sperm are relevant to AR activation, an understanding of the underlying molecular mechanism has been elusive.

As multivalent ligands have become more and more important in studying biological interactions due to their unique recognition properties, we proposed that synthetic glycopolymer probes would provide a powerful approach to investigate the molecular complexity of sperm AR. However, it is crucial to choose the proper structure of multivalent ligands to achieve specific and selective carbohydrate-protein binding. Linear polymers have long been proved a versatile strategy to investigate ligand-receptor interactions in many different biological systems (Kanai, Mortell et al. 1997, Manning, Strong et al. 1997, Baessler, Lee et al. 2006). Compared to the BSA-conjugated neoglycoproteins used to study AR previously (Loeser and Tulsiani 1999, Hanna, Kerr et al. 2004), linear glycopolymers are better defined, allow easier variation of the length and ligand density, and can be easily prepared by living polymerization methods. Moreover, linear polymers favor clustering receptors and activating signaling transduction pathway (Gestwicki, Cairo et al. 2002), functions that are essential for inducing the AR.

In our work, all of the ZP monosaccharides proposed to be involved in the AR: mannose, fucose, GlcNAc, and GalNAc were chosen as ligands. Although Loeser *et al.* demonstrated that galactose-BSA and glucose-BSA did not induce AR (Loeser and Tulsiani 1999) and glucose is not present on the ZP (Easton, Patankar et al. 2000), the properties of galactose and glucose polymers were still tested to confirm these results. Though NB monomers would produce stereochemically heterogeneous polymers, it still served as the scaffold in our work due to its significant reactivity and widespread adoption. Previously utilized linkers in BSA conjugated neoglycoproteins are 3 or 14 atoms long. However their structures are proprietary. Thus, we

chose a simple 3-atom ethyl amide linker to connect the NB-derived backbone and the monosaccharide ligand. The desired homogenous glycopolymers with two different average lengths (10-mer and 100-mer) (**Figure 2-11**) were synthesized via ROMP and tested to determine the better scaffold length for activating the AR with monosaccharide ligands.

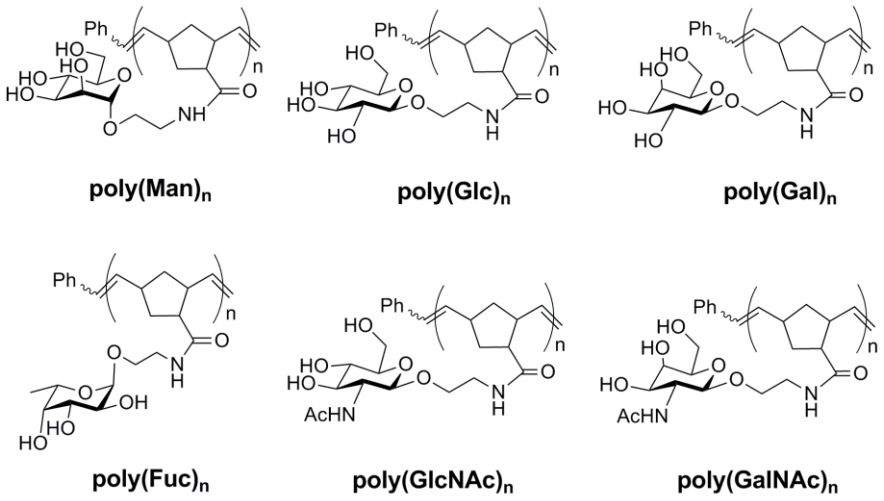

Figure 2-11. Glycopolymer structures.

Chapter 3

Results

1. Investigation of mouse sperm AR with synthetic glycopolymers
    1.1. Synthesis of homoglycopolymers
    1.2. Immunofluorescent assay for sperm acrosome reaction
    1.3. Effect of homoglycopolymers on the AR
    1.4. Effect of pairs of 100-mers on the AR
    1.5. Kinetics of AR induced by 100-mers
    1.6. Signaling pathway of glycopolymers induced AR
    1.7. Summary

2. Investigation of synthetic methods to prepare fertilization probes
    2.1. Synthesis of tripeptide-conjugated polymers
    2.2. The kinetics of ROMP
    2.3. Summary

1. Investigation of mouse sperm AR with synthetic glycopolymers

1. 1. Synthesis of homoglycopolymers

The synthesis of NB-mannose, NB-glucose and NB-galactose followed the same protocols (**Scheme 3-1** to **3-3**). A shorter synthesis route was utilized to prepare NB-fucose (**Scheme 3-4**). This route can also be applied for the synthesis of NB-mannose, NB-glucose and NB-galactose. However, GlcNAc and GalNAc showed distinct chemical properties from the other four carbohydrates, and a slightly different synthesis protocol was utilized to synthesize NB-GlcNAc and NB-GalNAc (**Scheme 3-5**, **3-6**).

The protocols are all conventional chemical glycosylation procedures. For mannose, fucose and GalNAc, only free sugars were commercial available, so an extra step of acetylation was carried out to generate protected sugars. The anomeric OAc was hydrolyzed by hydrazine acetate in DMF and followed by work-up to yield glycosides with a free anomeric OH group. No further chromatography purification was required in this step. The trichloroacetonitrile group was introduced to the anomeric OH under basic condition (DBU). Then, the addition of the three-atom linker could be easily achieved by glycosylation of the fully acetylated trichloroacetimidate with 2-chloroethanol and an activating agent BF_3•OEt_2. Subsequent displacement of the terminal Cl with NaN_3 afforded the 2-azidoethyl glycoside in good yields. The target norbornenyl glycosides were synthesized via Staudinger ligantion in a one-pot process.

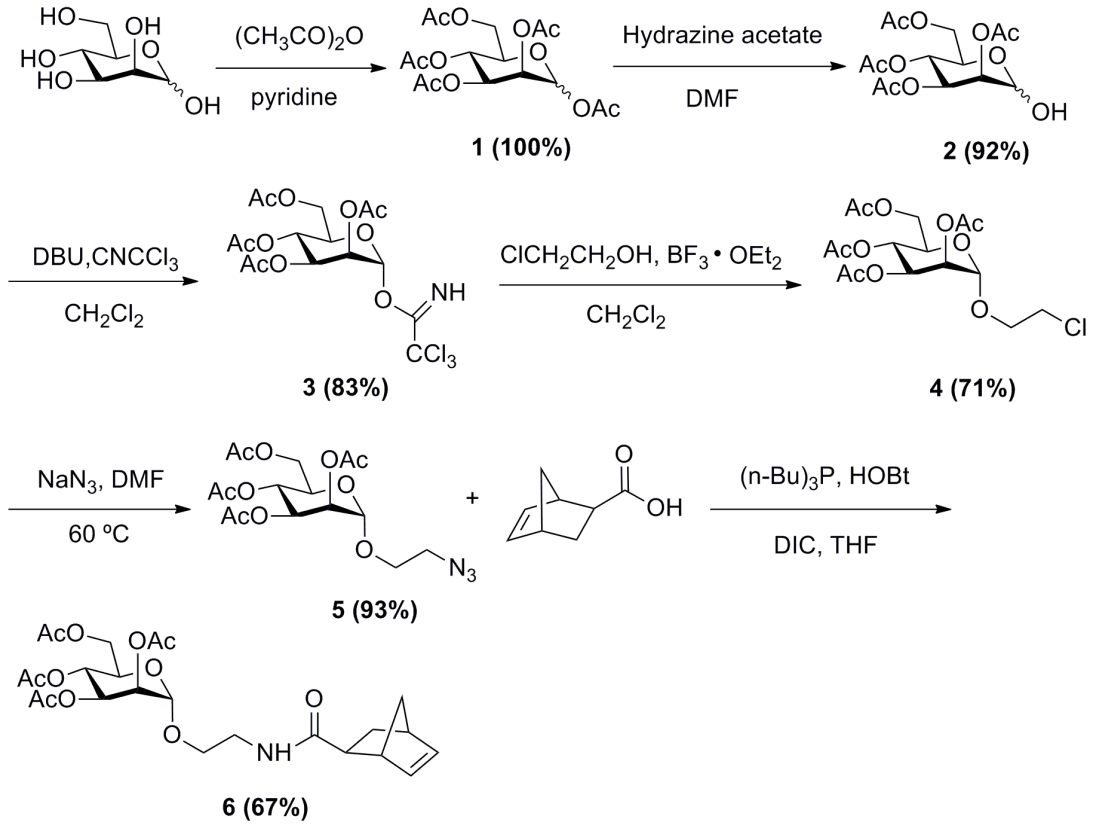

Scheme 3-1. Synthesis of NB-mannose.

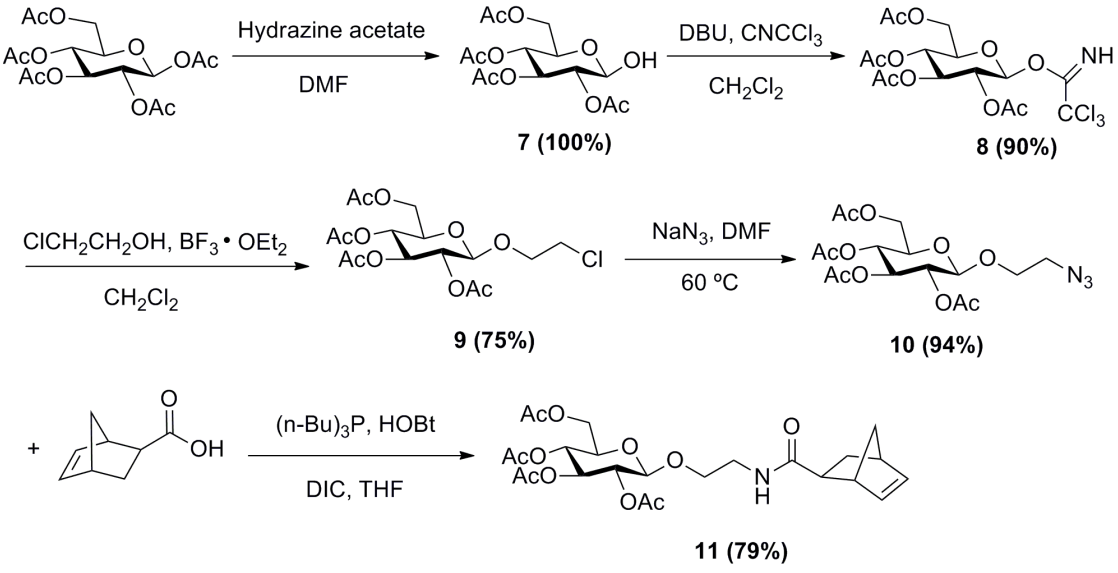

Scheme 3-2. Synthesis of NB-glucose.

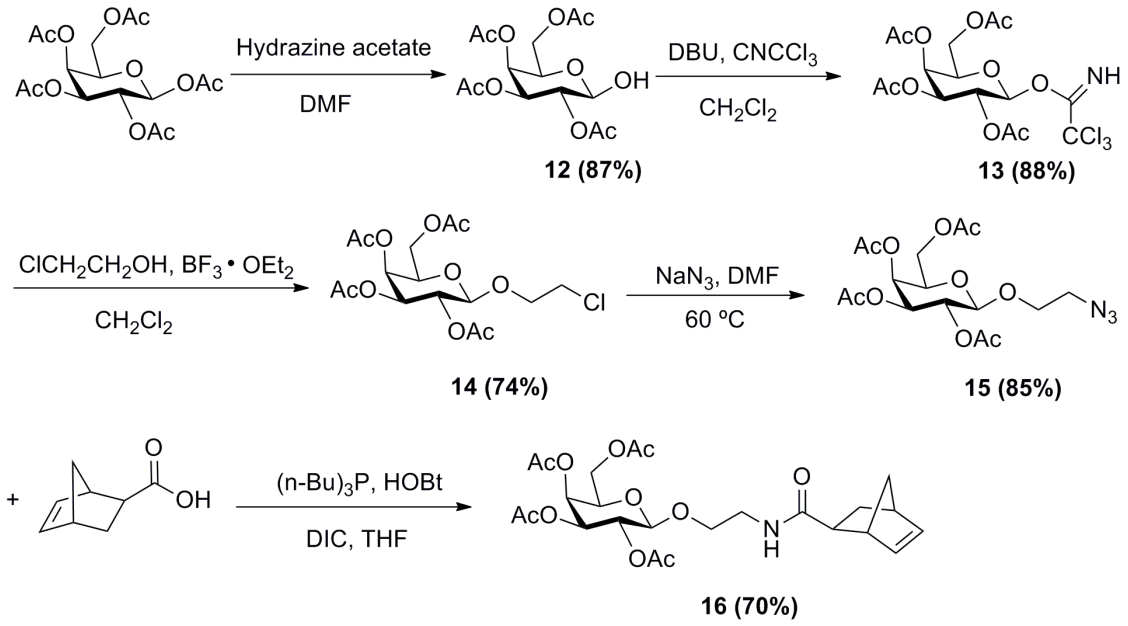

Scheme 3-3. Synthesis of NB-galactose.

In the shorter synthesis route of NB-fucose, compound **18** can be easily prepared in one step from fully protected fucose by initial condensation with 2-bromoethanol under excess Lewis acid mediated conditions. 2-bromoethanol can also be used to replace 2-chloroethanol in the previous schemes. Mixtures of α and β stereoisomers (about 1:1) were obtained in every step. The yields shown in the scheme were for the mixtures except the yield of the final product was only for the desired β anomer.

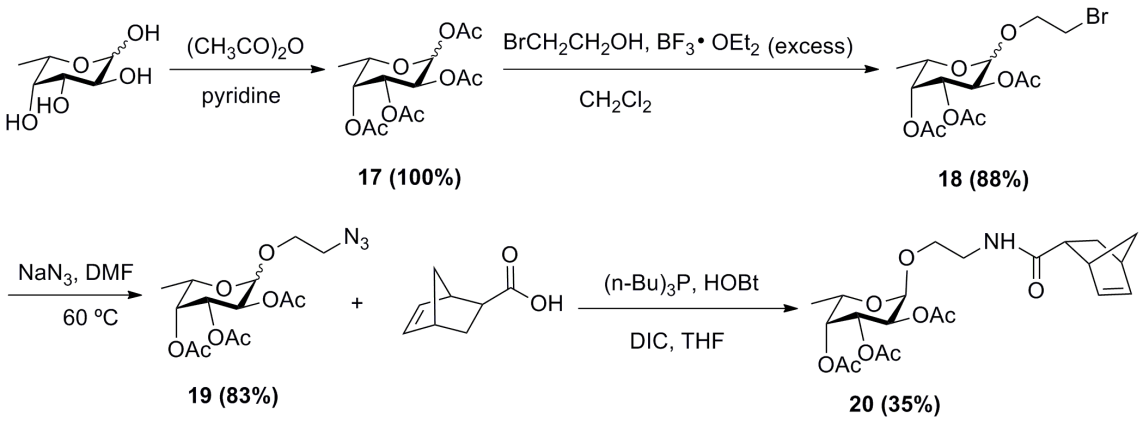

Scheme 3-4. Synthesis of NB-fucose.

Ammonium acetate was used to deprotect the acetyl group at the anomeric position of peracetylated GlcNAc and GalNAc, because many impurities were generated in the hydrazine acetate deprotection condition. Although some impurities were also observed in the ammonium acetate condition, the desired products (compound **21** in **Scheme 3-5**, compound **27** in **Scheme 3-6**) could be purified by chromatography with good yield. Compound **26** (**Scheme 3-6**) was used for the deprotection step directly without work-up because a large number of **26** was lost during extraction. The pyridine and the acetic anhydride in this step could be removed by forming azeotropes with toluene.

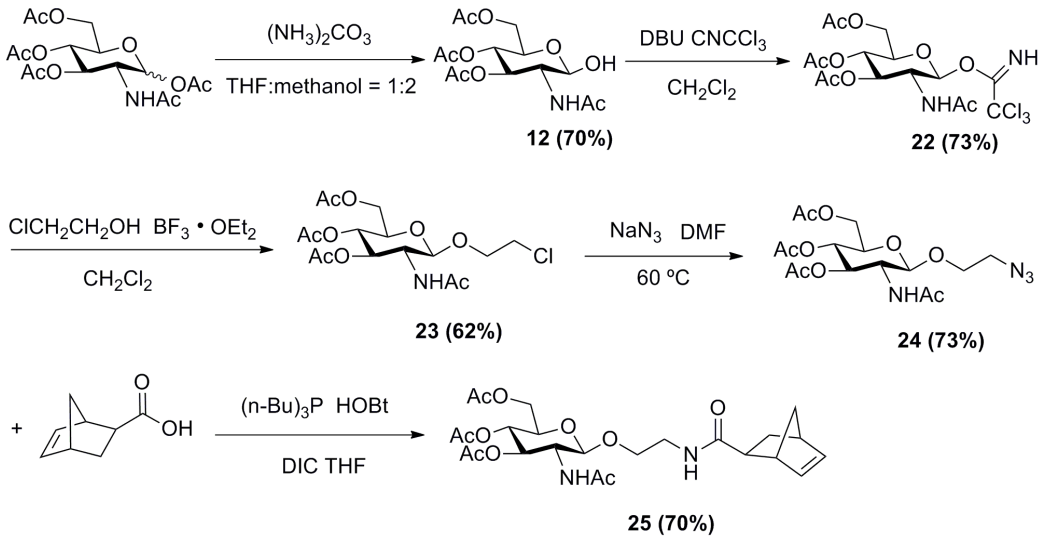

Scheme 3-5. Synthesis of NB-GlcNAc.

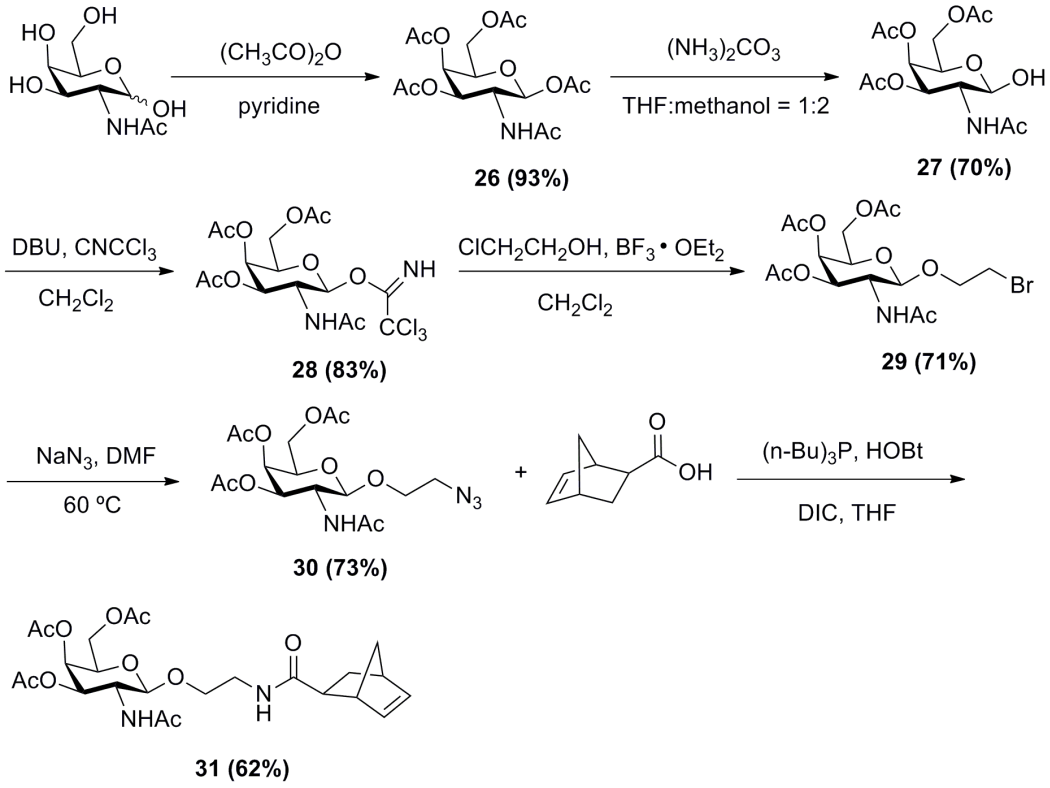

Scheme 3-6. Synthesis of NB-GalNAc.

The fully protected monomers were polymerized by ROMP in dichloromethane with catalyst (H_2IMes)(3-Br-pyr)$_2$$Cl_2$Ru=CHPh, **32** to form homoglycopolymers of two different length (10-mer and 100-mer), and the polymerizations were terminated with ethyl vinyl ether. Polymers were precipitated with an ether/dichloromethane mixture, and were deprotected by treating with excess K_2CO_3 in MeOH/THF followed by neutralization with a THF/H_2O/HCl cocktail mixture (**Scheme 3-7**). The deprotected polymers were purified by ion exchange (10-mers) or dialysis (100-mers), and stored in H_2O as stock solution.

The protected polymers were characterized by NMR spectroscopy, gel permeation chromatography (GPC), and laser light scattering. TLC and ^{1}H NMR spectra confirmed that no monomer was retained upon polymer precipitation. The number-average molecular weights (M_n), the weight average molecular weights (M_w), and the polydispersity index (PDI) (**Table 3-1**) were determined by gel permeation chromatography utilizing a differential refractometer and a multi-angle light scattering detector. The successful removal of the protecting acetyl groups was confirmed by ^{1}H NMR. The size distribution profiles of deprotected polymers in the assay buffer were monitored by dynamic light scattering to determine whether aggregates of polymers formed under the assay conditions.

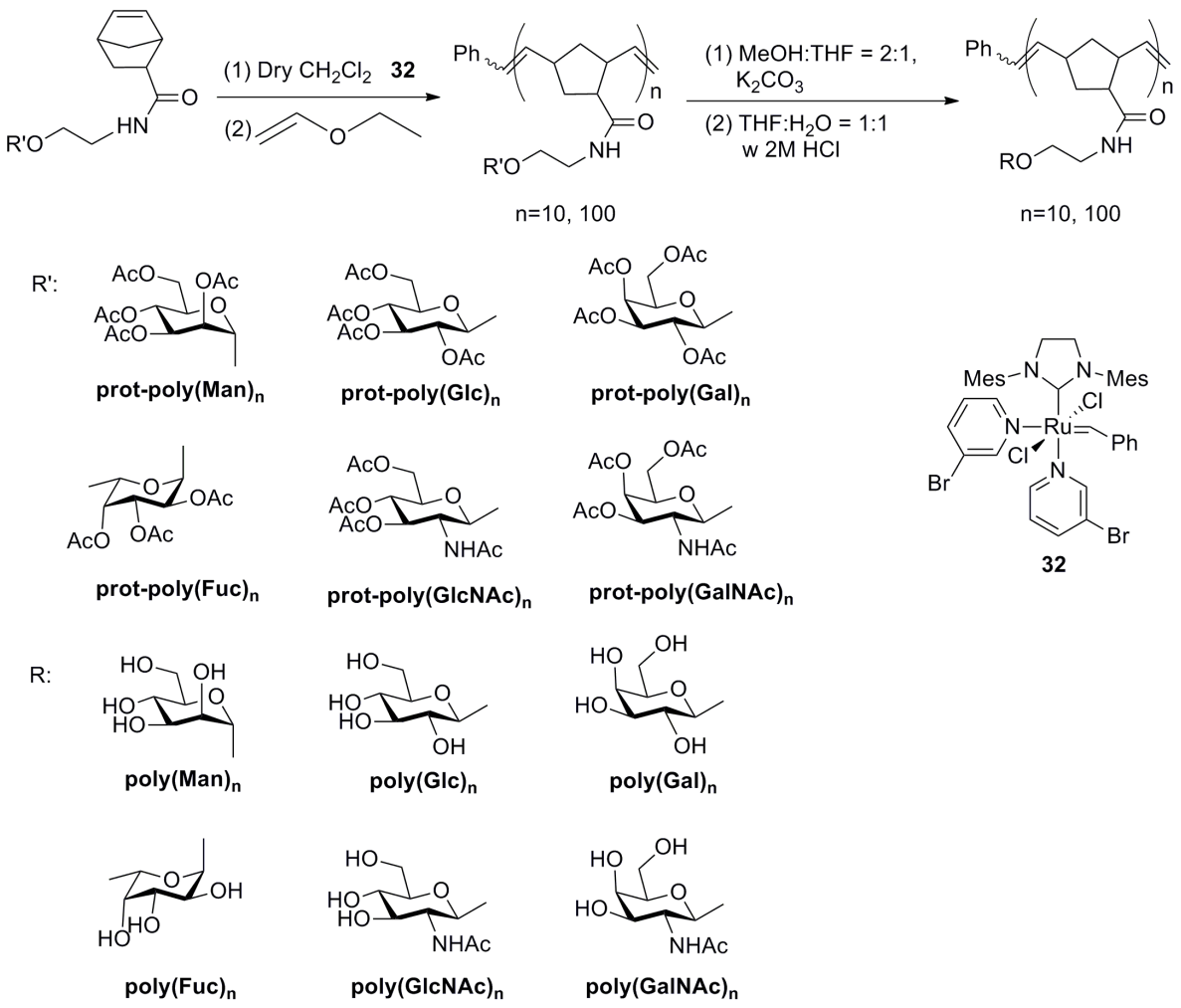

Scheme 3-7. ROMP and deacetylation of glycopolymers.

All the carbohydrates shown above are the D isomer except fucose which is the L isomer. Norbornene coupled with the unnatural D-fucose was also synthesized (**Scheme 3-8**) and polymerized (**Scheme 3-9**). Fucoses without an explicit prefix are L-fucose unless otherwise noted.

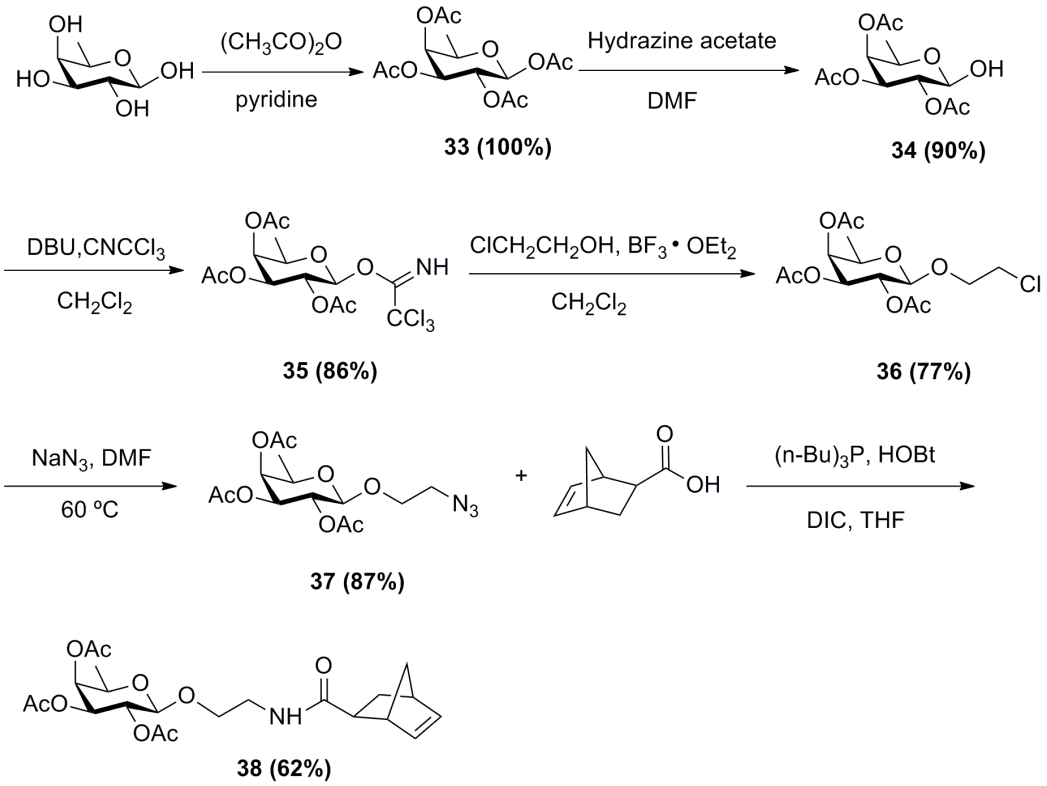

Scheme 3-8. Synthesis of NB-D-fucose.

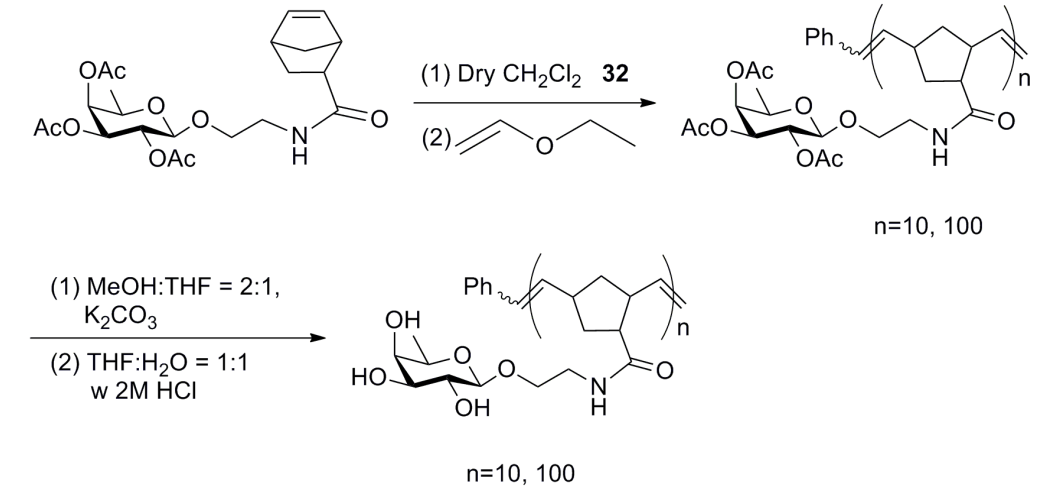

Scheme 3-9. ROMP and deacetylation of D-fucose.

Table 3-1. Analytical data for homoglycopolymers. [a]Theoretical molecular weights were calculated based on the catalyst-to-monomer ratio assuming full conversion. [b]Determined from GPC in THF utilizing a differential refractometer and a multiangle light scattering detector.

polymers	[Monomer]/ [Catalyst]	Rxn time (h)	Theo Mn[a]	Calcd Mn[b]	Calcd Mw[b]	PDI[b]
Poly(Man)$_{10}$	10/1	1	5189	3509	4316	1.23
Poly(Man)$_{100}$	100/1	1.5	51197	34397	38180	1.11
Poly(Glc)$_{10}$	10/1	1	5189	3509	4280	1.22
Poly(Glc)$_{100}$	100/1	1.5	51197	34397	44372	1.29
Poly(Gal)$_{10}$	10/1	1	5189	3509	4245	1.21
Poly(Gal)$_{100}$	100/1	1.5	51197	34397	41276	1.20
Poly(Fuc)$_{10}$	10/1	0.5	4534	2862	3692	1.29
Poly(Fuc)$_{100}$	100/1	1	45425	27928	32676	1.17
Poly(GlcNAc)$_{10}$	10/1	1	5179	3765	5158	1.37
Poly(GlcNAc)$_{100}$	100/1	1.5	51097	38497	50431	1.31
Poly(GalNAc)$_{10}$	10/1	0.5	5179	3998	5558	1.39
Poly(GalNAc)$_{100}$	100/1	1	51097	37977	50510	1.33
Poly(D-Fuc)$_{10}$	10/1	0.5	4534	3011	3957	1.31
Poly(D-Fuc)$_{100}$	100/1	1	45425	29071	34291	1.18

1.2. Immunofluorescent assay for sperm acrosome reaction

Deprotected glycopolymers were dissolved in phosphate buffered saline (PBS) to a final pH of 7 before use in assays. Sperm were first capacitated in M16 medium containing 0.3% BSA and then incubated with controls or glycopolymers for another 30 min followed by washing and fixation (**Figure 3-1**). After transfering to microscope slides, sperm samples were stained with rhodamine-labeled peanut agglutinin (PNA) and the number of acrosome reacted sperm were counted using an immunofluorescent microscope (20 ×/ 0.5 air) (**Figure 3-2**).

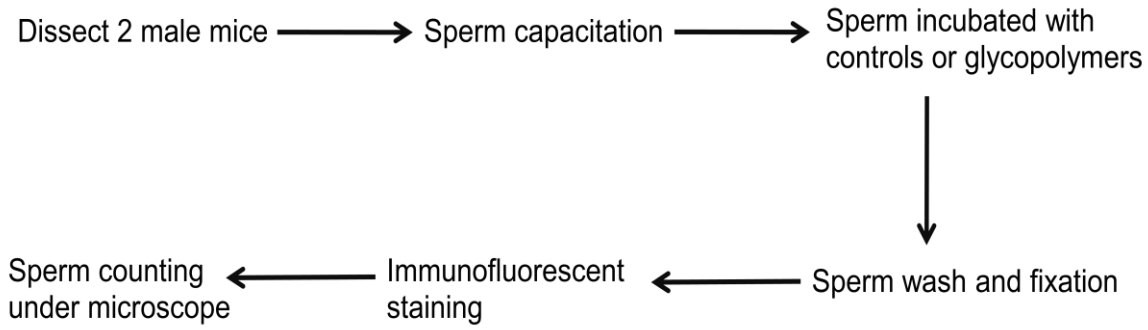

Figure 3-1. The procedure of sperm acrosome reaction immunofluorescent assay.

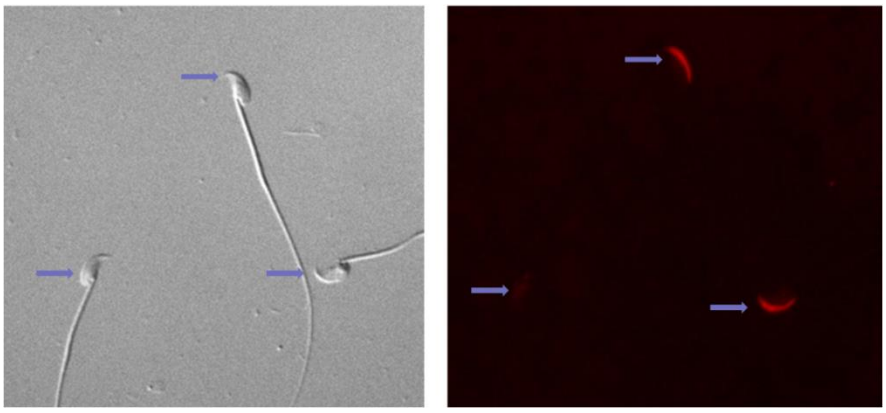

DIC **Cy3.5**

Figure 3-2. Sperm acrosome reaction immunofluorescent assay. Left: Differential interference contrast image (DIC). Right: Fluorescence image with Cy3.5 (585 nm). Sperm that displayed continuous red fluorescence along their acrosomal arcs were scored as acrosome-intact; those that displayed no red or punctuate fluorescence were scored as acrosome-reacted.

1.3. Effect of homoglycopolymers on the AR

First, the effect of homoglycopolymers on the sperm acrosome reaction was examined. A significantly greater number of sperm undergo the AR when treated with 100 μM poly(Man)$_{10}$, poly(Fuc)$_{10}$ or poly(GlcNAc)$_{10}$ than with the other three glycopolymers (**Figure 3-3a**). The activation of the AR by these three glycopolymers is dose dependent; at a 2-fold lower concentration, the AR is not activated. Sperm samples treated with a 2-fold higher concentration (200 μM) were AR activated with a lower efficiency or no efficacy. Neither poly(Glc)$_{10}$, poly(Gal)$_{10}$ or poly(GalNAc)$_{10}$ triggered the AR at concentrations of 100 or 200 μM. Induction of AR by poly(Fuc)$_{10}$ is not as effective as with poly(Man)$_{10}$ or poly(GlcNAc)$_{10}$. Similarly, dose-dependent AR initiation was observed when sperm were incubated with poly(Man)$_{100}$, poly(Fuc)$_{100}$ and poly(GlcNAc)$_{100}$, but not poly(Glc)$_{100}$ and poly(Gal)$_{100}$ and poly(GalNAc)$_{100}$ (**Figure 3-3b**). There is no statistically significant difference between the efficacy of mannose

polymers and GlcNAc polymers. Again, the AR initiation efficacy of poly(Fuc)$_{100}$ is lower than for poly(Man)$_{100}$, and poly(GlcNAc)$_{100}$, consistent with the lowered efficacy of poly(Fuc)$_{10}$. We have reported polymer efficacies in polymer concentrations. If the bulk concentration of glycan ligand utilized is considered in comparing the efficacies of 10-mers versus 100-mers, we observe that the 100-mers are more potent. Sperm did not undergo AR when incubated with the 10-mers at 500 μM (50 μM polymer) concentration (**Figure 3-3a**), whereas 500 μM (5 μM polymer) of poly(Man)$_{100}$, poly(Fuc)$_{100}$ and poly(GlcNAc)$_{100}$ (**Figure 3-3b**) successfully initiated the AR.

Surprisingly, D-fucose polymers also activate AR in a dose-dependent manner (**Figure 3-4**). Poly(D-Fuc)$_{10}$ showed almost the same AR activation pattern as poly(Fuc)$_{10}$. However, poly(D-Fuc)$_{100}$ could not fully activate the AR at 5 μM. The AR% also decreased when sperm were incubated with poly(D-Fuc)$_{100}$ at very high concentration (40 μM). The requirement for a higher concentration of poly(D-Fuc)$_{100}$ to maximally activate the AR indicated that poly(D-Fuc)$_{100}$ was less potent than the poly(Fuc)$_{100}$. In the following assays, the optimal concentration for poly(D-Fuc)$_{100}$ was 20 μM and for other 100-mers it was 10 μM.

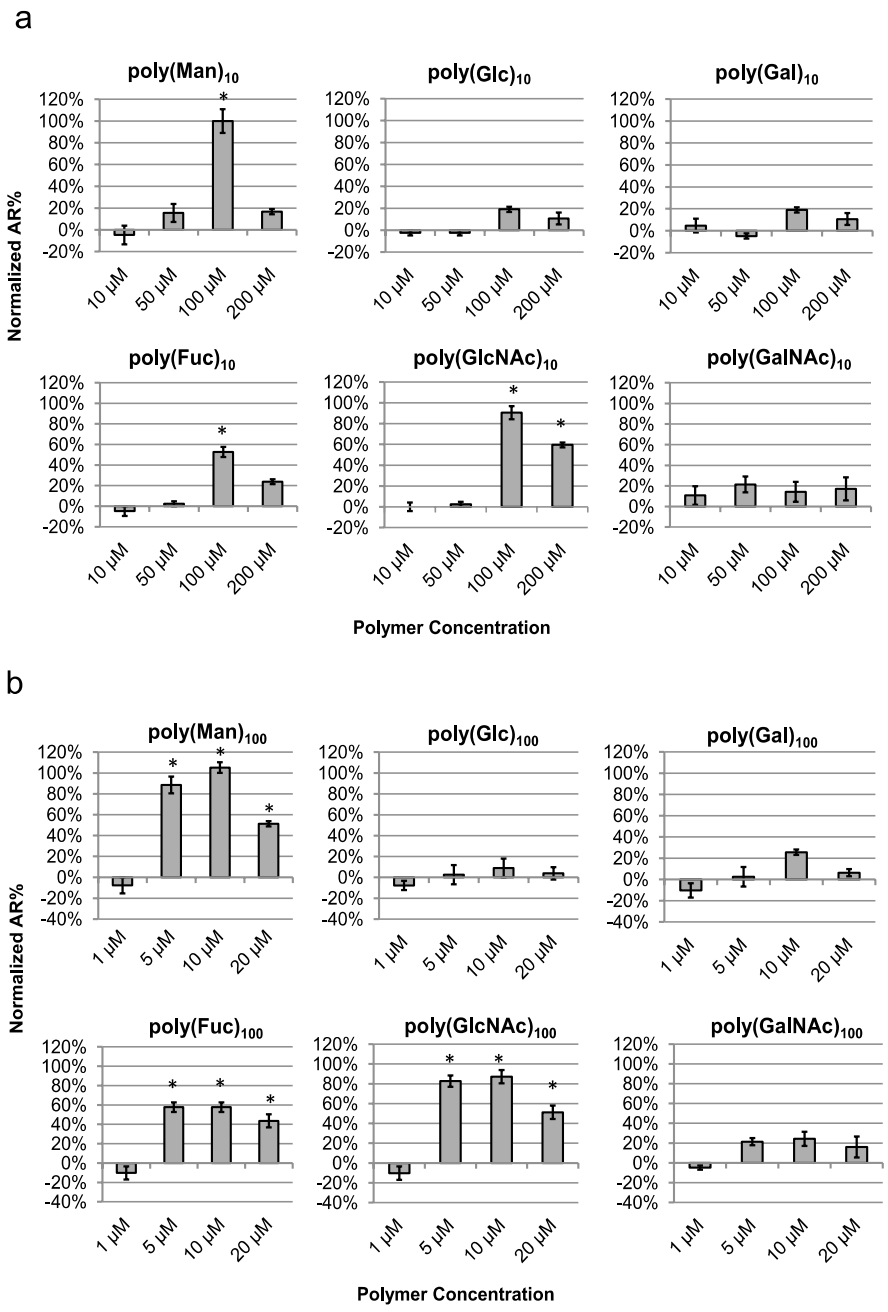

Figure 3-3. Capacitated sperm were incubated with glycopolymers at different concentrations (shown as polymer concentration). a) 10-mers. b) 100-mers. The average AR% of glycopolymer treated sperm were normalized using [AR%(glycopolymers) – AR%(negative control)]/[AR%(positive control) – AR%(negative control)]. The average AR% for the positive control, A23187–treated (5 μM) sperm, was 24% and for the negative control, PBS–treated sperm, was 10%. Data represent mean ± SEM of at least three independent experiments. * $p < 0.05$ when compared to the negative control.

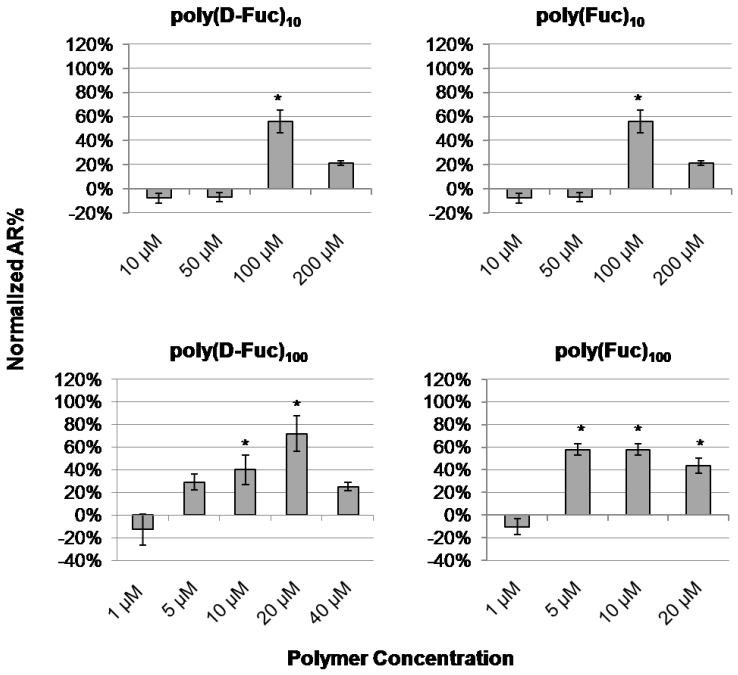

Figure 3-4. Comparison of D- and L-fucose polymers in the dose-dependent assay. The average AR% of glycopolymer treated sperm were normalized using [AR%(glycopolymers) – AR%(negative control)]/[AR%(positive control) – AR%(negative control)]. The average AR% for the positive control, A23187–treated (5 μM) sperm, was 24% and for the negative control, PBS–treated sperm, was 10%. Data represent mean ± SEM of at least three independent experiments. * $p < 0.05$ when compared to the negative control.

1.4. Effect of pairs of 100-mers on the AR

Next, the active 100-mers poly(Man)$_{100}$, poly(Fuc)$_{100}$, and poly(GlcNAc)$_{100}$ were paired at their optimal (10 μM) and at much lower concentrations (2.5 μM) to examine the effect of inducing the AR simultaneously with two different ligands. We saw no further increase in the amount of sperm AR comparing the polymer pairs and single glycopolymer at their optimal concentration; the efficacy remained at 100% of the positive control (**Figure 3-5a**). Mixtures of

three glycopolymers at their optimal concentrations were also tested, but no significant differences in AR percentage between a pair and a mixture of three were observed.

Although poly(GlcNAc)$_{100}$ and poly(Man)$_{100}$ had similar dose-dependent AR activating patterns (**Figure 3-3b**); poly(GlcNAc)$_{100}$ was more effective than poly(Man)$_{100}$ at 2.5 μM (**Figure 3-5b**). Poly(GlcNAc)$_{100}$ and poly(Man)$_{100}$ paired at 2.5 μM each showed a slight enhancement in AR activation compared to poly(GlcNAc)$_{100}$ at 2.5 μM, yet the mixture did not activate AR to the same level as 5 μM of a poly(GlcNAc)$_{100}$ or poly(Man)$_{100}$ (**Figure 3-5b**).

Sperm samples treated with the other two combinations of activating polymers (2.5 μM each) showed efficacies equal to treatment with a single polymer at 2.5 μM. In addition, the pairwise mixtures (2.5 μM each) were less effective activators of AR than a single polymer at 5 μM, which is equal to the total concentration of polymer in the paired mixture. Dynamic light scattering was also used to investigate whether polymer aggregation, which could interfere with sperm activation, had occurred. No aggregation was observed.

Similarly, poly(D-Fuc)$_{100}$ paired with the other two 100-mers at 10 μM or 2.5 μM each showed no increase in AR% (**Figure 3-6a**) compared to that of single glycopolymers at 10 μM or 2.5 μM. The pairwise mixtures (2.5 μM each) also did not activate AR to the same level as a single polymer at 5 μM. As poly(D-Fuc)$_{100}$ started significant AR activation at 10 μM instead of 5 μM, pairs of poly(D-Fuc)$_{100}$ at 5 μM with poly(GlcNAc)$_{100}$ and poly(man)$_{100}$ at 2.5 μM respectively were also examined (data not shown). The results were similar to those of poly(D-Fuc)$_{100}$ at 2.5 μM.

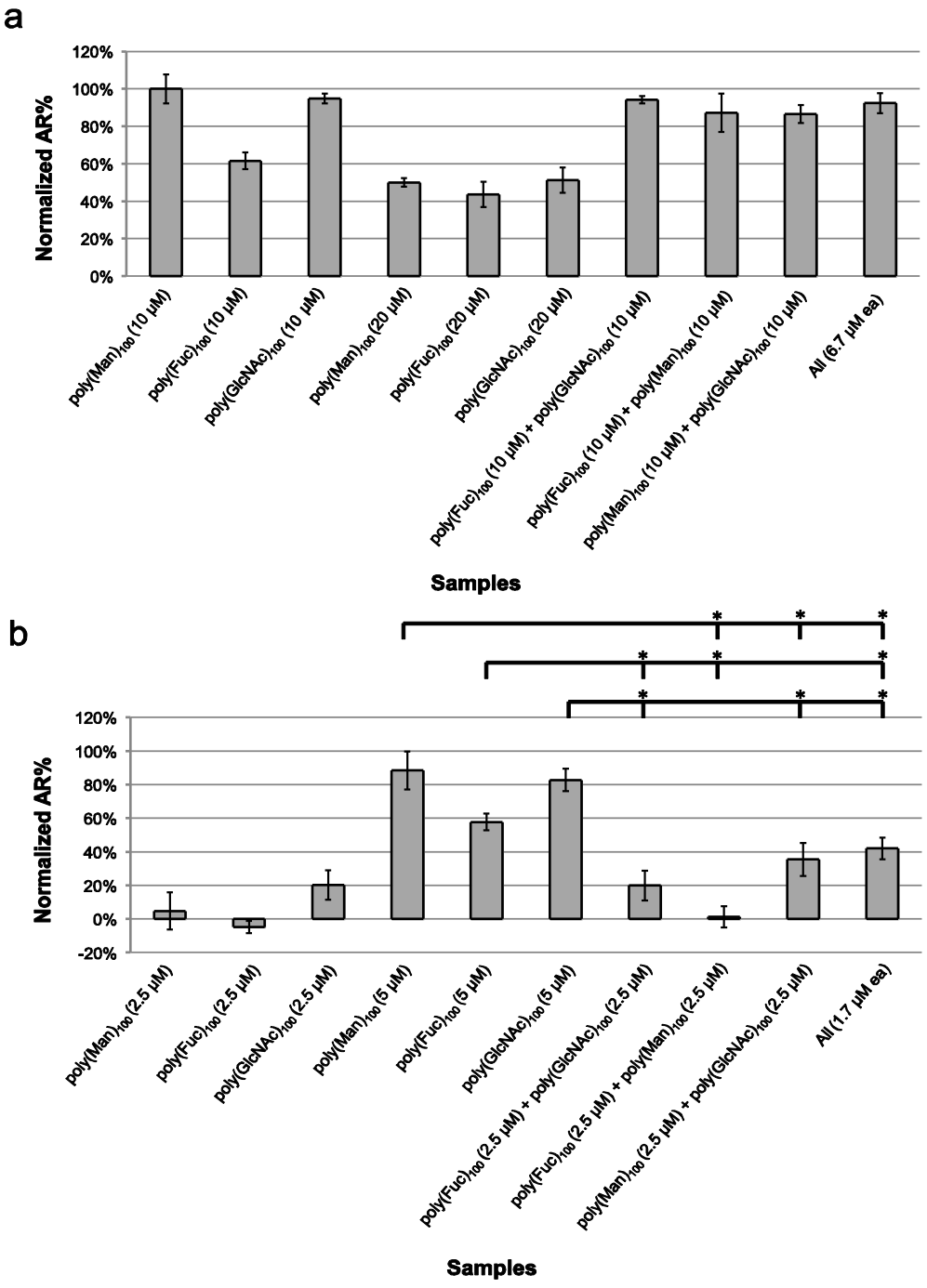

Figure 3-5. Comparison of mixed 100-mers and the corresponding single 100-mers. a) 100-mers paired at 10 μM each. b) 100-mers paired at 2.5 μM each. The concentration shown in the chart is polymer concentration. The average AR% of glycopolymer treated sperm were normalized using [AR%(glycopolymers) – AR%(negative control)]/[AR%(positive control) – AR%(negative control)]. The average AR% for the positive control, A23187–treated (5 μM) sperm, was 24% and for the negative control, Poly$(Glc)_{100}$–treated (10 μM) sperm, was 11%. Data represent mean ± SEM of at least three independent experiments. * $p < 0.05$ when compared to the corresponding single 100-mers.

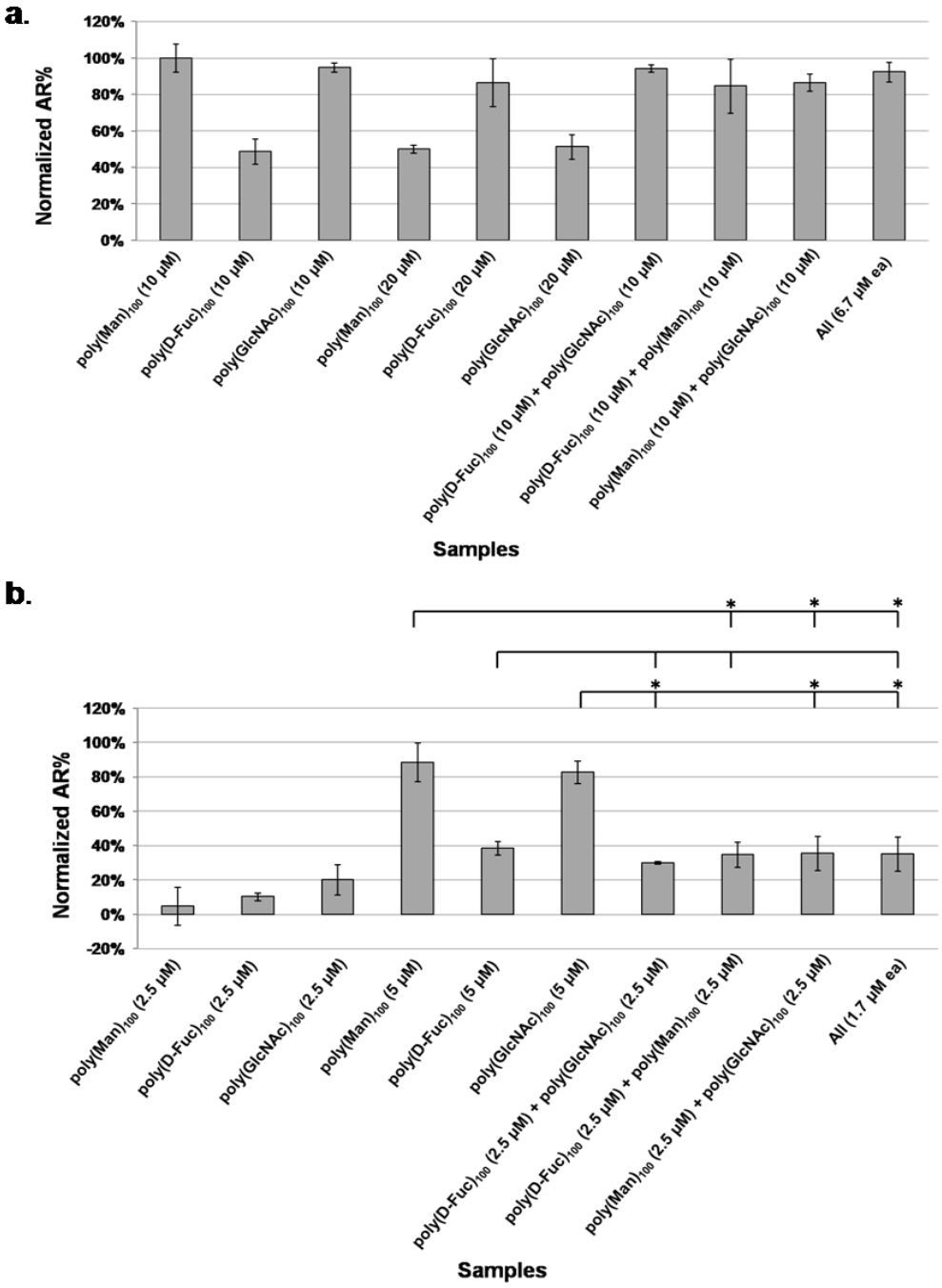

Figure 3-6. Comparison of mixed 100-mers with poly(D-Fuc)$_{100}$ and the corresponding single 100-mers. a) 100-mers paired at 10 μM each. b) 100-mers paired at 2.5 μM each. The concentration shown in the chart is polymer concentration. The average AR% of glycopolymer treated sperm were normalized using [AR%(glycopolymers) – AR%(negative control)]/[AR%(positive control) – AR%(negative control)]. The average AR% for the positive control, A23187–treated (5 μM) sperm, was 24% and for the negative control, poly(Glc)$_{100}$–treated (10 μM) sperm, was 11%. Data represent mean ± SEM of at least three independent experiments. * $p < 0.05$ when compared to the corresponding single 100-mers.

1.5. Kinetics of AR induced by 100-mers

The effects of the three active 100-mers on the AR were further studied as they were more potent than the 10-mers. The time courses for the three 100-mers were monitored in parallel for 45 minutes. Data for longer incubation periods were not included due to high AR in the negative control and reduced sperm viability.

At the three time points, the extent of AR in the positive control and the poly(Man)$_{100}$ and poly(GlcNAc)$_{100}$ treated samples is the same (**Figure 3-7**). However, poly(Fuc)$_{100}$ induced lower levels of the AR than poly(Man)$_{100}$ and poly(GlcNAc)$_{100}$ at 30 or 45 minutes, and there was no initiation after 15 minutes (**Figure 3-7**). These data indicate that the induction of the AR by poly(Man)$_{100}$ and poly(GlcNAc)$_{100}$ is more rapid than by poly(Fuc)$_{100}$, which is in agreement with the previous observation that poly(Man)$_{100}$ and poly(GlcNAc)$_{100}$ is more effective than poly(Fuc)$_{100}$. The AR% in the negative control increased sharply to 16% (38% after normalization) at 45 minutes due to spontaneous AR. Therefore, we selected 30 minutes for all of our endpoint assays because the level of spontaneous AR was much lower.

In the assay with D-fucose 100-mer (**Figure 3-8**), the extent of AR in the positive control and the glycopolymer-treated samples is the same after 15 minutes. By 30 minutes, poly(Man)$_{100}$ and poly(GlcNAc)$_{100}$ had induced higher levels of AR than poly(D-Fuc)$_{100}$. There was no statistically significant difference between the three 100-mers and A23187 at 30 or 45 minutes. However, sperm treated with poly(D-Fuc)$_{100}$ showed further AR at the last time point. These data confirm that poly(Man)$_{100}$ and poly(GlcNAc)$_{100}$ have faster AR activation rate, although poly(D-Fuc)$_{100}$ is equally effective at inducing the AR at the assay endpoint and at a 2-fold higher concentration.

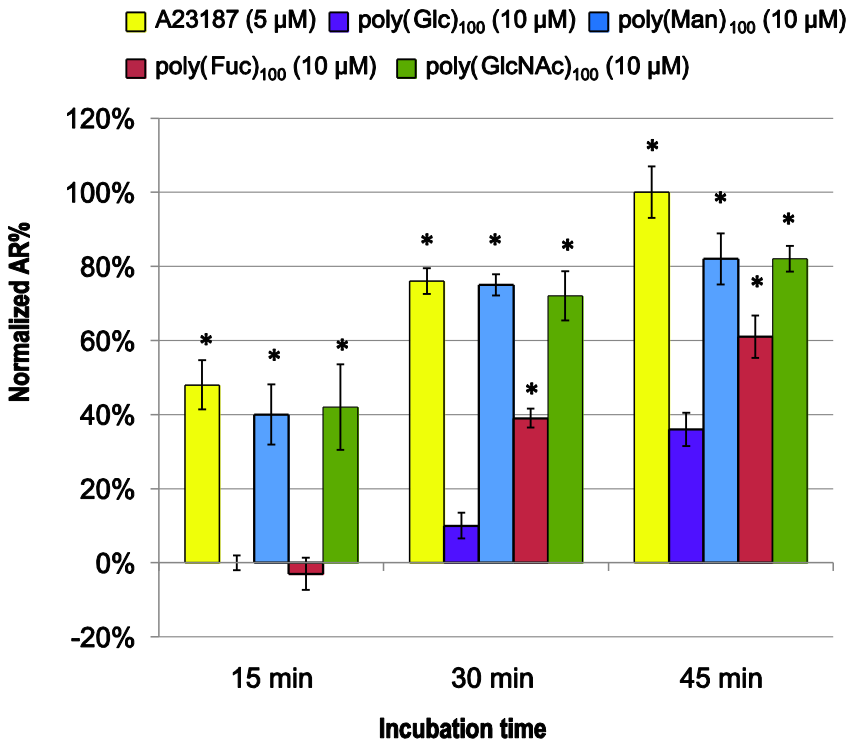

Figure 3-7. Poly(Fuc)$_{100}$, poly(Man)$_{100}$ and poly(GlcNAc)$_{100}$ have different AR activation rate. The concentration shown in the chart is polymer concentration. The average AR% of glycopolymer treated sperm were normalized using [AR%(glycopolymers) – AR%(negative control)]/[AR%(positive control) – AR%(negative control)]. The average AR% for the positive control, A23187-treated (5 μM) sperm at 45 min was 33% and for the negative control, poly(Glc)$_{100}$-treated sperm at 15 min, was 9%. Data represent mean ± SEM of at least three independent experiments. * $p < 0.05$ when compared to the AR% of poly(Glc)$_{100}$ at each time point.

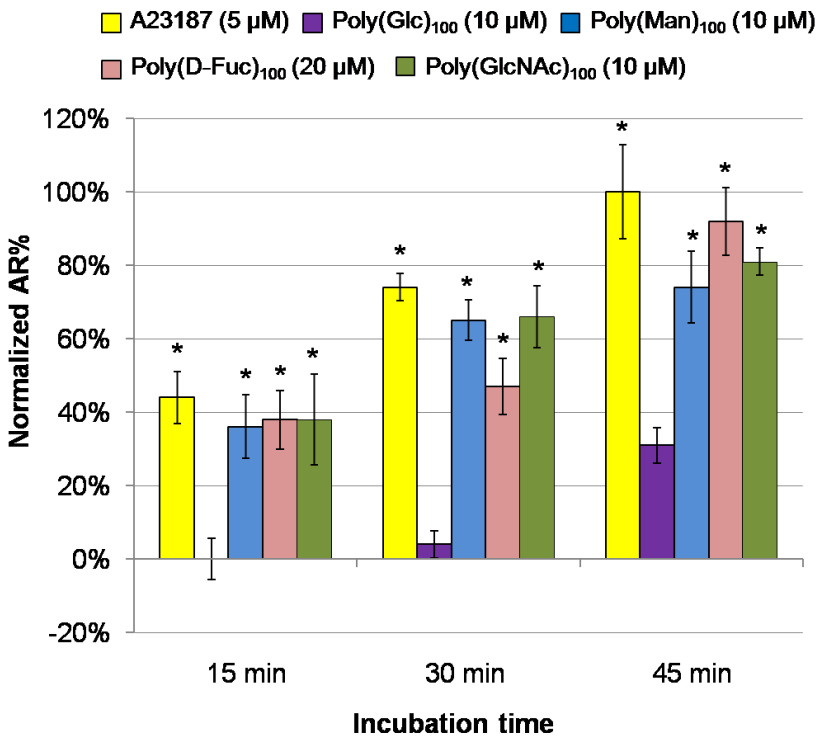

Figure 3-8. Poly(D-Fuc)$_{100}$ has similar AR activation rate as poly(Man)$_{100}$ and poly(GlcNAc)$_{100}$. The concentration shown in the chart is polymer concentration. The average AR% of glycopolymer treated sperm were normalized using [AR%(glycopolymers) – AR%(negative control)]/[AR%(positive control) – AR%(negative control)]. The average AR% for the positive control, A23187-treated (5 μM) sperm at 45 min was 33% and for the negative control, poly(Glc)$_{100}$-treated sperm at 15 min, was 9%. Data represent mean ± SEM of at least three independent experiments. * $p < 0.05$ when compared to the AR% of poly(Glc)$_{100}$ at each time point.

1.6. Signaling pathway of glycopolymers induced AR

Which signaling transduction events are activated by AR-active glycopolymers were also examined by using well characterized inhibitors for protein kinase A (PKA), protein kinase C (PKC), protein tyrosine kinase (PTK), G-protein, T-type/L-type Ca^{2+} channels and extracellular Ca^{2+}. These signaling molecules and channels have been detected in both mouse and human sperm and have been suggested to play an important role in both the mouse and the human ZP-

induced acrosome reaction (Loeser, Lynch et al. 1999, Chiu, Wong et al. 2008). In each signaling pathway inhibition assay, the glycopolymers were added to the sample 10 min after the incubation of the inhibitor with the sperm. Inhibitors do not completely abolish the spontaneous AR and sperm incubated with inhibitor alone served as a negative control. The inhibition was defined as no significant difference between the negative control and the sperm sample tread with both glycopolymer and inhibitor. In the results (**Figure 3-9**), all seven inhibitors significantly suppressed poly(Man)$_{100}$-, poly(GlcNAc)$_{100}$- and poly(Fuc)$_{100}$-activated AR with at least 60% inhibition. However, PKA inhibitor (H89) and PTK inhibitor (genistein) had limited effect on poly(D-Fuc)$_{100}$-induced AR (**Figure 3-10**).

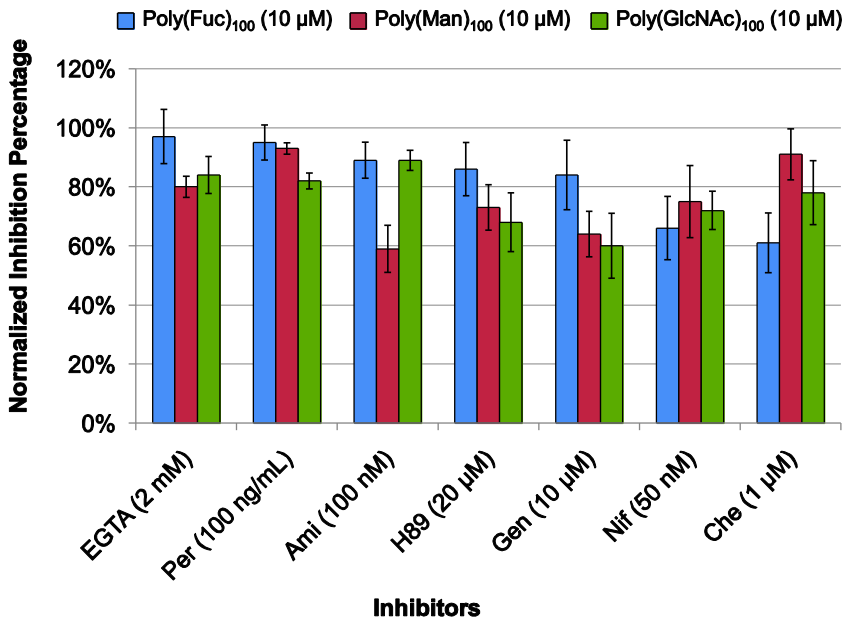

Figure 3-9. The signaling pathways of AR activation by the three inducing glycopolymers are similar. **EGTA**: ethylene glycol tetraacetic acid, extracellular Ca^{2+} inhibitor. **Per**: pertussis toxin, G-protein inhibitor. **Ami**: amiloride hydrochloride, T-type Ca^{2+} channel inhibitor. **H89**: protein kinase A inhibitor. **Gen**: genistein, protein tyrosine kinase inhibitor. **Nif**: nifedipine, L-type Ca^{2+} channel inhibitor. **Che**: chelerylthrine, protein kinase C inhibitor. The average AR% of inhibitor and glycopolymer treated sperm were normalized using [AR%(positive control) – AR%(glycopolymers)]/[AR%(positive control) – AR%(negative control)]. The average AR% for the positive control, A23187-treated (5 μM) sperm, was 24%, and for the negative control inhibitor-treated sperm, was 9-13%. Data represent mean ± SEM of three independent experiments.

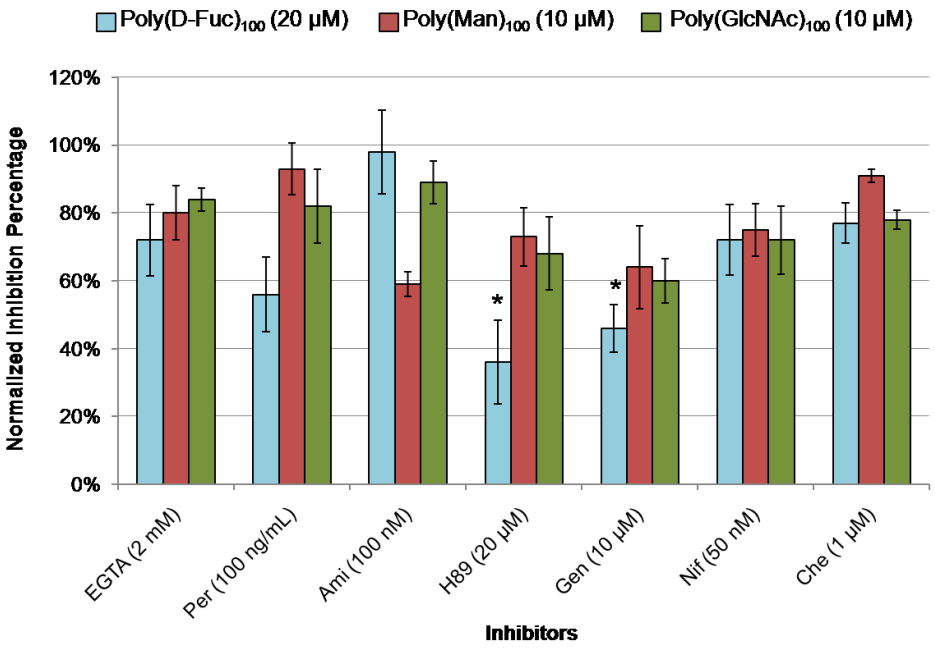

Figure 3-10. Poly(D-Fuc)$_{100}$-activated AR requires different signaling pathways. **EGTA**: ethylene glycol tetraacetic acid, extracellular Ca^{2+} inhibitor. **Per**: pertussis toxin, G-protein inhibitor. **Ami**: amiloride hydrochloride, T-type Ca^{2+} channel inhibitor. **H89**: protein kinase A inhibitor. **Gen**: genistein, protein tyrosine kinase inhibitor. **Nif**: nifedipine, L-type Ca^{2+} channel inhibitor. **Che**: chelerylthrine, protein kinase C inhibitor. The average AR% of inhibitor and glycopolymer treated sperm were normalized using [AR%(positive control) – AR%(glycopolymers)]/[AR%(positive control) – AR%(negative control)]. The average AR% for the positive control, A23187-treated (5 µM) sperm, was 24%, and for the negative control inhibitor-treated sperm, was 9-13%. Data represent mean ± SEM of three independent experiments. * $p < 0.05$ when compared to the sperm sample treated with 100-mer alone.

1.7. Summary

A multivalent display of mannose, GlcNAc, or fucose triggers sperm acrosome reaction in a concentration-dependent manner, and high (100 ligands) valency polymers are more effective than low (10 ligands) valency polymers. Though fucose showed lower AR activation potency and the kinetics of fucose-induced AR are distinct from those of mannose or GlcNAc-induced AR, the signaling pathways of the three glycopolymers-activated AR are similar. All the three

glycopolymers rely on G-protein, protein kinase C, protein kinase A, extracellular Ca^{2+}, L- and T-type Ca^{2+} channels, and protein tyrosine kinase. Interestingly, the D-fucose polymers also show concentration-dependent AR activation abilities, and poly(D-Fuc)$_{100}$ paired with poly(Man)$_{100}$ and poly(GlcNAc)$_{100}$ at high and low concentrations demonstrate similar AR activation pattern as the pairs of the above three 100-mers. However, the poly(D-Fuc)$_{100}$-induced AR does not require PKA and PTK for signaling transduction and proceeds at a slower rate than poly(Man)$_{100}$- or poly(GlcNAc)$_{100}$-activated AR.

2. Investigation of synthetic methods to prepare fertilization probes

2.1. Synthesis of tripeptide-conjugated polymers

The cyclobutyl tripeptide monomers, CB-E(OtBu)AD(OtBu), CB-GCD and CB-E(OtBu)C(Acm)D(OtBu) were synthesized by Fmoc or Cbz α-amino protection in solution phase. The side-chains on monomers were protected with *tert*-butyl, acetamidomethyl (Acm) or trityl groups. Typically amino acid couplings were performed in dichloromethane with N-(3-dimethylaminopropyl)-N′-ethylcarbodiimide hydrochloride (EDC), 1-hydroxy-benzotriazole (HOBT), and *N*,*N*,-diisopropylethylamine (DIPEA). The Fmoc group was removed with 1-octanethiol and a catalytic amount of 1,8-diazabicyclo[5.4.0]undec-7-ene (DBU), and the Cbz group was removed by hydrogenation with 10% Pd/C in dichloromethane/methanol. Coupling and deprotection reactions were monitored by thin layer chromatography (TLC). Synthesized compounds were purified by Combiflash chromatography and characterized by ^{1}H and ^{13}C NMR

spectroscopy and ESI mass spectroscopy. The full synthesis of tripeptide monomers are shown in **Scheme 3-10** to **Scheme 3-12**.

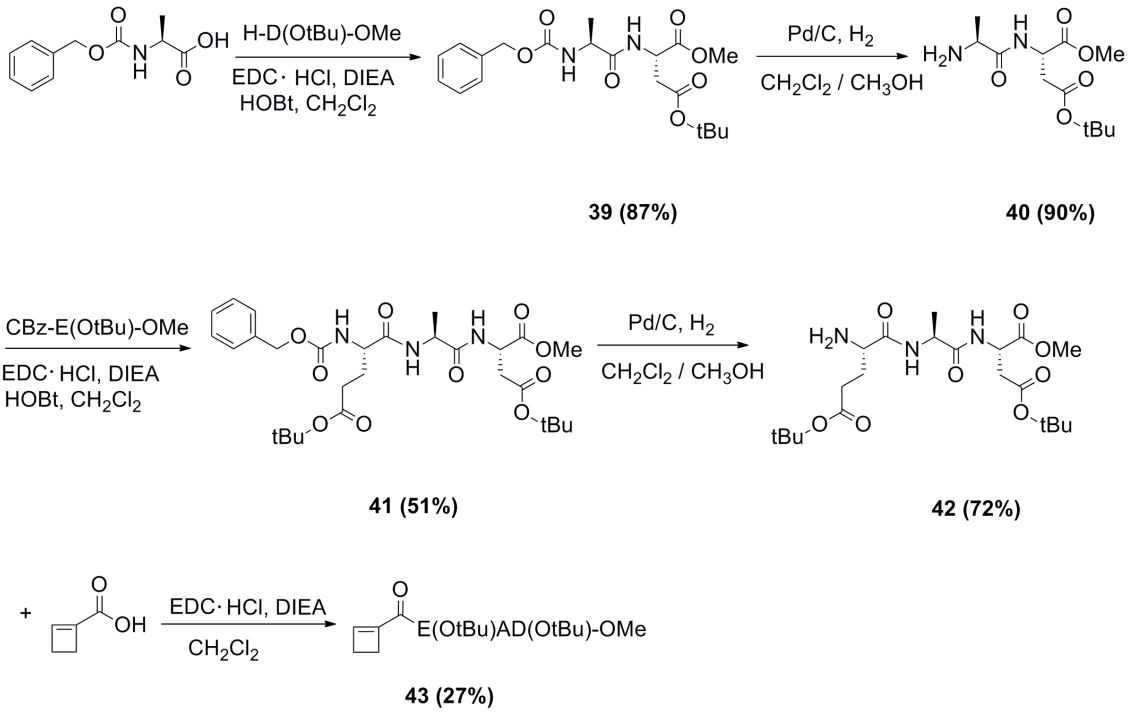

Scheme 3-10. Synthesis of CB-E(OtBu)AD(OtBu).

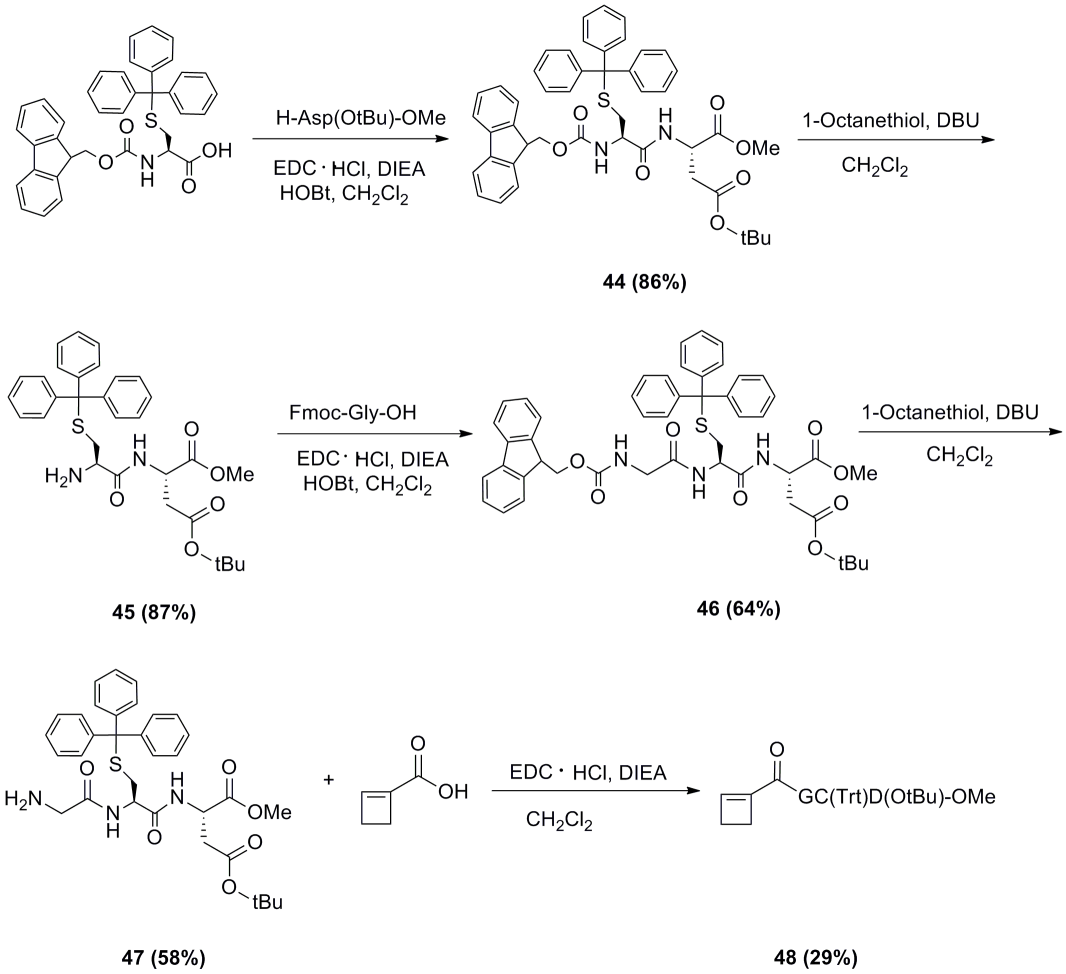

Scheme 3-11. Synthesis of CB-GC(Trt)D(OtBu).

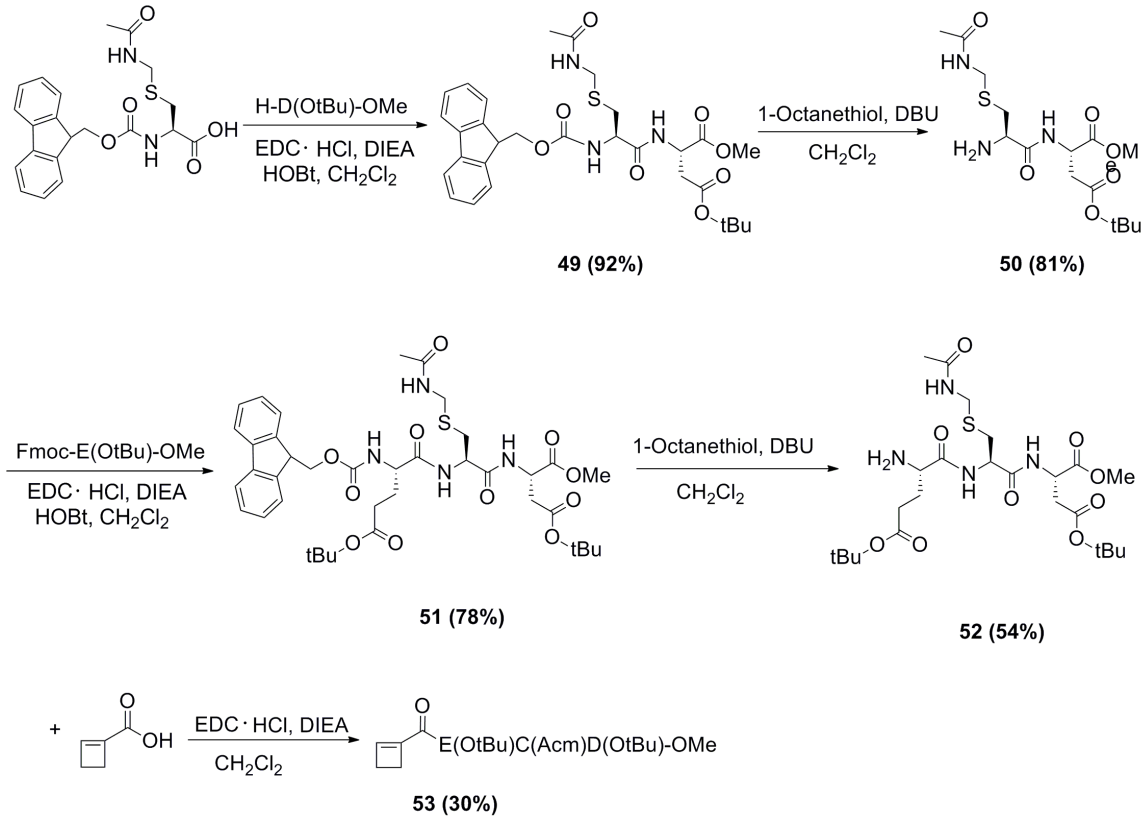

Scheme 3-12. Synthesis of CB-E(OtBu)C(Acm)D(OtBu).

The monomers were polymerized by ROMP with catalyst $(H_2IMes)(PCy_3)_2Cl_2Ru$=CHPh **32** in dichloromethane, and the polymerizations were terminated by adding ethylvinyl ether (**Scheme 3-12**). We tried to prepare 10-mers from the three tripeptide monomers. However, the polymerization did not go to completion and all of the cyclobutyl polymers were shorter than expected. CB-GC(Trt)D(OtBu) and CB-E(OtBu)AD(OtBu) both formed 6-mers based on crude NMR integration, while the ROMP of CB-E(OtBu)C(Acm)D(OtBu) only formed a 4-mer (from crude NMR integration), the same as that of CB-E(OtBu)C(Trt)D(OtBu).

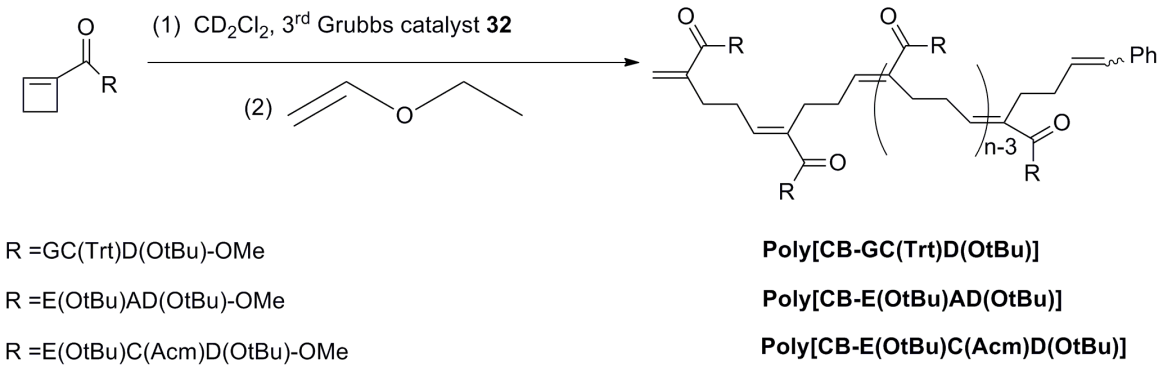

R =GC(Trt)D(OtBu)-OMe

R =E(OtBu)AD(OtBu)-OMe

R =E(OtBu)C(Acm)D(OtBu)-OMe

Poly[CB-GC(Trt)D(OtBu)]

Poly[CB-E(OtBu)AD(OtBu)]

Poly[CB-E(OtBu)C(Acm)D(OtBu)]

Scheme 3-13. ROMP of tripeptide-conjugated polymers.

None of the tripeptide monomers were completely consumed. The crude ^{1}H NMR spectra showed that CB-GC(Trt)D(OtBu) and CB-E(OtBu)AD(OtBu) formed 6-mers while CB-E(OtBu)C(Acm)D(OtBu) formed a 4-mer.

More polar solvents, CD_2Cl_2/CD_3OD (v/v = 3/1) with 3M LiCl or CD_2Cl_2/d_7-DMF (v/v = 1/1) were used to solubilize the polymers during the polymerization (**Scheme 3-13, Scheme 3-14**). However, no enhancement was observed and only 5-mer was obtained (based on crude NMR integration).

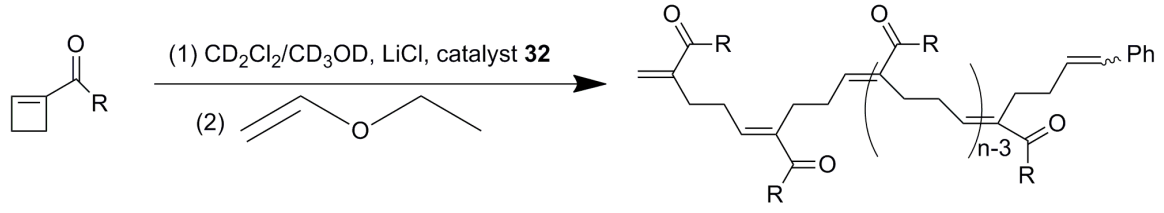

R =GC(Trt)D(OtBu)-OMe

Poly[CB-GC(Trt)D(OtBu)]

Scheme 3-14. ROMP of poly[CB-GC(Trt)D(OtBu)] with LiCl.

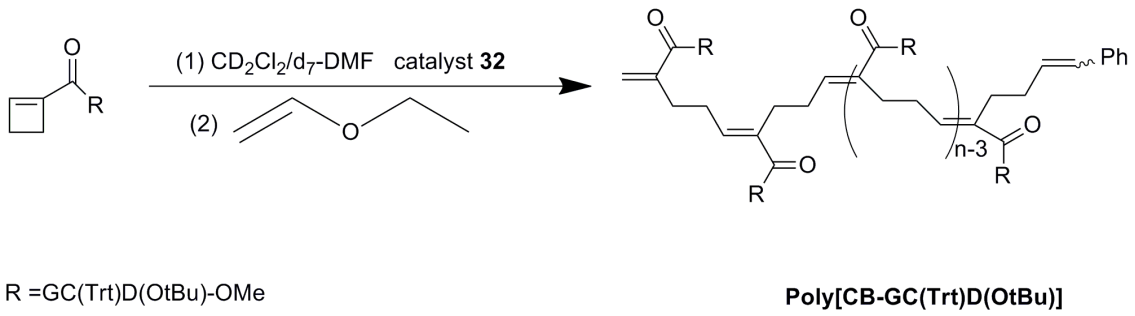

Scheme 3-15. ROMP of poly[CB-GC(Trt)D(OtBu)] with d_7-DMF.

2.2. The kinetics of ROMP

The kinetics of ROMP for these tripeptide-conjugated monomers were studied by NMR (**Figure 3-11**). The degree of polymerization was calculated by comparing the polymer peak integration at different time points to the theoretical peak integration at 100% conversion. In our experiments, 100% conversion is 10-mer, thus, 60% equals 6-mer. The polymerization was quenched, if no more conversion was observed. Among the three monomers, CB-E(OtBu)AD(OtBu) has the highest initiation and propagation rates, achieving the 60% conversion in the shortest time. CB-GC(Trt)D(OtBu) shows similar reaction trend to CB-E(OtBu)AD(OtBu) but is much slower to reach its conversion peak. The ROMP of CB-GC(Trt)D(OtBu) stops at about 600 min and that of CB-E(OtBu)AD(OtBu) stops at about 200 min. CB-E(OtBu)C(Acm)D(OtBu) has the slowest reaction rate and lowest conversion yield compared to the other two tripeptides. The conversion yield is about 40% which is similar to CB-E(OtBu)C(Trt)D(OtBu).

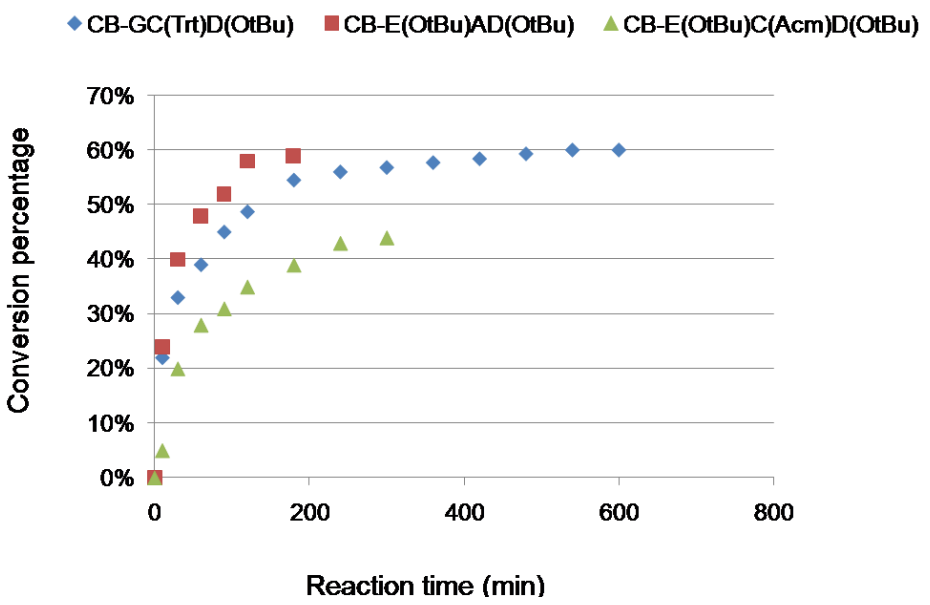

Figure 3-11. The kinetics of ROMP for the three tripeptide monomers.

To study the steric effects of the side chain, GGG was selected as a good candidate. Methylation of NH_2-GGG-CO_2H with CH_3COCl in methanol was successful. However, the reaction to couple CB with NH_2-GGG-OMe failed several times.

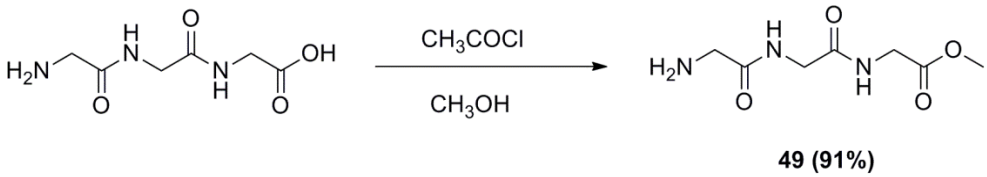

Scheme 3-16. Synthesis of GGG.

Due to the polarity of the tripeptides, the propagating polymer chains may precipitate prematurely in a nonpolar solvent, which may not be observed by eye. All the above ROMP experiments were run in CD_2Cl_2, a relatively nonpolar solvent, in an NMR tube. According to

the results from Roberts *et al.* (Roberts and Sampson 2003), the addition of LiCl to the solvent can greatly increase the polymer length of oligopeptide-substituted polynorbornenes by increasing the solubility of the propagating polymer chain. Thus, another ROMP reaction of CB-GC(Trt)D(OtBu) in CD_2Cl_2/CD_3OD (v:v=3:1) with LiCl was conducted and the degree of polymerization was also measured as above. In our result (**Figure 3-12**), the initiation rate was improved significantly, but the conversion percentage was even lower compared to that of NB-GC(Trt)D(OtBu) in CD_2Cl_2 alone. To promote ROMP of the monomers, another more polar solvent pair CD_2Cl_2/d_7-DMF (v/v=1:1) was applied. Similarly, no enhancement of polymerization rate was observed and only 5-mer was formed (**Figure 3-12**). The 1st Grubbs catalyst, $(PCy_3)_2Cl_2Ru$=CHPh was also tested to compare the activity of different catalysts. There was no initiation at all when CB-GC(Trt)D(OtBu) was mixed with the catalyst. Thus far, no further experiments have been performed to investigate the failed ROMP of cyclobutyl-tripeptides.

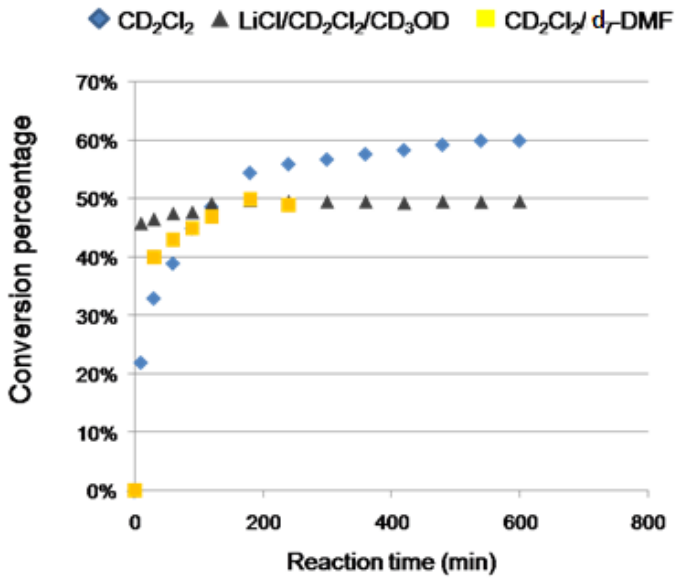

Figure 3-12. The solvent effects in the ROMP of the three monomers.

2.3. Summary

Less hindered cyclobutyl tripeptides, CB-E(OtBu)AD(OtBu), CB-GC(Trt)D(OtBu), CB-E(OtBu)C(Acm)D(OtBu) were prepared and their reactivity in ROMP were compared to CB-E(OtBu)C(Trt)D(OtBu). Though CB-E(OtBu)AD(OtBu) and CB-GC(Trt)D(OtBu) generated longer polymers in ROMP than CB- E(OtBu)C(Acm)D(OtBu) and CB-E(OtBu)C(Trt)D(OtBu), none of the polymerization reaction went to completion. LiCl and more polar solvents were added to the reaction, but no improvement of degree of polymerization was achieved. However, a large increase of the initiation rate was observed. A non-hindered CB-GGG could not be synthesized. Moreover, the 1st Grubbs catalyst could not initiate the ROMP of cyclobutyl tripeptides.

Chapter 4

Discussion

1. Analysis of ROMP-derived multivalent ligands

    1.1. Synthesis of glycomonomers

    1.2. ROMP of glycopolymers

    1.3. ROMP of tripeptide-conjugated polymers

2. Analysis of glycopolymers as probes for AR activation

    2.1. Mechanism of glycopolymers-activated AR

    2.2. Comparison of ROMP glycopolymers with other multivalent conjugates

4. Future plan

1. Analysis of ROMP-derived multivalent ligands

1.1. Synthesis of glycomonomers

Acetyl group is one of the most common protecting groups for carbohydrates, since it can be easily introduced with high yield and removed under simple basic conditions (Kováč, Sokoloski et al. 1984). However, regioselective deprotection of acetylated sugars is still a challenge. Generally, anomeric acetates are considerably more reactive than primary and secondary acetates. Hydrazine is broadly used to regioselectively deacetylate the anomeric acetate, and the reaction usually affords quantitative transformation within short reaction time (Greene, Wuts et al. 1999). However, the conventional hydrazine method did not work for GlcNAc and GalNAc. The yields for the target 1-hydroxyl GlcNAc and GalNAc were very low and over-deacetylation was observed. Therefore, a milder method with ammonium acetate was applied. The reaction was monitored by TLC to prevent over-deacetylation. Although longer reaction time (14 h for GlcNAc and 7 h for GalNAc) was needed and some impurities were also generated, ammonium acetate method was non-toxic and afforded the target product in good yield after chromatography purification.

Trichloroacetimidates have become popular glycoside intermediates since 1980 (Schmidt and Michel 1980). The use of trichloroacetimidates provides many advantages including ease of formation, excellent glycosyl-donor properties and stereochemical outcome (Zhu and Schmidt 2009). In our work, the stereoselective glycosides were generated after the trichloroacetonitrile

group was replaced by 2-chroloethanol. However, trichloroacetimidates are unstable. They should be purified quickly after the reaction and used immediately for the next step.

Norbornene coupled carbohydrates can be synthesized by the standard peptide-coupling of glycosylamines with activated carboxylic acids. However, glycosylamines are relatively unstable and thus this method has often been shown to be rather unsatisfactory. Staudinger ligation provides a facile alternative, which allows the formation of amide-linked glycosides from carbohydrate azides and carboxylic acids mediated by a combination of diisopropylcarbodiimide (DIC), 1-hydroxybenzotriazole (HOBt) and a suitable phosphane. Tri-*n*-butylphosphane was used in our synthesis. This method saves one step and has high conversion yield. However, it is important to conduct the reaction at a low temperature (0 ℃) in the beginning for the formation of the phosphane-azide intermediate. No ligation product was observed, if the reaction was carried out at room temperature (25 ℃).

Although the synthesis of glycomonomers followed similar protocols, the reaction conditions of each step for different carbohydrates were not exactly the same. Especially, the reaction time of a same step varied for different carbohydrates. A small scale reaction was usually conducted first to determine the optimal reaction conditions. Water can harm many glycosylation reactions. Thus, in many steps, water was removed from the sticky carbohydrate intermediates through formation of an azeotrope with toluene before use in the subsequent step. GalNAc is the most polar carbohydrate among the seven carbohydrates. Even fully acetylated GalNAc could dissolve in water. Therefore, aqueous work-ups were usually avoided to prevent product loss in the synthesis of NB-GalNAc.

1. 2. ROMP of glycopolymers

Though all glycopolymers were prepared with the same ROMP protocol (**Scheme 3-7**), not all of them showed the same polymerization rate. The reaction time for poly(Man)$_{10}$, poly(Glc)$_{10}$, poly(Gal)$_{10}$ and poly(GlcNAc)$_{10}$ was 1 h, but poly(Fuc)$_{10}$ and poly(GalNAc)$_{10}$ reacted in only 0.5 h (**Table 3-1**). The shorter reaction time for poly(Fuc)$_{10}$ and poly(GalNAc)$_{10}$ suggests that NB-fucose and NB-GalNAc have higher reactivity in ROMP. Why these two monomers react faster than the others is unclear. However, it is certain that polarity is not the driving force, because fucose is the least polar carbohydrate among all the carbohydrates, while GalNAc is the most polar one based on their Rf values on the TLC. Similarly, the ROMP of poly(Fuc)$_{100}$ and poly(GalNAc)$_{100}$ (1 h) was also more efficient than that of the other 100-mers (1.5 h) (**Table 3-1**). The monomers for the ROMP of 10-mers and 100-mers were all from the same batch, and they were pure based on NMR and TLC.

All of the glycopolymers have relatively low PDIs, ranging from 1.11 to 1.39. However, their calculated molecular weights (Mn) are smaller than the theoretical Mns (**Table 3-1**). To generate longer polymers, we lengthened the reaction time to 2 h for the 10-mers and 2.5 h for the 100-mers. Polymers with slightly increased Mns were obtained, but their PDIs were significantly broadened. Increasing temperature is another alternative to promote the polymerization, but high temperatures also produced broadly-distributed molecular weights. Since all of the monomers were consumed (monitored by TLC) and no chain-transfer reaction (**Figure 4-1**) was observed by NMR spectroscopy, no further modifications of the ROMP conditions were pursued. For more accurate interpretation of the biological assays, we utilized the glycopolymers with narrow PDIs although the Mns were lower. Altogether, these results

provide useful information for the preparation of hetero-glycopolymers in the future.

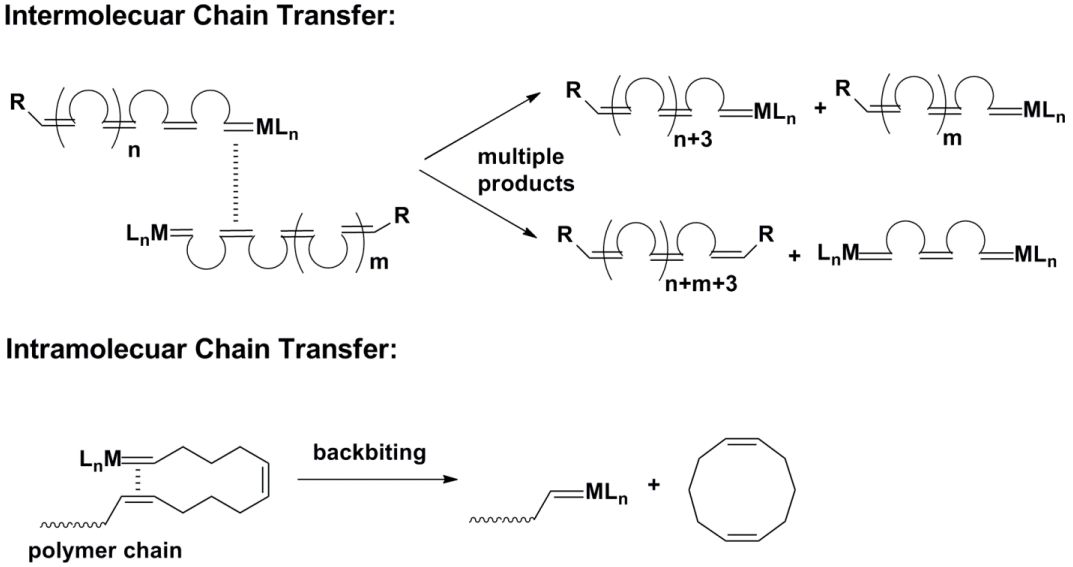

Figure 4-1. Examples of chain transfer in ROMP.

1. 3. ROMP of tripeptide-conjugated polymers

When the same ROMP protocol used for NB-E(OtBu)C(Trt)D(OtBu) 10-mer was applied to the three CB tripeptides, we were not able to prepare the desired 10-mers. Based on the monomer structures (**Figure 2-10**) and the mechanism of ROMP, it is possible that the steric hindrance on the 1-substituted cyclobutene prevents the complete polymerization of CB-E(OtBu)C(Trt)D(OtBu) (**Figure 4-2**). The kinetic results for the three tripeptide monomers (**Figure 3-7**) also showed that the ROMP propagation rate can be increased by reducing the steric hindrance on the peptide side chains. Meanwhile, a smaller amino acid instead of a bulky one coupled to CB directly [CB-**G**C(Trt)D(OtBu) Vs. CB-E(OtBu)**A**D(OtBu)] had no improvement on the polymerization rate and the degree of polymerization. The reason why CB-

GC(Trt)D(OtBu) has slower propagation rate than CB-E(OtBu)AD(OtBu) still needs further investigation. Although the relationship of ROMP reactivity to the distance between the backbone (CB) and amino acids is unclear from these results, the right linker inserted in between the CB and the peptide may be helpful to reduce the steric effect.

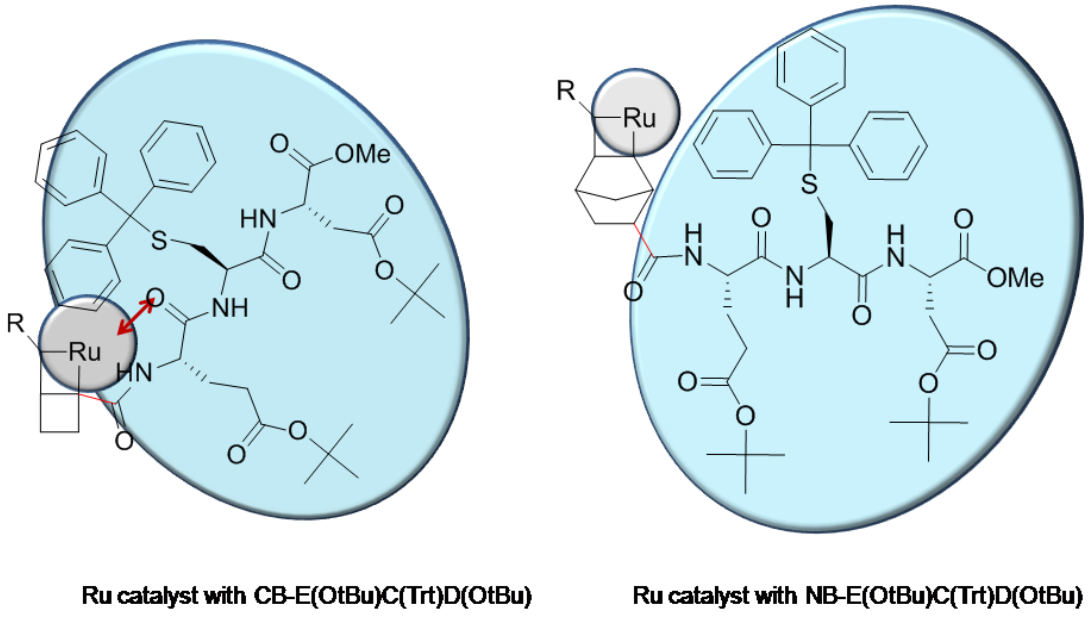

Figure 4-2. Steric hindrance between Ru catalyst and E(OtBu)C(Trt)D(OtBu) tripeptide.

In the study of solvent effects in ROMP (**Figure 3-8**), the replacement of CD_2Cl_2 with two more polar solvent pairs could not improve the ROMP of CB-GC(Trt)D(OtBu). In the case with the solvent pair CD_2Cl_2/CD_3OD (v:v=3:1) and LiCl, one possible reason is due to the immiscibility of the CD_3OD (containing LiCl) and the CD_2Cl_2 (containing polymer and catalyst) layers. It is likely that a small amount of LiCl dissolved in the CD_2Cl_2 layer can enhance the polymer chain solubility, which leads to a faster reaction rate in the first 20 minutes. As no more LiCl dissolves in CD_2Cl_2 layer, the immiscibility of solvents prevents the effective contact

between the polymer and the catalyst, and the reaction rate drops severely—it stopped at about 90 min. Another solvent pair CD_2Cl_2/d_7-DMF, which is miscible and dissolves both the monomer and the catalyst very well, was applied. However, complete polymerization of CB-GC(Trt)D(OtBu) failed to occur. We think the reason may also be due to the fact that the oxygen in CD_3OD and DMF chelate with the ruthenium in the catalyst (Haigh, Kenwright et al. 2005), which blocks the coordination between the monomer and the catalyst.

No initiation was observed when CB-GC(Trt)D(OtBu) was mixed with the 1st Grubbs catalyst, $(PCy_3)_2Cl_2Ru$=CHPh, which could be due to the lower stability and/or lower functional group tolerance of the catalyst. The 2nd Grubbs catalyst was not tested because it produces polymers with uncontrolled molecular weights and broad polydispersities according to Grubbs and coworkers (Maynard, Okada et al. 2001). Overall, new strategies to prepare stereo-selective E(OtBu)C(Trt)D(OtBu) polymers and even other functional biomolecule-bearing polymers are needed.

2. Analysis of glycopolymers as probes for AR activation

2. 1. Mechanism of glycopolymers-activated AR

Testing the functions of molecules that have been implicated in mediating sperm AR is the first step for understanding the molecular mechanisms of the AR. Probe-protein interaction studies are valuable tools in many biological systems, but they have been applied in a limited

fashion to fertilization because of the limited quantities of material available and the lack of cell culture models. Most experiments in the field of fertilization biology rely on genetic and immunohistochemical methods. Here, we employed synthetic polymers incorporated with ZP3 terminal carbohydrates to explore the mechanism of AR activation.

First, we examined the effect of glycopolymers on AR by sperm immunofluorescent assay (**Figure 3-3**). The data was normalized for better comparison. A significantly greater number of sperm underwent the AR when treated with 100 μM poly(Man)$_{10}$, poly(Fuc)$_{10}$, and poly(GlcNAc)$_{10}$. The AR induction by these three 10-mers is in a dose-dependent manner, but poly(Fuc)$_{10}$ is not as effective as the other two 10-mers. Similarly, dose-dependent AR initiation was also observed when sperm incubated with poly(Man)$_{100}$, poly(Fuc)$_{100}$, and poly(GlcNAc)$_{100}$, and poly(Fuc)$_{100}$ is less efficient in AR activation. Neither NB-galactose nor NB-glucose polymers induced the AR at different concentrations, indicating that galactose or GalNAc may play a role in sperm-egg binding but not the AR. Taken together; these results strongly suggest mannose, GlcNAc and fucose function as sperm AR activators, and the synthesized glycopolymers are useful multivalent tools to study the AR. The higher potency of the 100-mers further confirms that the polymers stimulate the AR through a multivalent interaction with sperm. At the maximal concentration tested (200 μM for the 10-mers and 20 μM for the 100-mers), reduced AR% were observed. We think this is because at high polymer concentrations multivalent binding and thus the clustering effect are not favored (**Figure 4-3**) (Gestwicki, Cairo et al. 2002).

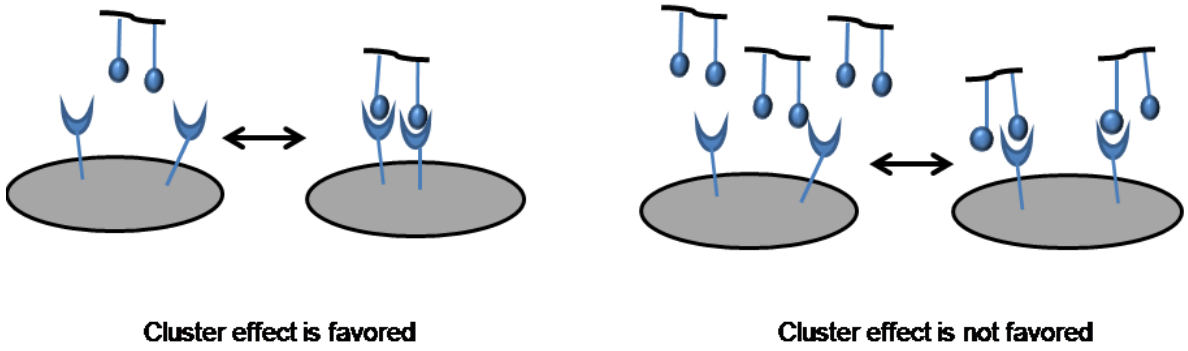

Figure 4-3. The cluster effect is not favored by the high local concentration of multivalent ligands.

In the study of D-fucose polymers (**Figure 3-4**), a dose-dependent AR activation by D-fucose polymers was also observed. Poly(D-Fuc)$_{100}$ could not activate AR at 5 μM, but it reached the maximum AR activation at 20 μM, two-fold higher than the optimal concentrations of other effective 100-mers. Interestingly, the maximum AR% activated by poly(D-Fuc)$_{100}$ was slightly higher than that by poly(Fuc)$_{100}$, though higher concentration of poly(D-Fuc)$_{100}$ was required. The lower potency of poly(D-Fuc)$_{100}$ is also consistent with the lower activation efficacy observed with poly(D-Fuc)$_{10}$. Why the unnatural D-fucose can also bind to sperm and trigger the AR is still unclear.

As 100-mers revealed better AR inducing ability, we further studied their characteristics and effects on the AR. The effect of mixed 100-mers on AR was measured and compared with that of the corresponding single 100-mers. No further increase in the amount of sperm AR comparing the polymer pairs and single glycopolymers at their optimal (10 μM) and much lower (2.5 μM) concentrations (**Figure 3-5**) was observed. This result reveals that the AR activation was maxed out at the optimal concentration of glycopolymers, and that the three carbohydrate ligands bind to different binding sites on the sperm. The pairwise mixtures (2.5 μM each) were less effective than a single polymer at 5 μM—the total concentration of the paired mixtures. We think that

there is a concentration threshold for glycopolymer-receptor binding and signal transduction. Altogether, the data suggests that maximal sperm AR is achieved upon treatment with a single homopolymer at its optimal concentration, and that the three sugars act independently to activate the AR. Poly(D-Fuc)$_{100}$ paired with poly(Man)$_{100}$ and poly(GlcNAc)$_{100}$ at 10 μM and 2.5 μM each also showed no AR% enhancement compared to their single 100-mers (**Figure 3-6**). Although poly(D-Fuc)$_{100}$ could not activate AR at 5 μM, it was slightly more effective than poly(Fuc)$_{100}$ at 2.5 μM.

In the time-course study assay (**Figure 3-7**, **Figure 3-8**), the AR activation kinetics of the four glycopolymers were tested at their optimal concentrations—20 μM for poly(D-Fuc)$_{100}$, and 10 μM for poly(Man)$_{100}$, poly(D-Fuc)$_{100}$, and poly(GlcNAc)$_{100}$. At the 15 min time point, poly(Fuc)$_{100}$-activated AR was very low but poly(D-Fuc)$_{100}$-activated AR was comparable to poly(Man)$_{100}$- and poly(GlcNAc)$_{100}$-activated AR. At 45 min, poly(D-Fuc)$_{100}$-activated AR even exceeded poly(Man)$_{100}$- and poly(GlcNAc)$_{100}$-activated AR. These observations together suggest that poly(D-Fuc)$_{100}$ needs longer time and higher concentration to achieve maximum AR activation, and poly(Fuc)$_{100}$ induce AR in a slower rate than the other glycopolymers.

The precise sperm AR signaling pathways are not completely elucidated, though several tentative signaling pathway mechanisms of ZP-initiated AR have been proposed (Breitbart and Spungin 1997, Gupta and Bhandari 2011, Tulsiani 2012). In these mechanisms (**Figure 1-5**), ZP is thought to bind to at least two receptors on the sperm membrane. One is a G-protein coupled receptor, which is thought to regulate adenylyl cyclase and activate PKA, phospholipase C (PLC) β1 and H^+ efflux. Upon activation, PKA phosphorylates and further triggers downstream factors. The other is a PTK receptor, which is suggested to trigger a sperm Na^+/H^+ exchanger promoting cell alkalinization, membrane depolarization, and T-type and L-type calcium channels activation

on the sperm plasma membrane. The calcium channels play vital roles in elevating intracellular Ca^{2+} and pH preceding the AR. G-protein and PTK can also activate PKC, which mediates calcium entry into the sperm cytosol from intracellular stores. These signaling factors all lead to an increase in cytosolic calcium, resulting in the fusion of sperm plasma membrane and the outer acrosomal membrane, and eventually the AR.

The seven chosen inhibitors do not have absolute specificity; they block AR activation non-selectively at high concentrations. The toxicity of the inhibitors was examined and the dose was carefully chosen in order to not affect sperm viability and motility. For EGTA, Per, and Ami, only one concentration (2mM for EGTA, 100 ng/mL for Per, 100 nM for Ami) was widely tested (Loeser, Lynch et al. 1999, Hanna, Kerr et al. 2004, Chiu, Wong et al. 2008), so we also chose the same concentration for our assay. Several concentrations of the other four inhibitors were reported previously (Loeser, Lynch et al. 1999, Chiu, Wong et al. 2008), therefore, we tested the effects of one high and one low concentrations of each inhibitor. Sperm motility is an important parameter to evaluate sperm function. In our results (**Figure 4-4**), most of the inhibitors did not affect the sperm motility except for Nif at 50 μM, indicating only Nif at 50 μM was toxic to the sperm. Though higher concentrations of some inhibitors did not harm sperm motility, we chose the lower concentrations to prevent non-selective inhibition.

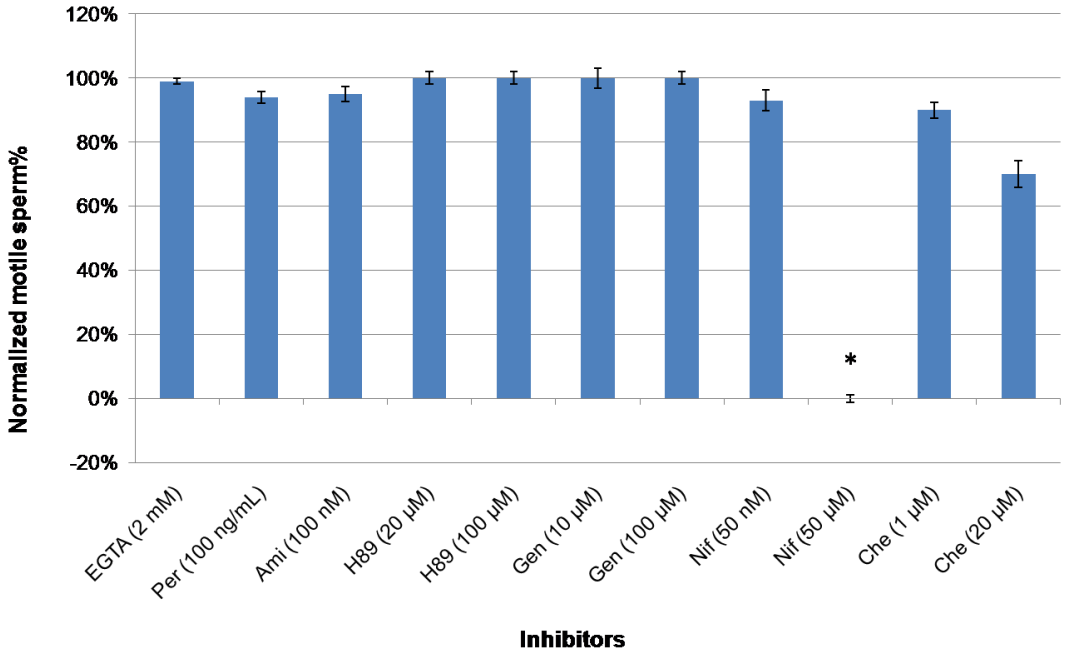

Figure 4-4. Inhibitor toxicity test. **EGTA**: ethylene glycol tetraacetic acid, extracellular Ca^{2+} inhibitor. **Per**: pertussis toxin, G-protein inhibitor. **Ami**: amiloride hydrochloride, T-type Ca^{2+} channel inhibitor. **H89**: protein kinase A inhibitor. **Gen**: genistein, protein tyrosine kinase inhibitor. **Nif**: nifedipine, L-type Ca^{2+} channel inhibitor. **Che**: chelerylthrine, protein kinase C inhibitor. The average percentage of motile sperm treated with inhibitor alone were normalized using motitle sperm (inhibitor)% / motitle sperm (control)%. The average motitle sperm% for the control (without inhibitor) was 85%. Data represent mean ± SEM of three independent experiments. * $p < 0.05$ when compared to the control.

The $poly(Man)_{100}$-, $poly(GlcNAc)_{100}$-, and $poly(Fuc)_{100}$-activated AR require all the above-described signaling factors (**Figure 3-9**). However, $poly(D\text{-}Fuc)_{100}$-activated AR does not rely on PKA and PTK for signaling transduction (**Figure 3-10**). These results demonstrate that glycopolymer-activated AR signaling pathways all terminate in a G-protein and PKC-dependent network that activates cytosolic Ca^{2+} stores, but the upstream signaling for $poly(D\text{-}Fuc)_{100}$ appears distinct from the signal pathway activated by the other three carbohydrates. As the four glycopolymers all activate AR, it is not surprising to find that they share some signaling pathways in common. Thus, $poly(Man)_{100}$, $poly(GlcNAc)_{100}$, and $poly(Fuc)_{100}$ activate the AR

though convergent signaling pathways, while poly(D-Fuc)$_{100}$ undergos divergent signaling pathways for AR activation. However, whether (D-Fuc)$_{100}$ binds to a different binding site on the sperm results in the distinct signaling pathways involved in poly(D-Fuc)$_{100}$-activated AR remains unknown. Sperm treated with inhibitors alone also showed a low AR percentage consistent with a low level of spontaneous AR that is independent of these pathways.

Our work emphasizes the high redundancy of carbohydrate ligands that can be used to activate the AR. In contrast to conditional genetic knockouts for which no AR phenotypes were observed, the use of glycopolymers has enabled the identification of which terminal carbohydrates are important for the AR. The glycopolymer chemotypes observed in this work suggest that at least three different sperm receptor binding sites can be utilized to initiate the AR in mouse. After receptor activation by glycopolymer, signaling converges onto the same pathways intracellularly.

The receptors activated by poly(Man)$_{100}$, poly(GlcNAc)$_{100}$, and poly(Fuc)$_{100}$ have not been definitively identified. None of the large number of egg binding receptors proposed and characterized has been demonstrated to be essential (Tsai and Silver 1996, Lu and Shur 1997, Muro, Buffone et al. 2012). Previous results also suggested a high level of redundancy, but whether multiple egg binding receptors acted individually or as a multi-protein complex was unclear. Our results favor the single ligand-receptor interaction model and provide further evidence that induction of the sperm acrosome reaction proceeds through duplicative sperm-egg interactions.

2.2. Comparison of ROMP glycopolymers with other multivalent conjugates

Table 4-1. Comparison of signaling pathways initiated by different activators.

Signaling molecule / AR activator	Extracellular Ca^{2+}	T-type Ca^{2+}	L-type Ca^{2+}	PKC	PKA	PTK	G protein
BSA-mannose/ GalNAc/GlcNAc[a]	-[b]	-	+[c]	-	-	-	-
BSA-Lewis X[d]	+	+	NA[e]	NA	NA	NA	-
BSA-Lewis A[f]	+	+	NA	NA	NA	NA	-
Mouse ZP[g]	+	+	+	+	+	+	+
$poly(Man)_{100}$	+	+	+	+	+	+	+
$poly(GlcNAc)_{100}$	+	+	+	+	+	+	+
$poly(Fuc)_{100}$	+	+	+	+	+	+	+
$poly(D\text{-}Fuc)_{100}$	+	+	+	+	-	-	+

[a]Data from ref (Loeser, Lynch et al. 1999). [b]–, Signaling pathway is not activated. [c]+, Signaling pathway is activated. [d]Data from ref (Hanna, Kerr et al. 2004). [e]NA, not available, no signaling pathway experiment was performed. [f]Data from ref (Hanna, Kerr et al. 2004). [g]Data from ref (Chiu, Wong et al. 2008).

All of the above-described signaling factors are involved in activation of the AR by $poly(Man)_{100}$, $poly(GlcNAc)_{100}$, and $poly(Fuc)_{100}$, but PKA and PTK are not required for the $poly(D\text{-}Fuc)_{100}$-activated AR. Compared with the globular BSA-conjugated neoglycoproteins, $poly(Man)_{100}$, $poly(GlcNAc)_{100}$, and $poly(Fuc)_{100}$ activate through the same pathways as mouse ZP (**Table 4-1**). Our data strongly support that glycopolymer-activated AR is analogous to ZP-activated AR and that these linear glycopolymers are suitable mimics of the ZP and/or other physiologic ligands for activating sperm AR. Moreover, the three single ligand-receptor

interactions are functionally equivalent, but they are redundant. In conclusion, the chemotypes of ROMP-derived glycopolymers mimic the biological function of physiologic AR-activation agents and provide evidence that occupation of one of at least three different receptor binding sites is sufficient to initiate the AR.

Understanding the mechanisms of the acrosome reaction is important to study the infertility problem, as the assessment of the AR has been shown to be a stable parameter of sperm function and a valid tool to predict the fertilizing potential of human sperm (Henkel, Miiller et al. 1993). Conventional semen analysis results do not correlate with fertility potential well because it only evaluate the sperm numbers but not sperm functional competence (Menkveld, Wong et al. 2001). AR testing has emerged as a useful tool in andrology for research purposes (Suri 2005), but it can also be utilized to predict fertilization success in assisted conception cycles. A common AR testing method, acrosome reaction to ionophore challenge (ARIC), which tests sperm AR function by incubating sperm with Ca^{2+} ionophore, has shown excellent predictive values for outcomes in assisted reproduction (Calvo, Dennison-Lagos et al. 1994). However, the mechanism of the acrosome reaction induced by ionophores differs from the physiological acrosome reaction induced by the ZP. Our synthetic glycopolymers involve the same signaling pathways as the ZP. They can be developed as potential *in vitro* biomarkers to aid in the selection of assisted conception treatment. Currently, AR testing is rarely used in the clinical setting. As a significant proportion of male patients showing unexplained infertility, the increasing demand for the non-invasive treatments could encourage the use of such prognostic sperm tests for both diagnosis and treatment.

4. Future plan

After identifying the effective glycopolymers and their activation mechanisms, there are two questions remained unclear: (1) is a closely-packed density of a single saccharide reqiured for the AR? (2) is the regularity of the spacing between identical saccharides important? To address the first question, a series of random copolymers *stat*-$(A_m/Glc_n)_{100}$ for which the m:n ratio is 1:1 or 1:9 should be prepared. A will be mannose, fucose, or GlcNAc, while our control glucose will be the spacer. Holding the number of active ligand monomers constant and increasing the number of spacer ligand monomers will reveal whether these local density are responsible for activity or whether the heterogeneous presentation of active ligands is the best for AR activation. Song *et. al.* (Song, Parker et al. 2009) have successfully developed a highly alternating polymerization (AROMP) method with cyclobutene 1-carboxylic esters and cyclohexene derivatives. In light of this, AROMP will be used to prepare regularly mixed *alt*-$(A/Glc)_{100}$ and *alt*-$(Glc/A)_{100}$ heteropolymers (**Figure 4-5**). The second question will be answered by direct comparison of regular spacing [*alt*-$(A/Glc)_{100}$ and *alt*-$(Glc/A)_{100}$] or random spacing [*stat*-$(A_m/Glc_n)_{100}$]. Different architectures may be optimal for different glycans.

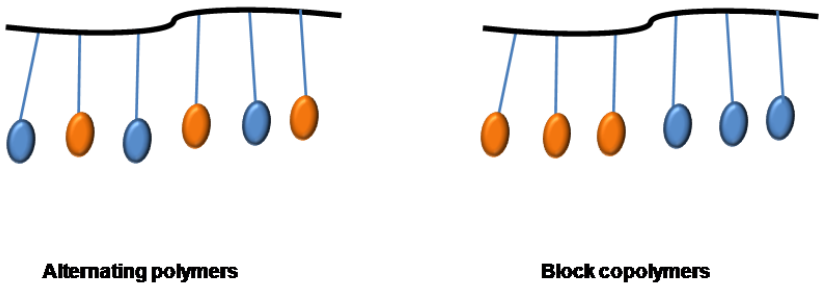

Figure 4-5. The structures of alternating polymer and block copolymer.

To further investigate what combinations of glycans best activate the AR, the three active sugars will be mixed in one mulvalent scaffold at random—*stat*-$(A_m/B_n)_{100}$ and *stat*-$(A_m/B_n/C_n)_{100}$, in sequence—*block*-$(A_m/B_n)_{100}$ and block-$(A_m/B_n/C_n)_{100}$ (**Figure 4-5**), or by alternating—*alt*-$(A_m/B_n)_{100}$ and *alt*-$(A_m/B_n/C_n)_{100}$. More complicated hetero-glycopolymers with spacers can also be generated. However, most importantly, the results from sperm immunofluorescent assay will guide future directions in designing effective polymers.

In our previous work, the general signaling pathways of glycopolymer-activated AR were studied. However, many downstream effectors of these pathways were not examined. In fact, some downstream pathways are still controversial, though they have been proposed in the mechanism of ZP3-activated AR (**Figure 1-5**). A deeper dig into one or some pathways by measuring the level of phospharylation or inhibiting the downstream effector(s) may provide more insights about the signaling mechanism of glycopolymer-activated AR.

Controversies also exist on the signaling pathways involved in progesterone activated AR and the indentification of progesterone receptor(s) on the sperm (Baldi, Luconi et al. 2009). To the best of our knowledge, no multivalent display of progesterone has been developed so far. Thus, progesterone may serve as the ligand for the synthesis of new ROMP derived polymers, and their effects in AR can be investigated by immunofluorescent assay as well. Although the feasibility of synthesizing progesterone polymer by ROMP is unknown, applying other AR activating agents to the multivalent scaffold is also an interesting future direction of our project.

Moreover, Chen et al. successfully identified the fertilinβ binding partner on the mouse oocyte surface by using a photoaffinity tagged fertilinβ peptide (Chen and Sampson 1999). Later, Jaechul Lee in the Sampson group prepared fluorphore-linked fertilinβ mimic block copolymers, and applied them for photoaffinity labeling to identify binding partners on the oocyte plasma

membrane (Lee 2006). Thus, discovery of sperm-surface receptors with photoaffinity tagged glycopolymers can be another future goal of our project. Introducing an azido-tagged target moiety such as fluorophore or biotin to the glycopolymer by “click chemistry” is feasible. However, to improve the labeling efficiency, many conditions such as the the suitable polymer and reagent concentrations should be carefully determined.

Chapter 5

Experimental procedures

1. Investigation of mouse sperm acrosome reaction with synthetic glycopolymers

    1.2. Synthesis of glycomonomers

    1.3. Synthesis of glycopolymers

    1.4. Sperm immunofluorescent assay

2. Investigation of synthetic methods to prepare fertilization probes

    2.1. Synthesis of tripeptides

    2.2. ROMP of tripeptide polymers

1. Investigation of mouse sperm acrosome reaction with synthetic glycopolymers

Materials. Carbohydrates and other chemicals used were purchased from Sigma-Aldrich (Milwaukee, WI) or Fisher Scientific, Inc. (Springfield, NJ). CH_2Cl_2, CH_3OH, THF and EtO_2 were purified by Pushstill solvent dispensing system (Pure Process Technology LLC, Nashua, NH); pyridine, hexane, pentane were used without further purification. $(H_2IMes)(3\text{-}BrPyr)_2Cl_2Ru{=}CHPh$, **32**, was prepared according to the literature (Love, Morgan et al. 2002). All reactions were carried out under an N_2 atmosphere in oven-dried glassware unless otherwise specified. Moisture and oxygen-sensitive reagents were handled in an N_2 filled dry box.

General Methods. Analytical thin layer chromatography (TLC) was performed on precoated silica gel plates (60F254). TLC spots were detected by UV and by staining with 10% phosphomolybdic acid (PMA) in ethanol. The usual workup mentioned in the following synthesis was three washes of the organic layer with 5% aq $NaHCO_3$, followed by three washes with 1 N aq HCl, and drying of the organic layer over Na_2SO_4. All intermediates and monomers were purified by Combiflash personal flash chromatography system (Teledyne Isco, NE), and analyzed by Inova500, Inova600, Bruker400 and Bruker500 MHz NMR spectrometers. ^{1}H-NMR spectra are reported as chemical shift in parts per million (multiplicity, coupling constant in Hz, integration) and assumed to be first order. The molecular weight of the polymers was assessed by gel permeation chromatography (Phenogel 5 μ Linear(2) GPC column, Phenomenex, CA) and light scattering (Brookhaven instrument) eluting with THF.

1. 1. Synthesis of glycomonomers

Penta-acetyl-D-mannopyranose 1. To a solution of D-mannopyranose (16.65 mmol, 3 g) in pyridine (64 mL) was added Ac_2O (333.04 mmol, 32 mL) (Fekete, Gyergyoi et al. 2006). After stirring 24 h at rt the mixture was concentrated. The residue was diluted with CH_2Cl_2, followed by workup and concentrated to yield **1** as colorless oil (6.49 g, 100%) (**Scheme 3-1**). Compound **1** was similar to the same compound reported previously (Šardzík, Noble et al. 2010). ^{1}H NMR (500 MHz, $CDCl_3$): δ 6.11 (d, *J* = 2.0 Hz, 1H), 5.38—5.35 (m, 2H), 5.28 (t, *J* = 2.2 Hz, 1H), 4.30 (dd, *J* = 12.4, 5.0 Hz, 1H), 4.12 (dd, *J* = 12.4, 2.5 Hz, 1H), 4.09—4.03 (m, 1H), 2.19 (d, *J* = 4.1 Hz, 6H), 2.11 (s, 3H), 2.07 (s, 3H), 2.03 (d, *J* = 0.8 Hz, 3H).

(1-Hydroxyl)-2,3,4,6-tetra-*O*-acetyl-D-mannopyranose 2. To a solution of compound **1** (5.02 mmol, 1.96 g) in dry DMF (60 mL) was added hydrazine acetate (5.53 mmol, 0.51 g) (Fekete, Gyergyoi et al. 2006). After stirring for 2 h at 40 ℃, the mixture was concentrated. The residue was diluted with EtOAc, and washed with cold brine, followed by workup, and concentrated to yield **2** as colorless oil (1.37 g, 78%) (**Scheme 3-1**). Compound **2** was similar to the same compound reported previously (Ikeda, Morimoto et al. 2010). ^{1}H NMR (500 MHz, $CDCl_3$): δ 5.44 (dd, *J* = 10.0, 3.4 Hz, 1H), 5.36—5.25 (m, 3H), 4.31—4.22 (m, 2H), 4.19—4.11 (m, 1H), 3.32 (d, *J* = 4.0 Hz, 1H), 2.18 (s, 3H), 2.12 (s, 3H), 2.07 (s, 3H), 2.02 (s, 3H).

2,3,4,6-Tetra-*O*-acetyl-α-D-mannopyranosyl trichloroacetimidate 3. To a solution of compound **2** (1.17 mmol, 0.41 g) in dry CH_2Cl_2 (25 mL) was added trichloroacetonenitrile (1.17 mmol, 1.18 mL) and DBU (0.12 mmol, 18 μL) (Fekete, Gyergyoi et al. 2006). After stirring for 3 h at rt the mixture was concentrated. The crude product was purified by Combiflash

(EtOAc:hexane = 3:7, v/v) to yield **3** as colorless oil (0.40 g, 69%) (**Scheme 3-1**). Compound **3** was similar to the same compound reported previously (Kerékgyártó, Kamerling et al. 1989). ^{1}H NMR (600 MHz, $CDCl_3$): δ 5.43 (dd, *J* = 10.1, 3.4 Hz, 1H), 5.36—5.24 (m, 3H), 4.32—4.19 (m, 2H), 4.18—4.11 (m, 1H), 2.92—2.82 (m, 1H), 2.16 (s, 3H), 2.11 (s, 3H), 2.05 (s, 3H), 2.00 (s, 3H).

1-Chloroethyl-2,3,4,6-tetra-*O*-acetyl-α-D-mannopyranoside 4. To a cooled solution of compound **3** (1.97 mmol, 0.97 g) and 2-chloroethanol (19.7 mmol, 1.32 ml) in dry CH_2Cl_2 (15 mL) was added BF_3-etherate (0.39 mmol, 36.5 μL) (Gu, Luo et al. 2008). The solution was stirred for 3 h at -80 ℃ and followed by workup. The crude product was concentrated and purified by Combiflash (EtOAc:hexane = 4:6, v/v) to yield **4** as a white solid (0.60 g, 74%) (**Scheme 3-1**). Compound **4** was similar to the same compound reported previously (Gu, Luo et al. 2008). ^{1}H NMR (600 MHz, $CDCl_3$): δ 5.35 (dd, *J* = 10.1, 3.4 Hz, 1H), 5.31—5.25 (m, 2H), 4.87 (d, *J* = 1.8 Hz, 1H), 4.27 (dd, *J* = 12.2, 5.4 Hz, 1H), 4.17—4.09 (m, 2H), 3.92 (dt, *J* = 11.5, 5.8 Hz, 1H), 3.82 (dt, *J* = 11.0, 5.4 Hz, 1H), 3.68 (t, *J* = 5.7 Hz, 2H), 2.16 (s, 3H), 2.10 (s, 3H), 2.05 (s, 3H), 2.00 (s, 3H).

1-Azidoethyl-2,3,4,6-tetra-*O*-acetyl-α-D-mannopyranoside 5. To a solution of compound **4** (1.02 mmol, 0.42 g) in dry DMSO (10 mL) was added sodium azide (10.2 mmol, 0.67 g). Then the reaction mixture was stirred for 72 h at 60 ℃ (Gu, Luo et al. 2008). After workup the mixture was concentrated and purified by Combiflash (EtOAc:hexane = 4:6, v/v) to yield **5** as a white solid (0.35 g, 82%) (**Scheme 3-1**). ^{1}H NMR (600 MHz, $CDCl_3$): δ 5.40—5.33 (m, 1H), 5.32—5.25 (m, 2H), 4.87 (d, *J* = 1.8 Hz, 1H), 4.29 (ddd, *J* = 12.3, 5.4, 1.3 Hz, 1H), 4.17—4.09 (m, 1H), 4.06 – 4.01 (m, 1H), 3.91—3.82 (m, 1H), 3.67 (m, 1H), 3.53—3.40 (m, 2H), 2.16 (s, 3H), 2.10 (s, 3H), 2.05 (s, 3H), 1.99 (s, 3H).

1-Aminoethyl-2,3,4,6-tetra-O-acetyl-α-D-mannopyranosyl bicyclo[2.2.1]hept-5-ene-exo-2-carboxamide 6. Compound **5** (0.22 mmol, 91 mg) and *exo*-5-norbornenecarboxylic acid (0.39 mmol, 54.2 mg) were combined with HOBt • H_2O (0.39mmol, 60.2 mg) in a round bottle flask and dried for more than 1 h in vacuo. This mixture was dissolved in dry THF under N2 and cooled to 0 ℃. Then N,N-diisopropylcarbodiimide (0.39 mmol, 49.6 mg) was added and the solution was stirred for 10 min, followed by the addition of tri-*n*-butylphosphane (0.39 mmol, 79.5 mg) and stirring for 1 h at 0 ℃. Then the reaction mixture was stirred for 15 h at rt (Schierholt, Shaikh et al. 2009). After the usual workup, the crude was concentrated and purified by Combiflash (acetone:CH_2Cl_2 = 1:4, v/v) to yield **6** as colorless oil (74 mg, 66%) (**Scheme 3-1**). ^{1}H NMR (500 MHz, $CDCl_3$): δ 6.16 (ddd, J = 8.9, 5.5, 2.9 Hz, 2H), 5.92 (s, 1H), 5.36 (dt, J = 10.0, 3.8 Hz, 1H), 5.31 – 5.25 (m, 2H), 4.84 (d, J = 1.8 Hz, 1H), 4.28 (ddd, J = 12.3, 5.7, 2.8 Hz, 1H), 4.13 (dd, J = 12.3, 2.5 Hz, 1H), 4.02 – 3.95 (m, 1H), 3.86 – 3.78 (m, 1H), 3.56 (ddd, J = 13.4, 7.4, 4.3 Hz, 2H), 3.48 (d, J = 6.4 Hz, 1H), 2.95 (s, 2H), 2.18 (s, 3H), 2.11 (s, 3H), 2.06 (s, 3H), 2.02 (s, 3H), 1.99 – 1.89 (m, 1H), 1.72 (t, J = 7.5 Hz, 1H), 1.36 (m, 2H). 13C NMR (125 MHz, $CDCl_3$): δ 178.53, 178.44, 173.25, 172.71, 172.28, 140.86, 138.62, 100.28, 79.97, 72.01, 71.66, 71.34, 70.08, 68.82, 65.12, 49.92, 48.94, 47.28, 44.24, 41.73, 33.24, 33.06, 23.51, 23.35. HRMS (ESI) Calcd for $C_{24}H_{33}NO_{11}$ $[M+H]^+$ 512.2127; found 512.2164.

(1-Hydroxyl)-2,3,4,6-tetra-*O*-acetyl-β-D-glucopyranose 7. Compound **7** (**Scheme 3-2**) was synthesized following the same procedure to prepare **2**, and was similar to the same compound reported previously (Pilgrim and Murphy 2010). Yield: 91%. ^{1}H NMR (600 MHz, $CDCl_3$): δ 5.53 (td, *J* = 9.8, 1.5 Hz, 1H), 5.46 (t, *J* = 3.7 Hz, 1H), 5.12—5.04 (m, 1H), 4.94—4.83 (m, 1H), 4.29—4.20 (m, 2H), 4.17—4.08 (m, 1H), 2.93—2.89 (m, 1H), 2.12—2.06 (d, *J* = 10 Hz, 6H), 2.02 (d, *J* = 10.7 Hz, 6H).

2,3,4,6-Tetra-*O*-acetyl-β-D-glucopyranosyl trichloroacetimidate 8. Compound **8** (**Scheme 3-2**) was synthesized following the same procedure to prepare **3**, and was similar to the same compound reported previously (Pilgrim and Murphy 2010). Yield: 90%. ^{1}H NMR (600 MHz, $CDCl_3$): δ 8.69 (s, 1H), 6.56 (d, *J* = 3.7 Hz, 1H), 5.57 (t, *J* = 9.9 Hz, 1H), 5.18 (t, *J* = 9.9 Hz, 1H), 5.14 (dd, *J* = 10.2, 3.7 Hz, 1H), 4.27 (dd, *J* = 12.4, 4.2 Hz, 1H), 4.22 (ddd, *J* = 10.3, 4.2, 2.1 Hz, 1H), 4.13 (dd, *J* = 12.5, 2.2 Hz, 1H), 2.08 (s, 3H), 2.05 (s, 3H), 2.03 (s, 3H), 2.02 (s, 3H).

1-Chloroethyl-2,3,4,6-tetra-*O*-acetyl-β-D-glucopyranoside 9. Compound **9** (**Scheme 3-2**) was synthesized following the same procedure to prepare **4**, and was similar to the same compound reported previously (Guchhait and Misra 2011). Yield: 75%. ^{1}H NMR (600 MHz, $CDCl_3$): δ 5.21 (dd, *J* = 10.1, 9.0 Hz, 1H), 5.08 (t, *J* = 9.7 Hz, 1H), 5.04—4.98 (m, 1H), 4.57 (dd, *J* = 8.1, 1.1 Hz, 1H), 4.26 (dd, *J* = 12.4, 4.8 Hz, 1H), 4.15 (dd, *J* = 12.3, 2.4 Hz, 1H), 4.09 (dt, *J* = 10.8, 5.2 Hz, 1H), 3.80—3.73 (m, 1H), 3.71 (ddd, *J* = 9.9, 4.8, 2.4 Hz, 1H), 3.65—3.59 (m, 2H), 2.09 (d, *J* = 1.2 Hz, 3H), 2.06 (d, *J* = 1.1 Hz, 3H), 2.02 (s, 3H), 2.00 (d, *J* = 1.0 Hz, 3H).

1-Azidoethyl-2,3,4,6-tetra-*O*-acetyl-β-D-glucopyranoside 10. Compound **10** (**Scheme 3-2**) was synthesized following the same procedure to prepare **5**, and was similar to the same compound reported previously (Paterson, Clark et al. 2011). Yield: 94%. ^{1}H NMR (500 MHz, $CDCl_3$): δ 5.20 (td, *J* = 9.5, 0.9 Hz, 1H), 5.12—5.05 (m, 1H), 5.00 (ddd, *J* = 9.4, 8.0, 1.0 Hz, 1H), 4.59 (dd, *J* = 7.9, 0.9 Hz, 1H), 4.28—4.21 (m, 1H), 4.18—4.11 (m, 1H), 4.06—3.98 (m, 1H), 3.75—3.64 (m, 2H), 3.53—3.43 (m, 1H), 3.28 (dt, *J* = 13.4, 4.1 Hz, 1H), 2.07 (s, 3H), 2.03 (s, 3H), 2.01 (s, 3H), 1.99 (s, 3H).

1-Aminoethyl-2,3,4,6-tetra-*O*-acetyl-β-D-glucopyranosyl bicyclo[2.2.1]hept-5-ene-exo-2-carboxamide 11. Compound **11** (**Scheme 3-2**) was synthesized following the same procedure to

prepare **6**. Yield: 79%. ^{1}H NMR (600 MHz, $CDCl_3$): δ 6.14 (dt, *J* = 5.2, 2.4 Hz, 1H), 6.09 (dt, *J* = 5.8, 3.0 Hz, 1H), 5.91 (s, 1H), 5.21 (t, *J* = 9.5 Hz, 1H), 5.07 (td, *J* = 9.7, 2.4 Hz, 1H), 4.99 (dd, *J* = 9.6, 8.0 Hz, 1H), 4.51 (dd, *J* = 8.0, 1.6 Hz, 1H), 4.26 (ddd, *J* = 12.3, 7.4, 4.9 Hz, 1H), 4.14 (dt, *J* = 12.4, 2.4 Hz, 1H), 3.89 – 3.80 (m, 1H), 3.71 (dtd, *J* = 10.2, 5.1, 1.7 Hz, 2H), 3.46 (t, *J* = 5.6 Hz, 2H), 2.91 (dt, *J* = 3.7, 1.8 Hz, 2H), 2.08 (d, *J* = 1.9 Hz, 3H), 2.05 (d, *J* = 9.6 Hz, 3H), 2.03 (s, 3H), 2.01 (d, *J* = 1.0 Hz, 3H), 1.93 – 1.87 (m, 1H), 1.70 (dt, *J* = 8.6, 2.9 Hz, 1H), 1.32 (m, 2H). ^{13}C NMR (125 MHz, $CDCl_3$): δ 178.38, 173.19, 172.78, 172.05, 159.74, 140.92, 138.60, 103.55, 75.32, 74.60, 74.01, 71.91, 70.92, 64.48, 49.83, 48.99, 48.92, 47.25, 44.60, 44.21, 41.91, 33.09, 26.16, 23.30. HRMS (ESI) Calcd for $C_{24}H_{33}NO_{11}$ $[M+H]^+$ 512.2127; found 512.2180.

(1-Hydroxyl)-2,3,4,6-tetra-*O*-acetyl-D-galactopyranose 12. Compound **12** (**Scheme 3-3**) was synthesized following the same procedure to prepare **2**, and was similar to the same compound reported previously (Pilgrim and Murphy 2010). Yield: 87%. ^{1}H NMR (600 MHz, $CDCl_3$): δ 5.52 (t, *J* = 3.5 Hz, 1H), 5.44—5.39 (m, 1H), 5.17 (dd, *J* = 10.9, 3.6 Hz, 1H), 5.07 (dd, *J* = 3.4, 2.2 Hz, 1H), 4.47 (t, *J* = 6.6 Hz, 1H), 4.18—4.05 (m, 3H), 2.89 (s, 1H), 2.15 (s, 3H), 2.10 (s, 3H), 2.05 (s, 3H), 1.99 (s, 3H).

2,3,4,6-Tetra-*O*-acetyl-β-D-galactopyranosyl trichloroacetimidate 13. Compound **13** (**Scheme 3-3**) was synthesized following the same procedure to prepare **3**, and was similar to the same compound reported previously (Pilgrim and Murphy 2010). Yield: 88%. ^{1}H NMR (600 MHz, $CDCl_3$): δ 8.66 (s, 1H), 6.60 (d, *J* = 3.6 Hz, 1H), 5.56 (dd, *J* = 3.2, 1.3 Hz, 1H), 5.45—5.34 (m, 2H), 4.48—4.40 (m, 1H), 4.17 (dd, *J* = 11.3, 6.6 Hz, 1H), 4.08 (dd, *J* = 11.4, 6.6 Hz, 1H), 2.16 (s, 3H), 2.03— 2.01 (m, 9H).

1-Chloroethyl-2,3,4,6-tetra-*O*-acetyl-β-D-galactopyranoside 14. Compound **14** (**Scheme 3-3**) was synthesized following the same procedure to prepare **4**, and was similar to the same compound reported previously (Gu, Luo et al. 2008). Yield: 74%. ^{1}H NMR (600 MHz, $CDCl_3$): δ 5.43— 5.37 (m, 1H), 5.23 (ddd, J = 10.2, 7.9, 1.5 Hz, 1H), 5.03 (ddd, J = 10.5, 3.5, 1.3 Hz, 1H), 4.54 (dd, J = 7.8, 1.3 Hz, 1H), 4.22—4.07 (m, 3H), 3.92 (ddd, J = 7.9, 6.0, 1.5 Hz, 1H), 3.77 (dtd, J = 11.1, 6.5, 1.4 Hz, 1H), 3.63 (ddd, J = 6.5, 5.0, 1.4 Hz, 2H), 2.15 (s, 3H), 2.07 (s, 3H), 2.05 (s, 3H), 1.99 (s, 3H).

1-Azidoethyl-2,3,4,6-tetra-*O*-acetyl-β-D-galactopyranoside 15. Compound **15** (**Scheme 3-3**) was synthesized following the same procedure to prepare **5**, and was similar to the same compound reported previously (Gu, Luo et al. 2008). Yield: 84.6%. ^{1}H NMR (600 MHz, $CDCl_3$): δ 5.39 (dd, *J* = 3.4, 1.3 Hz, 1H), 5.24 (dd, *J* = 10.5, 7.9 Hz, 1H), 5.02 (dd, *J* = 10.4, 3.4 Hz, 1H), 4.56 (d, *J* = 7.9 Hz, 1H), 4.23—4.09 (m, 2H), 4.04 (m, 1H), 3.92 (td, *J* = 6.6, 1.3 Hz, 1H), 3.69 (ddd, *J* = 10.7, 8.4, 3.4 Hz, 1H), 3.50 (ddd, *J* = 13.5, 8.5, 3.6 Hz, 1H), 3.30 (ddd, *J* = 13.4, 4.8, 3.4 Hz, 1H), 2.15 (s, 3H), 2.05 (d, *J* = 8.9 Hz, 6H), 1.98 (s, 3H).

1-Aminoethyl-2,3,4,6-tetra-*O*-acetyl-β-D-galactopyranosyl bicyclo[2.2.1]hept-5-ene-exo-2-carboxamide 16. Compound **16** (**Scheme 3-3**) was synthesized following the same procedure to prepare **6**. Yield: 69.8%. ^{1}H NMR (400 MHz, $CDCl_3$): δ 6.22 – 6.08 (m, 2H), 5.93 (s, 1H), 5.42 (dd, *J* = 3.5, 1.2 Hz, 1H), 5.22 (ddd, *J* = 10.5, 7.9, 1.2 Hz, 1H), 5.04 (ddd, *J* = 10.5, 3.4, 0.9 Hz, 1H), 4.50 (dd, *J* = 7.9, 1.7 Hz, 1H), 4.17 (ddd, *J* = 6.4, 2.1, 1.0 Hz, 2H), 3.98 – 3.86 (m, 2H), 3.72 (ddt, *J* = 10.6, 7.6, 3.9 Hz, 1H), 3.50 (m, 2H), 2.94 (dd, *J* = 3.6, 1.9 Hz, 2H), 2.18 (s, 3H), 2.12 – 2.06 (m, 6H), 2.01 (s, 3H), 1.94 (m, 1H), 1.73 (d, *J* = 8.4 Hz, 1H), 1.41 – 1.25 (m, 2H). ^{13}C NMR(125 MHz, $CDCl_3$): δ 175.83, 170.44, 170.25, 170.21, 169.68, 138.16, 135.98, 101.58,

70.97, 69.10, 68.99, 67.0, 61.30, 47.35, 47.22, 46.32, 44.62, 41.57, 39.33, 30.49, 29.73, 20.84, 20.66, 20.51. HRMS (ESI) Calcd for $C_{24}H_{33}NO_{11}$ $[M+H]^+$ 512.2127; found 512.2136.

Tetra-acetyl-α-L-fucopyranose 17. Compound **17** (**Scheme 3-4**) was synthesized following the same procedure to prepare **1**, and was similar to the same compound reported previously (Šardzík, Noble et al. 2010). Yield: 98%. ^{1}H NMR (500 MHz, $CDCl_3$): δ 6.34 (d, *J* = 2.8 Hz, 1H), 5.34 (m, 2H), 4.27 (q, *J* = 6.5 Hz, 1H), 2.18 (s, 3H), 2.15 (s, 3H), 2.01 (s, 3H), 2.00 (s, 3H), 1.16 (d, *J* = 6.5 Hz, 3H).

1-Bromoethyl-2,3,4-tri-*O*-acetyl-L-fucopyranoside 18. Compound **18** (**Scheme 3-4**) was synthesized according to the reference (Dasgupta, Rajput et al. 2007), and the product is a mixture of α and β diastereomers. Yield: 75%. The mixture was used for the next step without further separation.

1-Azidoethyl-2,3,4-tri-*O*-acetyl-α-L-fucopyranoside 19. Compound **19** (**Scheme 3-4**) was synthesized following the same procedure to prepare **5**, and was similar to the same compound reported previously (Park and Shin 2007). Yield: 82%. ^{1}H NMR (500 MHz, $CDCl_3$): δ 5.39 (dd, *J* = 10.5, 3.4 Hz, 1H), 5.34 (dd, *J* = 3.4, 1.3 Hz, 1H), 5.21—5.09 (m, 2H), 4.20 (dd, *J* = 10.5, 3.4 Hz, 1H), 3.88 (ddd, *J* = 10.8, 6.1, 3.2 Hz, 1H), 3.63 (ddd, *J* = 10.6, 7.1, 3.3 Hz, 1H), 3.44 (dddd, *J* = 41.9, 13.4, 6.6, 3.3 Hz, 2H), 2.19 (s, 3H), 2.10 (s, 3H), 2.01 (s, 3H), 1.17 (d, *J* = 6.5 Hz, 3H).

1-Aminoethyl-2,3,4-tri-*O*-acetyl-α-L-fucopyranosyl bicyclo[2.2.1]hept-5-ene-exo-2-carbox-amide 20. Compound **20** (**Scheme 3-4**) was synthesized following the same procedure to prepare **6**. Yield: 66%. ^{1}H NMR (500 MHz, $CDCl_3$): δ 6.17 (dd, *J* = 5.9, 2.8 Hz, 1H), 6.13 (ddd, *J* = 11.1, 5.7, 3.0 Hz, 1H), 5.94 (s, 1H), 5.38 (dt, *J* = 10.9, 3.4 Hz, 1H), 5.31 (s, 1H), 5.17 (ddd, *J* = 10.8, 3.7, 1.0 Hz, 1H), 5.08 (t, *J* = 3.1 Hz, 1H), 4.16 (dq, *J* = 8.5, 7.1, 6.1 Hz, 1H), 3.79 (m, 1H), 3.53

(m, 3H), 2.94 (dt, *J* = 5.2, 2.6 Hz, 2H), 2.19 (s, 3H), 2.09 (d, *J* = 7.0 Hz, 3H), 2.02 (s, 3H), 1.94 (dt, *J* = 10.9, 3.6 Hz, 1H), 1.73 (d, *J* = 8.3 Hz, 1H), 1.44 – 1.31 (m, 2H), 1.17 (dd, *J* = 6.6, 2.6 Hz, 3H). ^{13}C NMR(125 MHz, $CDCl_3$): δ 175.61, 170.62, 170.21, 170.20, 138.36, 135.91, 96.49, 71.02, 68.15, 67.92, 67.66, 64.68, 47.24, 46.35, 44.78, 41.58, 39.21, 30.53, 20.84, 20.75, 20.68, 20.51, 15.91. HRMS (ESI) Calcd for $C_{22}H_{31}NO_9$ $[M+H]^+$ 454.2078; found 454.2078.

1-Hydroxyl-2-acetamido-3,4,6-tri-*O*-acetyl-2-deoxy-D-glucopyranose 21. To a solution of 2-Acetamido-1,3,4,6-tetra-*O*-acetyl-2-deoxy-D-glucopyranose (0.77 mmol, 0.3 g) in dry THF and methanol mixture (1:2, v/v) (6 mL) was added ammonium carbonate (1.54 mmol, 0.15 g) (Chittaboina, Hodges et al. 2006). After stirring overnight at RT the mixture was concentrated and purified by Combiflash (EtOAc: CH_2Cl_2 = 3:2, v/v) to yield **21** as a colorless oil (0.19 g, 70%) (**Scheme 3-5**). Compound **21** was similar to the same compound reported previously (Chittaboina, Hodges et al. 2006). ^{1}H NMR (600 MHz, $CDCl_3$): δ 5.76 (d, *J* = 9.3 Hz, 1H), 5.34—5.26 (m, 2H), 5.14 (t, *J* = 9.8 Hz, 1H), 4.35—4.27 (m, 1H), 4.25—4.17 (m, 2H), 4.17—4.08 (m, 2H), 3.03 (s, 1H), 2.10 (s, 3H), 2.04 (s, 6H), 1.96 (s, 3H).

2-Acetamido-3,4,6-tri-*O*-acetyl-2-deoxy-β-D-glucopyranosyl trichloroacetimidate 22. Compound **22** (**Scheme 3-5**) was synthesized following the same procedure to prepare **3**, and was similar to the same compound reported previously (Sudibya, Ma et al. 2009). Yield: 73%. ^{1}H NMR (600 MHz, $CDCl_3$): δ 8.79 (s, 1H), 5.62 (d, *J* = 8.9 Hz, 1H), 5.35—5.22 (m, 2H), 4.55 (ddd, *J* = 10.7, 8.9, 3.7 Hz, 1H), 4.28— 4.22 (m, 1H), 4.15—4.09 (m, 2H), 2.07 (s, 3H), 2.06 (d, *J* = 5.3 Hz, 6H), 1.93 (s, 3H).

1-Chloroethy-2-Acetamido-3,4,6-tri-*O*-acetyl-2-deoxy-β-D-glucopyranoside 23. Compound **23** (**Scheme 3-5**) was synthesized following the same procedure to prepare **4**, and was similar to

the same compound reported previously (Sukhova, Dubrovskii et al. 2007). Yield: 62%. ^{1}H NMR (600 MHz, $CDCl_3$): δ 5.50 (d, *J* = 8.9 Hz, 1H), 5.34—5.27 (m, 1H), 5.08 (t, *J* = 9.7 Hz, 1H), 4.77 (dd, *J* = 8.4, 0.9 Hz, 1H), 4.26 (dd, *J* = 12.3, 4.7 Hz, 1H), 4.16—4.08 (m, 2H), 3.87 (dt, *J* = 10.5, 8.7 Hz, 1H), 3.77 (ddd, *J* = 11.0, 6.8, 5.8 Hz, 1H), 3.71 (ddd, *J* = 10.1, 4.8, 2.4 Hz, 1H), 3.64 (ddd, *J* = 6.1, 4.9, 1.0 Hz, 2H), 2.09 (s, 3H), 2.03 (d, *J* = 5.7, 6H), 1.97 (s, 3H).

1-Azidoethyl-2-acetamido-3,4,6-tri-*O*-acetyl-2-deoxy-β-D-glucopyranoside 24. Compound **24** (**Scheme 3-5**) was synthesized following the same procedure to prepare **5**, and was similar to the same compound reported previously (Park and Shin 2007). Yield: 73%. ^{1}H NMR (500 MHz, $CDCl_3$): δ 5.60 (d, *J* = 8.6 Hz, 1H), 5.38 (dd, *J* = 10.6, 9.3 Hz, 1H), 5.09 (t, *J* = 9.7 Hz, 1H), 4.85 (d, *J* = 8.3 Hz, 1H), 4.27 (dd, *J* = 12.3, 4.8 Hz, 1H), 4.17 (dd, *J* = 12.3, 2.4 Hz, 1H), 4.06 (ddd, *J* = 10.9, 4.8, 3.3 Hz, 1H), 3.83 (dt, *J* = 10.8, 8.5 Hz, 1H), 3.78—3.68 (m, 2H), 3.52 (ddd, *J* = 13.4, 8.6, 3.2 Hz, 1H), 3.28 (ddd, *J* = 13.5, 4.7, 3.2 Hz, 1H), 2.10 (s, 3H), 2.05 (d, *J* = 3.4 Hz, 6H), 1.97 (s, 3H).

1-Aminoethyl-2-acetamido-3,4,6-tri-*O*-acetyl-2-deoxy-β-D-glucotopyranosyl bicycle[2.2.1] hept-5-ene-exo-2-carboxamide 25. Compound **25** (**Scheme 3-5**) was synthesized following the same procedure to prepare **6**. Yield: 70%. ^{1}H NMR (400 MHz, $CDCl_3$): δ 6.25 (d, *J* = 4 Hz, 1H), 6.22 – 6.01 (m, 3H), 5.19 (td, *J* = 9.9, 4.7 Hz, 1H), 5.08 (td, *J* = 9.6, 2.7 Hz, 1H), 4.58 (d, *J* = 8.4 Hz, 1H), 4.26 (dt, *J* = 12.7, 5.0 Hz, 1H), 4.14 (dd, *J* = 12.2, 2.2 Hz, 1H), 3.96 (tq, *J* = 8.7, 3.9 Hz, 1H), 3.86 (ddt, *J* = 9.9, 6.5, 3.3 Hz, 1H), 3.70 (ddd, *J* = 10.0, 5.2, 2.4 Hz, 2H), 3.58 – 3.49 (m, 1H), 3.39 (m, 1H), 2.91 (s, 2H), 2.08 (d, *J* = 1.7 Hz, 3H), 2.04 (d, *J* = 4.6 Hz, 6H), 1.95 (d, *J* = 10.7 Hz, 3H), 1.90 (m, 1H), 1.70 (t, *J* = 8.0 Hz, 1H), 1.38 – 1.22 (m, 3H). ^{13}C NMR (125 MHz, $CDCl_3$): δ 178.55, 173.71, 173.28, 173.10, 171.98, 140.90, 138.65, 109.99, 103.75, 75.15, 74.65,

71.41, 71.02, 64.68, 57.15, 50.02, 49.77, 49.0, 47.19, 44.23, 41.77, 33.12, 26.06, 23.33. HRMS (ESI) Calcd for $C_{24}H_{34}N_2O_{10}$ $[M+H]^+$ 511.2300; found 511.2295.

2-Acetamido-1,3,4,6-tetra-*O*-acetyl-2-deoxy-D-galactopyranose 26. Compound **26** (**Scheme 3-6**) was synthesized following the same procedure to prepare **1**, and was similar to the same compound reported previously (Dowlut, Hall et al. 2005). Yield: 100%. ^{1}H NMR (600 MHz, $CDCl_3$): δ 6.21 (d, *J* = 3.7 Hz, 1H), 5.45—5.39 (m, 2H), 5.25—5.19 (m, 1H), 4.72 (ddd, *J* = 11.8, 8.7, 3.4 Hz, 1H), 4.23 (t, *J* = 6.8 Hz, 1H), 4.14—4.03 (m, 2H), 2.17 (s, 6H), 2.03 (s, 6H), 1.95 (s, 3H).

1-Hydroxyl-2-acetamido-3,4,6-tri-*O*-acetyl-2-deoxy-D-galactopyranose 27. Compound **27** (**Scheme 3-6**) was synthesized following the same procedure to prepare **21**, and was similar to the same compound reported previously (Wang, Wang et al. 2011). Yield: 70%. ^{1}H NMR (600 MHz, $CDCl_3$): δ 5.72 (d, *J* = 9.5 Hz, 1H), 5.39 (dd, *J* = 3.3, 1.4 Hz, 1H), 5.33 (t, *J* = 3.0 Hz, 1H), 5.25 (dd, *J* = 11.4, 3.2 Hz, 1H), 4.56 (td, *J* = 11.2, 10.5, 3.5 Hz, 1H), 4.42 (t, *J* = 6.5 Hz, 1H), 4.16—4.02 (m, 2H), 3.25 (s, 1H), 2.16 (s, 3H), 2.05 (s, 3H), 2.00 (s, 3H), 1.98 (s, 3H).

2-Acetamido-3,4,6-tri-*O*-acetyl-2-deoxy-β-D-galactopyranosyl trichloroacetimidate 28. Compound **28** (**Scheme 3-6**) was synthesized following the same procedure to prepare **3**, and was similar to the same compound reported previously (Wang, Wang et al. 2011). Yield: 83%. ^{1}H NMR (600 MHz, $CDCl_3$): δ 8.78 (s, 1H), 6.40 (d, *J* = 3.6 Hz, 1H), 5.52—5.46 (m, 2H), 5.31—5.25 (m, 1H), 4.80 (ddd, *J* = 11.4, 9.2, 3.7 Hz, 1H), 4.38—4.32 (m, 1H), 4.17 (dd, *J* = 11.4, 6.7 Hz, 1H), 4.07 (dd, *J* = 11.4, 6.6 Hz, 1H), 2.18 (s, 3H), 2.04 (s, 3H), 2.01 (s, 3H), 1.94 (s, 3H).

1-Bromoethyl-2-acetamido-3,4,6-tri-*O*-acetyl-2-deoxy-β-D-galactopyranoside 29. Compound **29** (**Scheme 3-6**) was synthesized following the same procedure to prepare **4**, and was similar to the same compound reported previously (Wang, Wang et al. 2011). Yield: 71%. ^{1}H NMR (600 MHz, $CDCl_3$): δ 5.54 (d, *J* = 8.4 Hz, 1H), 5.43—5.28 (m, 2H), 4.81 (d, *J* = 8.4 Hz, 1H), 4.26—4.08 (m, 3H), 4.05—3.90 (m, 2H), 3.85 (dt, *J* = 11.5, 6.4 Hz, 1H), 3.51 (dd, *J* = 6.4, 4.9 Hz, 2H), 2.16 (s, 3H), 2.07 (s, 3H), 2.02 (s, 3H), 1.99 (s, 3H).

1-Azidoethyl-2-acetamido-3,4,6-tri-*O*-acetyl-2-deoxy-β-D-galactopyranoside 30. Compound **30** (**Scheme 3-6**) was synthesized following the same procedure to prepare **5**, and was similar to the same compound reported previously (Park and Shin 2007). Yield: 73%. ^{1}H NMR (600 MHz, $CDCl_3$): δ 5.52 (d, *J* = 8.4 Hz, 1H), 5.44—5.28 (m, 2H), 4.87 (d, *J* = 8.3 Hz, 1H), 4.19—4.03 (m, 3H), 3.97—3.86 (m, 2H), 3.71 (ddd, *J* = 11.2, 8.5, 3.2 Hz, 1H), 3.52 (ddd, *J* = 13.8, 8.5, 3.4 Hz, 1H), 3.27 (ddd, *J* = 13.4, 4.7, 3.1 Hz, 1H), 2.14 (s, 3H), 2.04 (s, 3H), 2.00 (s, 3H), 1.96 (s, 3H).

1-Aminoethyl-2-acetamido-3,4,6-tri-*O*-acetyl-2-deoxy-β-D-galactopyranosyl bicyclo[2.2.1] hept-5-ene-exo-2-carboxamide 31. Compound **31** (**Scheme 3-6**) was synthesized following the same procedure to prepare **6**. Yield: 62%. ^{1}H NMR (400 MHz, $CDCl_3$): δ 6.21– 6.07 (m, 3H), 5.89 – 5.80 (m, 1H), 5.36 (dd, *J* = 3.4, 1.1 Hz, 1H), 5.14 (ddd, *J* = 11.3, 6.3, 3.4 Hz, 1H), 4.62 (dd, *J* = 8.4, 4.6 Hz, 1H), 4.22 – 4.05 (m, 3H), 3.98 – 3.85 (m, 2H), 3.71 (m, 1H), 3.63 – 3.50 (m, 1H), 3.46 – 3.33 (m, 1H), 2.93 (s, 1H), 2.17 (d, *J* = 6.2 Hz, 3H), 2.06 (d, *J* = 1.6 Hz, 3H), 2.02 (d, *J* = 0.9 Hz, 3H), 1.97 (d, *J* = 9.6 Hz, 3H), 1.95 – 1.84 (m, 2H), 1.71 (ddd, *J* = 6.0, 4.6, 3.0 Hz, 1H), 1.39 – 1.24 (m, 2H). ^{13}C NMR (125 MHz, $CDCl_3$): δ 176.13, 176.03, 170.84, 170.43, 170.25, 138.26, 136.0, 101.68, 70.77, 70.02, 68.50, 66.34, 61.30, 51.02, 47.35, 47.12, 46.22, 44.56, 41.57, 39.03, 30.39, 30.29, 23.64, 20.61. HRMS (ESI) Calcd for $C_{24}H_{34}N_2O_{10}$ $[M+H]^+$ 511.2300; found 511.2304.

Tetra-acetyl-D-fucopyranose 33. Compound **33** was synthesized following the same procedure to prepare **1**. Yield: 98%. ^{1}H NMR (500 MHz, $CDCl_3$): δ 6.36 (d, *J* = 2.9 Hz, 1H), 5.58 – 5.19 (m, 3H), 4.29 (q, *J* = 6.6 Hz, 1H), 2.20 (s, 3H), 2.17 (s, 3H), 2.03 (d, *J* = 5.8 Hz, 6H), 1.24 (d, *J* = 6.4 Hz, 3H).

(1-Hydroxyl)-2,3,4-tri-*O*-acetyl-D-fucopyranose 34. Compound **34** was synthesized following the same procedure to prepare **2.** Yield: 80%. ^{1}H NMR (600 MHz, $CDCl_3$): δ 5.47 (t, *J* = 3.4 Hz, 1H), 5.42 (dd, *J* = 10.8, 3.4 Hz, 1H), 5.11 – 5.01 (m, 1H), 4.66 (dd, *J* = 9.1, 7.2 Hz, 1H), 4.42 (q, *J* = 6.5 Hz, 1H), 2.66 (s, 1H), 2.17 (s, 3H), 2.10 (s, 3H), 2.00 (s, 3H), 1.15 (d, *J* = 6.4 Hz, 3H).

2,3,4-Tri-*O*-acetyl-D-fucopyranosyl trichloroacetimidate 35. Compound **35** was synthesized following the same procedure to prepare **3**. Yield: 71%. ^{1}H NMR (600 MHz, $CDCl_3$): δ 8.60 (d, *J* = 3.1 Hz, 1H), 6.55 (t, *J* = 3.5 Hz, 1H), 5.51 – 5.26 (m, 3H), 4.36 (dd, *J* = 6.3, 2.9 Hz, 1H), 2.18 (s, 3H), 2.06 – 1.95 (m, 6H), 1.18 (d, *J* = 6.4 Hz, 3H).

1-Chloroethyl-2,3,4-tri-*O*-acetyl-α-D-fucopyranoside 36. Compound **36** was synthesized following the same procedure to prepare **4**. Yield: 75%. ^{1}H NMR (600 MHz, $CDCl_3$): δ 5.26 – 5.16 (m, 1H), 5.02 (dd, *J* = 10.5, 3.6 Hz, 0H), 4.50 (d, *J* = 8.0 Hz, 0H), 4.12 (dt, *J* = 10.3, 5.0 Hz, 1H), 3.81 (q, *J* = 6.6 Hz, 1H), 3.74 (dt, *J* = 11.3, 6.5 Hz, 1H), 3.67 – 3.57 (m, 1H), 2.17 (s, 3H), 2.06 (s, 3H), 1.98 (s, 3H), 1.21 (d, *J* = 6.4 Hz, 3H).

1-Azidoethyl-2,3,4-tri-*O*-acetyl-α-D-fucopyranoside 37. Compound **37** was synthesized following the same procedure to prepare **5**. Yield: 82%. ^{1}H NMR (400 MHz, $CDCl_3$): δ 5.28 – 5.20 (m, 2H), 5.04 (dd, *J* = 10.4, 3.5 Hz, 1H), 4.54 (d, *J* = 7.9 Hz, 1H), 4.07 (ddd, *J* = 10.6, 4.6, 3.5 Hz, 1H), 3.84 (qd, *J* = 6.6, 1.3 Hz, 1H), 3.69 (ddd, *J* = 10.6, 8.5, 3.4 Hz, 1H), 3.52 (ddd, *J* =

13.3, 8.5, 3.5 Hz, 1H), 3.31 (ddd, *J* = 13.4, 4.7, 3.4 Hz, 1H), 2.19 (s, 3H), 2.08 (s, 3H), 2.00 (s, 3H), 1.24 (d, *J* = 6.4 Hz, 3H).

1-Aminoethyl-2,3,4-tri-*O*-acetyl-α-D-fucopyranosyl bicyclo[2.2.1]hept-5-ene-exo-2-carbox-amide 38. Compound **38** was synthesized following the same procedure to prepare **6**. Yield: 66%. ^{1}H NMR (600 MHz, $CDCl_3$): δ 6.14 (m, 1H), 6.09 (m, 1H), 5.96 (s, 1H), 5.23 (d, *J* = 3.8 Hz, 1H), 5.16 (m, 1H), 5.01 (ddd, *J* = 10.5, 3.6, 1.5 Hz, 1H), 4.44 (dt, *J* = 8.5, 2.6 Hz, 1H), 3.90 – 3.77 (m, 3H), 3.73 – 3.64 (m, 1H), 3.46 (m, 2H), 2.92 (dd, *J* = 11.8, 4.1 Hz, 2H), 2.17 (s, 3H), 2.05 (d, *J* = 12.1 Hz, 3H), 1.98 (s, 3H), 1.91 (m, 1H), 1.70 (d, *J* = 8.7 Hz, 1H), 1.37 – 1.27 (m, 3H). 1.21 (d, *J* = 6.4 Hz, 3H).

1. 2. Synthesis of glycopolymers

ROMP of glycopolymers. The monomer **6** (0.06 mmol, 30.7 mg) was dissolved in 0.3 mL CH_2Cl_2. To the reaction was added **32** (6 μmol, 5.3 mg for the 10-mers and 0.6 μmol, 0.53 mg for the 100-mers) in CH_2Cl_2 (0.3 mL for the 10-mers and 0.7 mL for the 100-mers) (Strong and Kiessling 1999). The reaction was monitored by TLC. Ethyl vinyl ether (0.1 mL) was added to quench the reaction when it was done, and the mixture was stirred for an additional 30 min (**Scheme 3-7**). The polymer was isolated by precipitation with cold Et_2O to yield 10-mers as brown sticky oil and 100-mers as light yellow sticky oil.

Deacetylation of glycopolymers. The protected polymer (28 mg) was dissolved in 2 mL MeOH/THF (2:1, v/v) and to this was added K_2CO_3 (75 mg) and the reaction stirred for 20-30 min. The solvents were evaporated and the solid was then poured into a solution of 10 mL

THF/H_2O (1:1, v/v) containing 1N HCl. This was then allowed to stir for 30–60 min (**Scheme 3-7**) and then the solvents removed in vacuo, followed by ion exchange chromatography for 10-mers or dialysis for 100-mers to afford the deprotected polymer as a white powder (Murphy, Furusho et al. 2007).

Polymer molecular weight and polydispersity index (PDI) determination. Purified protected polymers were dissolved in filtrated THF (about 1.2 mg/mL). An aliquot (100 μL) of the polymer solution was injected and analyzed by gel permeation chromatography and static light scattering. Elution was performed at 0.7 mL/min with THF and UV signals were measured at 220 nm and 256 nm at 30 ℃. Narrowly dispersed polystyrene standards from Sigma Aldrich were used as molecular weight calibrants. The number average and weighted average molecular weights were calculated from the chromatogram. The results are shown in **Table 3-1**.

prot-poly(Man)$_{10}$ Yield after purification: 58%. ^{1}H-NMR (600 MHz, $CDCl_3$): δ 7.32 (m), 5.85—6.2 (m), 5.20—5.5 (with max at 5.3, 5.25), 4.82 (br s), 4.27 (br s), 4.12 (br s), 3.97 (br s), 3.12—3.80 (with max at 3.52, 3.74), 3.02 (br s), 2.70 (br s), 2.33 (br s), 1.90—2.24 (with max at 2.0, 2.05, 2.10, 2.15), 1.55 (br s), 1.04—1.40 (m).

prot-poly(Man)$_{100}$ Yield after purification: 90%. ^{1}H-NMR (600 MHz, $CDCl_3$): δ 5.85—6.3 (m), 5.10—5.50 (with max at 5.23, 5.27, 5.34), 4.80 (br s), 4.26 (br s), 4.09 (br s), 3.96 (br s), 3.12—3.80 (with max at 3.52, 3.75), 3.02 (br s), 2.68 (br s), 2.33 (br s), 1.73—2.24 (with max at 2.0, 2.05, 2.10, 2.15), 1.60 (br s), 1.05—1.27 (m).

prot-poly(Glc)$_{10}$ Yield after purification: 68%. ^{1}H-NMR (600 MHz, $CDCl_3$): δ 7.32 (m), 5.68—6.07 (m), 4.78—5.51 (with max at 4.95, 5.06, 5.18, 5.23, 5.40), 4.51 (br s), 4.25 (br s), 4.12 (br s), 3.18—3.97 (with max at 3.30, 3.48, 3.66, 3.72, 3.81), 3.01 (br s), 2.67 (br s), 2.19—2.49 (with

max at 2.24, 2.41), 1.95—2.20 (with max at 1.99, 2.01, 2.03, 2.07), 1.79 (br s), 1.57 (br s), 1.01—1.38 (m).

prot-poly(Glc)$_{100}$ Yield after purification: 75%. ^{1}H-NMR (600 MHz, $CDCl_3$): δ 5.78—6.0 (m), 5.23—5.48 (with max at 5.28, 5.40), 5.20 (br s), 5.07 (br s), 4.96 (br s), 4.54 (br s), 4.26 (br s), 4.13 (br s), 3.82 (br s), 3.63—3.77 (with max at 3.67, 3.71), 3.18—3.62 (with max at 3.29, 3.47), 3.02 (br s), 2.67 (br s), 2.09—2.37 (with max at 2.13, 2.25), 1.94—2.10 (with max at 2.0, 2.02, 2.04, 2.05, 2.08), 1.85—1.94 (m), 1.56 (br s), 0.97—1.39 (m).

prot-poly(Gal)$_{10}$ Yield after purification: 72%. ^{1}H-NMR (600 MHz, $CDCl_3$): δ 7.32 (m), 5.75—6.10 (m), 4.90—5.50 (with max at 5.07, 5.18, 5.32, 5.42), 4.52 (br s), 4.15 (br s), 3.75—4.00 (with max at 3.80, 3.92), 3.20—3.74 (with max at 3.30, 3.50, 3.67), 3.05 (br s), 2.71 (br s), 2.26 (br, s), 1.80—2.24 (with max at 2.03, 2.11, 2.20), 1.60 (br s), 1.0—1.30 (m).

prot-poly(Gal)$_{100}$ Yield after purification: 93%. ^{1}H-NMR (400 MHz, $CDCl_3$): δ 5.75—6.20 (m), 4.98—5.51(with max at 5.03, 5.16, 5.29, 5.39), 4.52 (br s), 4.16 (br s), 3.95 (br s), 3.84 (br s), 3.19—3.75 (with max at 3.29, 3.51, 3.65), 3.01 (br s), 2.68 (br s), 2.27 (br s), 1.82—2.20 (with max at 1.98, 2.04, 2.16), 1.59 (br s), 1.0—1.27 (m).

prot-poly(Fuc)$_{10}$ Yield after purification: 59%. ^{1}H-NMR (500 MHz, $CDCl_3$): δ 7.32 (m), 5.66—6.58 (m), 4.85—5.54 (with max at 5.02, 5.12, 5.27, 5.31), 4.12 (br s), 3.20—3.81 (with max at 3.34, 3.51, 3.71), 3.03 (br s), 2.67 (br s), 2.21—2.42 (m), 1.80—2.20 (with max at 1.98, 2.06, 2.15), 1.60 (br s), 0.9—1.33 (with max at 1.13, 1.23).

prot-poly(Fuc)$_{100}$ Yield after purification: 77%. ^{1}H-NMR (500 MHz, $CDCl_3$): δ 5.75—6.47 (m), 4.89—5.56 (with max at 5.06, 5.15, 5.30, 5.34), 4.15 (br s), 3.25—3.94 (with max at 3.38, 3.54,

3.76), 3.07 (br s), 2.70 (br s), 2.26—2.47 (m), 1.78—2.24 (with max at 2.02, 2.09, 2.19), 1.63 (br s), 1.28 (br s), 1.16 (br s), 0.72—0.99 (with max at 0.90).

prot-poly(GlcNAc)$_{10}$ Yield after purification: 67%. ^{1}H-NMR (600 MHz, $CDCl_3$): δ 7.31 (m), 6.02—6.56 (m), 4.51—5.50 (with max at 4.75, 5.02, 5.18, 5.28), 3.12—4.48 (with max at 3.31, 3.50, 3.67, 3.83, 4.12, 4.26), 2.95 (br s), 2.63 (br s), 2.19—2.47 (with max at 2.33, 2.41), 1.71—2.19 (with max at 1.94, 2.0, 2.06), 1.59 (br s), 0.98—1.34 (with max at 1.14, 1.22).

prot-poly(GlcNAc)$_{100}$ Yield after purification: 81%. ^{1}H-NMR (500 MHz, $CDCl_3$): δ 6.01—6.62 (m), 5.14—5.54 (with max at 5.22, 5.31), 5.08 (br s), 4.48—4.96 (m), 4.27 (br s), 4.15 (br s), 2.84—4.06 (with max at 2.92, 2.99, 3.37, 3.54, 3.69, 3.80, 3.87, 3.98), 2.66 (br s), 2.38 (br s), 1.76—2.20 (with max at 1.91, 1.96, 2.04, 2.09), 1.62 (br s), 0.97—1.48 (with max at 1.16, 1.27, 1.35).

prot-poly(GalNAc)$_{10}$ Yield after purification: 90%. ^{1}H-NMR (500 MHz, $CDCl_3$): δ 7.34 (m), 6.01—6.82 (m), 5.01—5.68 (with max at 5.23, 5.28, 5.38), 2.90—4.39 (with max at 3.01, 3.34, 3.51, 3.58, 3.65, 3.89, 3.97, 4.16), 2.67 (br s), 2.39 (br s), 1.78—2.27 (with max at 1.93, 1.98, 2.01, 2.06, 2.16), 1.62 (br s), 1.06—1.41 (m).

prot-poly(GalNAc)$_{100}$ Yield after purification: 92%. ^{1}H-NMR (500 MHz, $CDCl_3$): 6.06—6.77 (m), 5.05—5.58 (with max at 5.23, 5.28, 5.38), 4.67 (br s), 3.77—4.30 (with max at 3.80, 3.93, 4.16), 2.80—3.78 (with max at 3.02, 3.34, 3.86), 2.67 (br s), 2.39 (br s), 1.78—2.27 (with max at 1.93, 1.98, 2.01, 2.06, 2.16), 1.62 (br s), 1.06—1.41 (m).

Prot-poly(D-Fuc)$_{10}$ Yield after purification: 64%. ^{1}H-NMR (600 MHz, $CDCl_3$): δ 7.33 (m), 5.70—6.0 (m), 5.06—5.48 (with max at 5.13, 5.23, 5.29, 5.40), 5.01 (br s), 4.45 (br s), 3.83 (br

s), 3.19—3.74 (with max at 3.27, 3.35, 3.49, 3.64), 3.02 (br s), 2.68 (br s), 2.20—2.45 (m), 1.80—2.20 (with max at 1.98, 2.04, 2.17), 1.56 (br s), 1.0—1.28 (with max at 1.13, 1.20).

Prot-poly(D-Fuc)$_{100}$ Yield after purification: 82%. ^{1}H-NMR (600 MHz, $CDCl_3$): δ 5.73—6.24 (m), 5.07—5.46 (with max at 5.13, 5.22, 5.28, 5.39), 5.01 (br s), 4.48 (br s), 3.83 (br s), 3.18—3.75 (with max at 3.25, 3.34, 3.46, 3.64), 3.00 (br s), 2.68 (br s), 2.22 (br s), 1.80—2.20 (with max at 1.97, 2.03, 2.13), 1.72 (br s), 1.56 (br s), 0.94—1.25 (with max at 1.09, 1.19).

poly(Man)$_{10}$ Yield after purification: 78%. ^{1}H-NMR (600 MHz, D_2O): δ 7.24 (m), 5.09—5.43 (m), 4.70—4.82 (with max at 4.75), 3.10—3.90 (with max at 3.25, 3.48, 3.55, 3.60, 3.75, 3.82), 2.23—3.0 (with max at 2.40, 2.85), 1.53—2.10 (with max at 1.57, 1.91), 1.10 (br s).

poly(Man)$_{100}$ Yield after purification: 85%. ^{1}H-NMR (600 MHz, D_2O): δ 5.12—5.43 (m), 4.77 (m), 3.17—3.92 (with max at 3.26, 3.51, 3.68, 3.77, 3.84), 2.29—3.17 (with max at 2.42, 2.94), 1.48—2.13 (with max at 1.59, 1.91), 1.13 (br s).

poly(Glc)$_{10}$ Yield after purification: 83%. ^{1}H-NMR (600 MHz, D_2O): δ 7.25 (m), 4.80—5.50 (with max at 5.03, 5.26), 4.43 (br s), 3.10—4.02 (with max at 3.31, 3.48, 3.55, 3.68, 3.73, 3.81), 2.25—3.04 (with max at 2.39, 2.90), 1.30—2.10 (with max at 1.56, 1.92), 1.09 (br s).

poly(Glc)$_{100}$ Yield after purification: 85%. ^{1}H-NMR (500 MHz, D_2O): δ 5.08—5.50 (m), 4.34 (br s), 3.85 (br s), 3.66 (br s), 3.18—3.50 (with max at 3.73, 3.78, 3.80), 2.20—3.10 (with max at 2.40, 2.68, 2.98), 1.30—2.10 (with max at 1.59, 1.98), 1.09 (br s).

poly(Gal)$_{10}$ Yield after purification: 75%. ^{1}H-NMR (600 MHz, D_2O): δ 7.24 (m), 5.0—5.50 (m), 4.23 (br s), 3.10—4.0 (with max at 3.25, 3.40, 3.51, 3.55, 3.76), 2.25—3.10 (with max at 2.40, 2.90), 1.42—2.05 (with max at 1.54, 1.68, 1.90), 1.10 (br s).

poly(Gal)$_{100}$ Yield after purification: 78%. ^{1}H-NMR (600 MHz, D_2O): δ 5.04—5.45 (m), 4.26 (br s), 3.84 (br s), 3.11—3.78 (with max at 3.28, 3.44, 3.55, 3.63, 3.66), 2.70—3.12 (m), 2.29—2.69 (with max at 2.40), 1.48—2.08 (with max at 1.59, 1.94), 1.10 (br s).

poly(Fuc)$_{10}$ Yield after purification: 77%. ^{1}H-NMR (400 MHz, D_2O): δ 7.34 (m), 5.00—5.58 (m), 4.51—4.68 (m), 4.35 (br s), 4.22 (br s), 3.18—4.12 (with max at 3.37, 3.52, 3.65, 3.76, 3.83, 3.98), 3.00 (br s), 2.36—2.80 (with max at 2.49), 1.48—2.21 (with max at 1.66, 1.87, 2.01), 1.01—1.43 (with max at 1.23, 1.24, 1.27, 1.28).

poly(Fuc)$_{100}$ Yield after purification: 85%. ^{1}H-NMR (400 MHz, D_2O): δ 5.03—5.40 (m), 4.15—4.36 (m), 3.10—3.90 (with max at 3.40, 3.54, 3.61, 3.64), 2.12—3.08 (with max at 2.39, 2.60, 2.98), 1.45—2.21 (with max at 1.56, 2.01), 1.0—1.40 (with max at 1.11, 1.16).

poly(GlcNAc)$_{10}$ Yield after purification: 78%. ^{1}H-NMR (600 MHz, D_2O): δ 7.24 (m), 4.94—5.50 (with max at 5.03, 5.26), 4.43 (br s), 3.04—4.02 (with max at 3.31, 3.48, 3.55, 3.68, 3.73, 3.81), 2.25—3.04 (with max at 2.39, 2.90), 1.30—2.10 (with max at 1.56, 1.92), 1.17 (br s).

poly(GlcNAc)$_{100}$ Yield after purification: 77%. ^{1}H-NMR (600 MHz, D_2O): δ 5.02—5.40 (m), 4.38 (br s), 3.66—3.83 (with max at 3.73, 3.78, 3.80), 3.47—3.66 (with max at 3.51, 3.57, 3.62), 3.32 (br s), 3.15 (br s), 2.86 (m), 2.42—2.66 (with max at 2.33, 2.57), 1.91 (br s), 1.52 (br s).

poly(GalNAc)$_{10}$ Yield after purification: 90%. ^{1}H-NMR (500 MHz, D_2O): δ 7.24 (br s), 5.02—5.40 (m), 4.35 (br s), 3.48—4.10 (with max at 3.59, 3.68, 3.70, 3.88), 2.30—3.44 (with max at 2.40, 2.60, 2.91, 3.22), 1.98 (br s), 0.98—1.70 (with max at 1.10, 1.60).

poly(GalNAc)$_{100}$ Yield after purification: 92%. ^{1}H-NMR (500 MHz, D_2O): δ 5.09—5.45 (m), 4.36 (br s), 3.50—3.91 (with max at 3.59, 3.69, 3.70, 3.81, 3.90), 2.30—3.41 (with max at 2.38, 2.62, 2.90, 3.20, 3.35), 1.98 (br s), 1.59 (br s), 1.01—1.23 (m).

Poly(D-Fuc)$_{10}$ Yield after purification: 72%. ^{1}H-NMR (600 MHz, D_2O): δ 7.34 (m), 5.00—5.58 (m), 4.51—4.68 (m), 4.35 (br s), 4.22 (br s), 3.18—4.12 (with max at 3.37, 3.52, 3.65, 3.76, 3.83, 3.98), 3.00 (br s), 2.36—2.80 (with max at 2.49), 1.48—2.21 (with max at 1.66, 1.87, 2.01), 1.01—1.43 (with max at 1.23, 1.24, 1.27, 1.28).

Poly(D-Fuc)$_{100}$ Yield after purification: 57%. ^{1}H-NMR (500 MHz, D_2O): δ 5.03—5.40 (m), 4.15—4.36 (m), 3.10—3.90 (with max at 3.40, 3.54, 3.61, 3.64), 2.12—3.08 (with max at 2.39, 2.60, 2.98), 1.45—2.21 (with max at 1.56, 2.01), 1.0—1.40 (with max at 1.11, 1.16).

1.3. Sperm immunofluorescent assay

General Methods and Materials. All experiments performed with mice were in accordance with the National Institute of Health and United States Department of Agriculture guidelines, and the specific procedures performed were approved by the Stony Brook University IACUC (protocol 0616). Chemicals for assay buffer were purchased from Sigma-Aldrich, Fisher Scientific and VWR. The culture medium M16 is a modified Krebs-Ringer bicarbonate medium containing the following: 94.6 mM NaCl, 4.8 mM KCl, 1.19 mM KH_2PO_4, 1.19 mM $MgSO_4 \cdot 7H_2O$, 23.28 mM sodium lactate, 5.56 mM glucose, 0.0006% penicillin G potassium salt, 0.0005% streptomycin sulfate, 25.0 mM $NaHCO_3$, 0.33 mM sodium pyruvate, 1.95 mM

$CaCl_2 \cdot 2H_2O$ (Table 5-1). All solutions were stored at 4 ℃. Stock B and stock C must be changed every other week, and stock A and D can be stored up to 3 months.

Table 5-1. Composition of M16 buffer.

Stock solutions	Component	Quantity (g)	Concentration in assay buffer
Stock A (50 mL) 10 × Conc.	NaCl	2.767	94.6 mM
	KCl	0.178	4.8 mM
	KH_2PO_4	0.081	1.2 mM
	$MgSO_4 \cdot 7H_2O$	0.1465	1.2 mM
	60% w/v sodium lactate	2.2715	23.3 mM
	glucose	0.5	5.6 mM
	penicillin K^+ salt	0.03	0.0006%
	streptomycin sulfate	0.025	0.0005%
Stock B (20 mL) 10 × Conc.	$NaHCO_3$	0.402	25.0 mM
	Phenol red	0.002	
Stock C (20 mL) 10 × Conc.	Sodium pyruvate	0.072	0.33 mM
Stock D (20 mL) 10 × Conc.	$CaCl_2 \cdot 2H_2O$	0.572	2.0 mM

Preparation of 0.3% BSA/M16 buffer. The 0.3% BSA/M16 modified Krebs-Ringer medium was made up as follows: The stock mixture solution of 2 mL stock A, 2 mL stock B, 0.2 mL stock C and 0.2 mL stock D was diluted to 20mL with ddH_2O. To the stock mixture solution, 60 mg BSA was added to make a final concentration of 0.3% BSA. The buffer was filtered through a 0.2 μm sterile filter and stored at 4 °C.

Sperm Treatment. Sperm were isolated from cauda epididymis of two 10 to 12-week-old ICR male breeders (Taconic, NJ) in M16 medium supplemented with 0.3% BSA (6 mL). The sperm suspension was then gently pipetted into a polypropylene culture tube (12 × 75 mm) and incubated at 37 ℃ for 30 min under 5% CO_2 in air. Once the incubation was complete, the sperm motility was examined by phase-contrast microscopy. Only samples of capacitated sperm displaying >80% motility were used in subsequent experiments. The concentration of sperm was accessed by hemocytometer.

Dose-dependent Assay. Aliquots (20 μL) containing about 5×10^5 capacitated sperm were transferred to microcentrifuge tubes and incubated with controls and glycopolymers at varying concentrations at 37 ℃ under 5% CO_2 for 30 min. Calcium ionophore A23187 (Sigma), a known sperm acrosome reaction stimulus, was used as a positive control instead of ZP, because the role of ZP in AR activation is controversial and the calcium concentration has been proved to be very essential to AR. Since all polymer samples were prepared in phosphate buffered saline (PBS), sperm with PBS alone was used as a negative control. After incubation, the sperm were pelleted by centrifugation at 500 *g* for 6 min. The supernatant was removed and the pelleted sperm were washed once with 40 μl PBS and fixed with 40 μl 70% ethanol. After fixing at 4 °C for 30 min, the sperm were pelleted and washed twice with PBS. The final pellet was resuspended in 40 μL of DDI water. Aliquots (10 μL) of each sample were transferred to cover slips and air-dried.

Time-course Study. Aliquots (20 μL) containing about 5×10^5 capacitated sperm were transferred to microcentrifuge tubes and incubated with controls and effective 100-mers at their optimal concentrations at 37 ℃ under 5% CO_2 for a specified time (15 min, 30 min and 45 min). Poly$(Glc)_{100}$ was utilized as negative control in this assay and the following steps were same as the dose-dependent assay.

Glycopolymer Combination Assay. Aliquots (20 μL) containing about 5×10^5 capacitated sperm were transferred to microcentrifuge tubes and incubated with controls and mixture of two or three active 100-mers at their optimal (10 μM) and much lower concentrations (2.5 μM) at 37 ℃ under 5% CO_2 for 30 min. Poly$(Glc)_{100}$ was utilized as negative control in this assay and the following steps were same as the dose-dependent assay.

Signaling Pathway Inhibition Assay. Inhibitor stock solutions were prepared by dissolving the reagents either in distilled water (pertussis toxin) or in DMSO. Aliquots of the stock solutions were mixed with the capacitated sperm solution to achieve the desired concentration, and pre-incubated for 5 min before treatment with glycopolymers for another 30 min. The concentrations of inhibitors were chosen based on references (Loeser, Lynch et al. 1999, Chiu, Wong et al. 2008) and toxicity test. Poly$(Glc)_{100}$ was utilized as negative control in this assay and the following steps were same as the dose-dependent assay.

Assessment of Sperm Acrosome Reaction. 10 μL Rhodamine labeled peanut agglutinin (PNA) (Vector labs) at a concentration of 20 μg/mL was incubated with fixed sperm on cover slips for 10 min at room temperature. After washing with 2 mL DDI water (twice of 10 mins each), the cover slips were mounted on SuperFrost Plus microscope slides (Fisher Scientific, Suwanee, GA) over a drop (6 μL) of mounting medium Vectashield (Vector labs), sealed with nail polish, and the acrosomal status was assessed by inverse fluorescence microscopy (Zeiss,

Oberkochen, Germany). Sperm that displayed continuous red fluorescence along their acrosomal arcs were scored as acrosome-intact; those that displayed no red or punctuate fluorescence were scored as acrosome-reacted. The slides were coded and counted blindly; all experiments were conducted at least three times. Each time, three independent replicates of each test group were analyzed, and 200 sperm from each replicate were counted.

Statistical Analysis. Comparisons of the average values for the control and experimental groups were carried out by a paired two-tailed *t*-test to determine statistically significant differences ($p < 0.05$). The results are presented as mean ± SEM.

2. Investigation of synthetic methods to prepare fertilization probes

Materials. Amino acids and coupling agents used were purchased from Advanced Chem Tech. (Louisville, KY) or Sigma-Aldrich (Milwaukee, WI). $(H_2IMes)(PCy)_2Cl_2Ru{=}CHPh$ and $(PCy)_2Cl_2Ru{=}CHPh$ were purchased from Sigma-Aldrich (Milwaukee, WI). $(H_2IMes)(3\text{-}BrPyr)_2Cl_2Ru{=}CHPh$, **32**, was prepared according to the literature (Love, Morgan et al. 2002). Solvents and chemical reagents were obtained from Fisher Scientific, Inc. (Springfield, NJ) or Sigma-Aldrich (Milwaukee, WI). CH_2Cl_2 and CH_3OH were purified by Pushstill solvent dispensing system (SG Water USA LLC, Nashua, NH); pyridine, pentane and Et_2O were used without further purification. All reactions were carried out under an Ar or N_2 atmosphere in oven-dried glassware unless otherwise specified. Cyclobut-1-enecarboxylic acid (CB) was synthesized according to the literature (Schueller, Manning et al. 1996).

General Methods. Analytical thin layer chromatography (TLC) was performed on precoated silica gel plates (60F254). TLC spots were detected by UV light and by staining with phosphomolybdic acid (PMA) or ninhydrin. Gemini 300, Inova400, Inova500 and Inova600 MHz NMR spectrometers were used to perform NMR analysis, and spectra were recorded in $CDCl_3$ unless otherwise noted. ^{1}H-NMR spectra are reported as chemical shift in parts per million (multiplicity, coupling constant in Hz, integration). ^{1}H-NMR data are assumed to be first order. The usual workup for peptide coupling reactions was three washes of the CH_2Cl_2 solution with 5% $NaHCO_3$, followed by three washes with 1 N HCl and drying of the organic layer over Na_2SO_4. After concentrated by rotary evaporation, product was purified by flash silica chromatography on silica gel-60 (230–400 mesh) or Combiflash chromatography system (Teledyne Isco, Inc, Lincoln NE).

2. 1. Synthesis of tripeptides

CBz-AlaAsp(OtBu)-OMe 39 CBz-Ala-OH (4.59 mmol, 1.024 g), H-D(OtBu)-OMe ·HCl (4.17 mmol, 1.00 g), HOBt (5.01 mmol, 0.68 g) and EDC ·HCl (5.01 mmol, 0.96 g) were dissolved in 15 mL dry CH_2Cl_2 with N,N-diisopropylethylamine (DIEA, 5.01 mmol, 0.89 mL). The solution was stirred at room temperature under N_2 for 15 h (**Scheme 3-10**). After workup, the solution was concentrated and purified by Combiflash (acetone:methylene chloride = 2:8, v/v) to yield compound **39** (1.48 g, 87%) as a white powder. ^{1}H-NMR (500 Hz, $CDCl_3$) : δ 7.36 (s, 5H), 6.83 (d, J = 6.0, 1H), 5.38 (s, 1H), 5.16(s, 2H), 4.80 (m, 1H), 4.23(m, 1H), 3.78 (s, 3H), 2.95 (dd, J = 18.0, 15.0, 1H), 2.72 (dd, J = 9.0, 1H), 1.42 (d, J = 6.0, 12H).

H-AlaAsp(OtBu)-OMe 40 CBz-AlaAsp(OtBu)-OMe (2.69 mmol, 1.10 g) was dissolved in 8 mL dry CH_2Cl_2/CH_3OH (1:1, v/v) and then 10% Pd/C (0.27 mmol, 29 mg) was added. The solution was evacuated and then stirred at rt under H_2 for 24 h (**Scheme 3-10**). After that, the Pd/C was filtrated by celite and the solution was collected and evaporated by rotary evaporator to yield compound **40** (0.66 mg, 90%) as a white powder. ^{1}H-NMR (600 Hz, $CDCl_3$): δ 8.02 (d, J = 6.0, 1H), 6.42 (s, 2H), 4.79 (m, 1H), 3.76 (s, 3H), 3.57 (m, 1H), 2.90 (dd, J = 18.0, 15.0, 1H), 2.74 (dd, J = 18.0, 15.0, 1H), 1.44 (s, 9H), 1.36 (d, J = 6.0, 3H).

CBz-Glu(OtBu)AlaAsp(OtBu)-OMe 41 Compound **41** (**Scheme 3-10**) was synthesized following the same procedure to prepare **39**. Yield: 51%. ^{1}H-NMR (600 Hz, $CDCl_3$): δ 7.35 (s, 5H), 6.85 (dd, J = 18.0, 15.0, 2H), 5.63 (d, J = 6.0, 1H), 5.10 (s, 2H), 4.78 (dd, J = 12.0, 6.0, 1H), 4.23 (m, 1H), 4.20 (dd, J = 12.0, 6.0, 1H), 3.76 (s, 3H), 2.90 (dd, J = 18.0, 6.0, 1H), 2.72 (d, J = 12.0, 1H), 2.30—2.50 (m, 2H), 1.90—2.18 (m, 2H), 1.42 (s, 9H), 1.40 (d, J = 6.0, 3H).

H-Glu(OtBu)AlaAsp(OtBu)-OMe 42 Compound **42** (**Scheme 3-10**) was synthesized following the same procedure to prepare **40**. Yield: 72%. ^{1}H-NMR (600 Hz, $CDCl_3$): δ 7.65 (d, J = 6.0, 1H), 6.96 (d, J = 6.0, 1H), 4.80 (m, 1H), 4.45 (m, 1H), 3.72 (s, 3H), 3.21-3.26 (m, 2H), 2.90 (dd, J = 18.0, 6.0, 1H), 2.70 (dd, J = 18.0, 6.0, 1H), 2.16 (m, 2H), 2.10 (m, 1H), 1.80 (m, 1H), 1.42 (s, 9H), 1.40 (d, J = 6.0, 3H).

Cyclobut-1-enecarbonyl-Glu(OtBu)AlaAsp(OtBu)-OMe 43 Compound **43** (**Scheme 3-10**) synthesized following the same procedure to prepare **39**. Yield: 27%. ^{1}H-NMR (600 Hz, $CDCl_3$): δ 6.98 (d, J = 6.0, 1H), 6.90 (d, J = 6.0, 1H), 6.80 (d, J = 6.0, 1H), 6.65 (s, 1H), 4.80 (m, 1H), 4.42 (m, 2H), 3.74 (s, 3H), 2.92 (dd, J = 18.0, 6.0, 1H), 2.71 (m, 3H), 2.52 (m, 1H), 2.48 (s, 2H), 2.37 (m, 1H), 2.01—2.10 (m, 2H), 1.38—1.48 (m, 20H), 1.42 (s, 2H).

Fmoc-Cys(Trt)Asp(OtBu)-OMe 44 Compound **44** (**Scheme 3-11**) was synthesized following the same procedure to prepare **39**. Yield: 86%. ^{1}H-NMR (300 Hz, $CDCl_3$): δ 7.74 (t, J = 9.0, 2H), 7.56 (s, 2H), 7.34 (m, 8H), 7.26 (m, 9H), 7.20 (t, J = 9.0, 3H), 6.76 (d, J=6.0, 1H), 4.98 (d, J = 6.0, 1H), 4.70 (m, 1H), 4.34 (m, 2H), 4.20 (t, J = 6.0, 1H), 3.76 (d, J = 6.0, 1H), 3.60 (s, 3H), 2.80 (dd, J=18.0, 15.0, 1H), 2.60—2.74 (m, 3H), 1.37 (s, 9H).

H-Cys(Trt)Asp(OtBu)-OMe 45 Fmoc-Cys(Trt)Asp(OtBu)-OH **45** (0.65 mmol, 0.50 g) was dissolved in 4mL dry CH_2Cl_2, then 1,8-diazabicyclo[5.4.0]undec-7-ene (DBU, 0.07 mmol, 9.75 μL) and 1-octanethiol (6.49 mmol, 1.13 mL) were added. The solution was stirred at rt under N_2 for 15 h (**Scheme 3-11**). After concentrated, the product was purified by Combiflash (ethyl acetate:methylene chloride = 2:8, v/v) to yield compound **7** (0.31g, 87%) as a white powder. ^{1}H-NMR (300 Hz, $CDCl_3$) : δ 7.90 (d, J = 9.0, 1H), 7.17—7.48 (m, 3H), 6.76 (d, J = 6.0, 1H), 4.98 (d, J = 6.0, 1H), 4.68—4.75 (m, 1H), 3.75 (dd, J = 9.0, 6.0, 1H), 3.71 (s, 3H), 3.00 (dd, J = 9.0, 6.0, 1H), 2.90 (dd, 1H), 2.52—2.75 (m, 3H), 1.40 (s, 9H).

Fmoc-GlyCys(Trt)Asp(OtBu)-OMe 46 Compound **46** (**Scheme 3-11**) was synthesized following the same procedure to prepare **39**. Yield: 64%. ^{1}H-NMR (300 Hz, $CDCl_3$): δ 7.76 (d, J = 6.0, 2H), 7.53 (d, J = 6.0, 2H), 7.43 (m, 8H), 7.32 (m, 6H), 7.20 (m, 3H), 6.77 (d, J = 6.0, 1H), 6.20 (d, J = 6.0, 1H), 4.70 (dd, J = 9.0, 6.0, 1H), 4.45 (d, J = 6.0, 2H), 4.17 (t, J = 6.0, 1H), 3.98 (d, J = 6.0, 1H), 3.75 (d, J = 6.0, 2H), 3.60 (s, 3H), 3.12—3.22 (m, 1H), 2.50—2.85 (m, 4H), 1.47 (s, 9H).

H-GlyCys(Trt)Asp(OtBu)-OMe 47 Compound **47** (**Scheme 3-11**) was synthesized following the same procedure to prepare **45**. Yield: 58%. ^{1}H-NMR (300 Hz, $CDCl_3$): δ 7.43 (d, J = 6.0,

7H), 7.15—7.33 (m, 10H), 6.80 (d, J = 6.0, 1H), 4.69 (m, J = 6.0, 1H), 4.12 (dd, J = 6.0, 9.0, 1H), 3.65 (s, 3H), 2.50—2.80 (m, 5H), 1.40 (s, 9H).

Cyclobut-1-enecarbonyl-GlyCys(Trt)Asp(OtBu)-OMe 48 Compound **48** (**Scheme 3-11**) was synthesized following the same procedure to prepare **39**. Yield: 29%. ^{1}H-NMR (600 Hz, $CDCl_3$): δ 7.42 (d, J = 6.0 Hz, 6H), 7.25—7.33 (m, 6H), 7.22—7.25 (m, 3H), 6.75 (d, J = 6.0 Hz, 1H), 6.62 (s, 1H), 6.25 (s, 1H), 6.09 (d, J = 6.0 Hz, 1H), 4.70 (dt, J = 8.8, 4.7 Hz, 1H), 3.98 (dd, J = 7.4, 5.4 Hz, 1H), 3.87 (d, J = 6.0 Hz, 2H), 3.68 (s, 3H), 2.75—2.88 (m, 2H), 2.50—2.68 (m, 4H), 2.04 (s, 2H), 1.40 (s, 9H).

Fmoc-Cys(Acm)Asp(OtBu)-OMe 49 Compound **49** (**Scheme 3-12**) was synthesized following the same procedure to prepare **39**. Yield: 92%. ^{1}H-NMR (600 Hz, $CDCl_3$): δ 7.75 (d, J =6.0 Hz, 2H), 7.61 (m, 2H), 7.41 (m, 2H), 7.30 (t, J = 6.0 Hz, 2H), 6.67 (d, 1H), 5.92 (d, J = 6.0 Hz, 1H), 4.82 (m, 1H), 4.38—4.41 (m, 2H), 4.21 (m, 2H), 4.35 (m, 1H), 4.22 (t, J = 6.0 Hz, 1H), 3.78 (s, 3H), 2.73—3.00 (m, 4H), 2.03 (s, 3H), 1.42 (s, 9H).

H-Cys(Acm)Asp(OtBu)-OMe 50 Compound **50** (**Scheme 3-12**) was synthesized following the same procedure to prepare **45**. Yield: 82%. ^{1}H-NMR (600 Hz, $CDCl_3$): δ 8.19 (d, J = 6.0 Hz, 1H), 6.55 (s, 1H), 4.79 (m, 1H), 4.43 (dd, J = 12.0, 6.0 Hz, 1H), 4.19 (dd, J = 12.0, 6.0 Hz, 1H), 3.78 (s, 3H), 3.65 (t, J = 6.0 Hz, 1H), 3.02 (dd, J = 12.0, 6.0 Hz, 1H), 2.83 (m, 2H), 2.70 (dd, J = 12.0, 6.0 Hz, 1H), 2.01 (s, 3H), 1.43 (s, 9H).

Fmoc-Glu(OtBu)Cys(Acm)Asp(OtBu)-OMe 51 Compound **51** (**Scheme 3-12**) was synthesized following the same procedure to prepare **39**. Yield: 78%. ^{1}H-NMR (600 Hz, $CDCl_3$): δ 7.75 (d, J =6.0 Hz, 2H), 7.59 (t, J = 6.0 Hz, 2H), 7.40 (m, 4H), 7.25 (t, J = 6.0 Hz, 2H), 6.80 (t, J = 6.0 Hz, 1H), 5.83 (d, J = 6.0 Hz, 1H), 4.82 (dd, J = 12.0, 6.0 Hz, 1H), 4.73 (dd, J = 12.0, 6.0 Hz, 1H),

4.53 (dd, J = 12.0, 6.0 Hz, 1H), 4.37—4.41 (m, 2H), 4.20—4.27 (m, 2H), 3.76 (s, 3H), 2.71—3.00 (m, 4H), 2.17—2.24 (m, 2H), 2.02 (s, 3H), 1.42 (d, J = 12.0 Hz, 18H).

H-Glu(OtBu)Cys(Acm)Asp(OtBu)-OMe 52 Compound **52** (**Scheme 3-12**) was synthesized following the same procedure to prepare **45**. Yield: 77.7 %. ^{1}H-NMR (600 Hz): δ 8.17 (d, J =6.0 Hz, 1H), 7.40 (d, J =6.0 Hz, 1H), 7.13 (t, J = 6.0 Hz, 1H), 4.76—4.85 (m, 1H), 4.65—4.71 (dd, J = 12.0, 6.0 Hz, 1H), 4.58—4.64 (dd, J = 12.0, 6.0 Hz, 1H), 4.30—4.44 (m, 1H), 3.92 (3.76 (s, 3H), 3.43—3.50 (m, 1H), 2.90—3.00 (m, 2H), 2.67—2.77 (m, 1H), 2.33—2.47 (m, 2H), 2.07—2.19 (m, 2H), 2.04 (s, 4H), 1.82—1.89 (m, 1H), 1.44 (d, J = 12.0, 18H).

Cyclobut-1-enecarbonyl-Glu(OtBu)Cys(Acm)Asp(OtBu)-OMe 53 Compound **53** (**Scheme 3-12**) was synthesized following the same procedure to prepare **39**. Yield: 30%. ^{1}H-NMR (500 Hz, $CDCl_3$) : δ 7.40 (t, J = 5.0 Hz, 2H), 7.02 (d, J = 5.0 Hz, 1H), 6.95 (t, J = 5.0 Hz, 1H), 6.70 (s, 1H), 4.84 (m, 1H), 4.70 (dd, J = 10.0, 5.0 Hz, 1H), 4.35—4.55 (m, 3H), 3.76 (s, 3H), 2.90—3.0 (m, 3H), 2.72—2.79 (m, 3H), 2.39—2.58 (m, 4H), 2.00—2.20 (m, 5H), 1.47 (d, J = 5.0 Hz, 18H).

GlyGlyGly-OMe 54 GlyGlyGly-OH (1.59 mmol, 0.30 g) was dissolved in excess CH_3OH, and then acetyl chloride (15.9 mmol, 1.13 mL) was added. The solution was stirred at rt under air for 1 h (**Scheme 3-16**). After remove the solvents, the product was neutralized with NaOH solution in 1:1 ratio to yield **54** (0.34 g, 91%) as a white powder. ^{1}H-NMR (600 Hz, D_2O): δ 3.96 (d, J = 6.0 Hz, 6H), 3.1 (s, 3H), 3.67 (s, 4H).

2. 2. ROMP of tripeptide polymers

General Procedure of NMR Tube Reactions: The NMR tube was evacuated for 15 min, and then was purged with N_2 gas for another 15 min. Under an N_2 atmosphere, a solution of tripeptide monomer in CD_2Cl_2 (0.06 mmol, 300 μL) was added to the NMR tube. And then a solution of catalyst $(H_2IMes)(3\text{-Br-Py})_2(Cl)_2Ru{=}CHPh$ **32** in CD_2Cl_2 (0.006 mmol, 300 μL) was added to the NMR tube. After complete mixing of the solution, the NMR tube was put into the 500 MHz or 600 MHz Varian NMR instrument, and was kept spinning for several hours at 25 ℃ (**Scheme 3-13**). The reaction was quenched with ethylvinyl ether when no more polymer chain growth was observed.

Poly[CB-GC(Trt)D(OtBu)] Crude ^{1}H-NMR (600 Hz, CD_2Cl_2): δ 7.06—7.57 (with max at 7.23, 7.30, 7.36), 6.87 (br, s), 6.42 (br, s), 3.75—4.32 (with max at 3.93, 3.96, 4.12, 4.14, 4.16), 3.48—3.74 (with max at 3.57, 3.62, 3.67), 1.90—2.99 (with max at 1.99, 2.07, 2.23, 2.40, 2.54, 2.74, 2.87), 1.14—1.55 (with max at 1.35,1.40).

Poly[CB-E(OtBu)AD(OtBu)] Crude ^{1}H-NMR (600 Hz, CD_2Cl_2): δ 7.26—7.48 (m), 6.88—7.10 (m), 6.66 (br, s), 4.44 (br, s), 3.74 (m), 2.64—2.98 (with max at 2.73, 2.76, 2.85, 2.90), 1.91—2.59 (with max at 1.99, 2.09, 2.36, 2.48), 1.23—1.55 (with max at 1.44, 1.45, 1.47).

Poly[CB-E(OtBu)C(Acm)D(OtBu)] Crude ^{1}H-NMR (500 Hz, CD_2Cl_2): δ 7.21—7.59 (m), 7.01—7.19 (with max at 7.07, 7.13), 6.68 (s), 4.66—4.93 (with max at 4.73, 4.81), 4.31—4.57 (m), 3.74 (br, s), 2.94—3.05 (m), 2.68—2.93 (with max at 2.73, 2.77, 2.85, 2.88), 1.90—2.54 (with max at 2.04, 2.12, 2.22, 2.38, 2.47), 1.34—1.54 (with max at 1.46,1.47).

CB-GC**(**Trt**)**D**(**OtBu**)** **48** and (H_2IMes)(3-Br-Py)$_2$(Cl)$_2$Ru=CHPh **32** were mixed in CD_2Cl_2 (450 μL). LiCl (46.20 mg, 1.2 mmol) was dissolved in CD_3OD and added to the mixture to run the NMR tube reaction (**Scheme 3-14**).

CB-GC**(**Trt**)**D**(**OtBu**)** **48** (41.11 mg, 0.06 mmol) was dissolved in CD_2Cl_2/d_7-DMF (3:1/v:v, 300 μL). (H_2IMes)(3-Br-Py)$_2$(Cl)$_2$Ru=CHPh **32** was dissolved in CD_2Cl_2 (300 μL) and mixed to the monomer solution to run the NMR tube reaction (**Scheme 3-15**).

References

Abou-haila, A. and D. R. P. Tulsiani (2009). "Signal transduction pathways that regulate sperm capacitation and the acrosome reaction." Arch. Biochem. Biophys. **485**(1): 72-81.

Al Samak, B., V. Amir-Ebrahimi, D. G. Corry, J. G. Hamilton, S. Rigby, J. J. Rooney and J. M. Thompson (2000). "Dramatic solvent effects on ring-opening metathesis polymerization of cycloalkenes." J. Mol. Catal. A: Chem. **160**(1): 13-21.

Arya, S. K., P. R. Solanki, M. Datta and B. D. Malhotra (2009). "Recent advances in self-assembled monolayers based biomolecular electronic devices." Biosens. Bioelectron. **24**(9): 2810-2817.

Baessler, K. A., Y. Lee, K. S. Roberts, N. Facompre and N. S. Sampson (2006). "Multivalent fertilinβ oligopeptides: the dependence of fertilization inhibition on length and density." Chem. biol. **13**(3): 251-259.

Baessler, K. A., Y. Lee and N. S. Sampson (2009). "β1 integrin is an adhesion protein for sperm binding to eggs." ACS Chem. Biol. **4**(5): 357-366.

Baibakov, B., L. Gauthier, P. Talbot, T. L. Rankin and J. Dean (2007). "Sperm binding to the zona pellucida is not sufficient to induce acrosome exocytosis." Development **134**: 933-943.

Baldi, E., M. Luconi, M. Muratori, S. Marchiani, L. Tamburrino and G. Forti (2009). "Nongenomic activation of spermatozoa by steroid hormones: Facts and fictions." Mol. Cell. Endocrinol. **308**(1–2): 39-46.

Barner-Kowollik, C., T. P. Davis, J. P. A. Heuts, M. H. Stenzel, P. Vana and M. Whittaker (2003). "RAFTing down under: Tales of missing radicals, fancy architectures, and mysterious holes." J. Polym. Sci., Part A: Polym. Chem. **41**(3): 365-375.

Beebe, S. J., L. Leyton, D. Burks, M. Ishikawa, T. Fuerst, J. Dean and P. Saling (1992). "Recombinant mouse ZP3 inhibits sperm binding and induces the acrosome reaction." Dev. Biol. **151**(1): 48-54.

Bertozzi, C. R., Kiessling and L. L. (2001). "Chemical Glycobiology." Science **291**(5512): 2357-2364.

Bi, M., J. R. Hickox, V. P. Winfrey, G. E. Olson and D. M. Hardy (2003). "Processing, localization and binding activity of zonadhesin suggest a function in sperm adhesion to the zona pellucida during exocytosis of the acrosome." Biochem. J. **375**: 477-488.

Biasutti, J. D., T. P. Davis, F. P. Lucien and J. P. A. Heuts (2005). "Reversible addition–fragmentation chain transfer polymerization of methyl methacrylate in suspension." J. Polym. Sci., Part A: Polym. Chem. **43**(10): 2001-2012.

Bielawski, C. W. and R. H. Grubbs (2007). "Living ring-opening metathesis polymerization." Prog. Polym. Sci. **32**(1): 1-29.

Blackmore, P. F. (1998). "News and views of non-genomic progesterone receptors on spermatozoa." Andrologia **30**(4-5): 255-261.

Bleil, J. D. and P. M. Wassarman (1983). "Sperm-egg interactions in the mouse: Sequence of events and induction of the acrosome reaction by a zona pellucida glycoprotein." Dev. Biol. **95**(2): 317-324.

Bleil, J. D. and P. M. Wassarman (1988). "Galactose at the nonreducing terminus of O-linked oligosaccharides of mouse egg zona pellucida glycoprotein ZP3 is essential for the glycoprotein's sperm receptor activity." Proc. Natl. Acad. Sci. USA **85**: 6778-6782.

Boivin, J., L. Bunting, J. A. Collins and K. G. Nygren (2007). "International estimates of infertility prevalence and treatment-seeking: potential need and demand for infertility medical care." hum. Reprod. **22**(6): 1506-1512.

Borg, C. L., K. M. Wolski, G. M. Gibbs and M. K. O'Bryan (2010). "Phenotyping male infertility in the mouse: how to get the most out of a 'non-performer'." Hum. Reprod. Update **16**(2): 205-224.

Breitbart, H. and B. Spungin (1997). "The biochemistry of the acrosome reaction." Mol. Hum. Reprod. **3**(3): 195-202.

Buffone, M. G., T. Zhuang, T. S. Ord, L. Hui, S. B. Moss and G. L. Gerton (2008). "Recombinant mouse sperm ZP3-binding protein (ZP3R/sp56) forms a high order oligomer that binds eggs and inhibits mouse fertilization in vitro." J. Biol. Chem. **283**(18): 12438-12445.

Calvo, L., L. Dennison-Lagos, S. M. Banks, A. Dorfmann, L. P. Thorsell, M. Bustillo, J. D. Schulman and R. J. Sherins (1994). "Andrology: Acrosome reaction inducibility predicts fertilization success at in-vitro fertilization." Hum. Reprod. **9**(10): 1880-1886.

Chakravarty, S., S. Kadunganattil, P. Bansal, R. K. Sharma and S. K. Gupta (2008). "Relevance of glycosylation of human zona pellucida glycoproteins for their binding to capacitated human spermatozoa and subsequent induction of acrosomal exocytosis." Mol. Reprod. Dev. **75**(1): 75-88.

Chakravarty, S., K. Suraj and S. K. Gupta (2005). "Baculovirus-expressed recombinant human zona pellucida glycoprotein-B induces acrosomal exocytosis in capacitated spermatozoa in addition to zona pellucida glycoprotein-C." Mol. Reprod. Dev. **11**(5): 365-372.

Chapman, N., E. Kessopoulou, P. Andrews, D. Hornby and C. R. Barratt (1998). "The polypeptide backbone of recombinant human zona pellucida glycoprotein-3 initiates acrosomal exocytosis in human spermatozoa in vitro." Biochem. J. **330 (Pt 2)**: 839-845.

Chen, H. and N. S. Sampson (1999). "Mediation of sperm-egg fusion: evidence that mouse egg ±6 ²1 integrin is the receptor for sperm fertilin ²." Chemistry & Biology **6**(1): 1-10.

Chen, H. and N. S. Sampson (1999). "Mediation of sperm-egg fusion: evidence that mouse egg α6β1 integrin is the receptor for sperm fertilinβ." Chem. biol. **6**(1): 1-10.

Cheng, A., T. Le, M. Palacios, L. H. Bookbinder, P. M. Wassarman, F. Suzuki and J. D. Bleil (1994). "Sperm-egg recognition in the mouse: characterization of sp56, a sperm protein having specific affinity for ZP3." J. Cell Biol. **125**(4): 867-878.

Chiefari, J., Y. K. Chong, F. Ercole, J. Krstina, J. Jeffery, T. P. T. Le, R. T. A. Mayadunne, G. F. Meijs, C. L. Moad, G. Moad, E. Rizzardo and S. H. Thang (1998). "Living Free-Radical Polymerization by Reversible Addition−Fragmentation Chain Transfer: The RAFT Process." Macromolecules **31**(16): 5559-5562.

Chittaboina, S., B. Hodges and B. Wang (2006). "A facile route for the regioselective deacetylation of peracetylated carbohydrates at anomeric position." Lett. Org. Chem. **3**: 35-38.

Chittaboina, S., B. Hodges and Q. Wang (2006). "A Facile Route for the Regioselective Deacetylation of Peracetylated Carbohydrates at Anomeric Position." Letters in Organic Chemistry **3**(1): 35-38.

Chiu, P. C. N., B. S. T. Wong, M.-K. Chung, K. K. W. Lam, R. T. K. Pang, K.-F. Lee, S.B. Sumitro, S.K. Gupta and W. S. B. Yeung (2008). "Effects of native human zona pellucida glycoproteins 3 and 4 on acrosome Reaction and zona pellucida binding of human spermatozoa." Biol. Reprod. **79**: 869-877.

Clark, G. F. (2011). "The molecular basis of mouse sperm–zona pellucida binding: a still unresolved issue in developmental biology." Reproduction **142**(3): 377-381.

Clark, G. F. (2011). "Molecular models for mouse sperm-oocyte binding." Glycobiology **21**(1): 3-5.

Clark, G. F. and A. Dell (2006). "Molecular models for murine sperm-egg binding." J. Biol. Chem. **281**: 13853-13856.

Cornwall, G. A., D. R. Tulsiani and M. C. Orgebin-Crist (1991). "Inhibition of the mouse sperm surface alpha-D-mannosidase inhibits sperm-egg binding in vitro." Biology of Reproduction **44**(5): 913-921.

Cornwell, G. A. and D. R. P. Tulsiani (1991). "Inhibition of the Mouse Sperm Surface a-D-Mannosidase Inhibits Sperm-Egg Binding in Vitro." Biol. Reprod. **44**: 913-921.

Crommelin, D. J. A. and G. Storm (2003). "Liposomes: from the bench to the bed." J. Liposome Res. **13**(1): 33-36.

Darling, T. R., T. P. Davis, M. Fryd, A. A. Gridnev, D. M. Haddleton, S. D. Ittel, R. R. Matheson, G. Moad and E. Rizzardo (2000). "Living polymerization: Rationale for uniform terminology." J. Polym. Sci., Part A: Polym. Chem. **38**(10): 1706-1708.

Dasgupta, S., V. K. Rajput, B. Roy and B. Mukhopadhyay (2007). "Lanthanum trifluoromethane-sulfonate ‐ catalyzed facile synthesis of per ‐ O ‐ acetylated sugars and their one ‐ pot conversion to S ‐ aryl and O ‐ alkyl/aryl glycosides." J. Carbohyd. Res. **26**(2): 91-106.

David, A., P. Kopečková, A. Rubinstein and J. Kopeček (2001). "Enhanced Biorecognition and Internalization of HPMA Copolymers Containing Multiple or Multivalent Carbohydrate Side-Chains by Human Hepatocarcinoma Cells." Bioconjug. Chem. **12**(6): 890-899.

Dowlut, M., D. G. Hall and O. Hindsgaul (2005). "Investigation of nonspecific effects of different dyes in the screening of labeled carbohydrates against immobilized proteins." J. Org. Chem. **70**(24): 9809-9813.

Easton, R. L., M. S. Patankar, F. A. Lattanzio, T. H. Leaven, H. R. Morris, G. F. Clark and A. Dell (2000). "Structural analysis of murine zona pellucida glycans. Evidence for the expression of core 2-type O-glycans and the Sd(a) antigen." J. Biol. Chem. **275**(11): 7731-7742.

Ensslin, M. A. and B. D. Shur (2003). "Identification of mouse sperm SED1, a bimotif EGF repeat and discoidin-domain protein involved in sperm-egg binding." Cell **114**(4): 405-417.

Eto, K., C. Huet, T. Tarui, S. Kupriyanov, H.-Z. Liu, W. Puzon-McLaughlin, X.-P. Zhang, D. Sheppard, E. Engvall and Y. Takada (2002). "Functional classification of ADAMs based on a conserved motif for binding to integrin α9β1: implications for sperm-egg binding and other cell interactions " J. biol. Chem. **277**(20): 17804-17810.

Evens, E. M. (2004). "A global perspective on infertility: an under recognized public health issue." (18): 1-45.

Fekete, A., K. Gyergyoi, K. E. Kover, I. Bajza and A. Liptak (2006). "Preparation of the pentasaccharide hapten of the GPL of Mycobacterium avium serovar 19 by achieving the glycosylation of a tertiary hydroxyl group." Carbohydr. Res. **341**(10): 1312-1321.

Florman, H. M. and B. T. Storey (1982). "Mouse gamete interactions: the zona pellucida is the site of the acrosome reaction leading to fertilization in vitro." Dev. Biol. **91**(1): 121-130.

Florman, H. M. and P. M. Wassarman (1985). "O-linked oligosaccharides of mouse egg ZP3 account for its sperm receptor activity." Cell **41**(1): 313-324.

Florman, H. M. and P. M. Wassarman (1985). "O-linked oligosaccharides of mouse egg ZP3 account for its sperm receptor activity." Cell **41**(1): 313-324.

Gahlay, G., L. Gauthier, B. Baibakov, O. Epifano and J. Dean (2010). "Gamete recognition in mice depends on the cleavage status of an egg's zona pellucida protein." Science **329**(5988): 216-219.

Gao, H. and K. Matyjaszewski (2009). "Synthesis of functional polymers with controlled architecture by CRP of monomers in the presence of cross-linkers: From stars to gels." Prog. Polym. Sci. **34**(4): 317-350.

Gestwicki, J. E., C. W. Cairo, L. E. Strong, K. A. Oetjen and L. L. Kiessling (2002). "Influencing receptor-ligand binding mechanisms with multivalent ligand architecture." J. Am. Chem. Soc. **124**(50): 14922-14933.

Gestwicki, J. E., C. W. Cairo, L. E. Strong, K. A. Oetjen and L. L. Kiessling (2002). "Influencing Receptor−Ligand Binding Mechanisms with Multivalent Ligand Architecture." Journal of the American Chemical Society **124**(50): 14922-14933.

Gestwicki, J. E., C. W. Cairo, L. E. Strong, K. A. Oetjen and L. L. Kiessling (2002). "Influencing receptor−ligand binding mechanisms with multivalent ligand architecture." J. Am. Chem. Soc. **124**(50): 14922-14933.

Gestwicki, J. E., L. E. Strong, S. L. Borchardt, C. W. Cairo, A. M. Schnoes and L. L. Kiessling (2001). "Designed potent multivalent chemoattractants for Escherichia coli." Bioorg. Med. Chem. **9**(9): 2387-2393.

Greene, T. W., P. G. Wuts and J. Wiley (1999). Protective groups in organic synthesis, Wiley New York.

Gregory, A. and M. H. Stenzel (2012). "Complex polymer architectures via RAFT polymerization: From fundamental process to extending the scope using click chemistry and nature's building blocks." Prog. Polym. Sci. **37**(1): 38-105.

Gu, L., P. Luo and H. Wang (2008). "Single-walled carbon nanotube as a unique scaffold for the multivalent display of sugars." Biomacromolecules (9): 2408-2418.

Guchhait, G. and A. K. Misra (2011). "Efficient glycosylation of unprotected sugars using sulfamic acid: A mild eco-friendly catalyst." Catal. Comm. **14**(1): 52-57.

Gupta, S. K. and B. Bhandari (2011). "Acrosome reaction: relevance of zona pellucida glycoproteins." Asian J. Androl. **13**(1): 97-105.

Haigh, D. M., A. M. Kenwright and E. Khosravi (2005). "Nature of the propagating species in ring-opening metathesis polymerizations of oxygen-containing monomers using well-defined ruthenium initiators." Macromolecules **38**(18): 7571-7579.

Hanna, W. F., C. L. Kerr, J. H. Shaper and W. W. Wright (2004). "Lewis X-containing neoglycoproteins mimic the intrinsic ability of Zona Pellucida glycoprotein ZP3 to induce the acrosome reaction in capacitated mouse sperm." Biol. Reprod. **71**: 778-789.

Hardy, D. M. and D. L. Garbers (1995). "A sperm membrane protein that binds in a species-specific manner to the egg extracellular matrix is homologous to von Willebrand factor." J. biol. Chem. **270**(44): 26025-26028.

Hejl, A., O. A. Scherman and R. H. Grubbs (2005). "Ring-opening metathesis polymerization of functionalized low-strain monomers with ruthenium-based catalysts." Macromolecules **38**(17): 7214-7218.

Henkel, R., C. Miiller, W. Miska, H. Gips and W.-B. Schill (1993). "Fertilization and early embryology: Determination of the acrosome reaction in human spermatozoa is predictive of fertilization in vitro." Hum. Reprod. **8**(12): 2128-2132.

Hernández-González, E. O., J. Sosnik, J. Edwards, J. J. Acevedo, I. Mendoza-Lujambio, I. López-González, I. Demarco, E. Wertheimer, A. Darszon and P. E. Visconti (2006). "Sodium and epithelial sodium channels participate in the regulation of the capacitation-associated hyperpolarization in mouse sperm." J. biol. Chem. **281**(9): 5623-5633.

Hilderbrandt, J. D., J. Codina, J. S. Tash, H. J. Kirchick, L. Lipschultz, R. D. Sekura and L. Birnbaumer (1985). "The membrane-bound spermatozoal adenylyl ccyclase system does not share coupling characteristics with somatic cell adenylyl cyclases." Endocrinology **116**(4): 1357-1366.

Hong, S.-J., P. C.-N. Chiu, K.-F. Lee, J. Y.-M. Tse, P.-C. Ho and W. S.-B. Yeung (2009). "Cumulus cells and their extracellular matrix affect the quality of the spermatozoa penetrating the cumulus mass." Fertil. Steril. **92**(3): 971-978.

Ickowicz, D., M. Finkelstein and H. Breitbart (2012). "Mechanism of sperm capacitation and the acrosome reaction: role of protein kinases." Asian J Androl **14**(6): 816-821.

Ickowicz, D., M. Finkelstein and H. Breitbart (2012). "Mechanism of sperm capacitation and the acrosome reaction: role of protein kinases." Asian J. Androl. **14**(6): 816-821.

Ikeda, K., T. Morimoto and K. Kakiuchi (2010). "Utilization of aldoses as a carbonyl source in cyclocarbonylation of enynes." J. biol. Chem. **75**(18): 6279-6282.

Jayaraman, N. (2009). "Multivalent ligand presentation as a central concept to study intricate carbohydrate-protein interactions." chem. Soc. Rev. **38**(12): 3463-3483.

Jin, M., E. Fujiwara, Y. Kakiuchi, M. Okabe, Y. Satouh, S. A. Baba, K. Chiba and N. Hirohashi (2011). "Most fertilizing mouse spermatozoa begin their acrosome reaction before contact with the zona pellucida during in vitro fertilization." Proc. Natl. Acad. Sci. USA **108**(12): 4892-4896.

Johnston, D. S., W. W. Wright and J. H. Shaper (1998). "Murine sperm-zona binding, a fucosyl residue is required for a high affinity sperm-binding ligand." J. Biol. Chem. **273**(4): 1888-1895.

Joshi, N. and M. Grinstaff (2008). "Applications of dendrimers in tissue engineering." Curr. Top. Med. Chem. **8**(14): 1225-1236.

Jovine, L., C. C. Darie, E. S. Litscher and P. M. Wassarman (2005). "Zona pellucida domain proteins." Annu. Rev. Biochem. **74**: 83-114.

Kanai, M., K. H. Mortell and L. L. Kiessling (1997). "Varying the size of multivalent ligands: The dependence of concanavalin a binding on neoglycopolymer length." J. Am. Chem. Soc. **119**(41): 9931-9932.

Kashir, J., B. Heindryckx, C. Jones, P. De Sutter, J. Parrington and K. Coward (2010). "Oocyte activation, phospholipase C zeta and human infertility." hum. Reprod. update **16**(6): 690-703.

Katz, T. J. and C. C. Han (1982). "Induction of olefin metathesis by phenylacetylene plus tungsten hexachloride." Organometallics **1**(8): 1093-1095.

Ker ékgy árt ó, J., J. P. Kamerling, J. B. Bouwstra, J. F. G. Vliegenthart and A. Lipt ák (1989). "Synthesis of four structural elements of xylose-containing carbohydrate chains from N-glycoproteins." Carbohyd. Res. **186**(1): 51-62.

Khalil, M. B., K. Chakrabandhu, H. Xu, W. Weerachatyanukul, M. Buhr, T. Berger, E. Carmona, N. Vuong, P. Kumarathasan, P. T. T. Wong, D. Carrier and N. Tanphaichitr (2006). "Sperm capacitation induces an increase in lipid rafts having zona pellucida binding ability and containing sulfogalactosylglycerolipid." Dev. Biol. **290**(1): 220-235.

Kiessling, L. L., J. E. Gestwicki and L. E. Strong (2000). "Synthetic multivalent ligands in the exploration of cell-surface interactions." Curr. Opin. Struct. Biol. **4**(6): 696-703.

Kim, K.-S. and G. L. Gerton (2003). "Differential release of soluble and matrix components: evidence for intermediate states of secretion during spontaneous acrosomal exocytosis in mouse sperm." Dev. Biol. **264**: 141-152.

Kobayashi, S., L. M. Pitet and M. A. Hillmyer (2011). "Regio- and stereoselective ring-opening metathesis polymerization of 3-substituted cyclooctenes." J. Am. Chem. Soc. **133**(15): 5794-5797.

Kováč, P., E. A. Sokoloski and C. P. J. Glaudemans (1984). "Synthesis and characterization of methyl 6-O-α- and -β-d-galactopyranosyl-β-d-galactopyranoside." Carbohyd. Res. **128**(1): 101-109.

Kress, J. and J. A. Osborn (1983). "Tungsten carbene complexes in olefin metathesis: a cationic and chiral active species." Journal of the American Chemical Society **105**(20): 6346-6347.

Leclerc, P. and G. S. Kopf (1995). "Mouse sperm adenylyl cyclase: general properties and regulation by the zona pellucida." Biol. Repord. **52**(6): 1227-1233.

Lee, J. (2006). "Probing ligand-receptor interactions in mammalian fertilization using ring opening metathesis polymerization." Ph. D. Thesis: Stony Brook University, Stony Brook.

Lee, J., K. A. Parker and N. S. Sampson (2006). "Amino acid-bearing ROMP polymers with a stereoregular backbone." J. Am. Chem. Soc. **128**: 4578-4579.

Lee, J. C., K. A. Parker and N. S. Sampson (2006). "Amino acid-bearing ROMP polymers with a stereoregular backbone." Journal of the American Chemical Society **128**(14): 4578-4579.

Lee, J. W., B.-K. Kim, H. J. Kim, S. C. Han, W. S. Shin and S.-H. Jin (2006). "Convergent synthesis of symmetrical and unsymmetrical PAMAM dendrimers." Macromolecules **39**(6): 2418-2422.

Li, D., S. Cao and C. Xu (2007). "Polypeptide backbone derived from carboxyl terminal of mouse ZP3 inhibits sperm-zona binding." Mol. Reprod. Dev. **74**(10): 1327-1336.

Lindhorst, T. (2002). Artificial multivalent sugar ligands to understand and manipulate carbohydrate-protein interactions. Host-Guest Chemistry. S. Penadés, Springer Berlin Heidelberg. **218:** 201-235.

Litscher, E. S. and P. M. Wassarman (1996). "Characterization of mouse ZP3-derived glycopeptide, gp55, that exhibits sperm receptor and acrosome reaction-inducing activity in vitro." Biochemistry **35**(13): 3980-3985.

Liu, C., E. S. Litscher and P. M. Wassarman (1997). "Zona pellucida glycoprotein mZP3 bioactivity is not dependent on the extent of glycosylation of its polypeptide or on sulfation and sialylation of its oligosaccharides." J Cell Sci **110 (Pt 6)**: 745-752.

Loeser, C. R., C. Lynch and D. R. P. Tulsiani (1999). "Characterization of the pharmacological-sensitivity profile of neoglycoprotein induced acrosome reaction in mouse spermatozoa." Biol. Reprod. **61**: 629-634.

Loeser, C. R. and D. R. P. Tulsiani (1999). "The role of carbohydrates in the induction of the acrosome reaction in mouse spermatozoa." Biol. Reprod. **60**: 94-101.

Love, J. A., J. P. Morgan, T. M. Trnka and R. H. Grubbs (2002). "A practical and highly active ruthenium-based catalyst that effects the cross metathesis of acrylonitrile." Angew. Chem. Int. Ed. **41**(21): 4035-4037.

Lu, Q. and B. D. Shur (1997). "Sperm from beta 1,4-galactosyltransferase-null mice are refractory to ZP3-induced acrosome reactions and penetrate the zona pellucida poorly." Development **124**(20): 4121-4131.

Mammen, M., S.-K. Choi and G. M. Whitesides (1998). "Polyvalent Interactions in Biological Systems: Implications for Design and Use of Multivalent Ligands and Inhibitors." Angew. Chem. Int. Ed. **37**(20): 2754-2794.

Manning, D. D., L. E. Strong, X. Hu, P. J. Beck and L. L. Kiessling (1997). "Neoglycopolymer inhibitors of the selectins." Tetrahedron **53**(35): 11937-11952.

Martinez, H., P. Miró, P. Charbonneau, M. A. Hillmyer and C. J. Cramer (2012). "Selectivity in ring-opening metathesis polymerization of Z-cyclooctenes catalyzed by a second-generation Grubbs catalyst." ACS Catal. **2**(12): 2547-2556.

Maughon, B. R. and R. H. Grubbs (1997). "Ruthenium Alkylidene Initiated Living Ring-Opening Metathesis Polymerization (ROMP) of 3-Substituted Cyclobutenes." Macromolecules **30**(12): 3459-3469.

Maynard, H. D., S. Y. Okada and R. H. Grubbs (2001). "Inhibition of cell adhesion to fibronectin by oligopeptide-substituted polynorbornenes." J. Am. Chem. Soc. **123**(7): 1275-1279.

Menkveld, R., W. Y. Wong, C. J. Lombard, A. M. Wetzels, C. M. Thomas, H. M. Merkus and R. P. Steegers-Theunissen (2001). "Semen parameters, including WHO and strict criteria morphology, in a fertile and subfertile population: an effort towards standardization of in-vivo thresholds." Hum. Reprod. **16**(6): 1165-1171.

Miller, D. J., X. Gong and D. B. Shur (1993). "Sperm require β-N-acetylglucosaminidase to penetrate through the egg zona pellucida." Development **118**: 1279-1289.

Miller, D. J., M. B. Macek and B. D. Shur (1992). "Complementarity between sperm surface beta-1,4-galactosyltransferase and egg-coat ZP3 mediates sperm-egg binding." Nature **357**(6379): 589-593.

Miura, Y. (2012). "Design and synthesis of well-defined glycopolymers for the control of biological functionalities." Polym. J. **44**(7): 679-689.

Muro, Y., M. G. Buffone, M. Okabe and G. L. Gerton (2012). "Function of the Acrosomal Matrix: Zona Pellucida 3 Receptor (ZP3R/sp56) Is Not Essential for Mouse Fertilization." Biology of Reproduction **86**(1): 1-6.

Muro, Y., M. G. Buffone, M. Okabe and G. L. Gerton (2012). "Function of the acrosomal matrix: zona pellucida 3 receptor (ZP3R/sp56) is not essential for mouse fertilization." Biol. Repord. **86**(1): 1-6.

Murphy, J. J., H. Furusho, R. M. Paton and K. Nomura (2007). "Precise synthesis of poly(macromonomer)s containing sugars by repetitive ROMP and their attachments to poly(ethylene glycol): Synthesis, TEM analysis and their properties as amphiphilic block fragments." Chem.-a Euro. J. **13**(32): 8985-8997.

Mutch, A., M. Leconte, F. Lefebvre and J.-M. Basset (1998). "Effect of alcohols and epoxides on the rate of ROMP of norbornene by a ruthenium trichloride catalyst." J. Mol. Catal. A: Chem. **133**(1–2): 191-199.

Myung, J. H., K. A. Gajjar, J. Saric, D. T. Eddington and S. Hong (2011). "Dendrimer-mediated multivalent binding for the enhanced capture of tumor cells." Angew. Chem. Int. Ed. **50**(49): 11769-11772.

Nagdas, S. K., Y. Araki, C. A. Chayko, M. C. Orgebin-Crist and D. R. Tulsiani (1994). "O-linked trisaccharide and N-linked poly-N-acetyllactosaminyl glycans are present on mouse ZP2 and ZP3." Biol. Repord. **51**(2): 262-272.

Nixon, B., R. J. Aitken and E. A. McLaughlin (2007). "New insights into the molecular mechanisms of sperm-egg interaction." Cellular and Molecular Life Sciences **64**(14): 1805-1823.

Oh, Y. S., H. S. Ahn and M. C. Gye (2012). "Fucosyl neoglycoprotein binds to mouse epididymal spermatozoa and inhibits sperm binding to the egg zona pellucida." Andrologia: doi: 10.1111/and.12024.

Ombelet, W., I. Cooke, S. Dyer, G. Serour and P. Devroey (2008). "Infertility and the provision of infertility medical services in developing countries." hum. Reprod. update **14**(6): 605-621.

Park, S. and I. Shin (2007). "Carbohydrate microarrays for assaying galactosyltransferase activity." Org. Lett. **9**(9): 1675-1678.

Paterson, S. M., J. Clark, K. A. Stubbs, T. V. Chirila and M. V. Baker (2011). "Carbohydrate-based crosslinking agents: potential use in hydrogels." J. Polym. Sci., Part A: Polym. Chem. **49**(20): 4312-4315.

Pilgrim, W. and P. V. Murphy (2010). "SnCl4- and TiCl4-catalyzed anomerization of acylated O- and S-glycosides: analysis of factors that lead to higher α:β anomer ratios and reaction rates." J. biol. Chem. **75**(20): 6747-6755.

Rankin, T. L., J. S. Coleman, O. Epifano, T. Hoodbhoy, S. G. Turner, P. E. Castle, E. Lee, R. Gore-Langton and J. Dean (2003). "Fertility and Taxon-Specific Sperm Binding Persist after Replacement of Mouse Sperm Receptors with Human Homologs." Developmental cell **5**(1): 33-43.

Ren, D. and J. Xia (2010). "Calcium Signaling Through CatSper Channels in Mammalian Fertilization." Physiology **25**(3): 165-175.

Roberts, K. S. and N. S. Sampson (2003). "Increased polymer length of oligopeptide-substituted polynorbornenes with LiCl." J. Org. Chem. **68**(5): 2020-2023.

Roldan, E. R. S., T. Murase and Q. X. Shi (1994). "Exocytosis in spermatozoa in response to progesterone and zona pellucida." science **266**: 1579-1581.

Šardzík, R., G. T. Noble, M. J. Weissenborn, A. Martin, S. J. Webb and S. L. Flitsch (2010). "Preparation of aminoethyl glycosides for glycoconjugation." Beil. J. Org. Chem. **6**: 699-703.

Schierholt, A., H. A. Shaikh, J. Schmidt-Lassen and T. K. Lindhorst (2009). "Utilizing staudinger ligation for the synthesis of glycoamino acid building blocks and other glycomimetics." Eur. J. Org. Chem.(22): 3783-3789.

Schleyer, P. v. R., J. E. Williams and K. R. Blanchard (1970). "Evaluation of strain in hydrocarbons. The strain in adamantane and its origin." J. Am. Chem. Soc. **92**(8): 2377-2386.

Schmidt, R. R. and J. Michel (1980). "Facile synthesis of α - and β - O - glycosyl imidates; preparation of glycosides and disaccharides." Angew. Chem. Int. Ed. **19**(9): 731-732.

Schrock, R. R. and J. D. Fellmann (1978). "Multiple metal-carbon bonds. 8. Preparation, characterization, and mechanism of formation of the tantalum and niobium neopentylidene complexes, M(CH2CMe3)3(CHCMe3)." Journal of the American Chemical Society **100**(11): 3359-3370.

Schrock, R. R., J. S. Murdzek, G. C. Bazan, J. Robbins, M. DiMare and M. O'Regan (1990). "Synthesis of molybdenum imido alkylidene complexes and some reactions involving acyclic olefins." Journal of the American Chemical Society **112**(10): 3875-3886.

Schueller, C. M., D. D. Manning and L. L. Kiessling (1996). "Preparation of (r)-(+)-7-oxabicyclo[2.2.1]hept-5-ene-exo-2-carboxylic acid, a precursor to substrates for the ring opening metathesis polymerization." Tetrahedron Letters **37**(49): 8853-8856.

Senaratne, W., L. Andruzzi and C. K. Ober (2005). "Self-assembled monolayers and polymer brushes in biotechnology: current applications and future perspectives." Biomacromolecules **6**(5): 2427-2448.

Shur, B. D., C. Rodeheffer, M. A. Ensslin, R. Lyng and A. Raymond (2006). "Identification of novel gamete receptors that mediate sperm adhesion to the egg coat." Mol. Cell Endocrinol. **250**(1–2): 137-148.

Siegwart, D. J., J. K. Oh and K. Matyjaszewski (2012). "ATRP in the design of functional materials for biomedical applications." Prog. Polym. Sci. **37**(1): 18-37.

Song, A., J. C. Lee, K. A. Parker and N. S. Sampson (2010). "Scope of the Ring-Opening Metathesis Polymerization (ROMP) Reaction of 1-Substituted Cyclobutenes." Journal of the American Chemical Society **132**(30): 10513-10520.

Song, A., K. A. Parker and N. S. Sampson (2009). "Synthesis of copolymers by alternating ROMP (AROMP)." J. Am. Chem. Soc. **131**(10): 3444-3445.

Strong, L. E. and L. L. Kiessling (1999). "A general synthetic route to defined, biologically active multivalent arrays." Journal of the American Chemical Society **121**(26): 6193-6196.

Sudibya, H. G., J. Ma, X. Dong, S. Ng, L.-J. Li, X.-W. Liu and P. Chen (2009). "Interfacing glycosylated carbon-nanotube-network devices with living cells to detect dynamic secretion of biomolecules." Angew. Chem. Int. Ed. **48**(15): 2723-2726.

Sukhova, E. V., A. V. Dubrovskii, Y. E. Tsvetkov and N. E. Nifantiev (2007). "Synthesis of oligosaccharides related to the HNK-1 antigen. 5. Synthesis of a sulfo-mimetic of the HNK-1 antigenic trisaccharide." Russ. Chem. Bull. **56**(8): 1655-1670.

Suri, A. (2005). "Contraceptive vaccines targeting sperm." Expert opin. biol. th. **5**(3): 381-392.

Szwarc, M. (1970). "Living polymers: a tool in studies of ions and ion-pairs." Science **170**(3953): 23-31.

Takeo, T., T. Hoshii, Y. Kondo, H. Toyodome, H. Arima, K.-i. Yamamura, T. Irie and N. Nakagata (2008). "Methyl-beta-cyclodextrin improves fertilizing ability of C57BL/6 mouse sperm after freezing and thawing by facilitating cholesterol efflux from the cells." Biol. Repord. **78**(3): 546-551.

Tanghe, S., A. Van Soom, H. Nauwynck, M. Coryn and A. de Kruif (2002). "Minireview: functions of the cumulus oophorus during oocyte maturation, ovulation, and fertilization." Mol. Reprod. Dev. **61**(3): 414-424.

Tanphaichitr, N., E. Carmona, M. Bou Khalil, H. Xu, T. Berger and G. L. Gerton (2007). "New insights into sperm-zona pellucida interaction: involvement of sperm lipid rafts." Front. Biosci. **12**: 1748-1766.

Tebbe, F. N., G. W. Parshall and D. W. Ovenall (1979). "Titanium-catalyzed olefin metathesis." Journal of the American Chemical Society **101**(17): 5074-5075.

Torchilin, V. P. (2006). "Multifunctional nanocarriers." Adv. Drug Delivery Rev. **58**(14): 1532-1555.

Tsai, J.-Y. and L. M. Silver (1996). "Sperm-egg binding protein or proto-oncogene?" Science **271**(5254): 1432-1434.

Tulsiani, D. R., H. Yoshida-Komiya and Y. Araki (1997). "Mammalian fertilization: a carbohydrate-mediated event." Biol. Reprod. **57**(3): 487-494.

Tulsiani, D. R. P. (2012). "Mechanisms of mammalian sperm-egg interaction leading to fertilization." Gynecol. Obstet. **2**(5): doi:10.4172/2161-0932.1000e4107.

Tulsiani, D. R. P. and A. Abou-Haila (2012). "Biological processes that prepare mammalian spermatozoa to interact with an egg and fertilize it." Scientifica **2012**: 12.

Tulsiani, D. R. P., A. Abou-Haila, C. R. Loeser and B. M. J. Pereira (1998). "The biological and functional significance of the sperm acrosome and acrosomal enzymes in mammalian fertilization." Exp. Cell Res. **240**(2): 151-164.

van Baal, I., H. Malda, S. A. Synowsky, J. L. J. van Dongen, T. M. Hackeng, M. Merkx and E. W. Meijer (2005). "Multivalent peptide and protein dendrimers using native chemical ligation." Angew. Chem. Int. Ed. Engl. **44**(32): 5052-5057.

van Duin, M., J. E. Polman, I. T. De Breet, K. van Ginneken, H. Bunschoten, A. Grootenhuis, J. Brindle and R. J. Aitken (1994). "Recombinant human zona pellucida protein ZP3 produced by chinese hamster ovary cells induces the human sperm acrosome reaction and promotes sperm-egg fusion." Biol. Repord. **51**(4): 607-617.

Visconti, P. E. and H. M. Florman (2010). "Mechanisms of Sperm-Egg Interactions: Between Sugars and Broken Bonds." Sci. Signal. **3**(142): pe35-.

Vjugina, U., X. Zhu, E. Oh, N. J. Bracero and J. P. Evans (2009). "Reduction of mouse egg surface integrin alpha9 subunit (ITGA9) reduces the egg's ability to support sperm-egg binding and fusion." Biol. Repord. **80**(4): 833-841.

Wang, J.-S. and K. Matyjaszewski (1995). "Controlled/"living" radical polymerization. atom transfer radical polymerization in the presence of transition-metal complexes." J. Am. Chem. Soc. **117**(20): 5614-5615.

Wang, W., H. Wang, C. Ren, J. Wang, M. Tan, J. Shen, Z. Yang, P. G. Wang and L. Wang (2011). "A saccharide-based supramolecular hydrogel for cell culture." Carbohyd. Res. **346**(8): 1013-1017.

Wassarman, P. M. (1999). "Mammalian fertilization: molecular aspects of gamete adhesion, exocytosis, and fusion." cell **96**: 175-183.

Wassarman, P. M. (2005). "Contribution of mouse egg zona pellucida glycoproteins to gamete recognition during fertilization." J. Cell. Physiol. **204**: 388-391.

Wassarman, P. M. (2005). "Contribution of mouse egg zona pellucida glycoproteins to gamete recognition during fertilization." J. biol. Chem. **204**(2): 388-391.

Wassarman, P. M. (2009). "Mammalian fertilization: the strange case of sperm protein 56." BioEssays **31**(2): 153-158.

Wassarman, P. M., L. Jovine and E. S. Litscher (2001). " A profile of fertilization in mammals." Nat. Cell Biol. **3**(2): 59-64.

Wassarman, P. M., L. Jovine, H. Qi, Z. Williams, C. Darie and E. S. Litscher (2004). "Recent aspects of mammalian fertilization research." Mol. Cell. Endocrinol. **234**: 95-103.

Williams, S. A., L. Xia, R. D. Cummings, R. P. McEver and P. Stanley (2007). "Fertilization in mouse does not require terminal galactose or N-acetylglucosamine on the zona pellucida glycans." J. Cell Sci. **120**: 1341-1349.

Wolfsberg, T. G., P. D. Straight, R. L. Gerena, A.-P. J. Huovila, P. Primakoff, D. G. Myles and J. M. White (1995). "ADAM, a widely distributed and developmentally regulated gene family encoding membrane proteins with A Disintegrin And Metalloprotease domain." Dev. Biol. **169**(1): 378-383.

Wolfsberg, T. G. and J. M. White (1996). "ADAMs in fertilization and development." Dev. Biol. **180**(2): 389-401.

Yanagimachi, R. (2011). "Mammalian sperm acrosome reaction: where does it begin before fertilization." Biol. Reprod. **85**: 4-5.

Yuan, R., P. Primakoff and D. G. Myles (1997). "A role for the disintegrin domain of cyritestin, a sperm surface protein belonging to the ADAM family, in mouse sperm–egg plasma membrane adhesion and fusion." J. Cell Biol. **137**(1): 105-112.

Zhu, X., N. P. Bansal and J. P. Evans (2000). "Identification of key functional amino acids of the mouse fertilin beta (ADAM2) disintegrin loop for cell-cell adhesion during fertilization." J. Biol. Chem. **275**: 7677-7683.

Zhu, X. and R. R. Schmidt (2009). "New principles for glycoside-bond formation." Angew. Chem. Int. Ed. **48**(11): 1900-1934.

Appendix

Checklist for compounds

Compound #	Ref.	^{1}H NMR	^{13}C NMR	LRMS	HRMS	Other
1	(Šardzík, Noble et al. 2010)	√				
2	(Ikeda, Morimoto et al. 2010)	√				
3	(Fekete, Gyergyoi et al. 2006)	√				
4	(Gu, Luo et al. 2008)	√				
5	(Gu, Luo et al. 2008)	√				
6		√	√		√	
7	(Pilgrim and Murphy 2010)	√				
8	(Pilgrim and Murphy 2010)	√				
9	(Guchhait and Misra 2011)	√				
10	(Paterson, Clark et al. 2011)	√				
11		√	√		√	
12	(Pilgrim and Murphy 2010)	√				
13	(Pilgrim and Murphy 2010)	√				
14	(Gu, Luo et al. 2008)	√				
15	(Gu, Luo et al. 2008)	√				
16		√	√		√	
17	(Šardzík, Noble et al. 2010)	√				
19	(Park and Shin 2007)	√				
20		√	√		√	
21	(Chittaboina, Hodges et al. 2006)	√				
22	(Sudibya, Ma et al. 2009)	√				
23	(Sukhova, Dubrovskii et al. 2007)	√				
24	(Park and Shin 2007)	√				
25		√	√		√	
26	(Dowlut, Hall et al. 2005)	√				
27	(Wang, Wang et al. 2011)	√				
28	(Wang, Wang et al. 2011)	√				
29	(Wang, Wang et al. 2011)	√				
30	(Park and Shin 2007)	√				
31		√	√		√	
32	(Love, Morgan et al. 2002)					

Checklist – continuation page

Compound #	Ref.	^{1}H NMR	^{13}C NMR	LRMS	HRMS
Prot-poly(Man)$_{10}$		√			
Prot-poly(Man)$_{100}$		√			
Prot-poly(Glc)$_{10}$		√			
Prot-poly(Glc)$_{100}$		√			
Prot-poly(Gal)$_{10}$		√			
Prot-poly(Gal)$_{100}$		√			
Prot-poly(Fuc)$_{10}$		√			
Prot-poly(Fuc)$_{100}$		√			
Prot-poly(GlcNAc)$_{10}$		√			
Prot-poly(GlcNAc)$_{100}$		√			
Prot-poly(GalNAc)$_{10}$		√			
Prot-poly(GalNAc)$_{100}$		√			
Poly(Man)$_{10}$		√			
Poly(Man)$_{100}$		√			
Poly(Glc)$_{10}$		√			
Poly(Glc)$_{100}$		√			
Poly(Gal)$_{10}$		√			
Poly(Gal)$_{100}$		√			
Poly(Fuc)$_{10}$		√			
Poly(Fuc)$_{100}$		√			
Poly(GlcNAc)$_{10}$		√			
Poly(GlcNAc)$_{100}$		√			
Poly(GalNAc)$_{10}$		√			
Poly(GalNAc)$_{100}$		√			
33		√			
34		√			
35		√			
36		√			
37		√			
38		√			
Prot-poly(D-Fuc)$_{10}$		√			
Prot-poly(D-Fuc)$_{100}$		√			
Poly(D-Fuc)$_{10}$		√			
Poly(D-Fuc)$_{100}$		√			
39		√			
40		√			
41		√			

Checklist – continuation page

Compound #	Ref.	^{1}H NMR	^{13}C NMR	LRMS	HRMS
42		√			
43		√			
44		√			
45		√			
46		√			
47		√			
48		√			
49		√			
50		√			
51		√			
52		√			
53		√			
54		√			
Poly[CB-GC(Trt)D(OtBu)]		√			
Poly[CB-E(OtBu)AD(OtBu)]		√			
Poly[CB-E(OtBu)C(Trt)D(OtBu)]		√			

	Parameter	Value
1	Data File Name	C:/ Users/ Stella/ Dropbox/ RESEARCH/ NMR/ NMR Varian 500 600/ 600/ mannose/ nb-man04012010.fid/ fid
2	Origin	Varian
3	Spectrometer	inova
4	Solvent	CDCl3
5	Temperature	25.0
6	Pulse Sequence	s2pul
7	Experiment	1D
8	Number of Scans	27
9	Receiver Gain	60
10	Pulse Width	0.0000
11	Acquisition Date	2010-04-01T12:17:33
12	Modification Date	2010-04-01T00:00:00
13	Spectrometer Frequency	499.90
14	Spectral Width	7998.4
15	Lowest Frequency	-999.9
16	Nucleus	1H
17	Acquired Size	15133
18	Spectral Size	65536

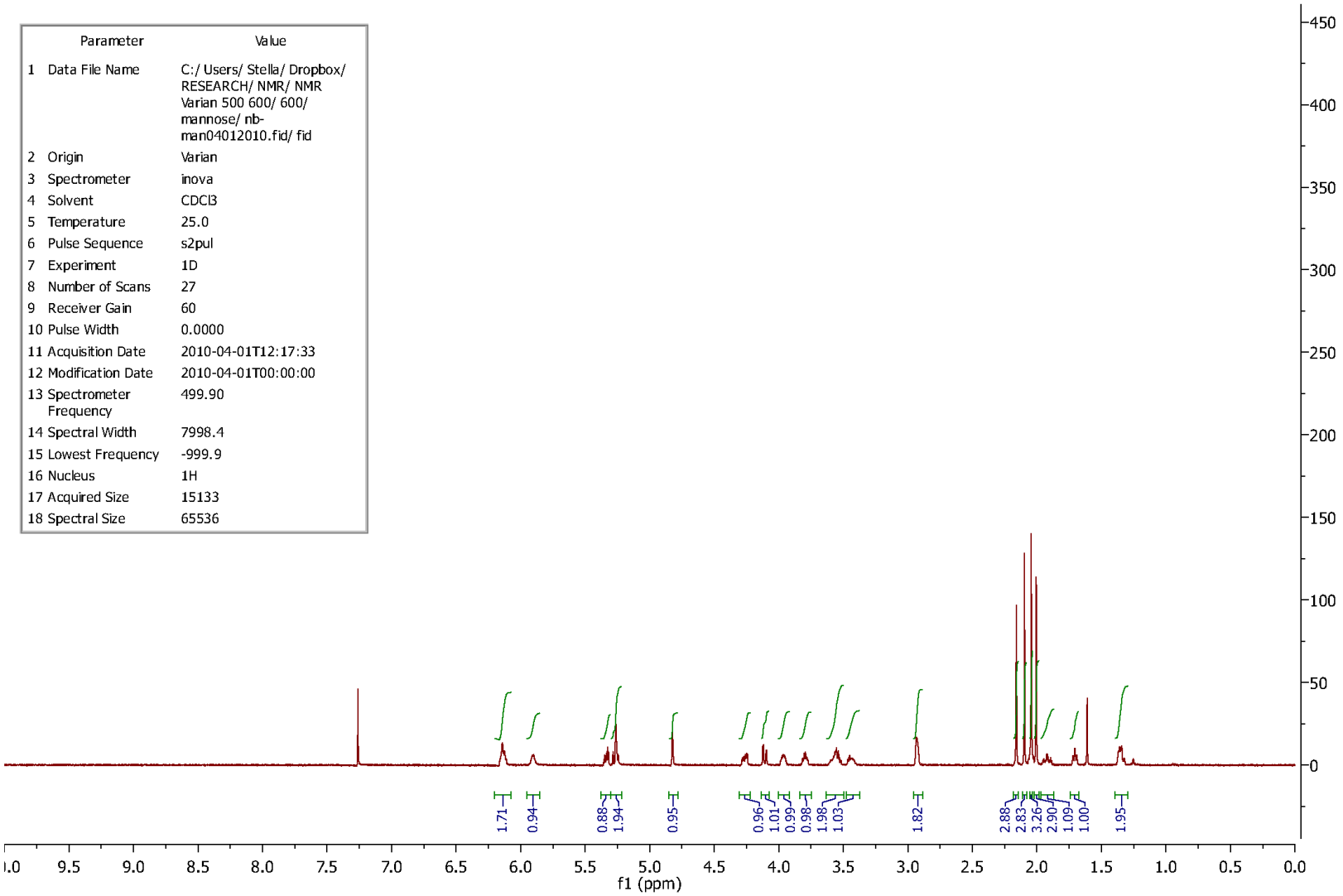

^{1}H-NMR spectrum of NB-mannose 6

	Parameter	Value
1	Data File Name	D:/ Dropbox/ RESEARCH/ NMR/ NMR Varian 500 600/ 600/ mannose/ c13-nb-mannose.fid/ fid
2	Origin	Varian
3	Solvent	CDCl3
4	Temperature	25.0
5	Pulse Sequence	s2pul
6	Experiment	1D
7	Number of Scans	133
8	Receiver Gain	60
9	Relaxation Delay	1.0000
10	Pulse Width	0.0000
11	Acquisition Date	2010-03-03T20:48:04
12	Modification Date	2010-03-03T03:00:00
13	Spectrometer Frequency	125.71
14	Spectral Width	31421.8
15	Lowest Frequency	-1884.1
16	Nucleus	13C
17	Acquired Size	40863
18	Spectral Size	131072

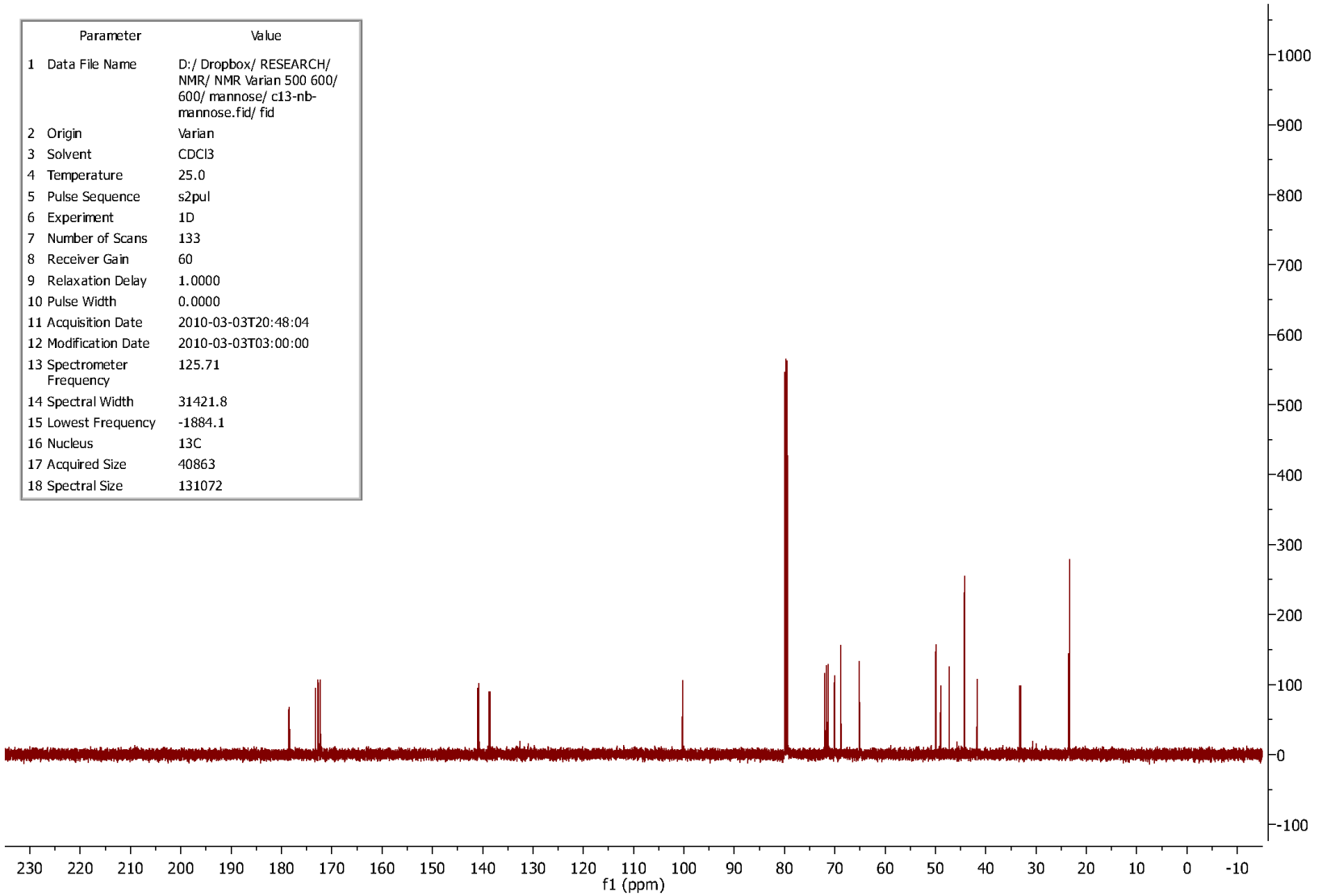

^{13}C-NMR spectrum of NB-mannose 6

	Parameter	Value
1	Data File Name	C:/ Users/ Stella/ Dropbox/ RESEARCH/ NMR/ NMR Varian 500 600/ 600/ glucose/ nb-glucose-11092010.fid/ fid
2	Origin	Varian
3	Spectrometer	inova
4	Solvent	CDCl3
5	Temperature	25.0
6	Pulse Sequence	s2pul
7	Experiment	1D
8	Number of Scans	30
9	Receiver Gain	46
10	Pulse Width	0.0000
11	Acquisition Date	2010-11-10T13:59:29
12	Modification Date	2010-11-10T17:05:38
13	Spectrometer Frequency	599.72
14	Spectral Width	8000.0
15	Lowest Frequency	-1001.3
16	Nucleus	1H
17	Acquired Size	15136
18	Spectral Size	65536

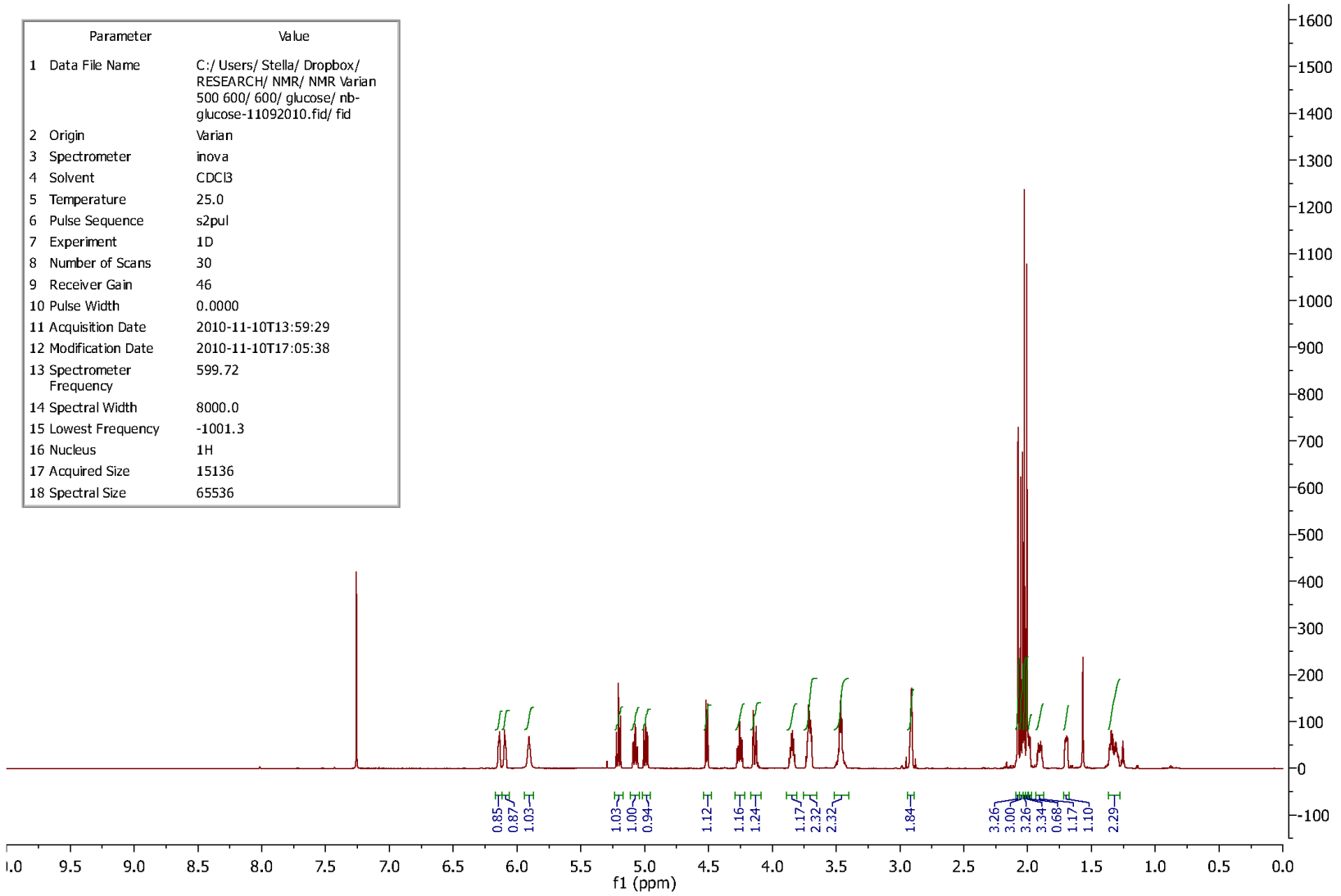

^{1}H-NMR spectrum of NB-glucose 11

	Parameter	Value
1	Data File Name	D:/ Dropbox/ RESEARCH/ NMR/ NMR Varian 500 600/ 600/ glucose/ c13_nb-glucose_staudinger_02192010.fid/ fid
2	Origin	Varian
3	Solvent	CDCl3
4	Temperature	25.0
5	Pulse Sequence	s2pul
6	Experiment	1D
7	Number of Scans	323
8	Receiver Gain	60
9	Relaxation Delay	1.0000
10	Pulse Width	0.0000
11	Acquisition Date	2010-02-19T12:09:43
12	Modification Date	2010-02-19T03:00:00
13	Spectrometer Frequency	125.71
14	Spectral Width	31421.8
15	Lowest Frequency	-1884.1
16	Nucleus	13C
17	Acquired Size	40863
18	Spectral Size	131072

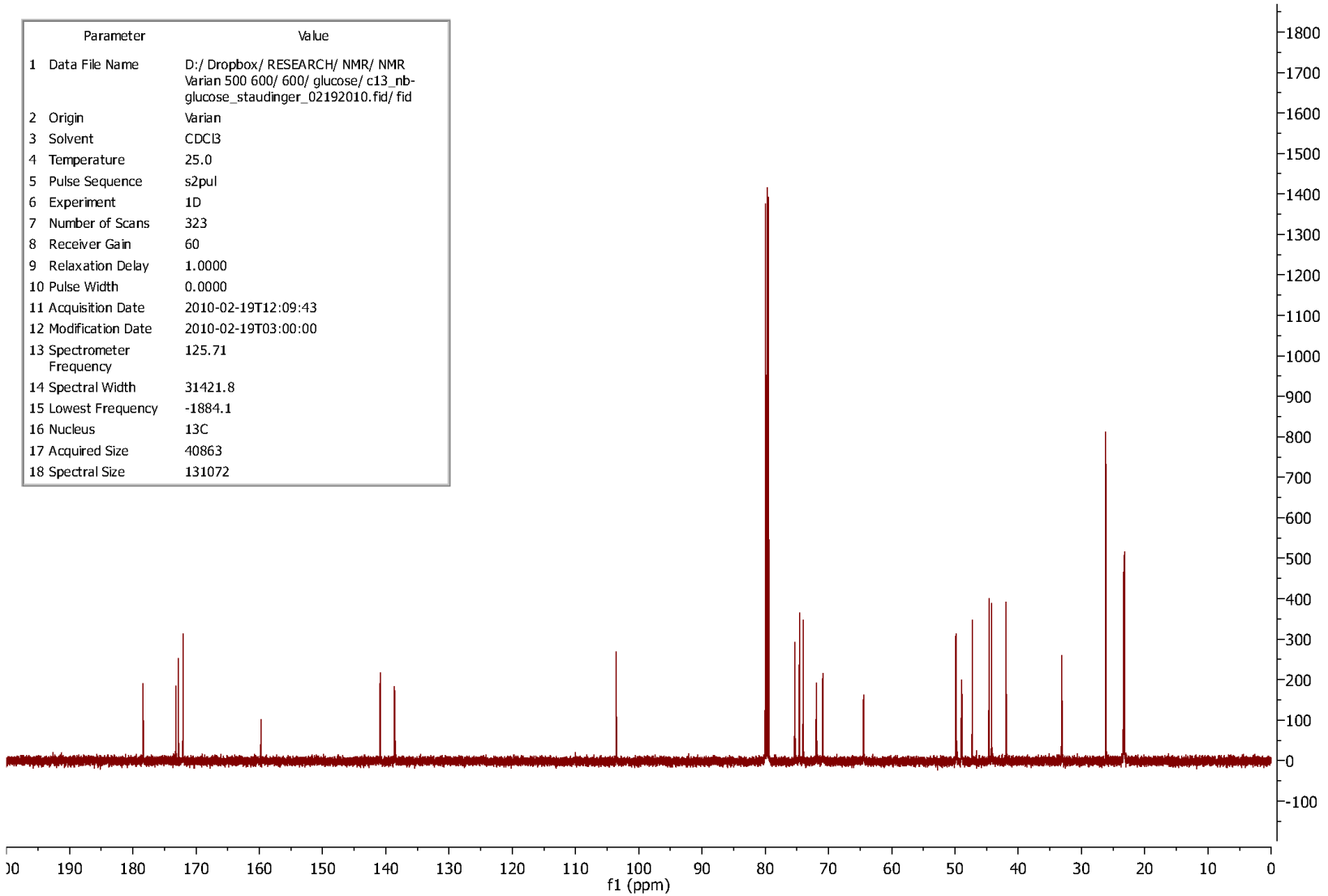

^{13}C-NMR spectrum of NB-glucose 11

	Parameter	Value
1	Data File Name	F:/ Old/ HH NMR data/ lw-nb-galactose-08292012/ 1/ fid
2	Title	lw-nb-galactose-08292012.1.fid
3	Origin	Bruker BioSpin GmbH
4	Spectrometer	spect
5	Solvent	CDCl3
6	Temperature	298.1
7	Pulse Sequence	zg30
8	Experiment	1D
9	Probe	5 mm PABBO BB/ 19F-1H/ D Z-GRD Z116098/ 0058
10	Number of Scans	16
11	Receiver Gain	101
12	Relaxation Delay	1.0000
13	Pulse Width	10.1000
14	Modification Date	2012-08-29T17:05:08
15	Spectrometer Frequency	399.83
16	Spectral Width	8223.7
17	Lowest Frequency	-1642.7
18	Nucleus	1H
19	Acquired Size	32768
20	Spectral Size	65536

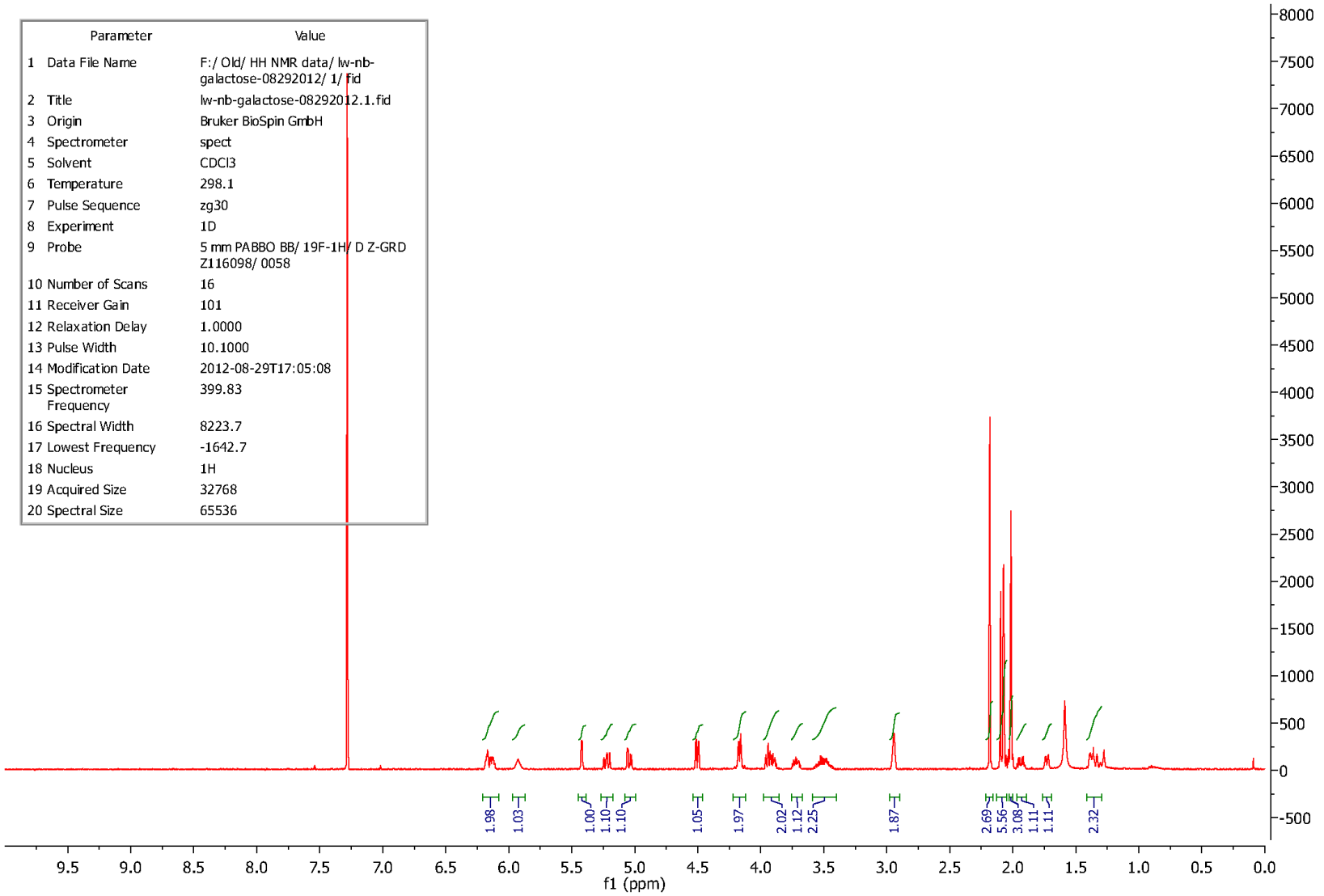

^{1}H-NMR spectrum of NB-galactose 16

	Parameter	Value
1	Data File Name	F:/ NMR/ galactose/ C13-NB-Galactose-09062012/ 1/ fid
2	Title	C13-NB-Galactose-09062012.1.fid
3	Origin	Bruker BioSpin GmbH
4	Spectrometer	spect
5	Solvent	CDCl3
6	Temperature	298.1
7	Pulse Sequence	zgpg30
8	Experiment	1D
9	Probe	5 mm CPPBBO BB-1H/ 19F/ D Z-GRD Z122624/ 0008
10	Number of Scans	201
11	Receiver Gain	197
12	Relaxation Delay	2.0000
13	Pulse Width	10.0000
14	Modification Date	2012-09-06T17:40:34
15	Spectrometer Frequency	125.71
16	Spectral Width	29761.9
17	Lowest Frequency	-2311.3
18	Nucleus	13C
19	Acquired Size	32768
20	Spectral Size	65536

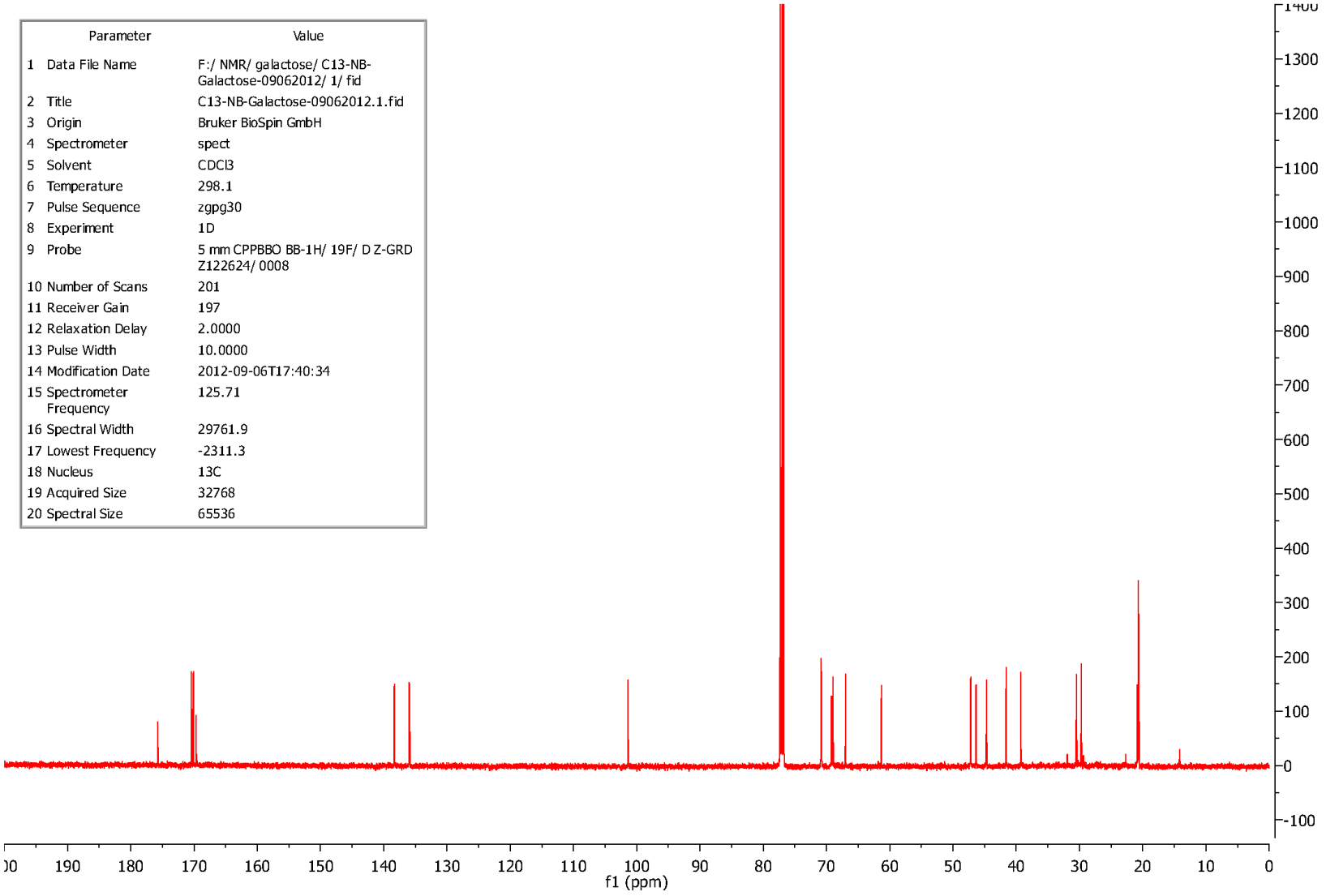

^{13}C-NMR spectrum of NB-galactose 16

	Parameter	Value
1	Data File Name	F:/ fucose/ nb-l-fucose-top/ 1/ fid
2	Title	nb-l-fucose-top.1.fid
3	Origin	Bruker BioSpin GmbH
4	Spectrometer	spect
5	Solvent	CDCl3
6	Temperature	298.1
7	Pulse Sequence	zg30
8	Experiment	1D
9	Probe	5 mm CPPBBO BB-1H/ 19F/ D Z-GRD Z122624/ 0008
10	Number of Scans	16
11	Receiver Gain	32
12	Relaxation Delay	1.0000
13	Pulse Width	12.0000
14	Modification Date	2013-04-12T14:38:34
15	Spectrometer Frequency	499.89
16	Spectral Width	10000.0
17	Lowest Frequency	-1913.0
18	Nucleus	1H
19	Acquired Size	32768
20	Spectral Size	65536

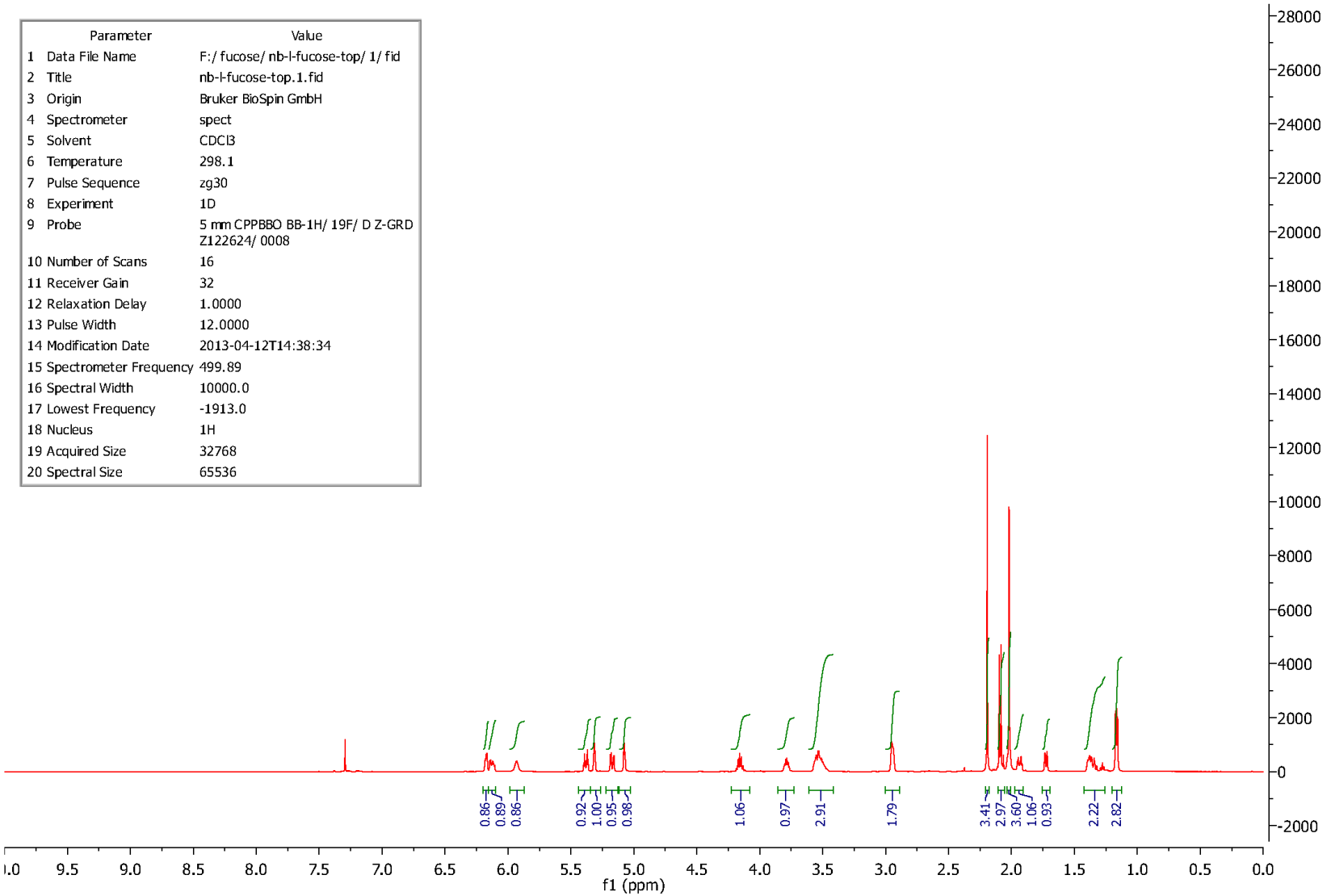

^{1}H-NMR spectrum of NB-fucose 20

	Parameter	Value
1	Data File Name	F:/ fucose/ c13-nb-l-fucose-top/ 2/ fid
2	Title	c13-nb-l-fucose-top.2.fid
3	Origin	Bruker BioSpin GmbH
4	Spectrometer	spect
5	Solvent	CDCl3
6	Temperature	298.1
7	Pulse Sequence	zgpg30
8	Experiment	1D
9	Probe	5 mm CPPBBO BB-1H/ 19F/ D Z-GRD Z122624/ 0008
10	Number of Scans	182
11	Receiver Gain	197
12	Relaxation Delay	2.0000
13	Pulse Width	10.0000
14	Modification Date	2013-04-12T19:04:02
15	Spectrometer Frequency	125.71
16	Spectral Width	29761.9
17	Lowest Frequency	-2311.3
18	Nucleus	13C
19	Acquired Size	32768
20	Spectral Size	65536

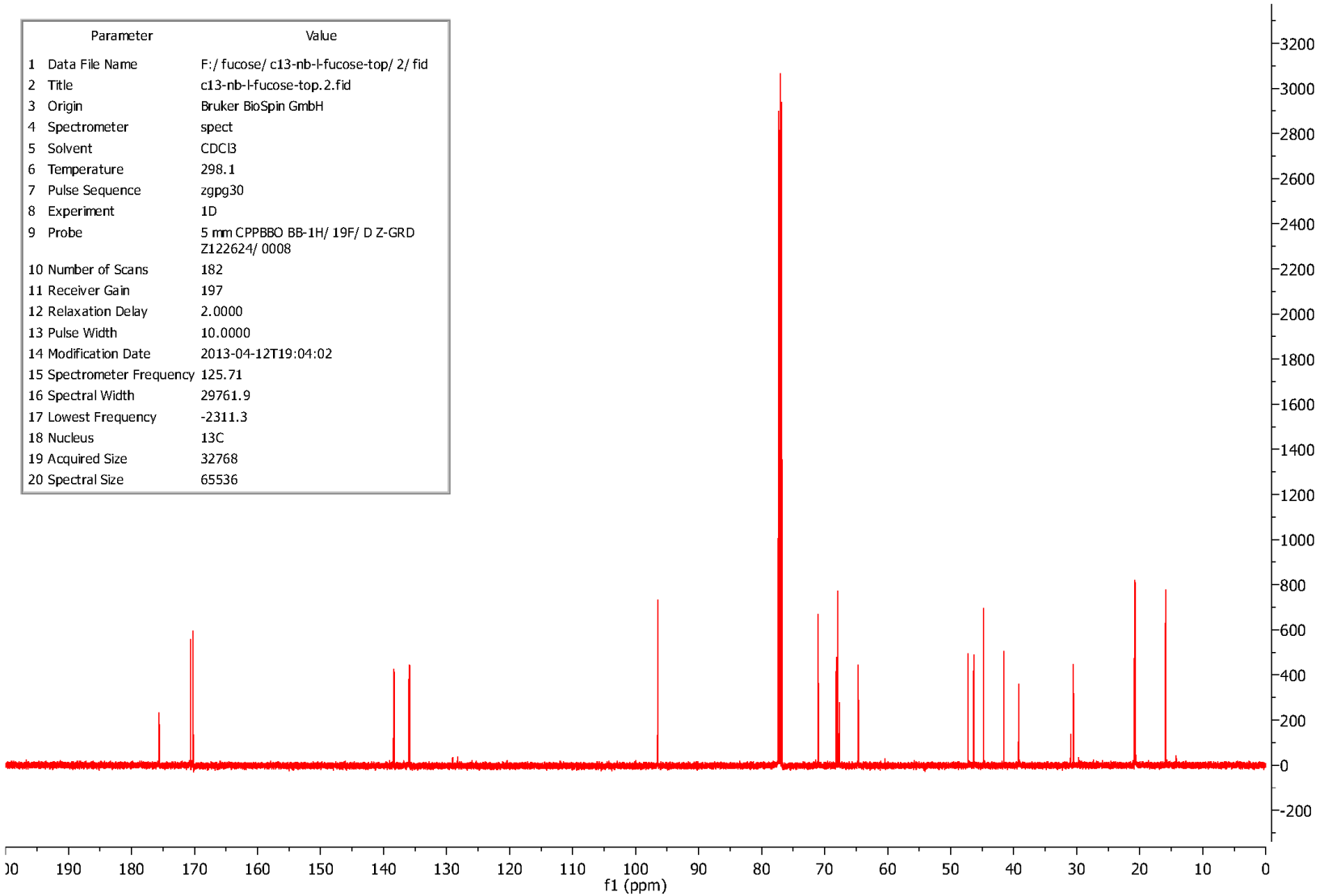

150

^{13}C-NMR spectrum of NB-fucose 20

	Parameter	Value
1	Data File Name	F:/ Old/ NMR data/ NB-glcnac-03022010/ 1/ fid
2	Title	NB-glcnac-03022010.fid
3	Origin	Bruker BioSpin GmbH
4	Spectrometer	spect
5	Solvent	CDCl3
6	Temperature	298.0
7	Pulse Sequence	zg30
8	Experiment	1D
9	Probe	5 mm PABBO BB/ 19F-1H/ D Z-GRD Z116098/ 0058
10	Number of Scans	16
11	Receiver Gain	32
12	Relaxation Delay	1.0000
13	Pulse Width	10.1000
14	Modification Date	2010-03-02T16:19:06
15	Spectrometer Frequency	399.83
16	Spectral Width	8223.7
17	Lowest Frequency	-1639.0
18	Nucleus	1H
19	Acquired Size	32768
20	Spectral Size	65536

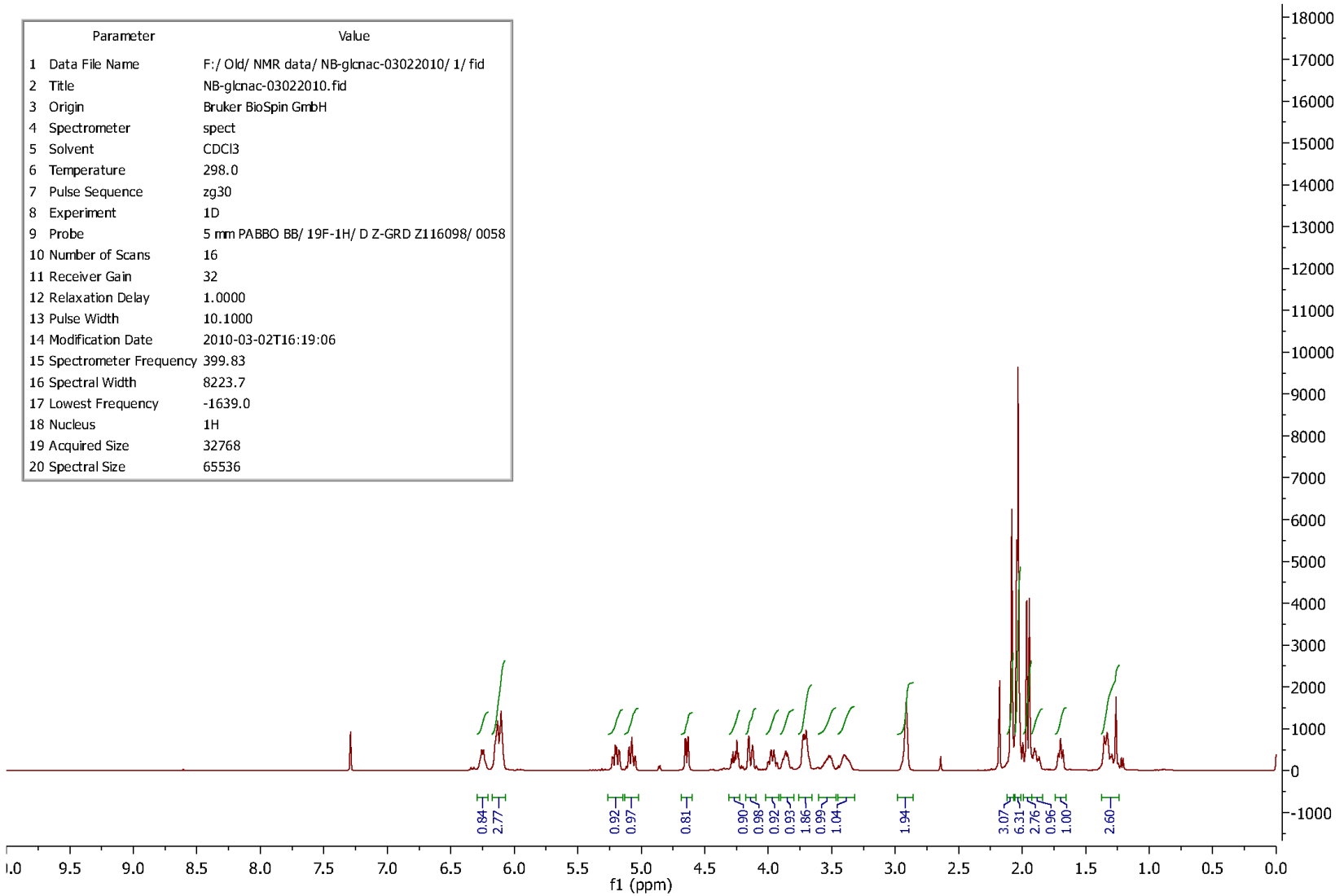

^{1}H-NMR spectrum of NB-GlcNAc 25

	Parameter	Value
1	Data File Name	D:/ Dropbox/ RESEARCH/ NMR/ NMR Varian 500 600/ 600/ glcNAc/ c13_nb-glcnac03082010.fid/ fid
2	Origin	Varian
3	Solvent	CDCl3
4	Temperature	25.0
5	Pulse Sequence	s2pul
6	Experiment	1D
7	Number of Scans	64
8	Receiver Gain	60
9	Relaxation Delay	1.0000
10	Pulse Width	0.0000
11	Acquisition Date	2010-03-08T11:52:32
12	Modification Date	2010-03-08T03:00:00
13	Spectrometer Frequency	125.71
14	Spectral Width	31421.8
15	Lowest Frequency	-1884.1
16	Nucleus	13C
17	Acquired Size	40863
18	Spectral Size	131072

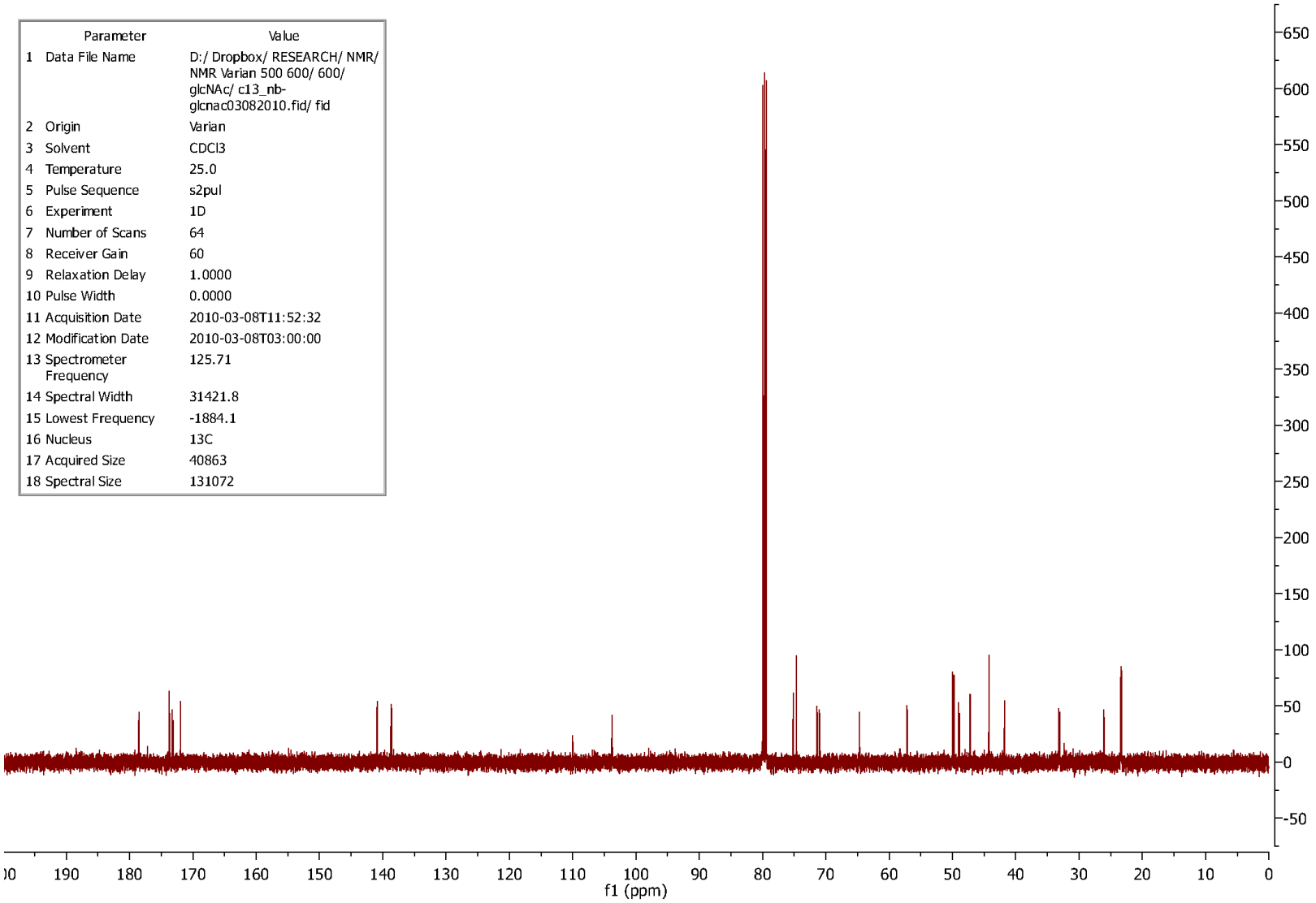

^{13}C-NMR spectrum of NB-GlcNAc 25

	Parameter	Value
1	Data File Name	F:/ NMR/ galNAc/ NB-GalNAc-08292012/ 1/ fid
2	Title	NB-GalNAc-08292012.1.fid
3	Origin	Bruker BioSpin GmbH
4	Spectrometer	spect
5	Solvent	CDCl3
6	Temperature	298.1
7	Pulse Sequence	zg30
8	Experiment	1D
9	Probe	5 mm PABBO BB/ 19F-1H/ D Z-GRD Z116098/ 0058
10	Number of Scans	16
11	Receiver Gain	32
12	Relaxation Delay	1.0000
13	Pulse Width	10.1000
14	Modification Date	2012-08-29T18:49:56
15	Spectrometer Frequency	399.83
16	Spectral Width	8223.7
17	Lowest Frequency	-1642.7
18	Nucleus	1H
19	Acquired Size	32768
20	Spectral Size	65536

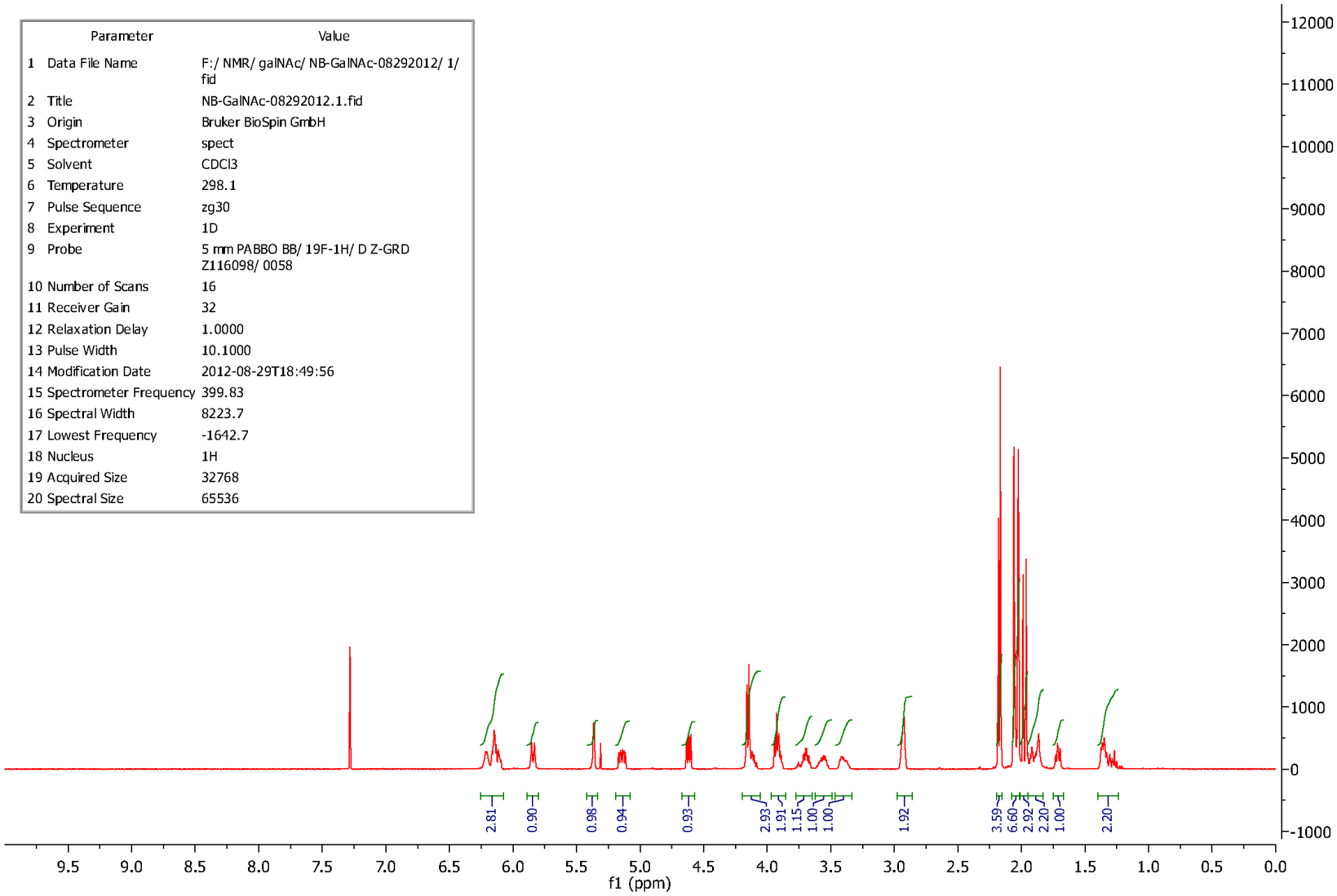

^{1}H-NMR spectrum of NB-GalNAc 31

	Parameter	Value
1	Data File Name	F:/ NMR/ galNAc/ c13-nb-GalNAC-08292012/ 1/ fid
2	Title	c13-nb-GalNAC-08292012.1.fid
3	Origin	Bruker BioSpin GmbH
4	Spectrometer	spect
5	Solvent	CDCl3
6	Temperature	298.1
7	Pulse Sequence	zgpg30
8	Experiment	1D
9	Probe	5 mm CPPBBO BB-1H/ 19F/ D Z-GRD Z122624/ 0008
10	Number of Scans	176
11	Receiver Gain	197
12	Relaxation Delay	2.0000
13	Pulse Width	10.0000
14	Modification Date	2012-08-29T23:26:54
15	Spectrometer Frequency	125.71
16	Spectral Width	29761.9
17	Lowest Frequency	-2311.3
18	Nucleus	13C
19	Acquired Size	32768
20	Spectral Size	65536

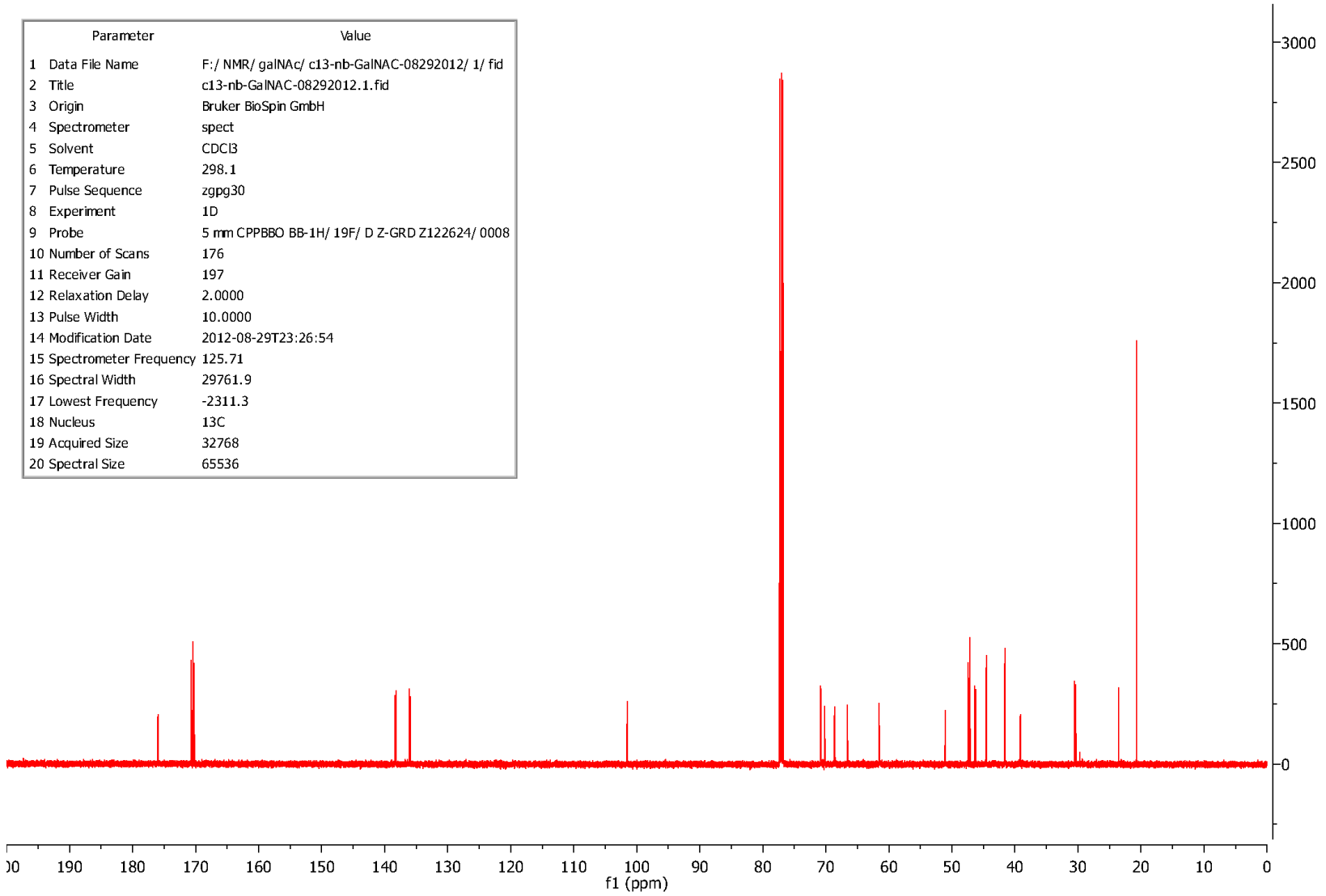

^{13}C-NMR spectrum of NB-GalNAc 31

	Parameter	Value
1	Data File Name	C:/ Users/ Stella/ Dropbox/ RESEARCH/ NMR/ NMR Varian 500 600/ 600/ fucose/ nb-fucose-12062010.fid/ fid
2	Origin	Varian
3	Spectrometer	inova
4	Solvent	CDCl3
5	Temperature	25.0
6	Pulse Sequence	s2pul
7	Experiment	1D
8	Number of Scans	35
9	Receiver Gain	44
10	Pulse Width	0.0000
11	Acquisition Date	2010-12-07T22:15:38
12	Modification Date	2010-12-07T22:21:26
13	Spectrometer Frequency	599.72
14	Spectral Width	8000.0
15	Lowest Frequency	-1001.3
16	Nucleus	1H
17	Acquired Size	15136
18	Spectral Size	65536

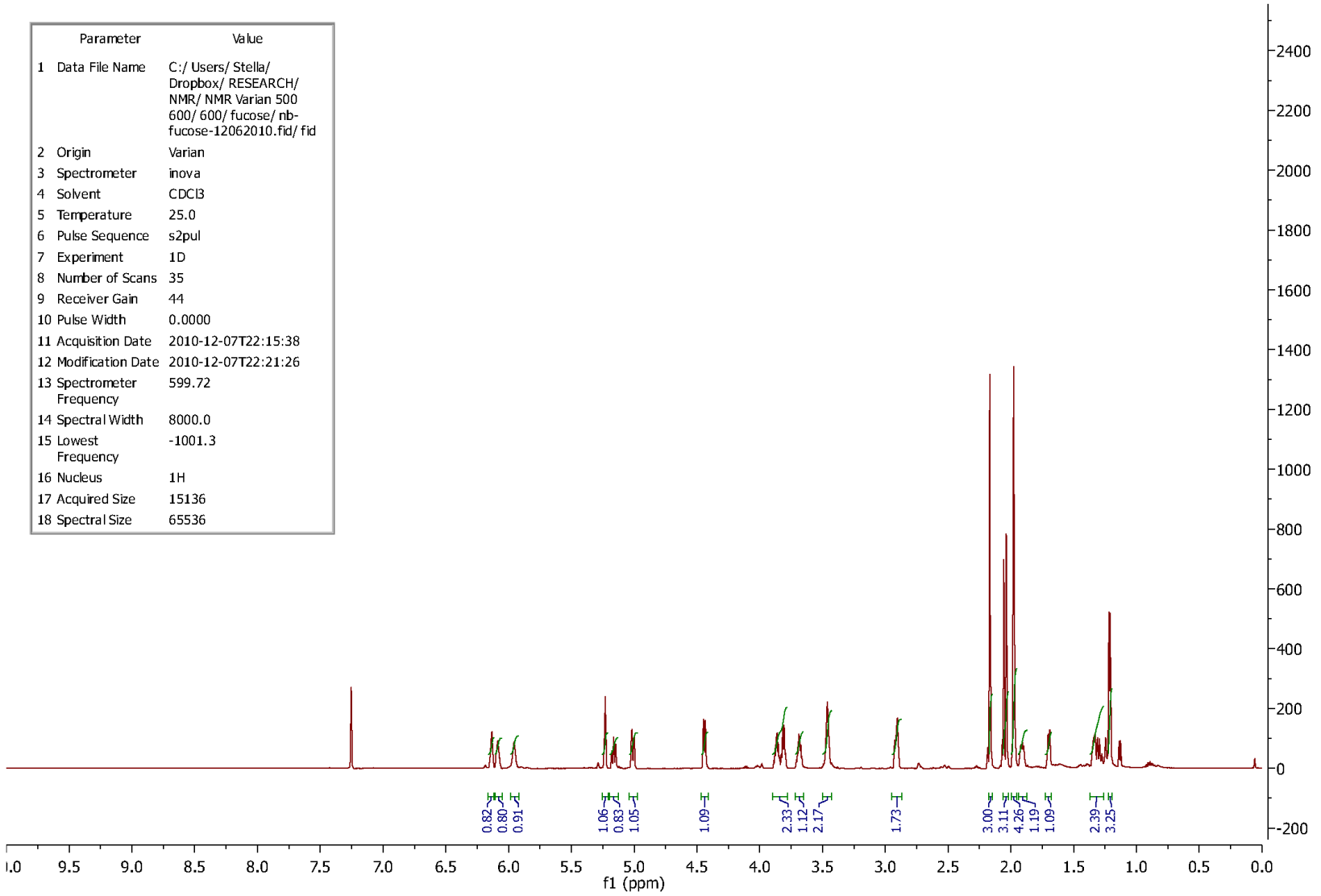

^{1}H-NMR spectrum of NB-D-fucose 38

	Parameter	Value
1	Data File Name	F:/ NMR/ mannose/ nb-mannoside10merpure-04162009.fid/ fid
2	Origin	Varian
3	Spectrometer	inova
4	Solvent	CDCl3
5	Temperature	25.0
6	Pulse Sequence	s2pul
7	Experiment	1D
8	Probe	hcx
9	Number of Scans	24
10	Receiver Gain	56
11	Relaxation Delay	1.0000
12	Pulse Width	0.0000
13	Acquisition Time	1.8920
14	Acquisition Date	2009-04-16T18:47:29
15	Spectrometer Frequency	599.72
16	Spectral Width	8000.0
17	Lowest Frequency	-1001.3
18	Nucleus	1H
19	Acquired Size	15136
20	Spectral Size	65536

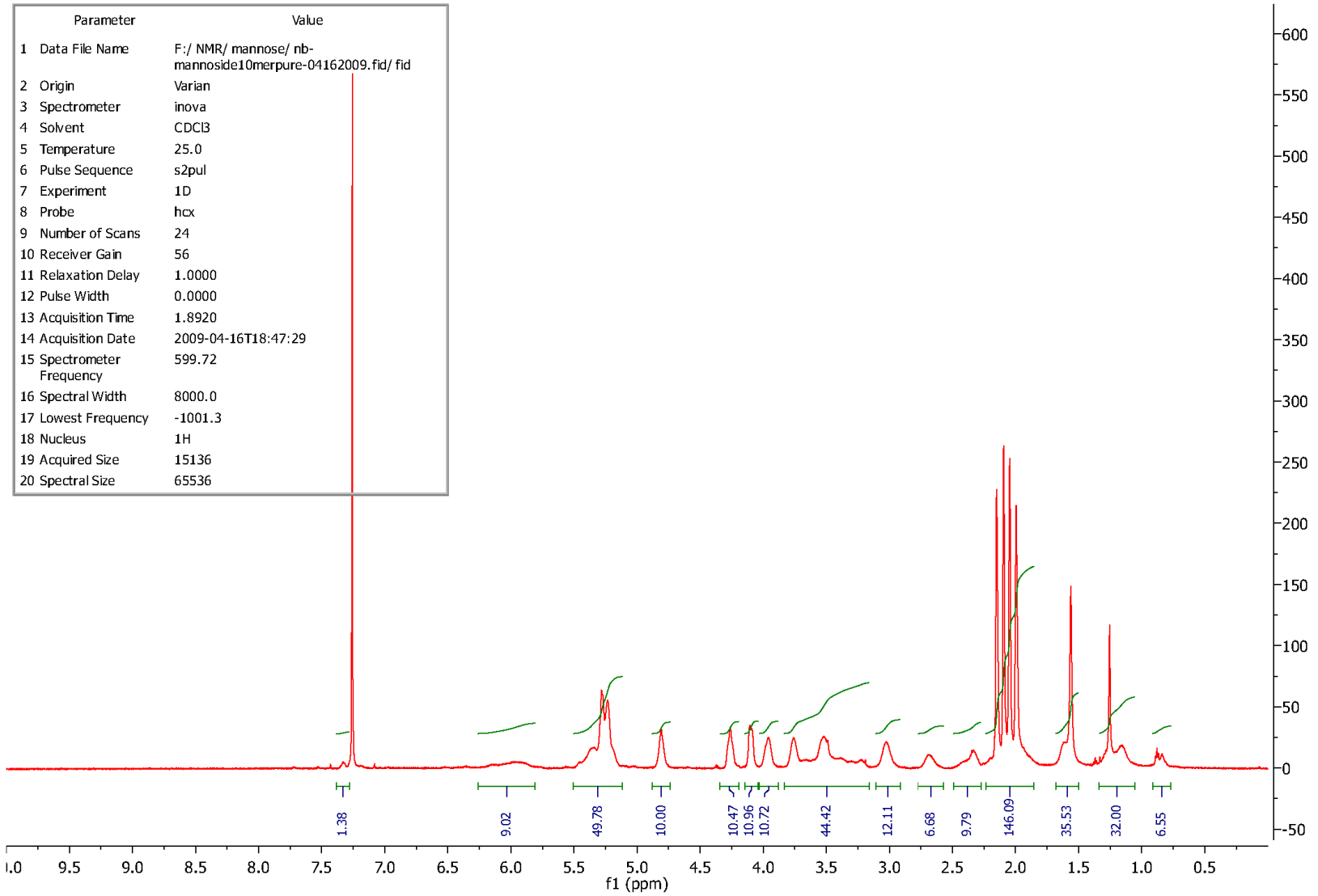

^{1}H-NMR spectrum of prot-poly(Man)$_{10}$

	Parameter	Value
1	Data File Name	F:/ NMR/ mannose/ nb-man100mer-3-tlc-02202011.fid/ fid
2	Origin	Varian
3	Spectrometer	inova
4	Solvent	CDCl3
5	Temperature	25.0
6	Pulse Sequence	s2pul
7	Experiment	1D
8	Probe	hcx
9	Number of Scans	28
10	Receiver Gain	40
11	Relaxation Delay	1.0000
12	Pulse Width	0.0000
13	Acquisition Time	1.8920
14	Acquisition Date	2011-02-25T14:56:48
15	Spectrometer Frequency	599.72
16	Spectral Width	8000.0
17	Lowest Frequency	-1001.3
18	Nucleus	1H
19	Acquired Size	15136
20	Spectral Size	65536

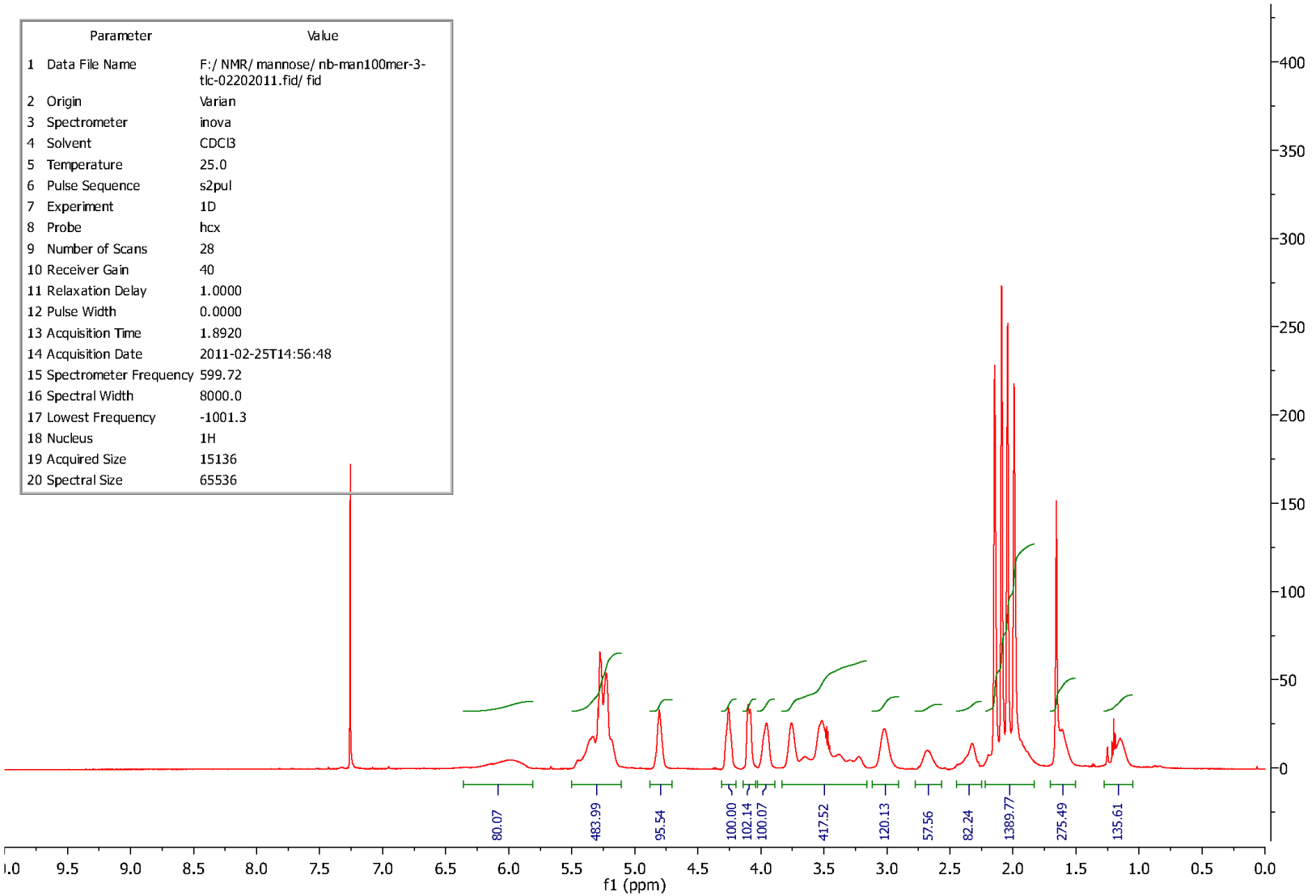

^{1}H-NMR spectrum of prot-poly(Man)$_{100}$

	Parameter	Value
1	Data File Name	D:/ Dropbox/ RESEARCH/ NMR/ NMR Varian 500 600/ 600/ glucose/ nb-glucose10mer-2-tlc-02212011.fid/ fid
2	Origin	Varian
3	Solvent	CDCl3
4	Temperature	25.0
5	Pulse Sequence	s2pul
6	Experiment	1D
7	Number of Scans	26
8	Receiver Gain	34
9	Relaxation Delay	1.0000
10	Pulse Width	0.0000
11	Acquisition Date	2011-02-25T15:10:51
12	Modification Date	2011-02-25T18:14:34
13	Spectrometer Frequency	599.72
14	Spectral Width	8000.0
15	Lowest Frequency	-1001.3
16	Nucleus	1H
17	Acquired Size	15136
18	Spectral Size	65536

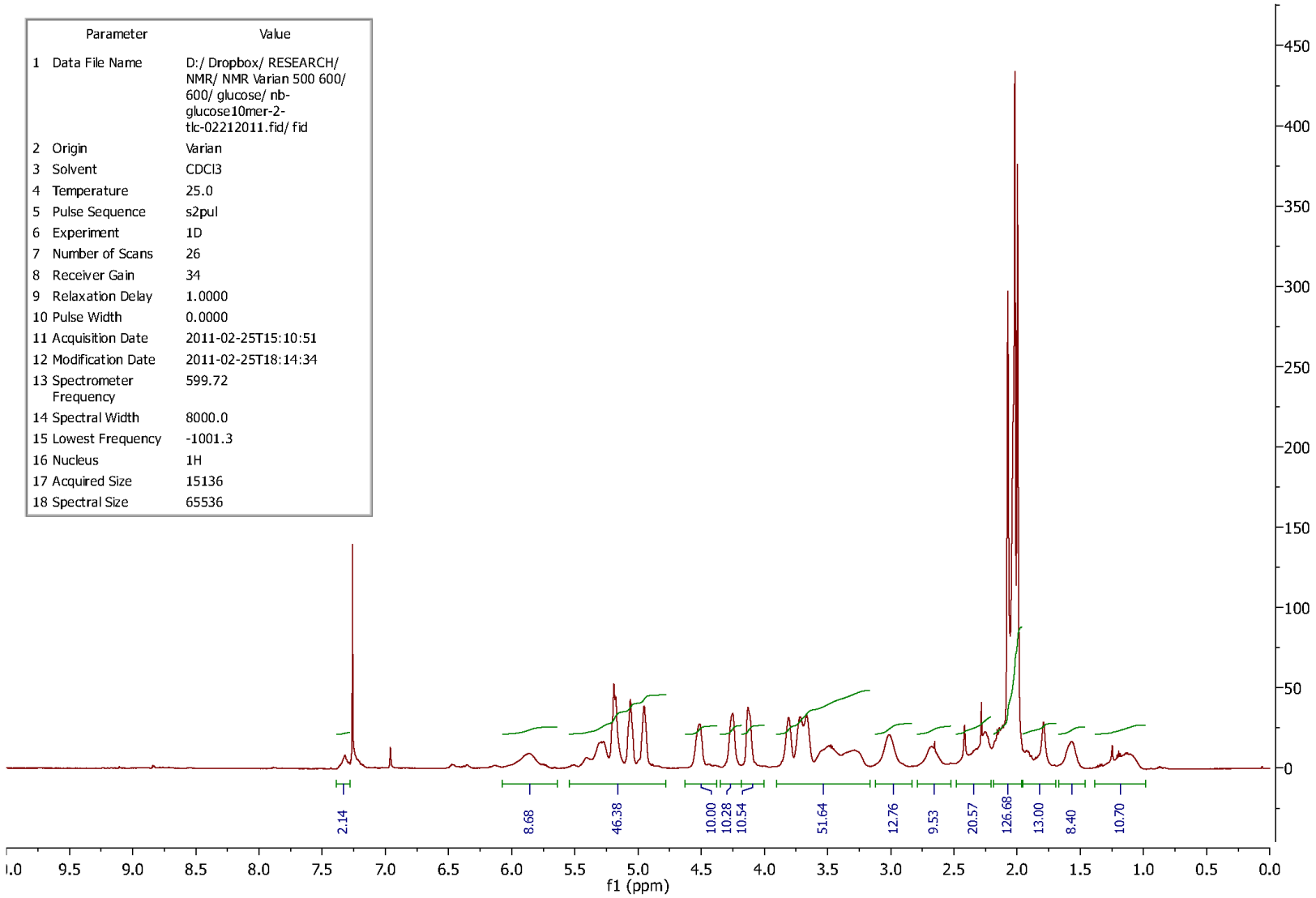

^{1}H-NMR spectrum of prot-poly(Glc)$_{10}$

	parameters	value
1	Data File Name	I:/ NMR/ glucose/ nb-glucose100mer04162010.fid/ fid
2	Origin	Varian
3	Spectrometer	inova
4	Solvent	CDCl3
5	Temperature	25.0
6	Pulse Sequence	s2pul
7	Probe	HCN
8	Number of Scans	16
9	Receiver Gain	38
10	Relaxation Delay	1.0000
11	Pulse Width	0.0000
12	Acquisition Time	1.8920
13	Acquisition Date	2010-04-16T15:41:28
14	Spectrometer Frequency	599.72
15	Spectral Width	8000.0
16	Lowest Frequency	-1001.3
17	Nucleus	1H
18	Acquired Size	15136
19	Spectral Size	65536

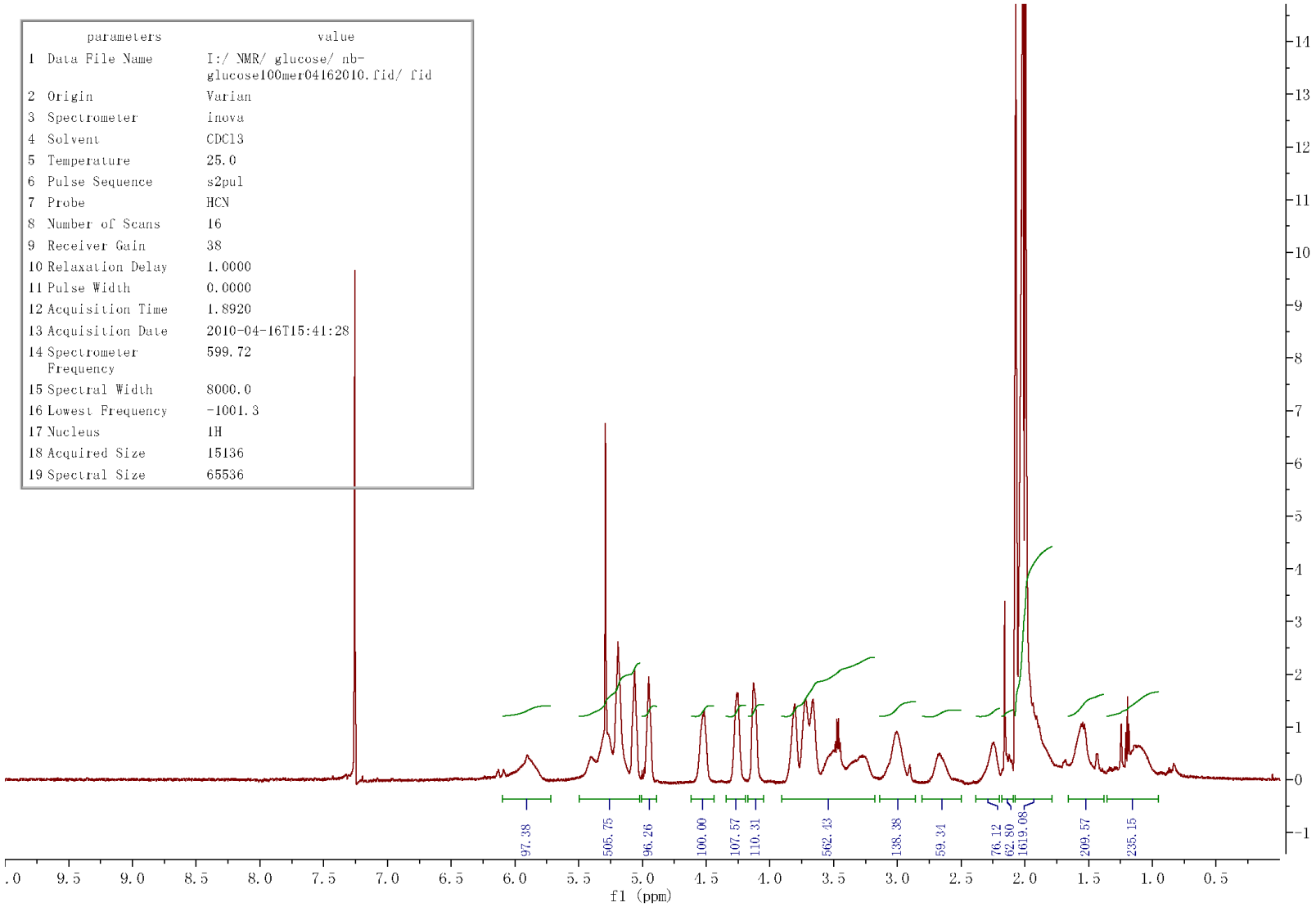

^{1}H NMR spectra of prot-poly(Glc)$_{100}$

	Parameter	Value
1	Data File Name	F:/ NMR/ galactose/ nb-galactose-10mer-09092010.fid/ fid
2	Origin	Varian
3	Spectrometer	inova
4	Solvent	CDCl3
5	Temperature	25.0
6	Pulse Sequence	s2pul
7	Experiment	1D
8	Probe	hcx
9	Number of Scans	1
10	Receiver Gain	34
11	Relaxation Delay	1.0000
12	Pulse Width	0.0000
13	Acquisition Time	1.8920
14	Acquisition Date	2010-09-09T21:19:26
15	Spectrometer Frequency	599.72
16	Spectral Width	8000.0
17	Lowest Frequency	-1001.3
18	Nucleus	1H
19	Acquired Size	15136
20	Spectral Size	65536

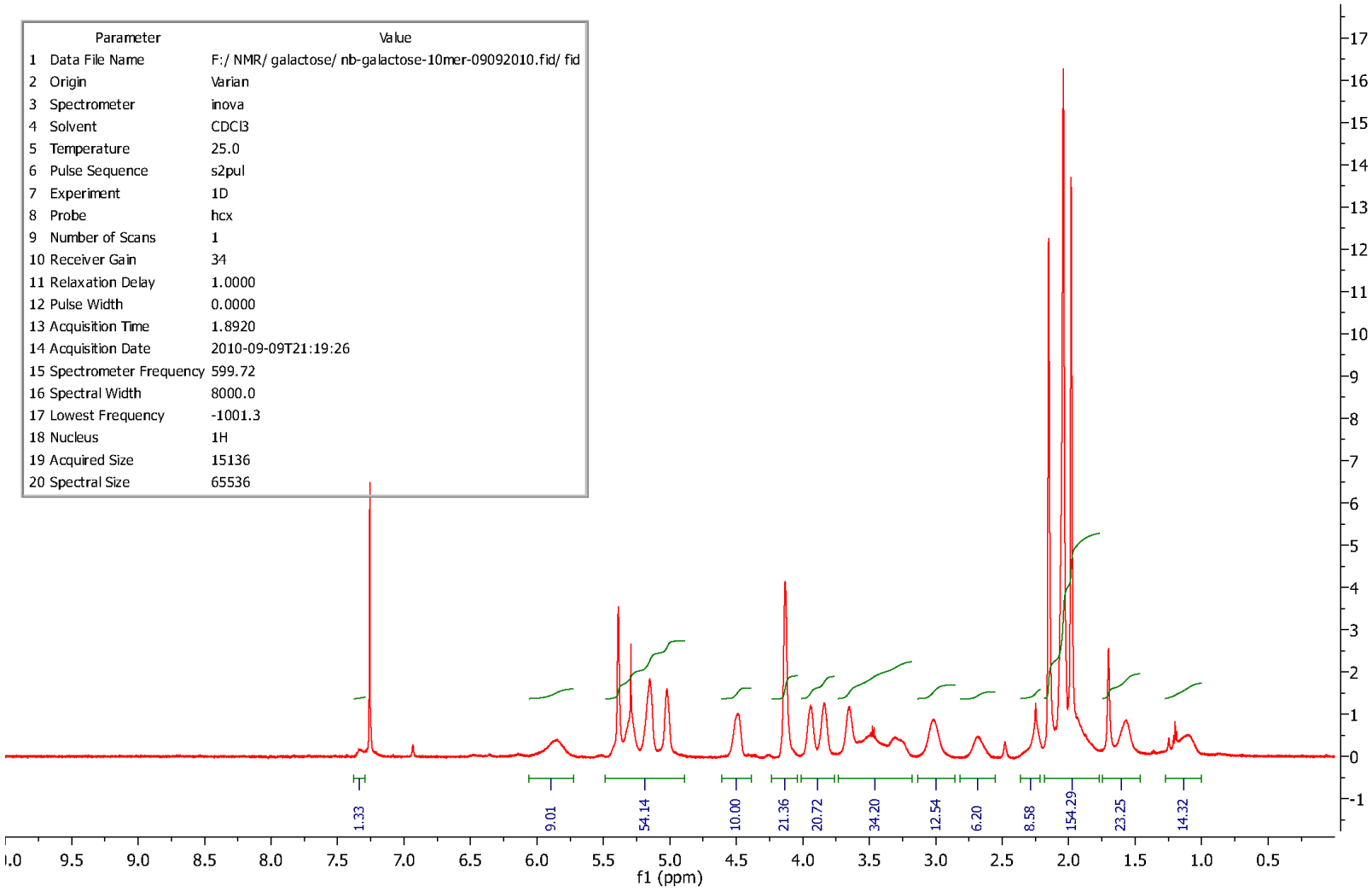

^{1}H-NMR spectrum of prot-poly(Gal)$_{10}$

	Parameter	Value
1	Data File Name	F:/ Old/ HH NMR data/ nb-galacotse-100mer-3-09042010/ 1/ fid
2	Title	nb-galacotse-100mer-3-09042010.1.fid
3	Origin	Bruker BioSpin GmbH
4	Spectrometer	spect
5	Solvent	CDCl3
6	Temperature	298.1
7	Pulse Sequence	zg30
8	Experiment	1D
9	Probe	5 mm PABBO BB/ 19F-1H/ D Z-GRD Z116098/ 0058
10	Number of Scans	16
11	Receiver Gain	85
12	Relaxation Delay	1.0000
13	Pulse Width	10.1000
14	Modification Date	2012-09-04T15:49:24
15	Spectrometer Frequency	399.83
16	Spectral Width	8223.7
17	Lowest Frequency	-1642.7
18	Nucleus	1H
19	Acquired Size	32768
20	Spectral Size	65536

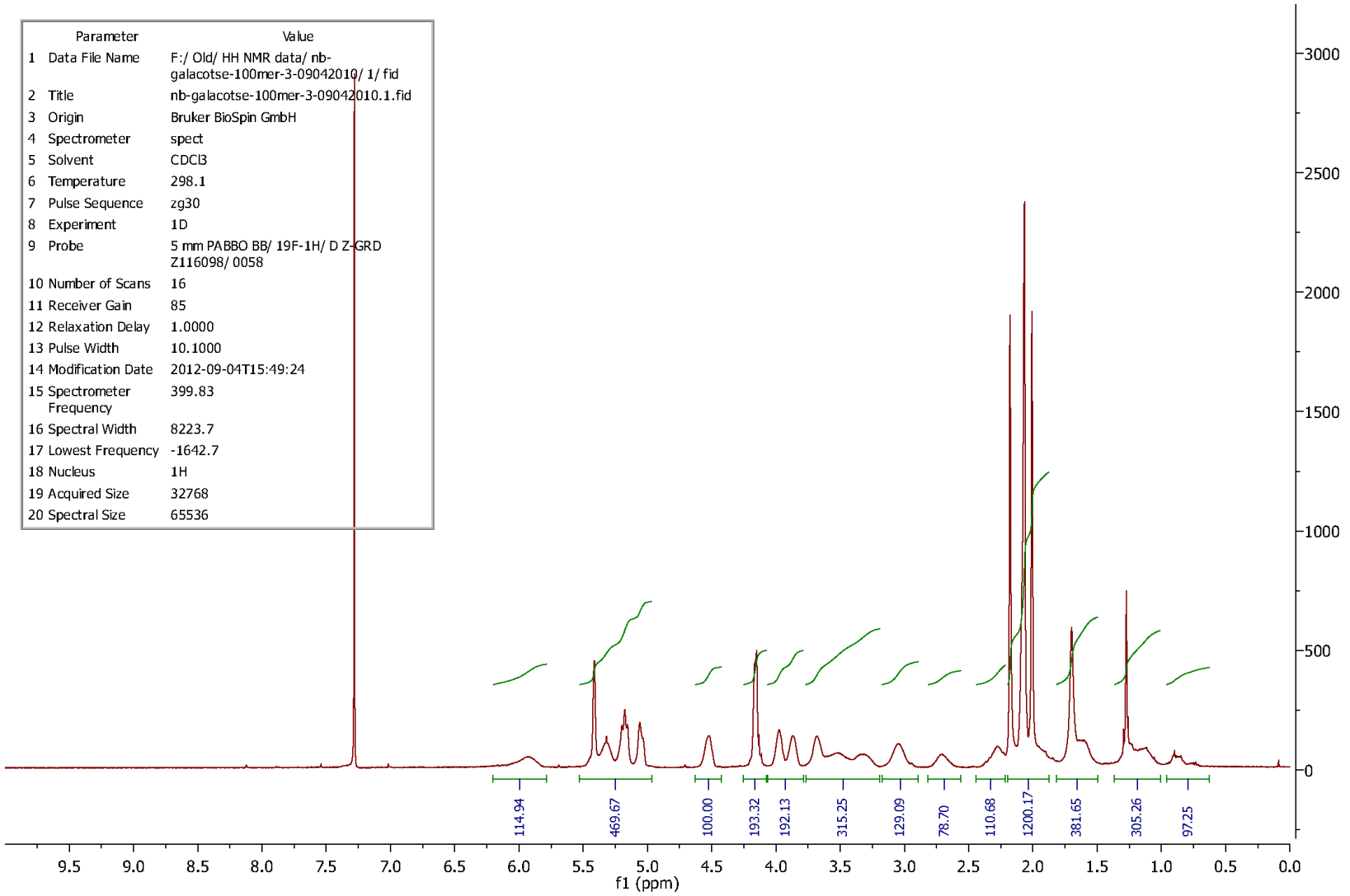

^{1}H-NMR spectrum of prot-poly(Gal)$_{100}$

	Parameter	Value
1	Data File Name	F:/ fucose/ nb-l-fucose-10mer dry04162013/ 1/ fid
2	Title	nb-l-fucose-10mer dry04162013.1.fid
3	Origin	Bruker BioSpin GmbH
4	Spectrometer	spect
5	Solvent	CDCl3
6	Temperature	298.2
7	Pulse Sequence	zg30
8	Experiment	1D
9	Probe	5 mm CPPBBO BB-1H/ 19F/ D Z-GRD Z122624/ 0008
10	Number of Scans	16
11	Receiver Gain	32
12	Relaxation Delay	1.0000
13	Pulse Width	12.0000
14	Modification Date	2013-04-16T17:50:50
15	Spectrometer Frequency	499.89
16	Spectral Width	10000.0
17	Lowest Frequency	-1913.0
18	Nucleus	1H
19	Acquired Size	32768
20	Spectral Size	65536

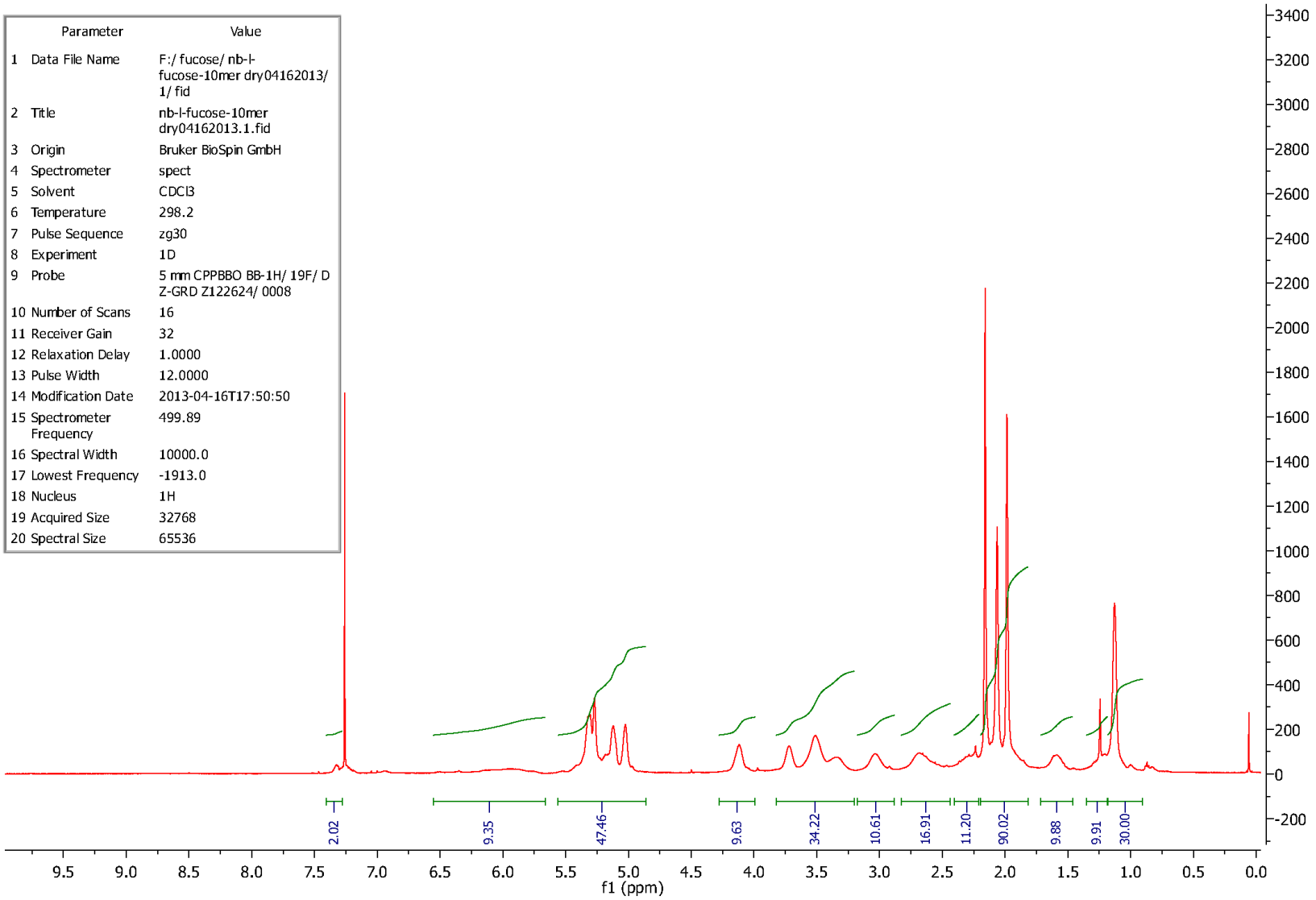

^{1}H-NMR spectrum of prot-poly(Fuc)$_{10}$

	Parameter	Value
1	Data File Name	F:/ fucose/ nb-l-fucose-100mer dry04162013/ 1/ fid
2	Title	nb-l-fucose-100mer dry04162013.1.fid
3	Origin	Bruker BioSpin GmbH
4	Spectrometer	spect
5	Solvent	CDCl3
6	Temperature	298.1
7	Pulse Sequence	zg30
8	Experiment	1D
9	Probe	5 mm CPPBBO BB-1H/ 19F/ D Z-GRD Z122624/ 0008
10	Number of Scans	16
11	Receiver Gain	32
12	Relaxation Delay	1.0000
13	Pulse Width	12.0000
14	Modification Date	2013-04-16T17:56:32
15	Spectrometer Frequency	499.89
16	Spectral Width	10000.0
17	Lowest Frequency	-1913.0
18	Nucleus	1H
19	Acquired Size	32768
20	Spectral Size	65536

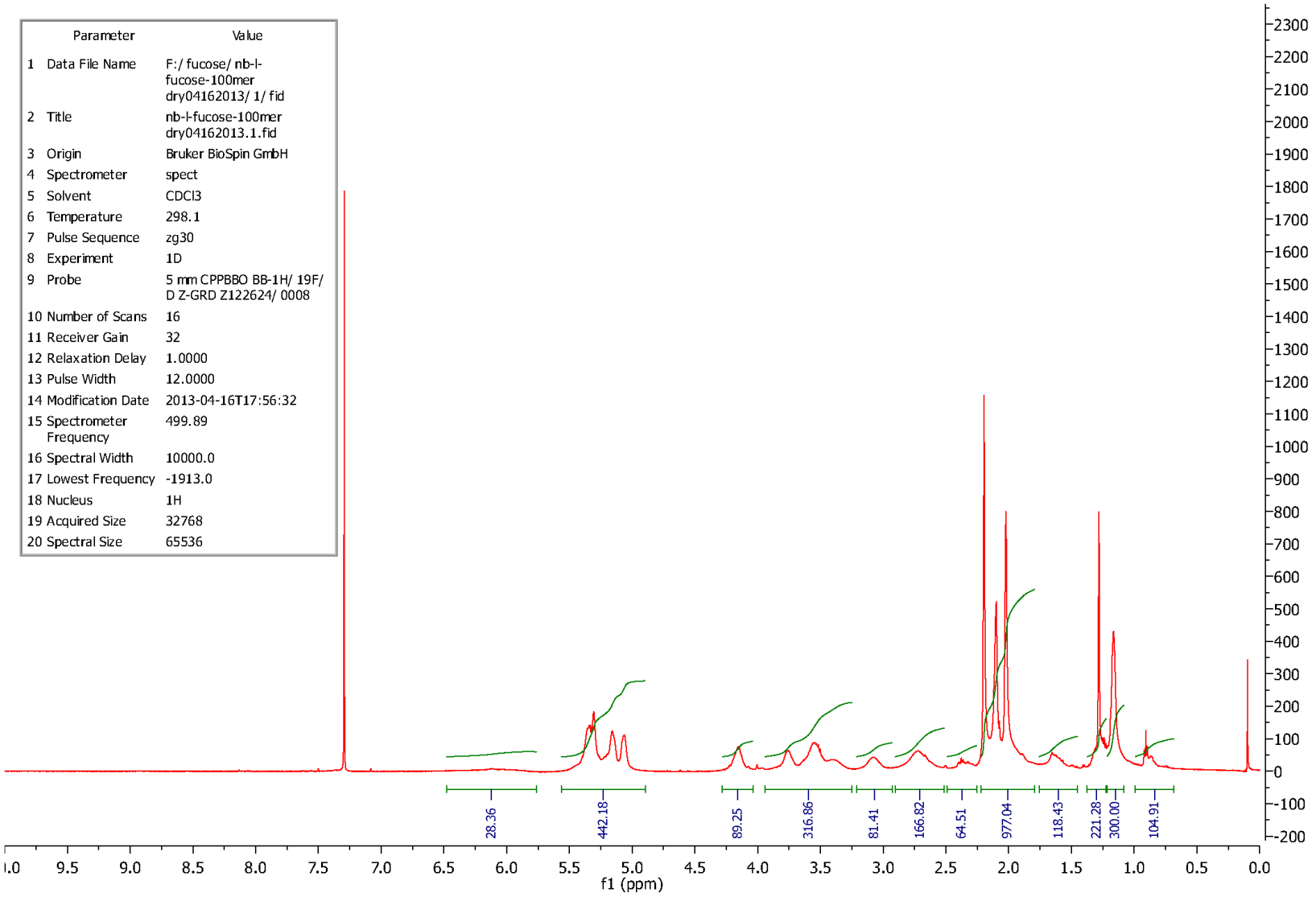

^{1}H-NMR spectrum of prot-poly(Fuc)$_{100}$

	Parameter	Value
1	Data File Name	C:/ Users/ Stella/ Dropbox/ RESEARCH/ NMR/ NMR Varian 500 600/ 600/ glcNAc/ nb-glcnac10mer-03192010.fid/ fid
2	Origin	Varian
3	Spectrometer	inova
4	Solvent	CDCl3
5	Temperature	25.0
6	Pulse Sequence	s2pul
7	Experiment	1D
8	Number of Scans	29
9	Receiver Gain	40
10	Pulse Width	0.0000
11	Acquisition Date	2010-03-19T15:33:48
12	Modification Date	2010-03-19T19:40:48
13	Spectrometer Frequency	599.72
14	Spectral Width	8000.0
15	Lowest Frequency	-1001.3
16	Nucleus	1H
17	Acquired Size	15136
18	Spectral Size	65536

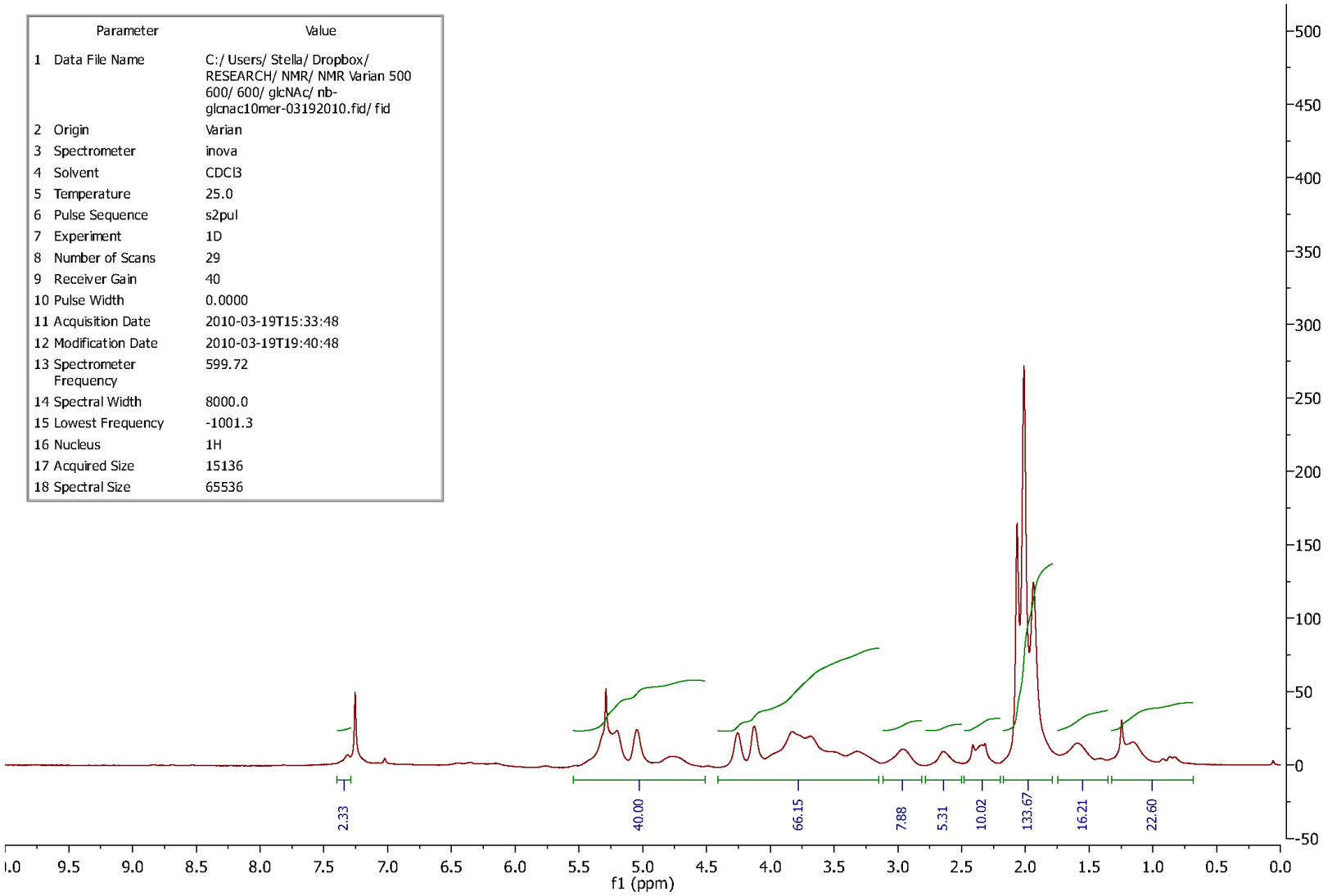

^{1}H-NMR spectrum of prot-poly(GlcNAc)$_{10}$

	Parameter	Value
1	Data File Name	F:/ nmr/ nb-glcnac100mer-06222010.fid/ fid
2	Origin	Varian
3	Spectrometer	inova
4	Solvent	CDCl3
5	Temperature	25.0
6	Pulse Sequence	s2pul
7	Experiment	1D
8	Probe	hcx2
9	Number of Scans	141
10	Receiver Gain	60
11	Relaxation Delay	1.0000
12	Pulse Width	0.0000
13	Acquisition Time	1.8920
14	Acquisition Date	2010-06-22T17:36:04
15	Spectrometer Frequency	499.90
16	Spectral Width	7998.4
17	Lowest Frequency	-999.9
18	Nucleus	1H
19	Acquired Size	15133
20	Spectral Size	65536

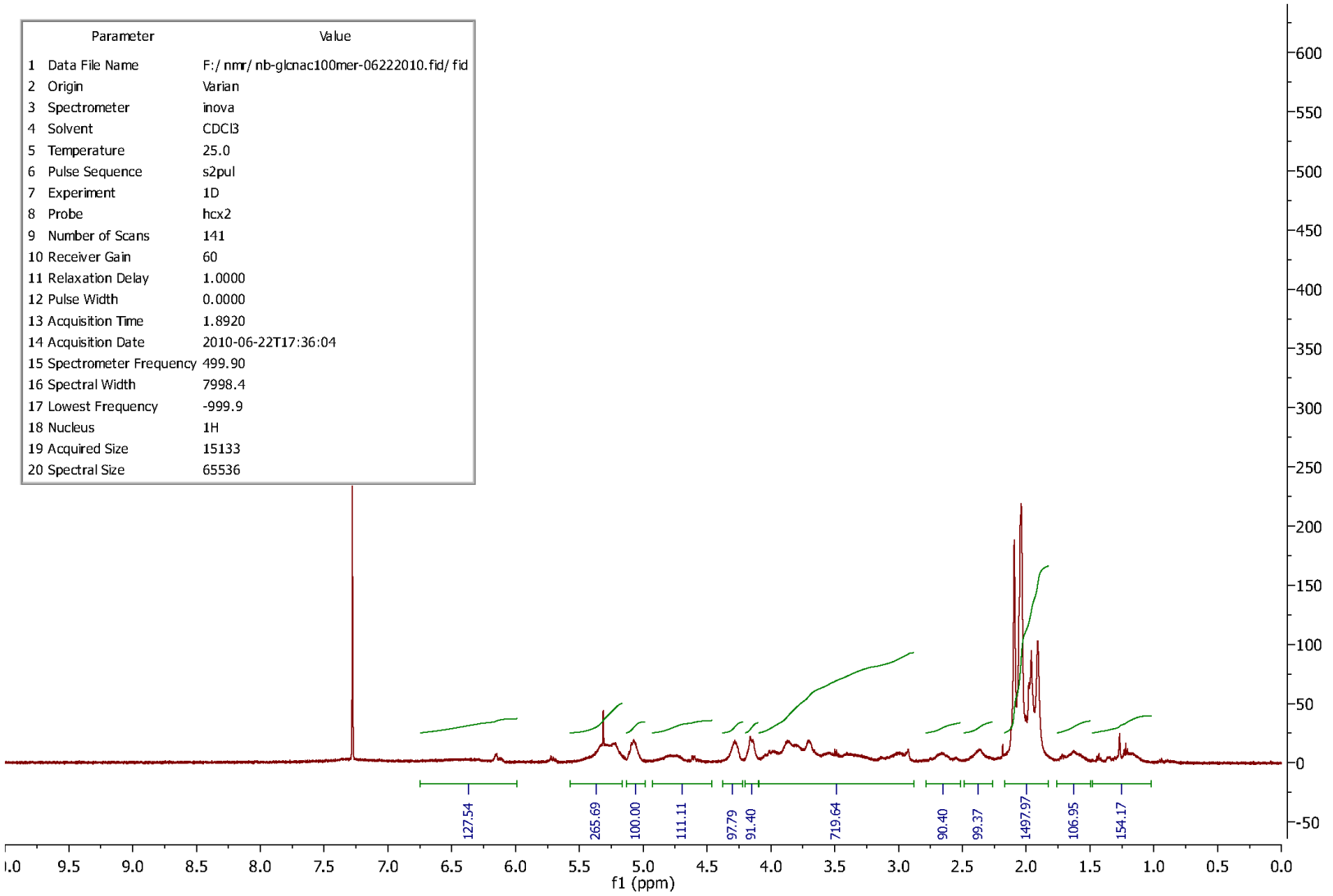

^{1}H NMR spectrum of prot-poly(GlcNAc)$_{100}$

	Parameter	Value
1	Data File Name	F:/ NMR/ galNAc/ nb-galnac-10mer-10042012/ 1/ fid
2	Title	nb-galnac-10mer-10042012.1.fid
3	Origin	Bruker BioSpin GmbH
4	Spectrometer	spect
5	Solvent	CDCl3
6	Temperature	298.2
7	Pulse Sequence	zg30
8	Experiment	1D
9	Probe	5 mm CPPBBO BB-1H/ 19F/ D Z-GRD Z122624/ 0008
10	Number of Scans	14
11	Receiver Gain	32
12	Relaxation Delay	1.0000
13	Pulse Width	12.0000
14	Modification Date	2012-10-04T11:50:54
15	Spectrometer Frequency	499.89
16	Spectral Width	15000.0
17	Lowest Frequency	-4413.0
18	Nucleus	1H
19	Acquired Size	32768
20	Spectral Size	65536

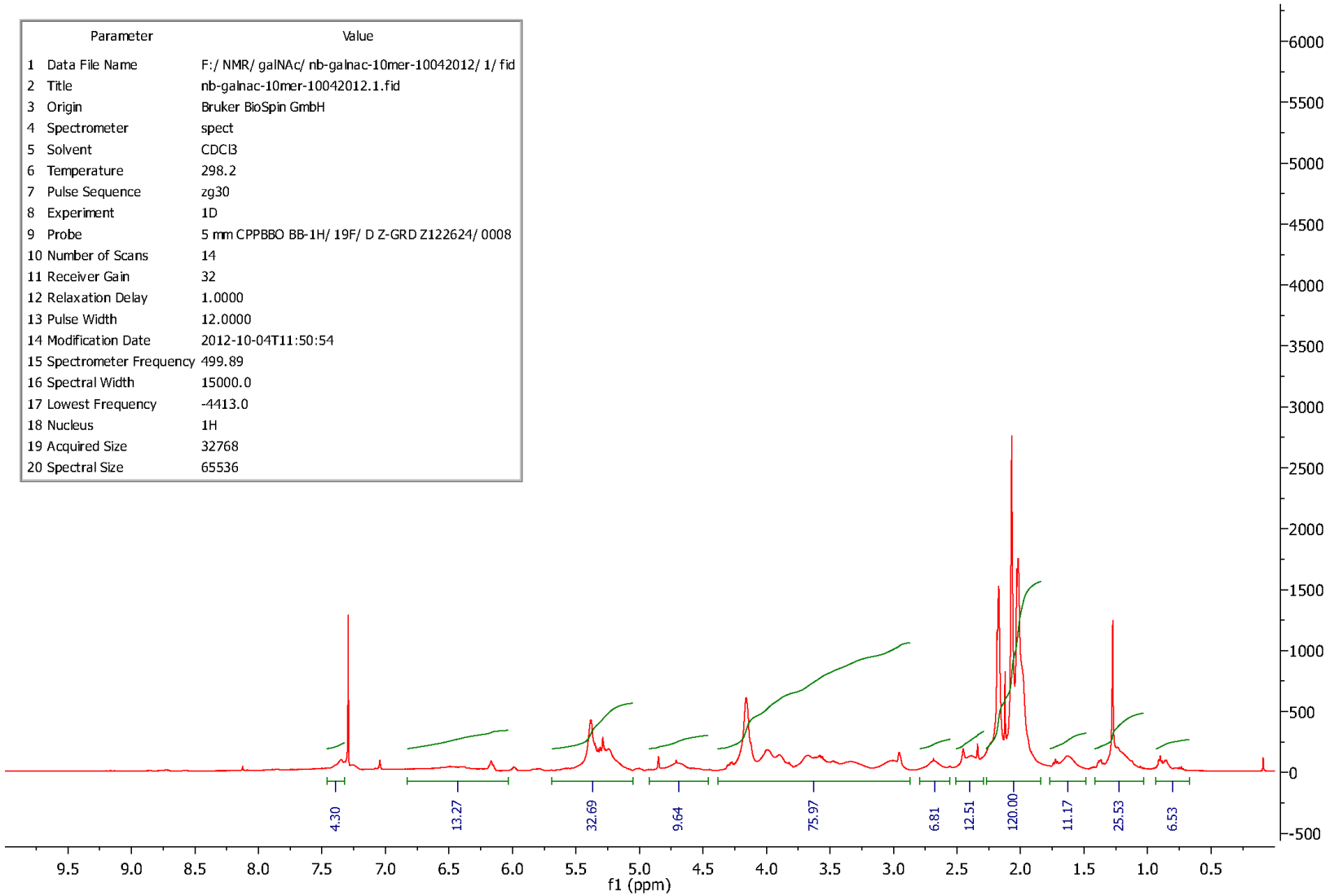

^{1}H-NMR spectrum of prot-poly(GalNAc)$_{10}$

	Parameter	Value
1	Data File Name	F:/ NMR/ galNAc/ nb-galnac-100mer-1-09032012/ 1/ fid
2	Title	NB-Galnac-100mer-1-09032012.1.fid
3	Origin	Bruker BioSpin GmbH
4	Spectrometer	spect
5	Solvent	CDCl3
6	Temperature	298.1
7	Pulse Sequence	zg30
8	Experiment	1D
9	Probe	5 mm CPPBBO BB-1H/ 19F/ D Z-GRD Z122624/ 0008
10	Number of Scans	16
11	Receiver Gain	32
12	Relaxation Delay	1.0000
13	Pulse Width	12.0000
14	Modification Date	2012-09-04T01:19:48
15	Spectrometer Frequency	499.89
16	Spectral Width	10000.0
17	Lowest Frequency	-1913.0
18	Nucleus	1H
19	Acquired Size	32768
20	Spectral Size	65536

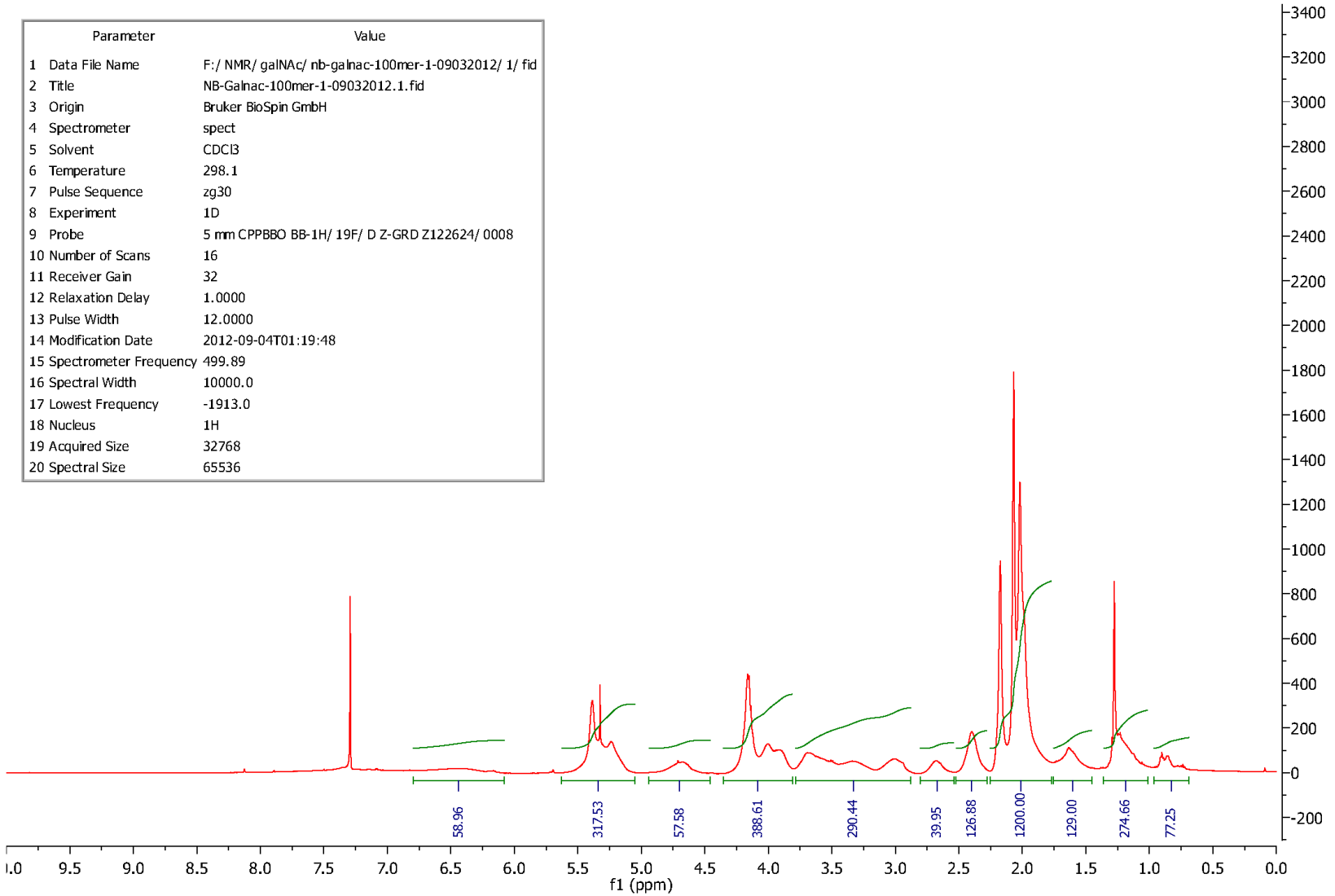

^{1}H-NMR spectrum of prot-poly(GalNAc)$_{100}$

	Parameter	Value
1	Data File Name	D:/ Dropbox/ RESEARCH/ NMR/ NMR Varian 500 600/ 600/ fucose/ nb-fucose10mer-1-12142010.fid/ fid
2	Origin	Varian
3	Solvent	CDCl3
4	Temperature	25.0
5	Pulse Sequence	s2pul
6	Experiment	1D
7	Number of Scans	43
8	Receiver Gain	40
9	Relaxation Delay	1.0000
10	Pulse Width	0.0000
11	Acquisition Date	2010-12-14T22:46:19
12	Modification Date	2010-12-15T01:51:02
13	Spectrometer Frequency	599.72
14	Spectral Width	8000.0
15	Lowest Frequency	-1001.3
16	Nucleus	1H
17	Acquired Size	15136
18	Spectral Size	65536

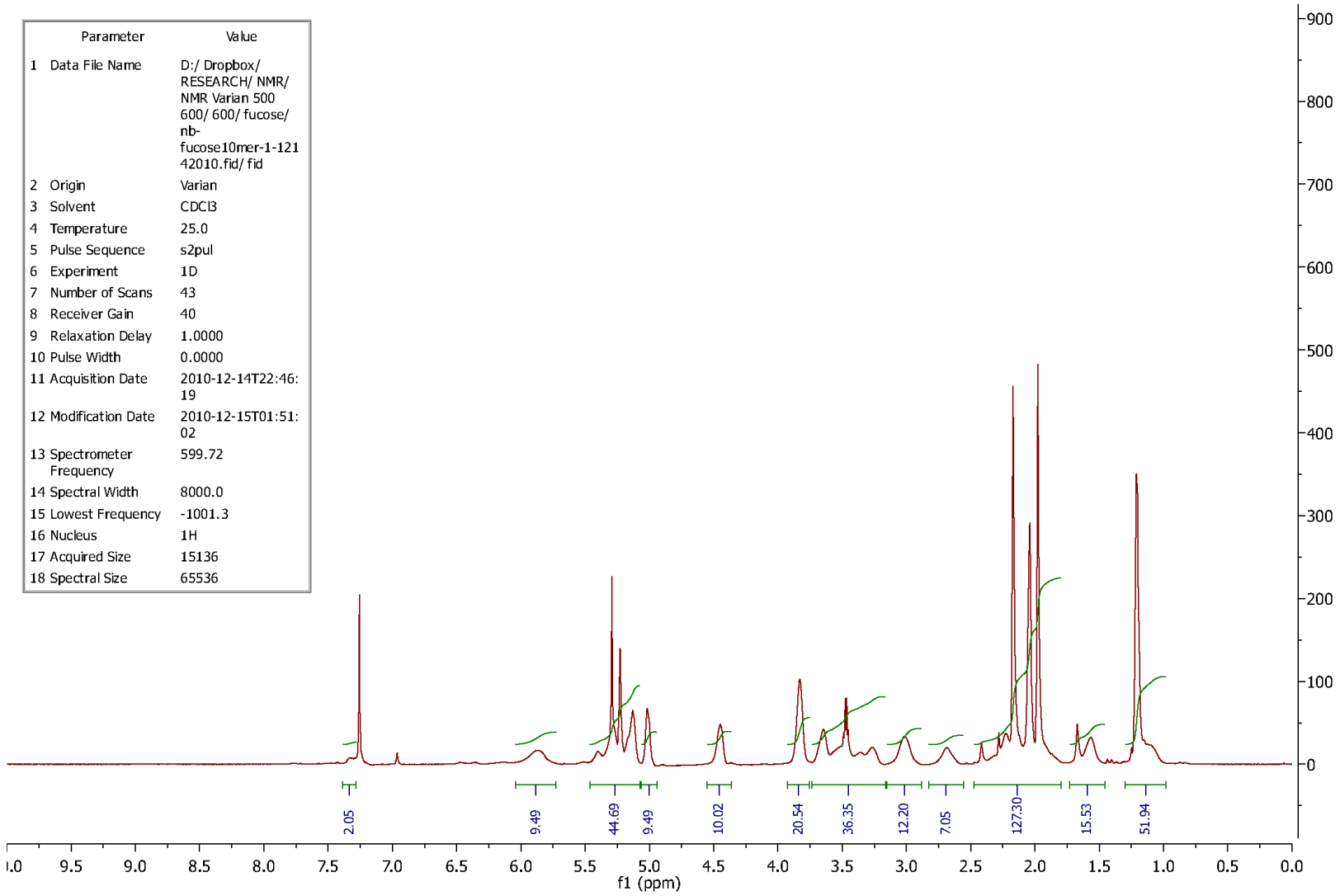

^{1}H-NMR spectrum of prot-poly(D-Fuc)$_{10}$

	Parameter	Value
1	Data File Name	C:/ Users/ Stella/ Dropbox/ RESEARCH/ NMR/ NMR Varian 500 600/ 600/ fucose/ nb-fucose100mer-1-121 42010.fid/ fid
2	Origin	Varian
3	Spectrometer	inova
4	Solvent	CDCl3
5	Temperature	25.0
6	Pulse Sequence	s2pul
7	Experiment	1D
8	Number of Scans	53
9	Receiver Gain	38
10	Pulse Width	0.0000
11	Acquisition Date	2010-12-14T22:52:45
12	Modification Date	2010-12-15T01:57:46
13	Spectrometer Frequency	599.72
14	Spectral Width	8000.0
15	Lowest Frequency	-1001.3
16	Nucleus	1H
17	Acquired Size	15136
18	Spectral Size	65536

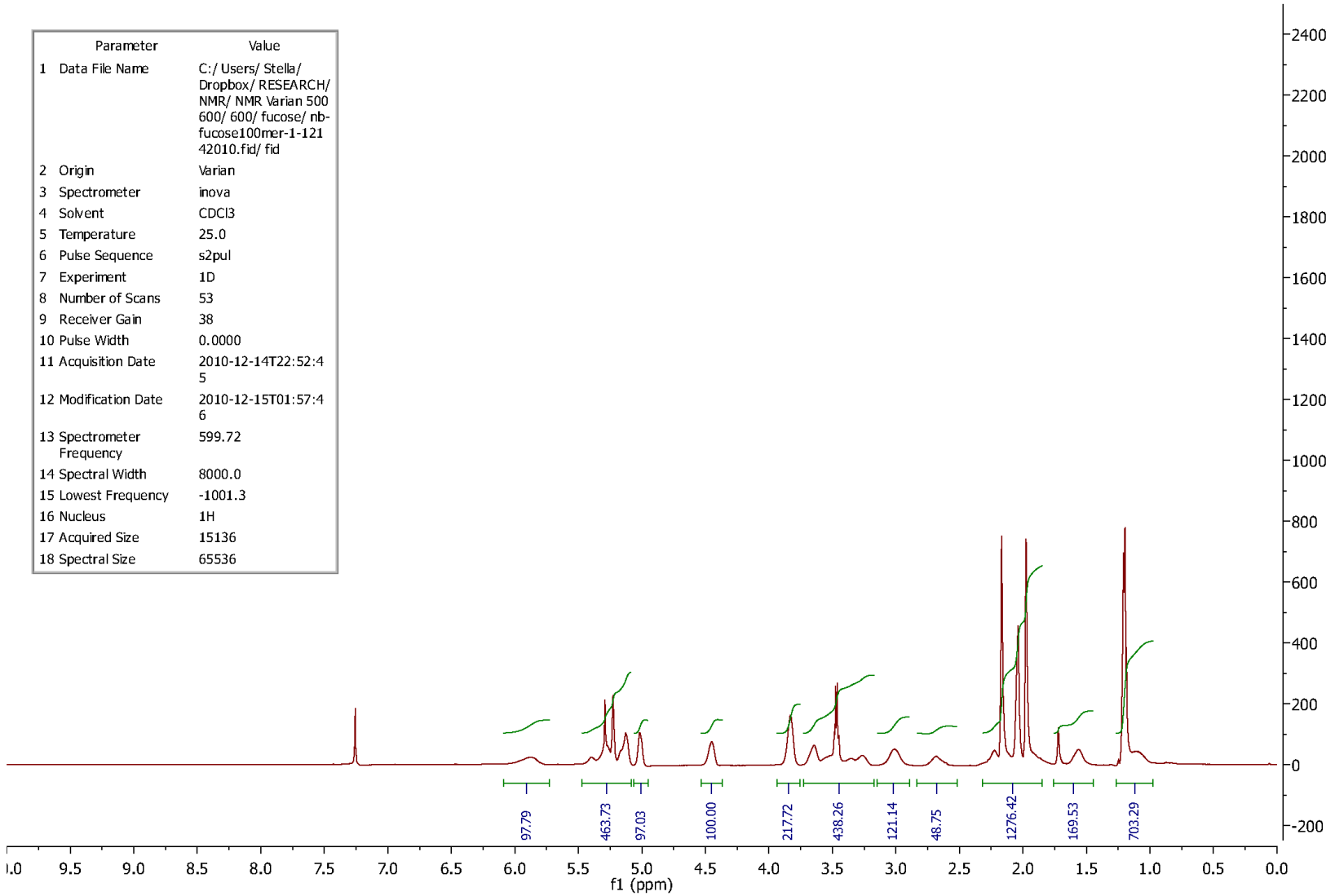

^{1}H-NMR spectrum of prot-poly(D-Fuc)$_{100}$

	Parameter	Value
1	Data File Name	D:/ Dropbox/ RESEARCH/ NMR/ NMR Varian 500 600/ 600/ mannose/ others/ nb-man10mer-3-deprot-03072011.fid/ fid
2	Origin	Varian
3	Solvent	D2O
4	Temperature	25.0
5	Pulse Sequence	s2pul
6	Experiment	1D
7	Number of Scans	79
8	Receiver Gain	40
9	Relaxation Delay	1.0000
10	Pulse Width	0.0000
11	Acquisition Date	2011-03-07T15:33:12
12	Modification Date	2011-03-07T18:38:00
13	Spectrometer Frequency	599.72
14	Spectral Width	8000.0
15	Lowest Frequency	-1001.3
16	Nucleus	1H
17	Acquired Size	15136
18	Spectral Size	65536

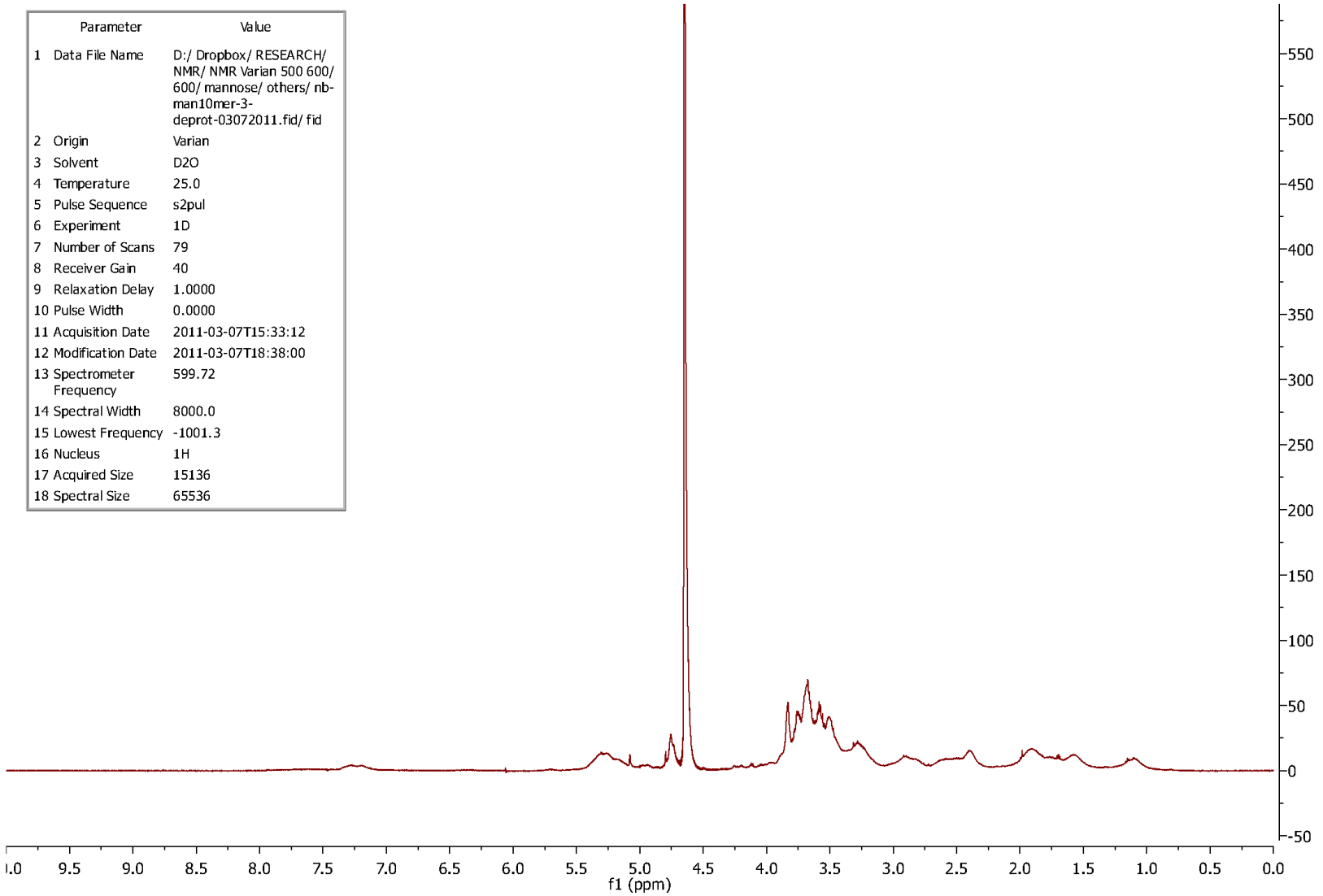

^{1}H-NMR spectrum of poly(Man)$_{10}$

	Parameter	Value
1	Data File Name	D:/ Dropbox/ RESEARCH/ NMR/ NMR Varian 500 600/ 600/ mannose/ nb-man100mer-3-deprot-03102011.fid/ fid
2	Origin	Varian
3	Solvent	D2O
4	Temperature	25.0
5	Pulse Sequence	s2pul
6	Experiment	1D
7	Number of Scans	64
8	Receiver Gain	40
9	Relaxation Delay	1.0000
10	Pulse Width	0.0000
11	Acquisition Date	2011-03-10T15:33:37
12	Modification Date	2011-03-10T18:39:00
13	Spectrometer Frequency	599.72
14	Spectral Width	8000.0
15	Lowest Frequency	-1001.3
16	Nucleus	1H
17	Acquired Size	15136
18	Spectral Size	65536

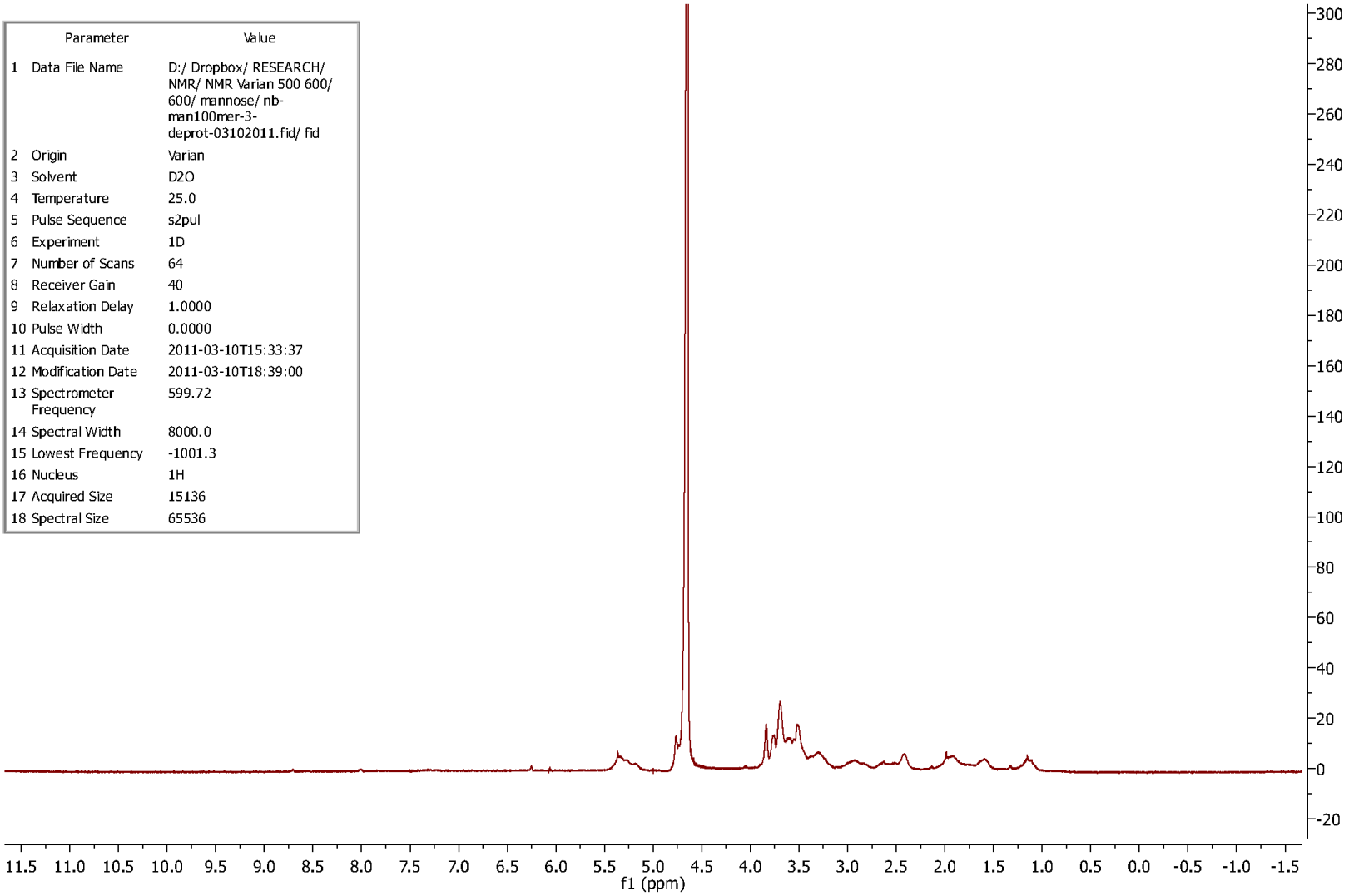

^{1}H-NMR spectrum of poly(Man)$_{100}$

	Parameter	Value
1	Data File Name	C:/ Users/ Stella/ Dropbox/ RESEARCH/ NMR/ NMR Varian 500 600/ 600/ glucose/ nb-glucose10mer-deprot-03092011.fid/ fid
2	Origin	Varian
3	Spectrometer	inova
4	Solvent	D2O
5	Temperature	25.0
6	Pulse Sequence	s2pul
7	Experiment	1D
8	Number of Scans	53
9	Receiver Gain	38
10	Pulse Width	0.0000
11	Acquisition Date	2011-03-10T11:53:12
12	Modification Date	2011-03-10T14:57:10
13	Spectrometer Frequency	599.72
14	Spectral Width	8000.0
15	Lowest Frequency	-1001.3
16	Nucleus	1H
17	Acquired Size	15136
18	Spectral Size	65536

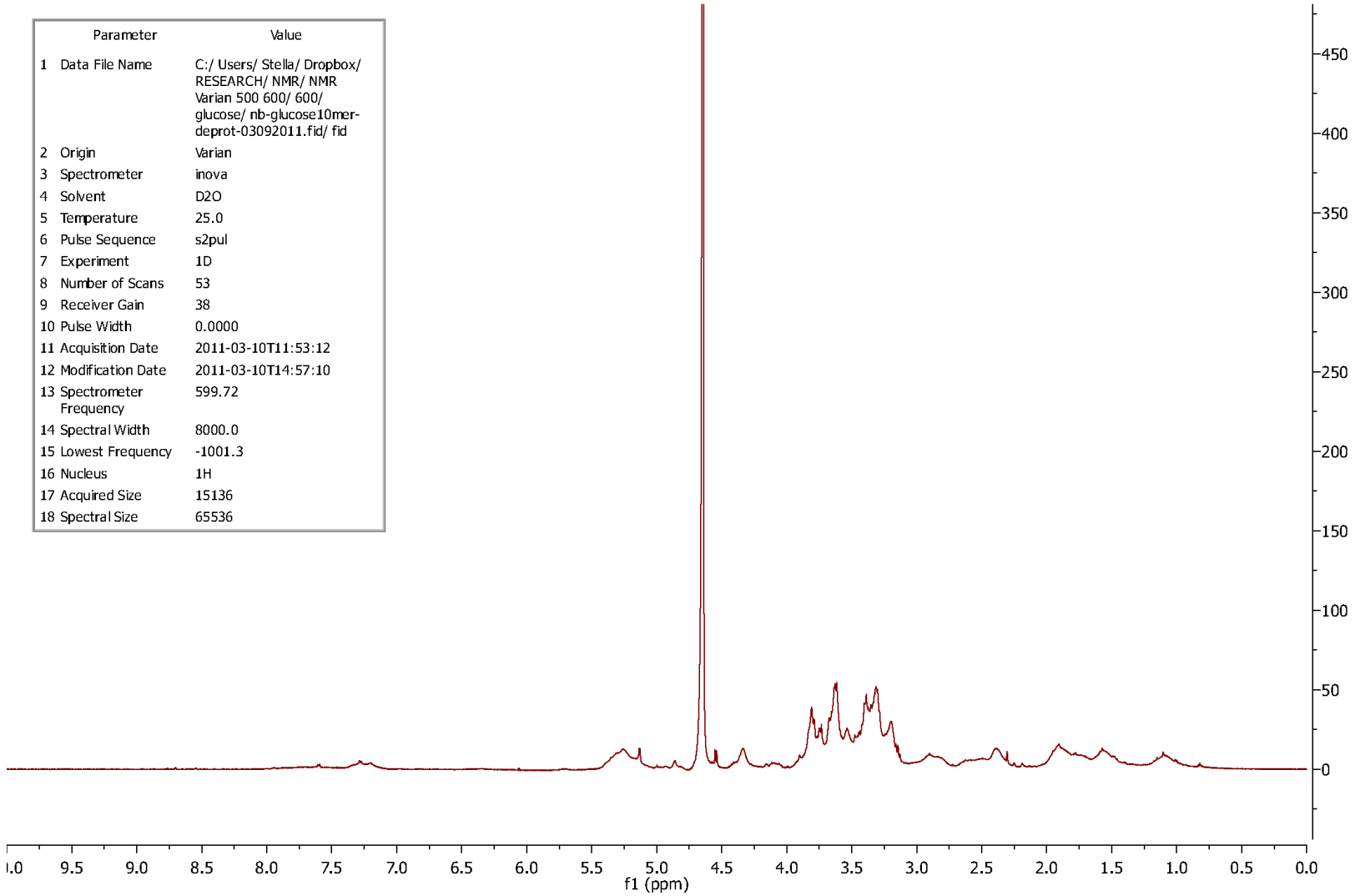

^{1}H-NMR spectrum of poly(Glc)$_{10}$

	parameters	value
1	Data File Name	J:/ nmr/ deprotectedNB-glucose 100mer-09172012/ 1/ fid
2	Origin	Bruker BioSpin GmbH
3	Spectrometer	spect
4	Solvent	D2O
5	Temperature	298.1
6	Pulse Sequence	zg30
7	Experiment	1D
8	Probe	5 mm CPPBBO BB-1H/ 19F/ D Z-GRD Z122624/ 0008
9	Number of Scans	241
10	Receiver Gain	32
11	Relaxation Delay	1.0000
12	Pulse Width	12.0000
13	Acquisition Time	3.2768
14	Acquisition Date	2012-09-17T14:13:00
15	Spectrometer Frequency	499.89
16	Spectral Width	10000.0
17	Lowest Frequency	-1913.0
18	Nucleus	1H
19	Acquired Size	32768
20	Spectral Size	65536

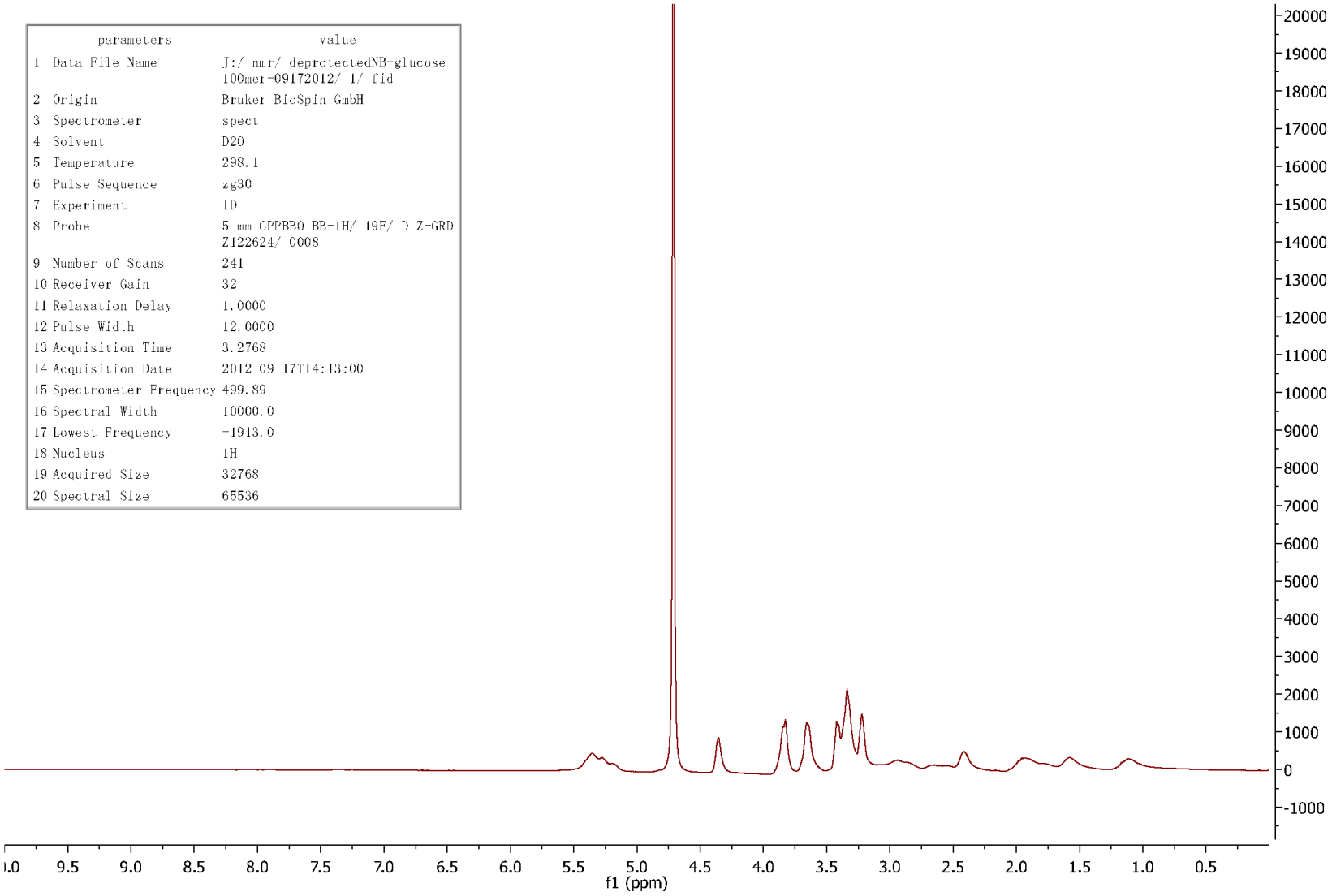

^{1}H NMR spectra of poly(Glc)$_{100}$

	Parameter	Value
1	Data File Name	C:/ Users/ Stella/ Dropbox/ RESEARCH/ NMR/ NMR Varian 500 600/ 600/ galactose/ nb-galactose-deprot-10mer 01292011.fid/ fid
2	Origin	Varian
3	Spectrometer	inova
4	Solvent	D2O
5	Temperature	25.0
6	Pulse Sequence	s2pul
7	Experiment	1D
8	Number of Scans	53
9	Receiver Gain	34
10	Pulse Width	0.0000
11	Acquisition Date	2011-01-31T12:19:18
12	Modification Date	2011-01-31T15:23:54
13	Spectrometer Frequency	599.72
14	Spectral Width	8000.0
15	Lowest Frequency	-1001.3
16	Nucleus	1H
17	Acquired Size	15136
18	Spectral Size	65536

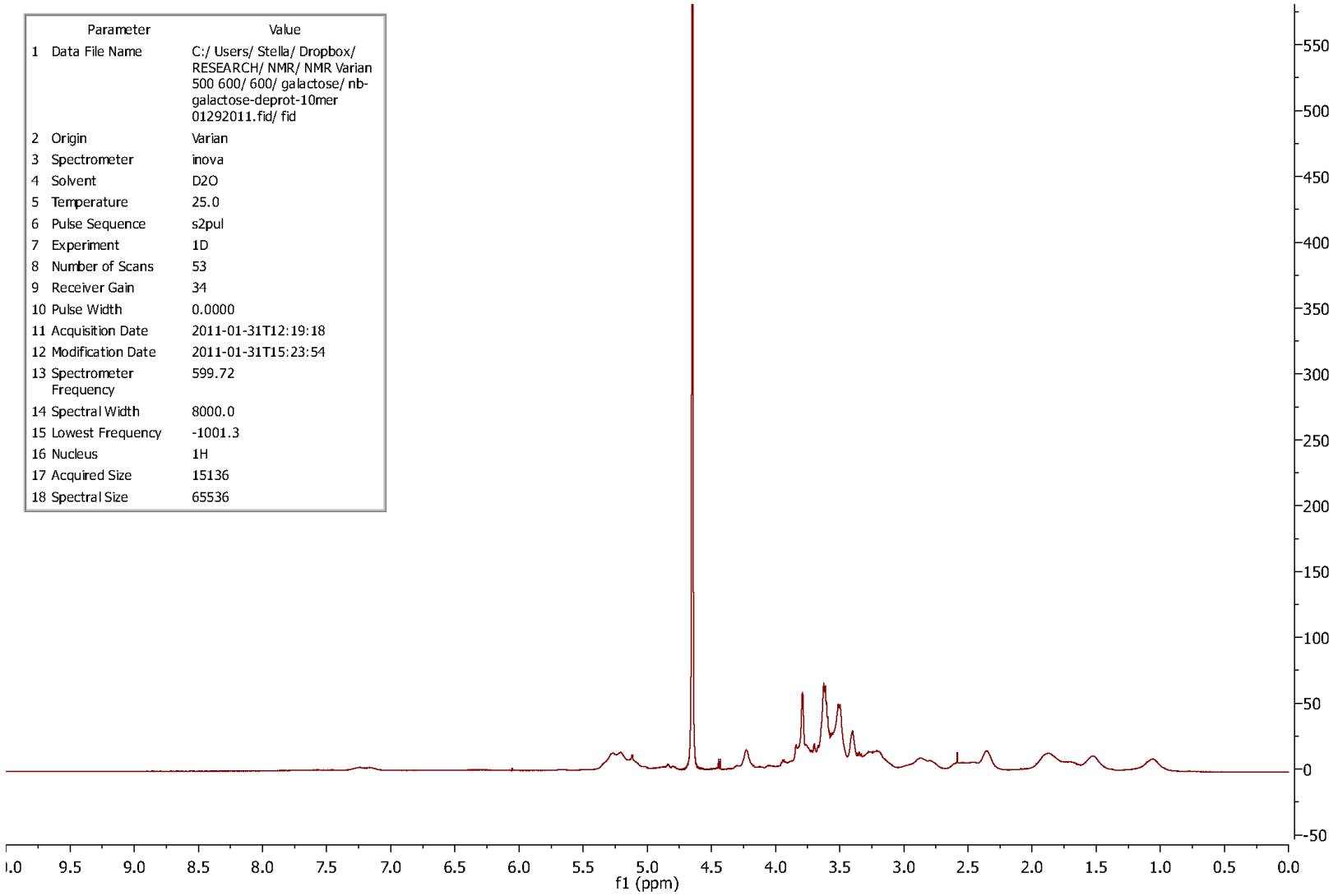

^{1}H-NMR spectrum of poly(Gal)$_{10}$

parameters	value
1 Data File Name	I:/ NMR with fixed fid/ galactose/ nb-galactose100mer-deprot-02072011.fid/ fid
2 Origin	Varian
3 Spectrometer	inova
4 Solvent	D2O
5 Temperature	25.0
6 Pulse Sequence	s2pul
7 Probe	hcx
8 Number of Scans	69
9 Receiver Gain	38
10 Relaxation Delay	1.0000
11 Pulse Width	0.0000
12 Acquisition Time	1.8920
13 Acquisition Date	
14 Spectrometer Frequency	599.72
15 Spectral Width	8000.0
16 Lowest Frequency	-1001.3
17 Nucleus	1H
18 Acquired Size	
19 Spectral Size	65536

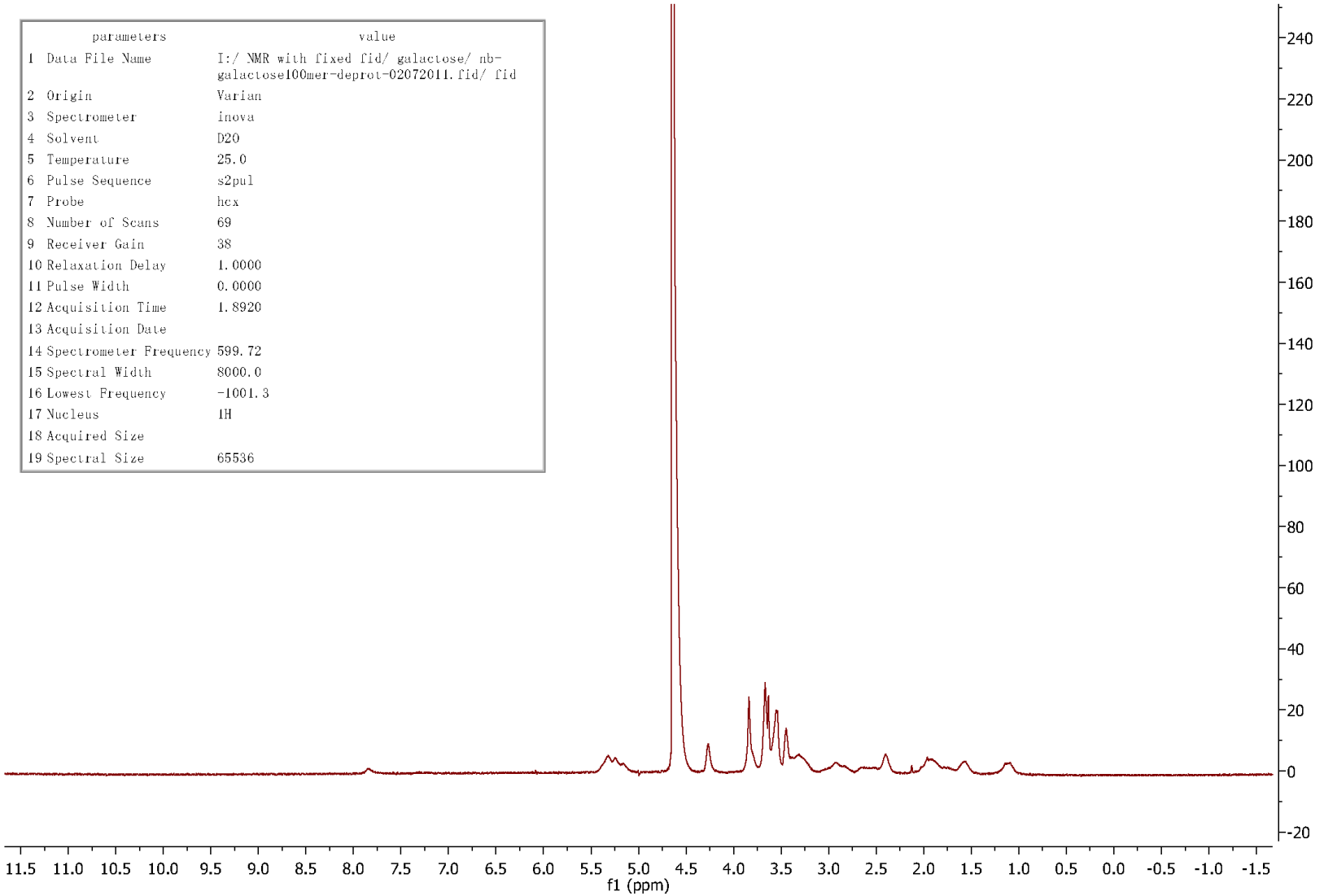

^{1}H NMR spectra of poly(Gal)$_{100}$

	Parameter	Value
1	Data File Name	F:/ fucose/ fucose-10mer/ 1/ fid
2	Title	fucose-10mer.1.fid
3	Origin	Bruker BioSpin GmbH
4	Spectrometer	spect
5	Solvent	D2O
6	Temperature	308.2
7	Pulse Sequence	zg30
8	Experiment	1D
9	Probe	5 mm PABBO BB/ 19F-1H/ D Z-GRD Z116098/ 0058
10	Number of Scans	164
11	Receiver Gain	32
12	Relaxation Delay	1.0000
13	Pulse Width	10.1000
14	Modification Date	2013-05-04T14:50:28
15	Spectrometer Frequency	399.83
16	Spectral Width	8223.7
17	Lowest Frequency	-1603.6
18	Nucleus	1H
19	Acquired Size	32768
20	Spectral Size	65536

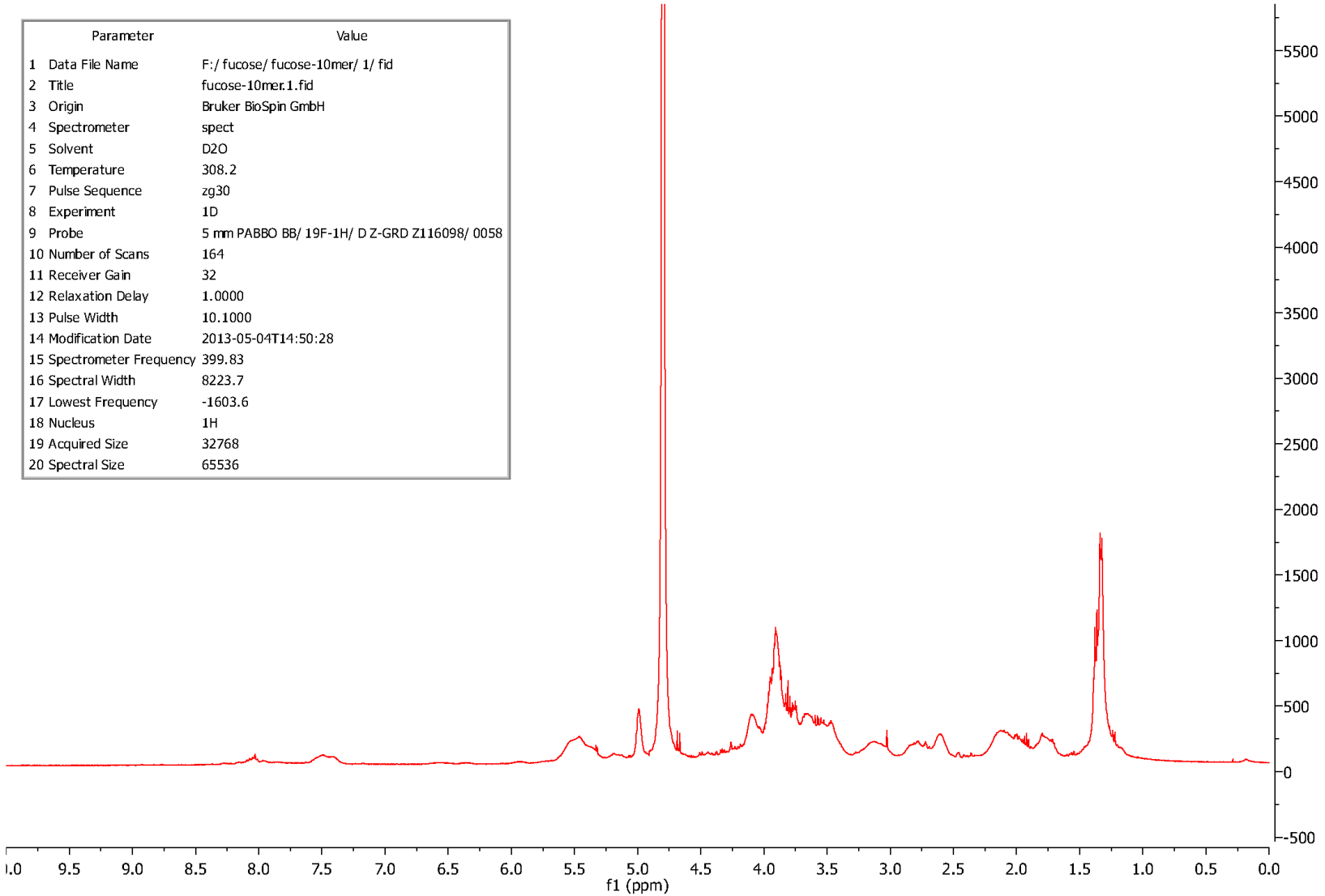

^{1}H-NMR spectrum of poly(Fuc)$_{10}$

	Parameter	Value
1	Data File Name	F:/ fucose/ fucose-100mer/ 1/ fid
2	Title	fucose-100mer.1.fid
3	Origin	Bruker BioSpin GmbH
4	Spectrometer	spect
5	Solvent	D2O
6	Temperature	308.2
7	Pulse Sequence	zg30
8	Experiment	1D
9	Probe	5 mm PABBO BB/ 19F-1H/ D Z-GRD Z116098/ 0058
10	Number of Scans	340
11	Receiver Gain	59
12	Relaxation Delay	1.0000
13	Pulse Width	10.1000
14	Modification Date	2013-05-04T15:46:20
15	Spectrometer Frequency	399.83
16	Spectral Width	8223.7
17	Lowest Frequency	-1602.6
18	Nucleus	1H
19	Acquired Size	32768
20	Spectral Size	65536

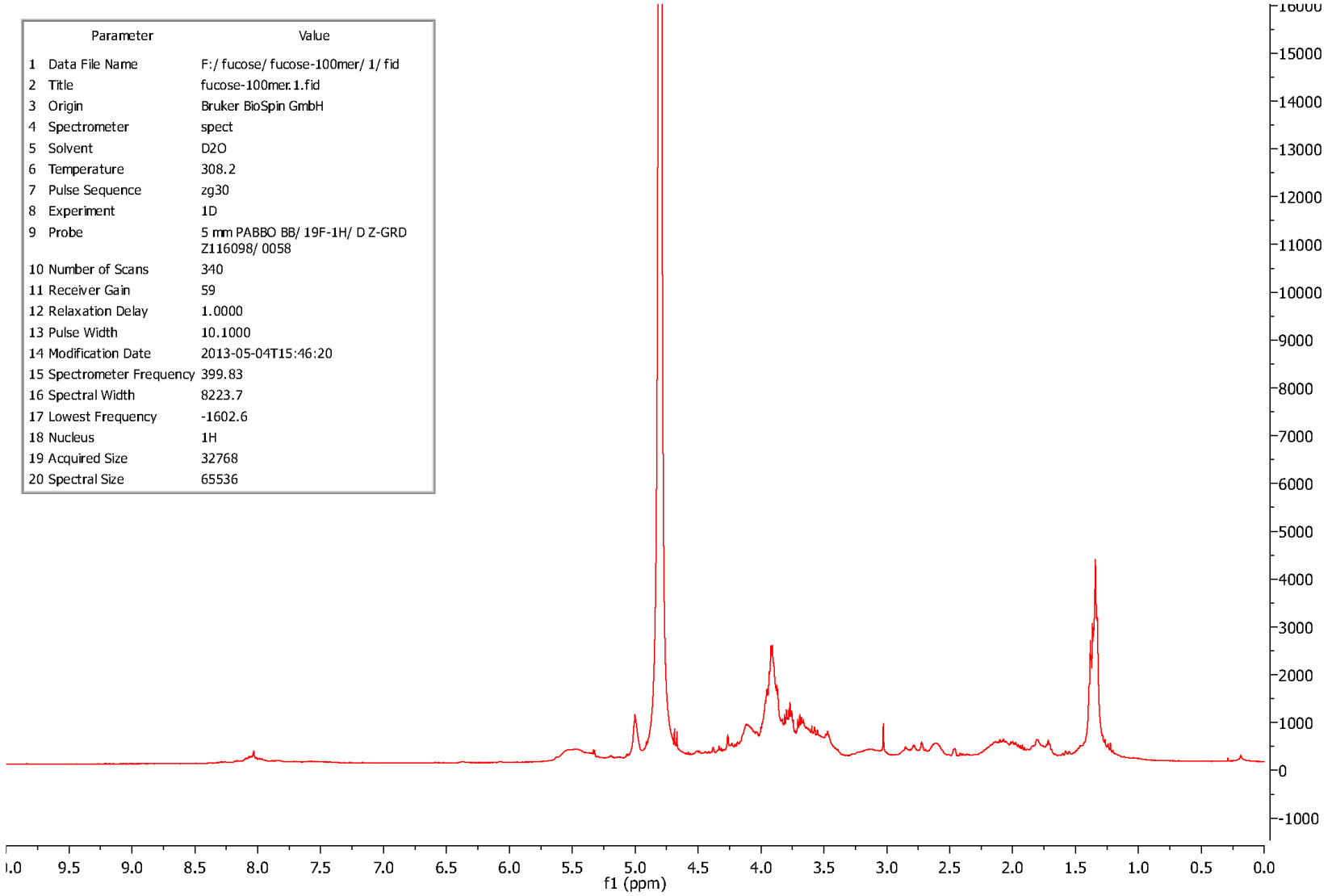

^{1}H-NMR spectrum of poly(Fuc)$_{100}$

	Parameter	Value
1	Data File Name	F:/ NMR/ glcNAc/ nb-glcnac10mer-2-deprot-12102010.fid/ fid
2	Origin	Varian
3	Spectrometer	inova
4	Solvent	D2O
5	Temperature	25.0
6	Pulse Sequence	s2pul
7	Experiment	1D
8	Probe	hcx
9	Number of Scans	48
10	Receiver Gain	40
11	Relaxation Delay	1.0000
12	Pulse Width	0.0000
13	Acquisition Time	1.8920
14	Acquisition Date	2010-12-11T17:26:54
15	Spectrometer Frequency	599.72
16	Spectral Width	8000.0
17	Lowest Frequency	-1001.3
18	Nucleus	1H
19	Acquired Size	15136
20	Spectral Size	65536

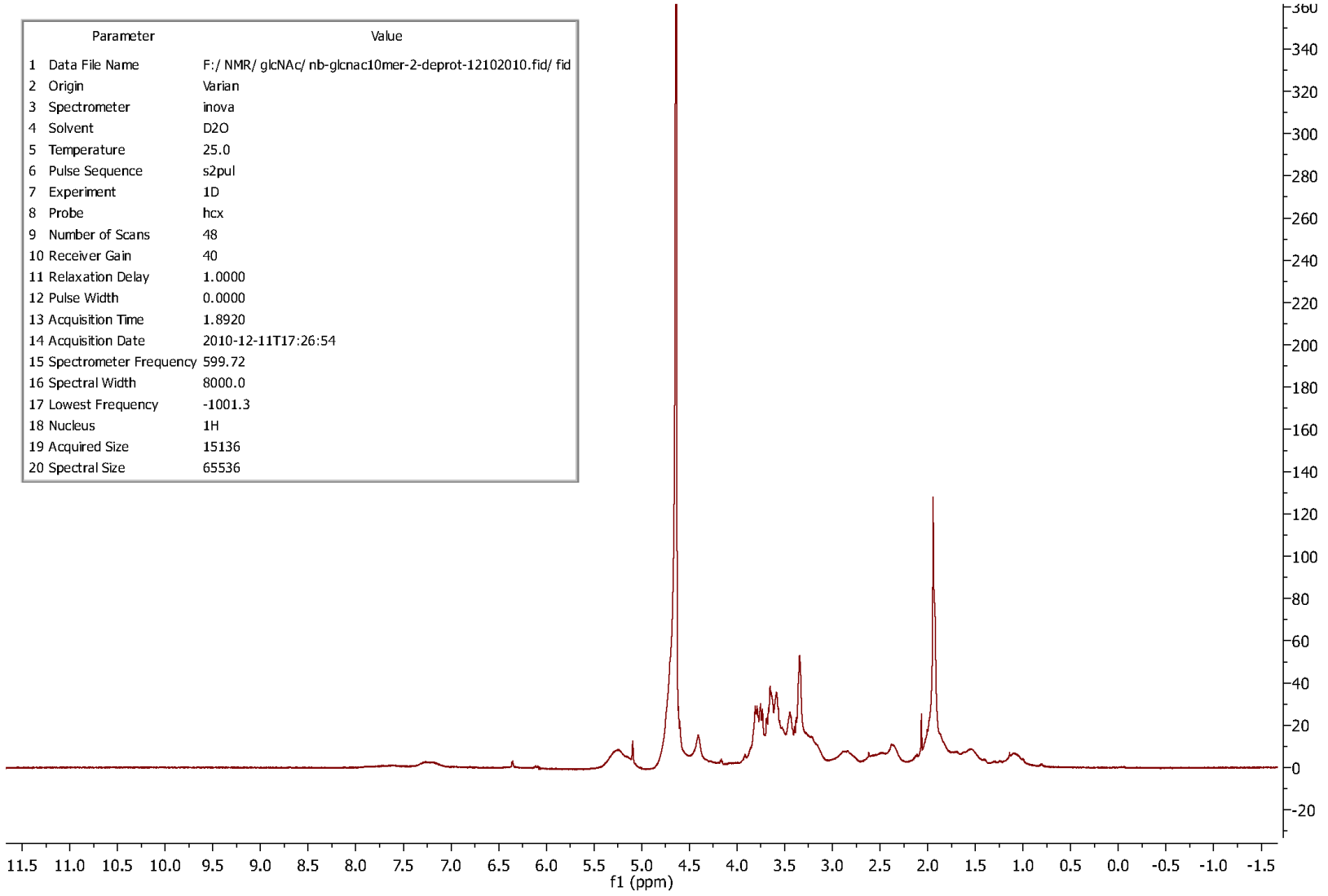

^{1}H-NMR spectrum of poly(GlcNAc)$_{10}$

Parameters	value
1 Data File Name	I:/ NMR/ glcNAc/ deprot nb glcnac 100mer 12062010.fid/ fid
2 Origin	Varian
3 Spectrometer	inova
4 Solvent	D2O
5 Temperature	25.0
6 Pulse Sequence	s2pul
7 Probe	hcx
8 Number of Scans	100
9 Receiver Gain	28
10 Relaxation Delay	1.0000
11 Pulse Width	0.0000
12 Acquisition Time	1.8920
13 Acquisition Date	2010 12 06T13:17:09
14 Spectrometer Frequency	599.72
15 Spectral Width	8000.0
16 Lowest Frequency	1001.3
17 Nucleus	1H
18 Acquired Size	15136
19 Spectral Size	65536

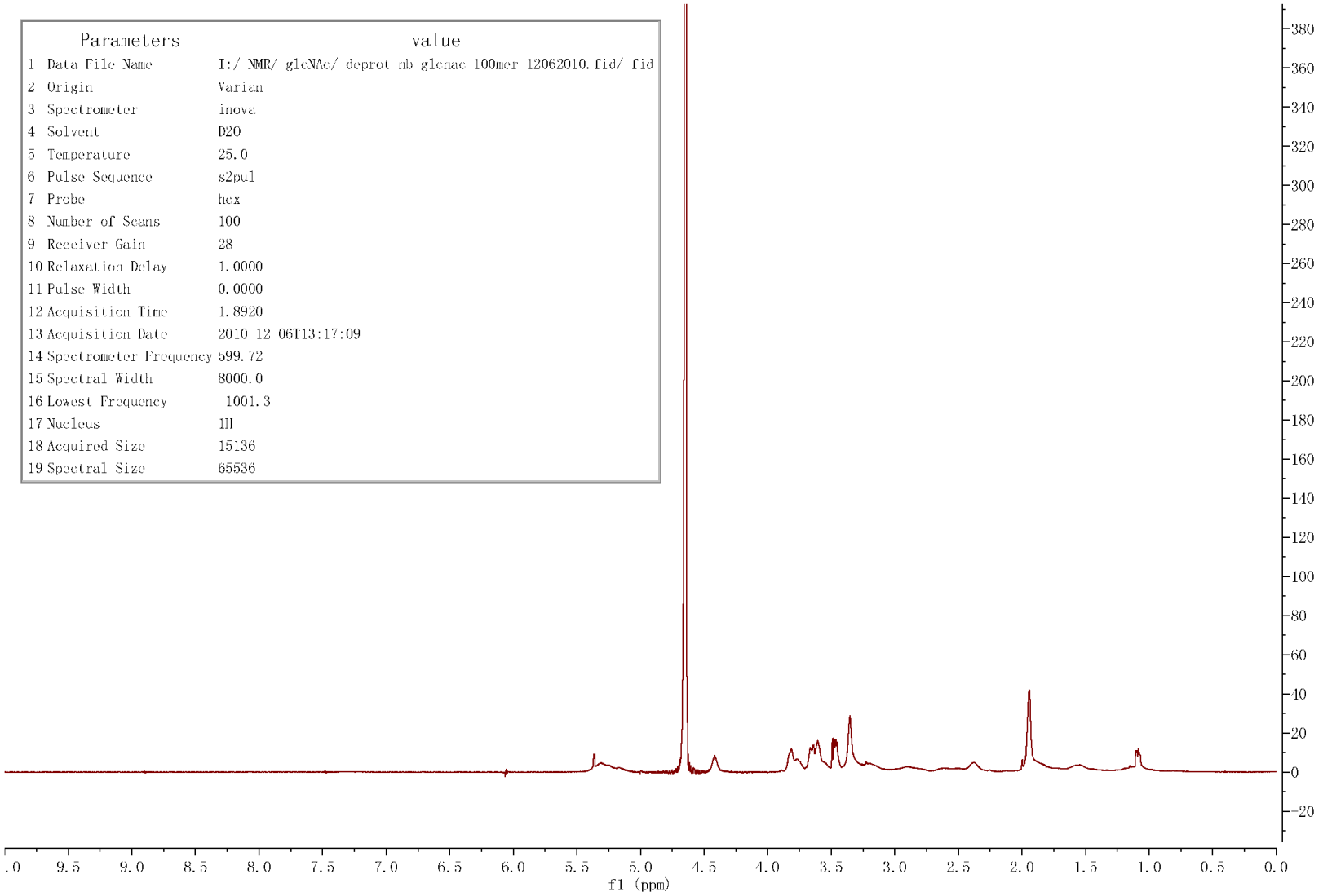

^{1}H NMR spectra of poly(GlcNAc)$_{100}$

	Parameter	Value
1	Data File Name	F:/ NMR/ galNAc/ deprot-nb-galnac-10mer-10042012/ 1/ fid
2	Title	deprot-nb-galnac-10mer-10042012.1.fid
3	Origin	Bruker BioSpin GmbH
4	Spectrometer	spect
5	Solvent	D2O
6	Temperature	298.1
7	Pulse Sequence	zg30
8	Experiment	1D
9	Probe	5 mm CPPBBO BB-1H/ 19F/ D Z-GRD Z122624/ 0008
10	Number of Scans	100
11	Receiver Gain	32
12	Relaxation Delay	1.0000
13	Pulse Width	12.0000
14	Modification Date	2012-10-05T11:45:02
15	Spectrometer Frequency	499.89
16	Spectral Width	10000.0
17	Lowest Frequency	-1913.0
18	Nucleus	1H
19	Acquired Size	32768
20	Spectral Size	65536

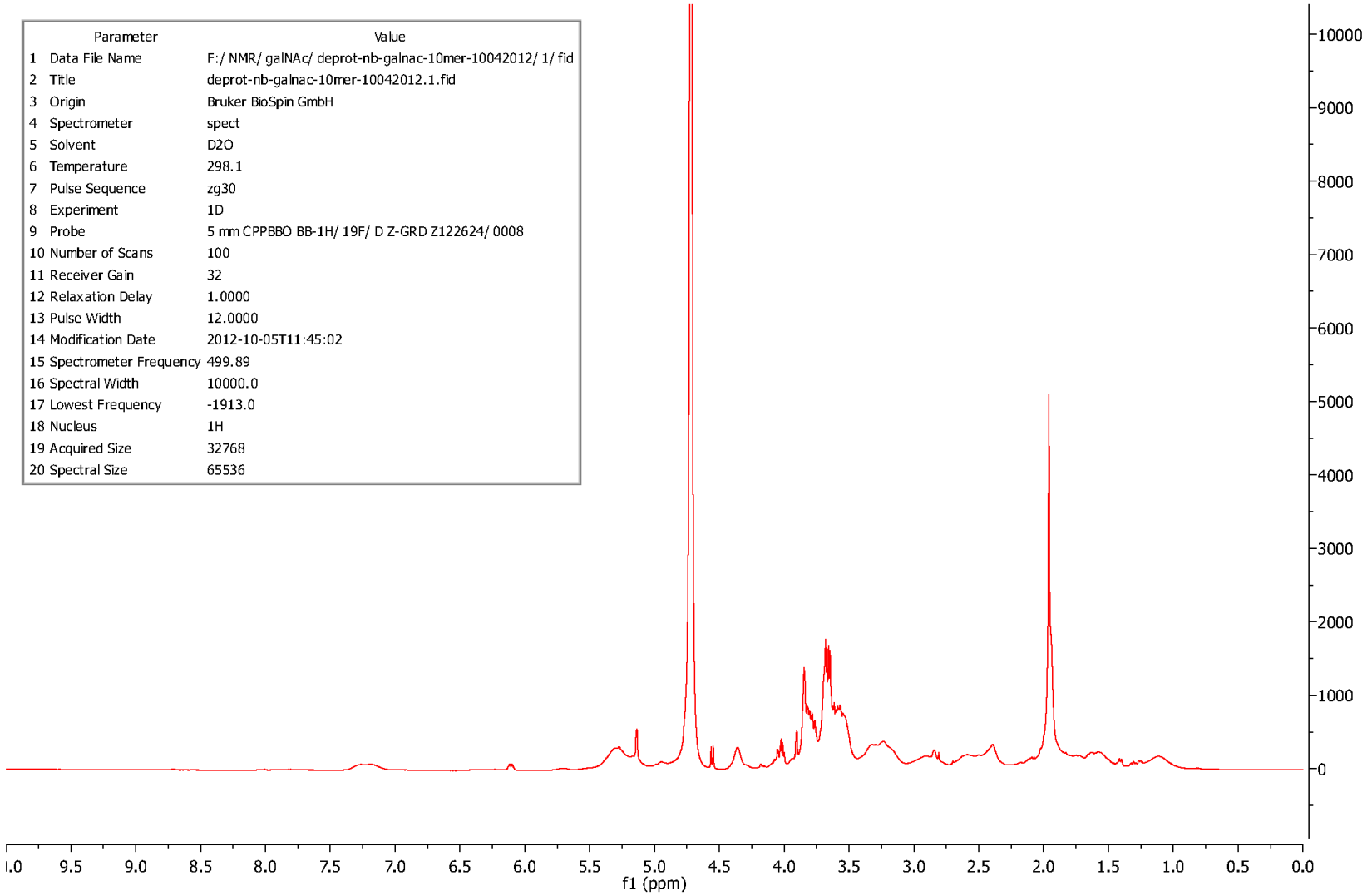

^{1}H-NMR spectrum of poly(GalNAc)$_{10}$

	Parameter	Value
1	Data File Name	F:/ NMR/ galNAc/ deacetyl-NB-GalNAc100mer-1-09062012/ 1/ fid
2	Title	deacetyl-NB-GalNAc100mer-1-09062012.1.fid
3	Origin	Bruker BioSpin GmbH
4	Spectrometer	spect
5	Solvent	D2O
6	Temperature	298.1
7	Pulse Sequence	zg30
8	Experiment	1D
9	Probe	5 mm CPPBBO BB-1H/ 19F/ D Z-GRD Z122624/ 0008
10	Number of Scans	52
11	Receiver Gain	32
12	Relaxation Delay	1.0000
13	Pulse Width	12.0000
14	Modification Date	2012-09-06T17:22:54
15	Spectrometer Frequency	499.89
16	Spectral Width	10000.0
17	Lowest Frequency	-1913.0
18	Nucleus	1H
19	Acquired Size	32768
20	Spectral Size	65536

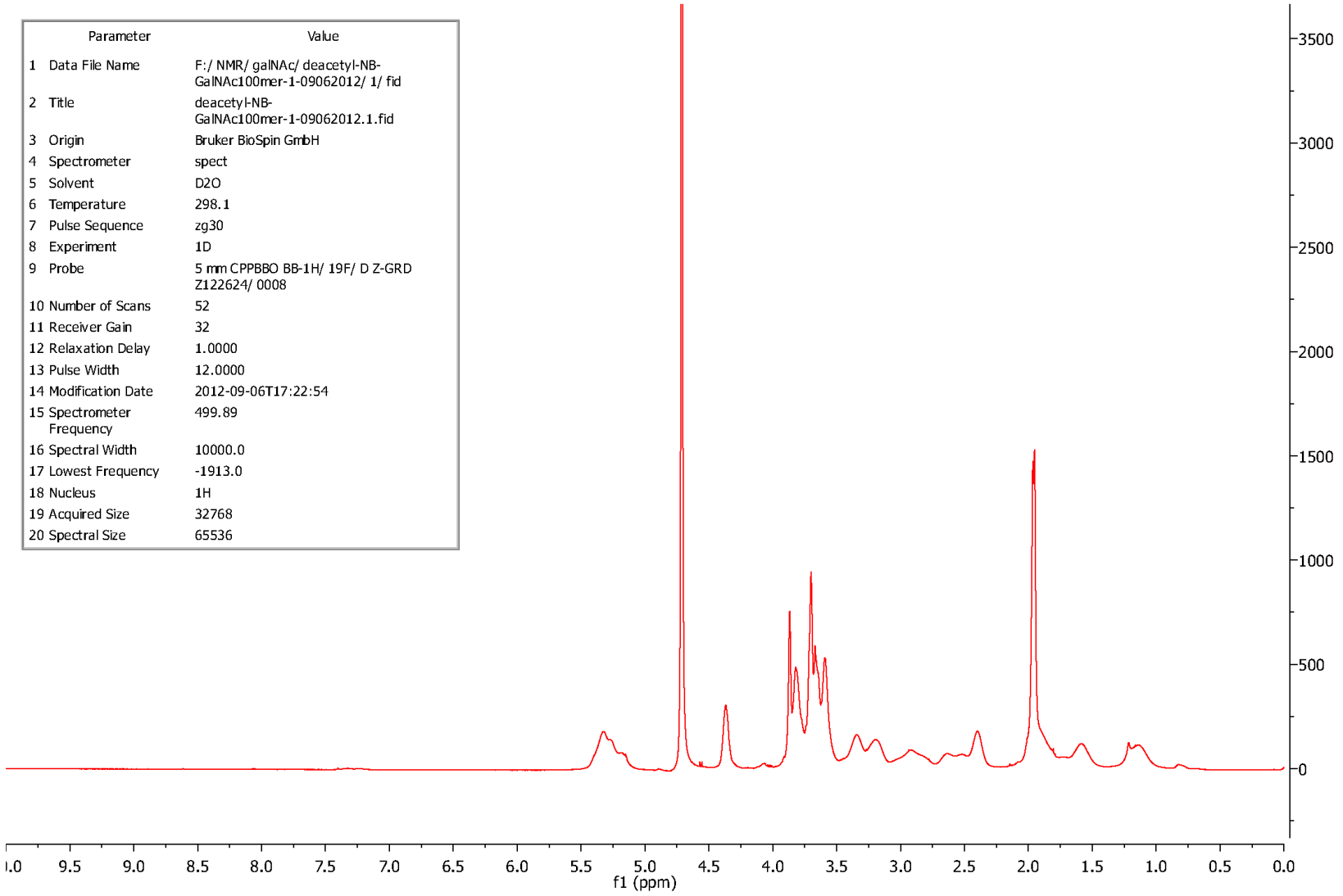

^{1}H-NMR spectrum of poly(GalNAc)$_{100}$

	Parameter	Value
1	Data File Name	C:/ Users/ Stella/ Dropbox/ RESEARCH/ NMR/ NMR Varian 500 600/ 600/ fucose/ nb-fucose10mer-1-deprot12162010.fid/ fid
2	Origin	Varian
3	Spectrometer	inova
4	Solvent	D2O
5	Temperature	25.0
6	Pulse Sequence	s2pul
7	Experiment	1D
8	Number of Scans	83
9	Receiver Gain	40
10	Pulse Width	0.0000
11	Acquisition Date	2010-12-17T21:11:34
12	Modification Date	2010-12-18T00:18:56
13	Spectrometer Frequency	599.72
14	Spectral Width	8000.0
15	Lowest Frequency	-921.4
16	Nucleus	1H
17	Acquired Size	15136
18	Spectral Size	65536

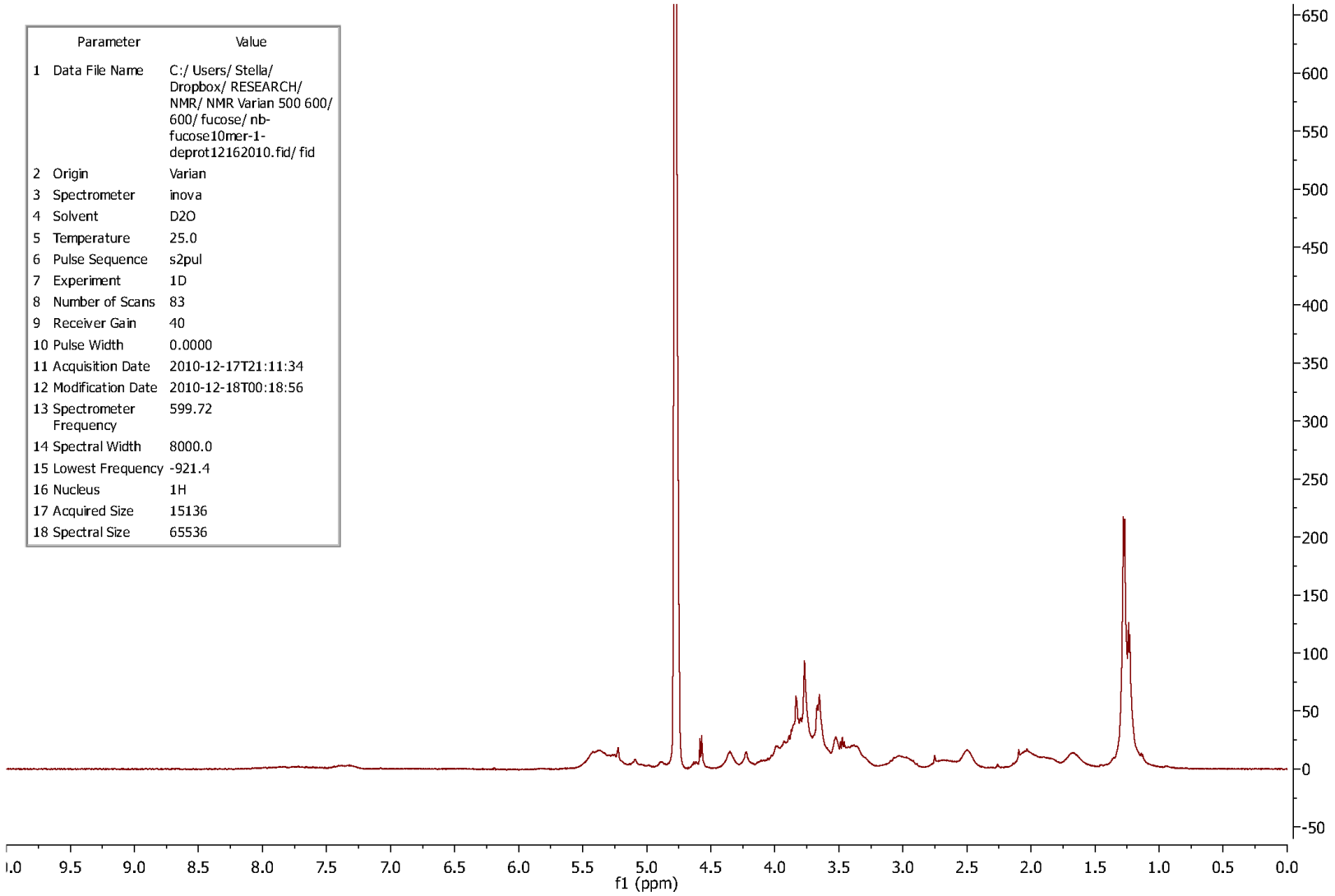

^{1}H-NMR spectrum of poly(D-Fuc)$_{10}$

Parameter	Value
1 Data File Name	I:/ fucose/ nb fucose 100mer deprotected01062011/1/fid
2 Origin	Bruker BioSpin GmbH
3 Spectrometer	spect
4 Solvent	D2O
5 Temperature	298.2
6 Pulse Sequence	zg30
7 Experiment	1D
8 Probe	5 mm CPPBBO BB 1H/ 19F/ D Z GRD Z122624/ 0008
9 Number of Scans	393
10 Receiver Gain	49
11 Relaxation Delay	1.0000
12 Pulse Width	12.0000
13 Acquisition Time	
14 Acquisition Date	
15 Spectrometer Frequency	499.89
16 Spectral Width	10000.0
17 Lowest Frequency	1913.0
18 Nucleus	1H
19 Acquired Size	
20 Spectral Size	65536

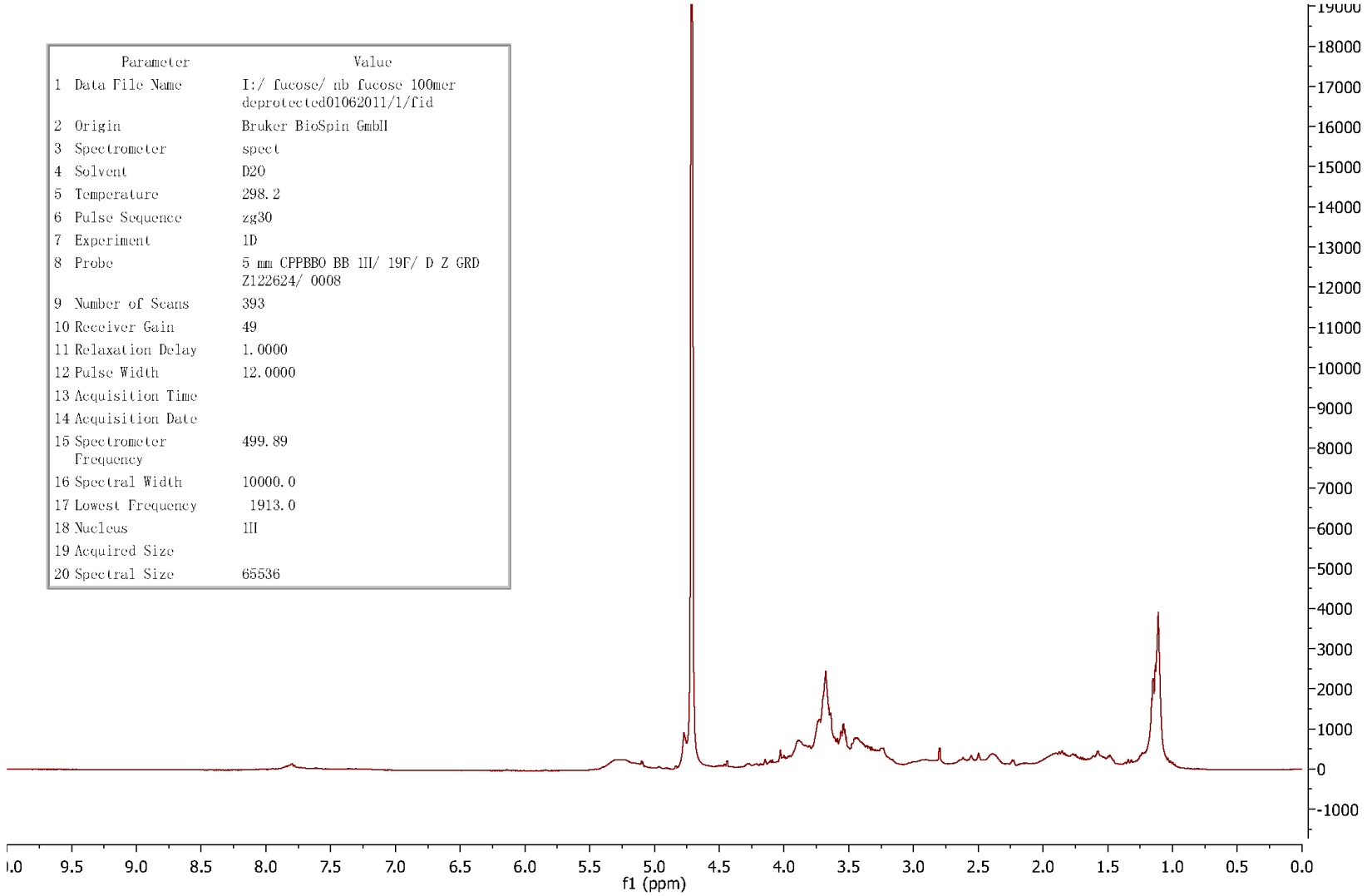

^{1}H-NMR spectrum of prot-poly(D-Fuc)$_{100}$

	Parameter	Value
1	Data File Name	F:/ peptide NMR/ CB-EAD/ cb-ead17-20-02042009.fid/ fid
2	Origin	Varian
3	Spectrometer	inova
4	Solvent	CDCl3
5	Temperature	25.0
6	Pulse Sequence	s2pul
7	Experiment	1D
8	Probe	hcx
9	Number of Scans	20
10	Receiver Gain	60
11	Relaxation Delay	1.0000
12	Pulse Width	0.0000
13	Acquisition Time	1.8920
14	Acquisition Date	2009-02-04T13:22:08
15	Spectrometer Frequency	599.72
16	Spectral Width	8000.0
17	Lowest Frequency	-1001.3
18	Nucleus	1H
19	Acquired Size	15136
20	Spectral Size	65536

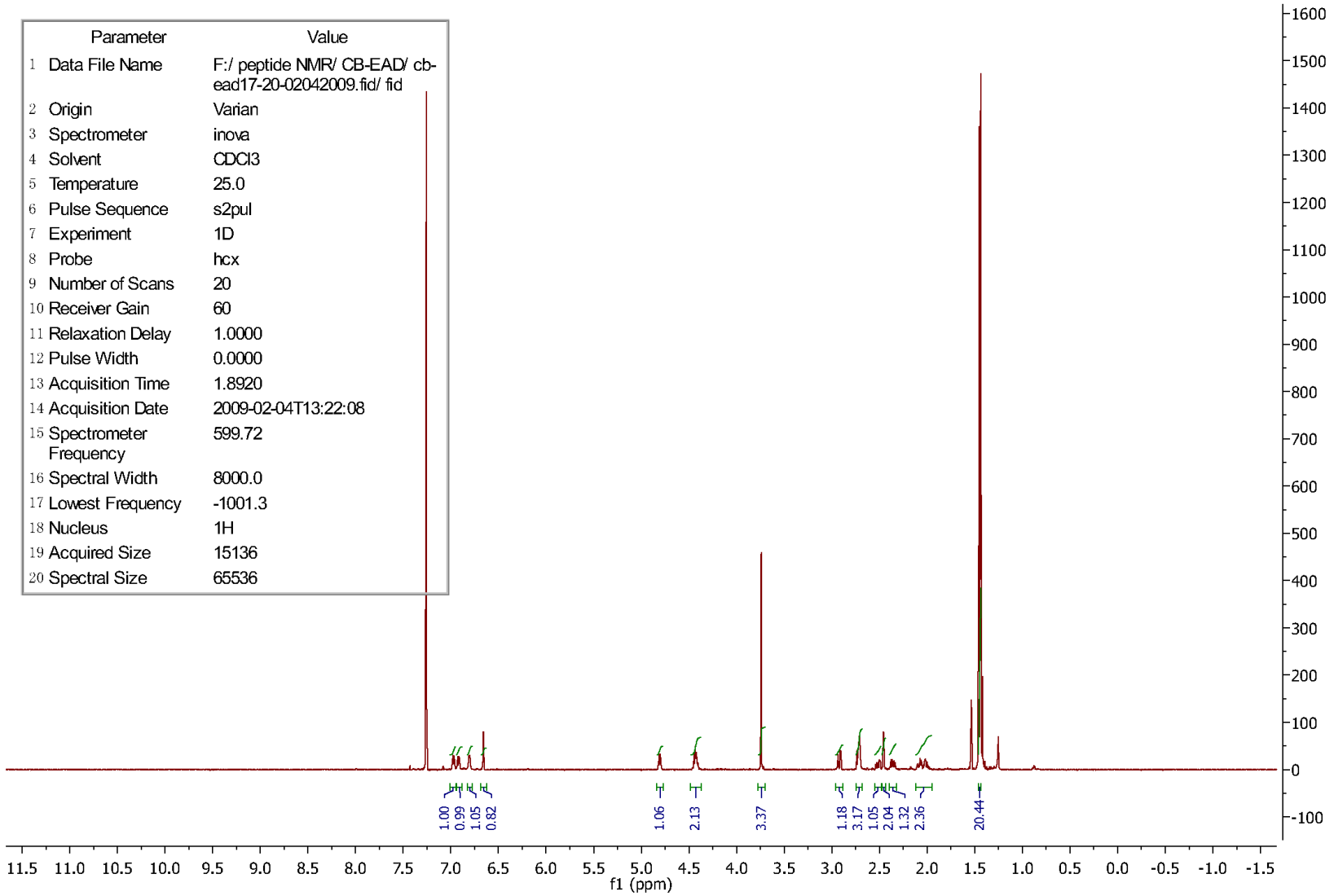

^{1}H NMR spectrum of CB-EAD 37

	Parameter	Value
1	Data File Name	F:/ peptide NMR/ cb-gcd/ cb-gcd07_23_08.fid/ fid
2	Origin	Varian
3	Spectrometer	inova
4	Solvent	CDCl3
5	Temperature	25.0
6	Pulse Sequence	s2pul
7	Experiment	1D
8	Probe	hcx
9	Number of Scans	32
10	Receiver Gain	52
11	Relaxation Delay	1.0000
12	Pulse Width	0.0000
13	Acquisition Time	1.8920
14	Acquisition Date	2008-07-23T14:59:52
15	Spectrometer Frequency	599.72
16	Spectral Width	8000.0
17	Lowest Frequency	-1000.5
18	Nucleus	1H
19	Acquired Size	15136
20	Spectral Size	65536

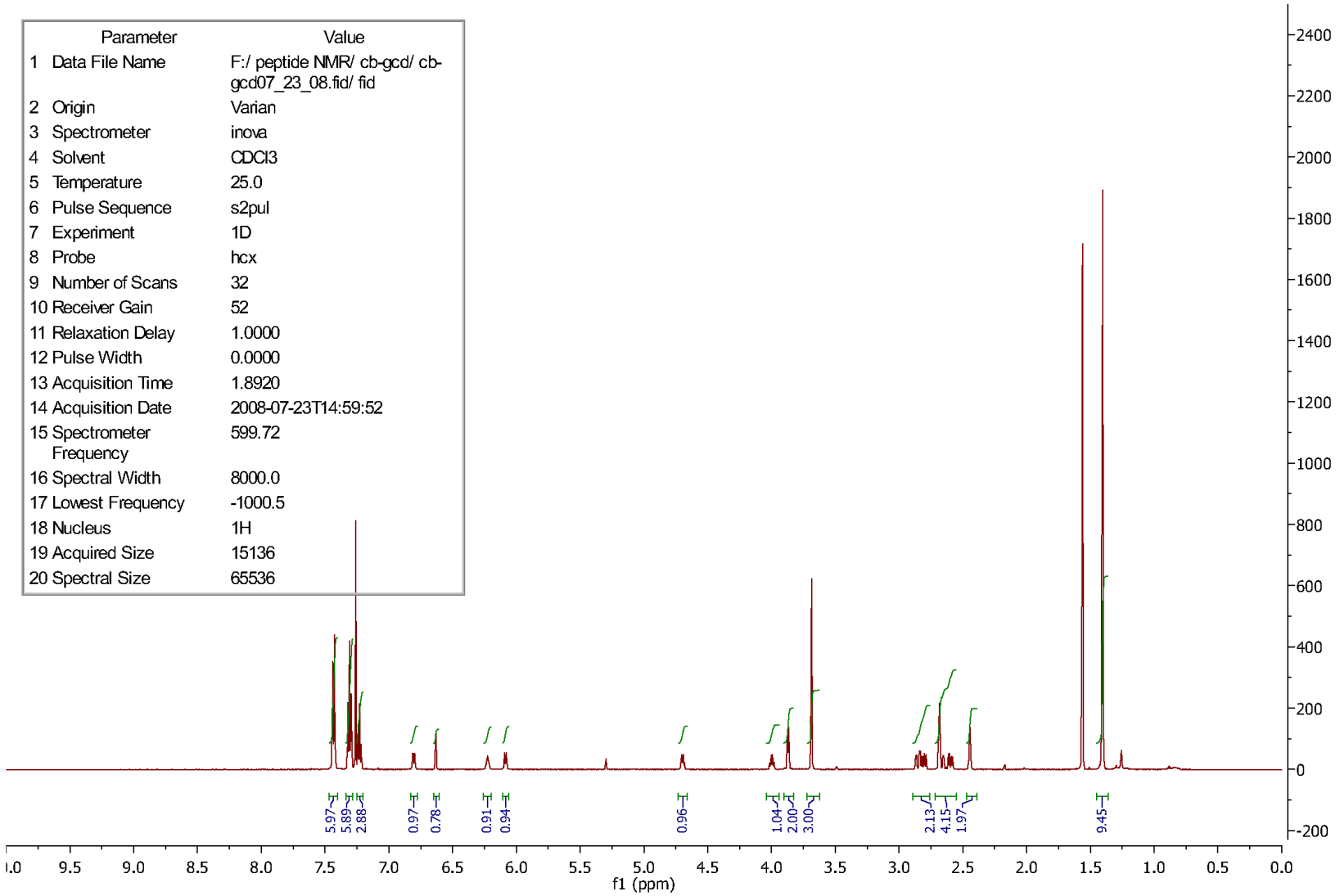

^{1}H NMR spectrum of CB-GCD 42

	Parameter	Value
1	Data File Name	F:/ peptide NMR/ CB-ec(acm)d/ cb-ec-acm-d02172009.fid/ fid
2	Origin	Varian
3	Spectrometer	inova
4	Solvent	CDCl3
5	Temperature	25.0
6	Pulse Sequence	s2pul
7	Experiment	1D
8	Probe	hcx
9	Number of Scans	30
10	Receiver Gain	56
11	Relaxation Delay	1.0000
12	Pulse Width	0.0000
13	Acquisition Time	1.8920
14	Acquisition Date	2009-02-17T11:04:39
15	Spectrometer Frequency	499.90
16	Spectral Width	7998.4
17	Lowest Frequency	-999.9
18	Nucleus	1H
19	Acquired Size	15133
20	Spectral Size	65536

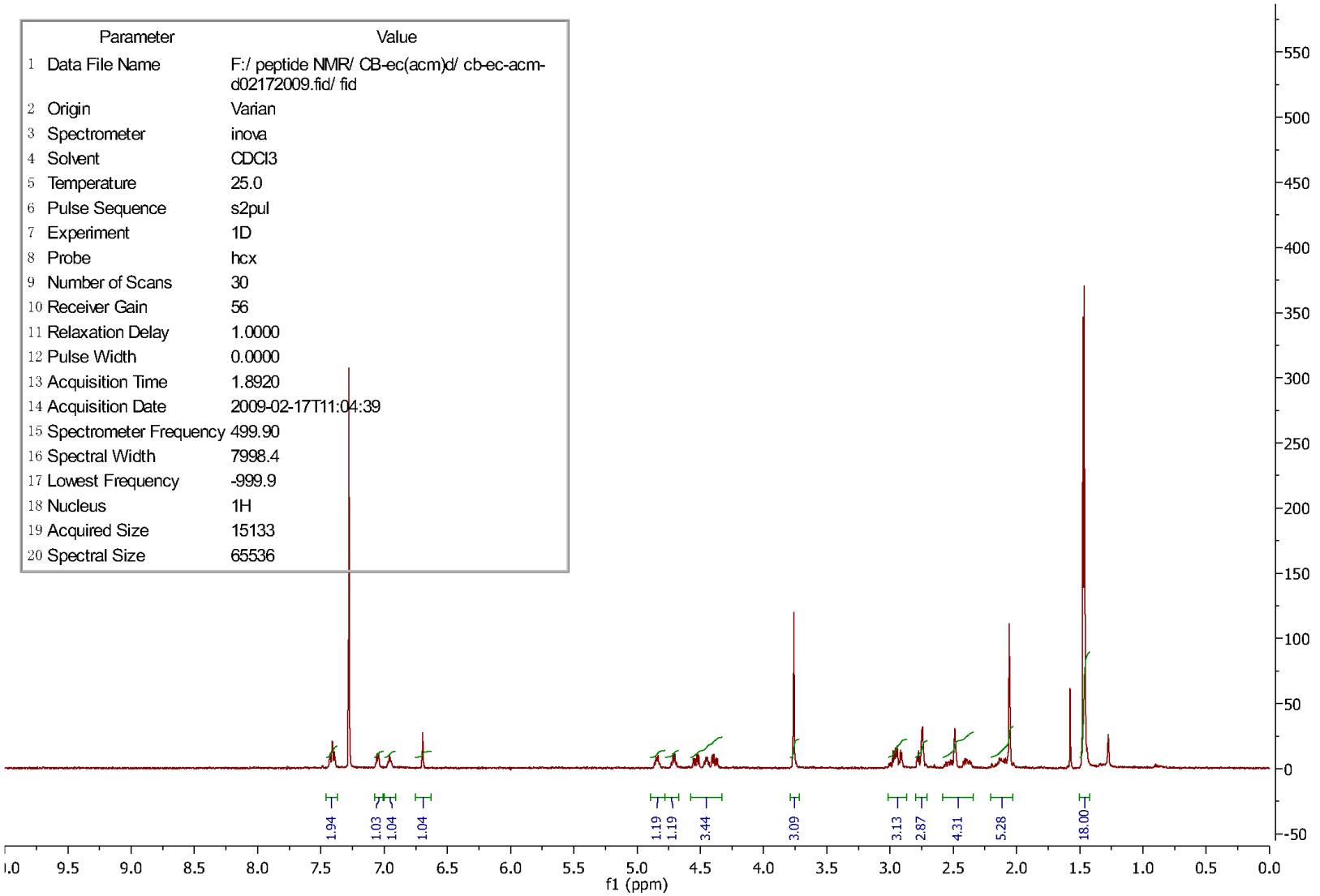

^{1}H NMR spectrum of CB-EC(Acm)D 47

	Parameter	Value
1	Data File Name	F:/ peptide NMR/ CB-EAD/ cb-ead10mer-3h30min02052009.fid/ fid
2	Origin	Varian
3	Spectrometer	inova
4	Solvent	cd2cl2
5	Temperature	25.0
6	Pulse Sequence	s2pul
7	Experiment	1D
8	Probe	hcx
9	Number of Scans	8
10	Receiver Gain	40
11	Relaxation Delay	1.0000
12	Pulse Width	0.0000
13	Acquisition Time	1.8920
14	Acquisition Date	2009-02-05T14:09:32
15	Spectrometer Frequency	499.90
16	Spectral Width	25000.0
17	Lowest Frequency	-9500.7
18	Nucleus	1H
19	Acquired Size	47300
20	Spectral Size	131072

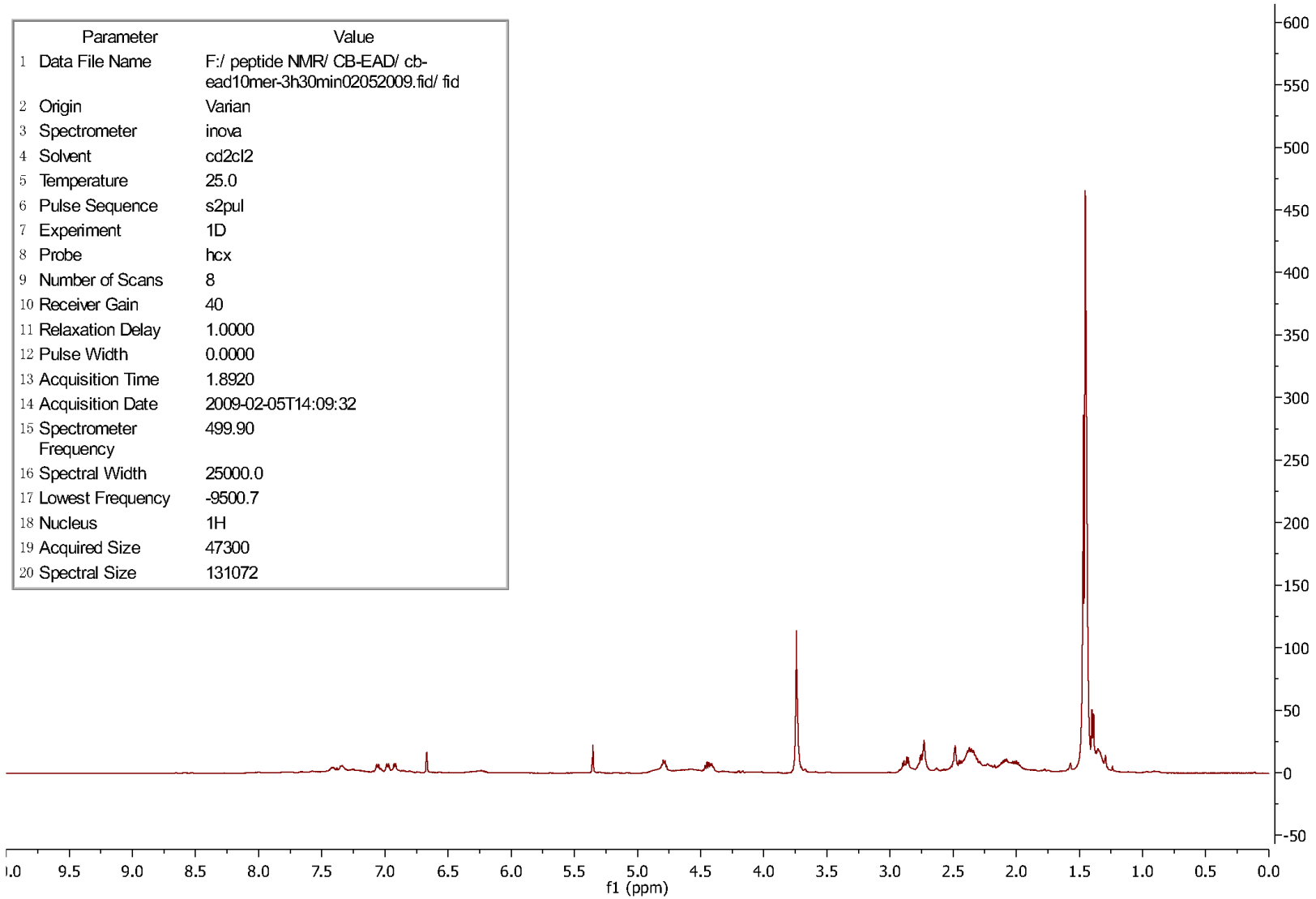

^{1}H NMR spectrum of poly(CB-EAD)

	Parameter	Value
1	Data File Name	I:/ peptide NMR/ cb-gcd/ cb-gcd10h12032008.fid/ fid
2	Origin	Varian
3	Spectrometer	inova
4	Solvent	cd2cl2
5	Temperature	25.0
6	Pulse Sequence	s2pul
7	Probe	hcx
8	Number of Scans	8
9	Receiver Gain	26
10	Relaxation Delay	1.0000
11	Pulse Width	0.0000
12	Acquisition Time	1.8920
13	Acquisition Date	
14	Spectrometer Frequency	599.72
15	Spectral Width	25000.0
16	Lowest Frequency	-10681.5
17	Nucleus	1H
18	Acquired Size	
19	Spectral Size	131072

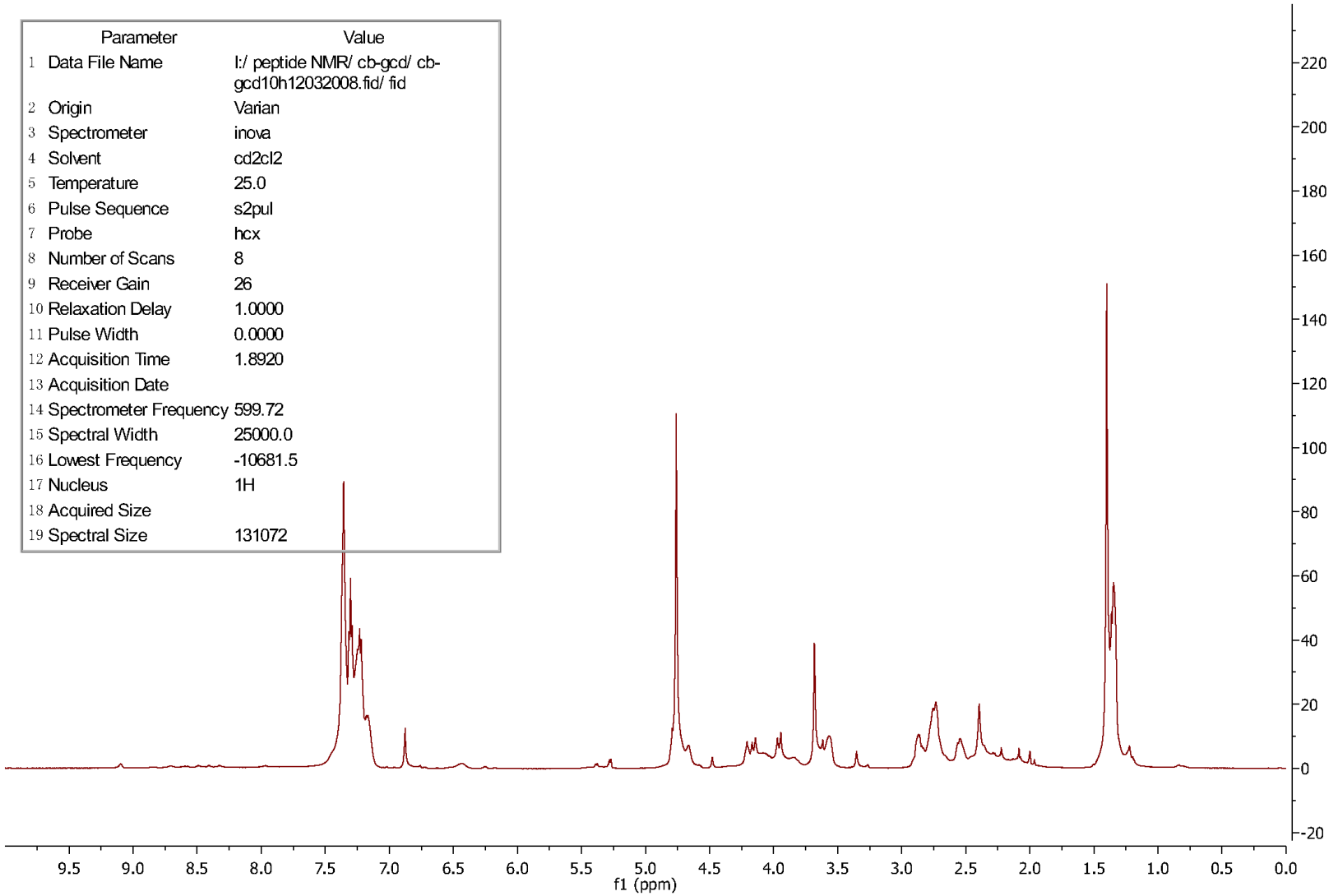

^{1}H NMR spectrum of poly(CB-GCD)

	Parameter	Value
1	Data File Name	I:/ peptide NMR/ CB-ec(acm)d/ cb-ec-acm-d10mer-6h30min02202009.fid/ fid
2	Origin	Varian
3	Spectrometer	inova
4	Solvent	cd2cl2
5	Temperature	25.0
6	Pulse Sequence	s2pul
7	Probe	hcx
8	Number of Scans	8
9	Receiver Gain	40
10	Relaxation Delay	1.0000
11	Pulse Width	0.0000
12	Acquisition Time	1.8920
13	Acquisition Date	
14	Spectrometer Frequency	499.90
15	Spectral Width	25000.0
16	Lowest Frequency	-9500.7
17	Nucleus	1H
18	Acquired Size	
19	Spectral Size	131072

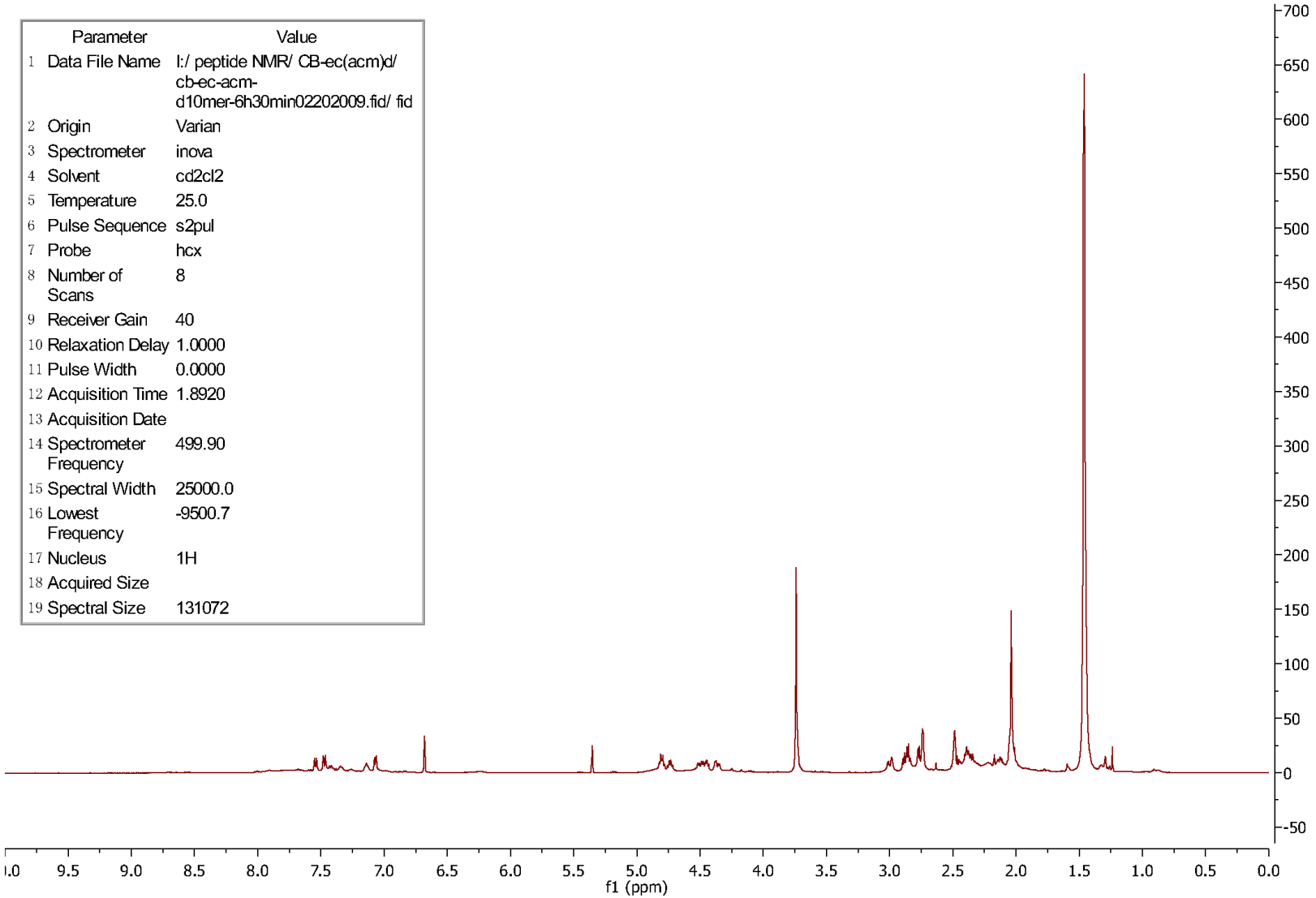

^{1}H NMR spectrum of poly[CB-EC(Acm)D]